

Some pages of this thesis may have been removed for copyright restrictions.

If you have discovered material in Aston Research Explorer which is unlawful e.g. breaches copyright, (either yours or that of a third party) or any other law, including but not limited to those relating to patent, trademark, confidentiality, data protection, obscenity, defamation, libel, then please read our [Takedown policy](#) and contact the service immediately (openaccess@aston.ac.uk)

Development of mass spectrometry protocols for analysis of oxidised lipidome in inflammatory disease models

**Using semi-targeted mass spectrometry based approach & optimized
chromatographic separation**

Alpesh Thakker

**A thesis submitted for the degree of
Doctor of Philosophy**



Dec 2016

©Alpesh Thakker, 2016

Alpesh Thakker asserts his moral right to be identified as the author of this thesis. This copy of the thesis has been supplied on condition that anyone who consults it is understood to recognise that its copyright rests with its author and that no quotation from the thesis and no information derived from it may be published without appropriate permission or acknowledgement.

Alpesh Thakker

Doctor of Philosophy

2016

Thesis Summary

Phospholipid oxidation generates a wide variety of products with potentially novel biological activities that may be associated with disease pathogenesis. To understand their role in disease requires precise information about their abundance in biological samples. Liquid chromatography-mass spectrometry (LCMS) is a sensitive technique that can provide detailed information about the oxidative lipidome, but challenges still remain.

The work in this thesis developed improved methods for detection of OxPLs by improvement of chromatographic separation through the comparison and optimisation of several HPLC columns such as C8, C18 and C30 reverse phase, polystyrene-divinylbenzene based monolithic, and mixed-mode hydrophilic interaction (HILIC) columns & solvent systems, with use of semi-targeted mass spectrometry approaches. The results suggests that the monolithic column was the most robust method for separating short chain oxPLs from long chain oxidised and native PLs. In addition, several approaches for method validation were explored such as testing of reproducibility and repeatability of the methods, together with the reanalysis of samples on a high resolution QToF mass spectrometer with automated quantitative data analysis using the Progenesis QI software to validate the identification. The combination of the developed methods allowed the identification of several oxPLs in biological samples. These were: i) ascites fluid of lean and obese rat model of acute pancreatitis; ii) isolated components of red blood cells (RBCs) infected with the malarial parasite *Plasmodium falciparum*; and iii) plasma samples of healthy and diabetic patients. In addition, an evaluation of post-acquisition data handling to minimise inherent biological variation was performed. Quantitative differences in oxPLs were observed in isolated malarial components as well as other studied disease models.

Overall, several protocols were developed that provide improved performance for the identification of OxPL in biological samples that can be used as a reference method by research laboratories interested in oxidative lipidomics work.

Keywords: Oxidised phospholipids (oxPLs), Liquid chromatography-mass spectrometry (LCMS), oxidative stress, Inflammation, Lipidomics

Dedication

“It is not the critic who counts: not the man who points out how the strong man stumbles or where the doer of deeds could have done better. The credit belongs to the man who is actually in the arena, whose face is marred by dust and sweat and blood, who strives valiantly, who errs and comes up short again and again, because there is no effort without error or shortcoming, but who knows the great enthusiasms, the great devotions, who spends himself for a worthy cause; who, at the best, knows, in the end, the triumph of high achievement, and who, at the worst, if he fails, at least he fails while daring greatly, so that his place shall never be with those cold and timid souls who knew neither victory nor defeat”

Theodore Roosevelt, 26th US President on ***Statistics and data science***

Acknowledgements

First and foremost, I would like to thank my supervisor Prof Corinne Spickett and co-supervisor Prof Andrew Pitt for giving me this opportunity to pursue PhD in the Oxidative Stress group. Their excellent supervisory skills and forward thinking approach to science made my PhD journey progressive and enriching. I am really grateful to them for the insightful discussions and scientific advice that inspired me to progress in my research. I am indebted to Corinne for her useful guidance and continuous support that helped me improve my academic writing as well as presentation skills, and that, ultimately, made me a better researcher than I was three and half years ago when I first started.

I cannot forget the support that I had from late Dr Mike Davies whose practical guidance on NMR instrument and guidance on general health and safety in the lab helped me develop into a better researcher. His knowledge in organic chemistry and synthesis was inspiring.

I also would like to express my gratitude to Dr James Brown, Prof Juan Sastre, Dr Evelin Schwarzer and Prof Roslyn Bill for their collaboration and providing biological samples.

I would also like to thank all the other - past and present - members of the Oxidative Stress group and lab MB358 for their help both inside and outside the lab, and for making me feel always welcome from day one. My last thanks go to the family, specially my wife without whom I could not have dreamed of pursuing this PhD. Her moral support and selfless love motivated me daily and kept me focussed.

List of abbreviations

AU- arbitrary unit

CID collision induced dissociation

eNOS endothelial nitric oxide synthase

EI- Electron impact ionisation

ESI electrospray ionization

FAB fast atom bombardment

FTICR Fourier transform ion cyclotron resonance

GC gas chromatography

GC-MS-gas chromatography

GPx4 glutathione peroxidase

GST glutathione transferase

HAEC human aortic endothelial cells

HDL high density lipoprotein

HETE-PL hydroxy-eicosatetraenoic acid-phospholipid

H(p)ETE-PL hydroperoxy-eicosatetraenoic acid-phospholipid

HPLC high performance liquid chromatography

HZ Hemozoin

ICAM-1 intracellular cell adhesion molecule -1

IsoP isoprostanes

LCAT lecithin-cholesterol acyl transferases

LC-MS liquid chromatography-mass spectrometry

LDL low density lipoprotein

LOX lipoxygenase

LPC lysophosphatidylcholines

MALDI matrix-assisted laser desorption ionization

MCP-1 monocyte chemoattractant protein-1

MDA malonaldehyde

MPO myeloperoxidase

MRM multiple reaction monitoring

MS mass spectrometry

MS/MS tandem mass spectrometry

NADPH nicotinamide adenine dinucleotide phosphate

NL neutral loss scanning

NMR nuclear magnetic resonance spectroscopy

NO nitric oxide

OxPL oxidised phospholipid

PAF platelet –activating factor

PAPC 1-palmitoyl-2-arachidonoyl-sn-glycerophosphatidylcholine

PC phosphatidylcholine

PE phosphatidylethanolamine

PEIPC 1-palmitoyl-2-(5-6 epoxyisoprostane E2) -sn-glycerophosphatidylcholine

PG phosphatidylglycerol

PAzPC-1-palmitoyl-2-azealoyl-sn-glycerophosphatidylcholine

PGPC 1-palmitoyl-2-glutaroyl-sn-glycerophosphatidylcholine

PLPC-1-palmitoyl-2-lineoyl-sn-glycerophosphatidylcholine

POVPC 1-palmitoyl-2-oxo-valeroyl-sn-glycerophosphatidylcholine

PONPC-1-palmitoyl-2-oxo-nonanoyl-sn-glycerophosphatidylcholine

PI phosphatidylinositol

PIS precursor ion scanning

PL phospholipids

PLA2 phospholipase A2

PS phosphatidylserine

PUFA poly-unsaturated fatty acids

QLIT quadrupole linear ion trap

QqQ triple quadrupole

QqTOF quadrupole time-of-flight

RB- Residual bodies

RBC-Red blood cells

ROS reactive oxygen species

RNS reactive nitrogen species

SH- Schizonts

SLPC-1-stearoyl-2-lineoyl-sn-glycerophosphatidylcholine

SM Sphingomyelin

SPE solid phase extraction

SRM selected reaction monitoring

TIC- Total ion chromatogram

TLC thin layer chromatography

TAG triacylglycerol

TOF time-of-flight

UPLC ultra performance liquid chromatography

VCAM-1 vascular cell adhesion molecule-1

List of Contents

THESIS SUMMARY	I
DEDICATION	II
ACKNOWLEDGEMENTS	III
LIST OF ABBREVIATIONS	IV
1 INTRODUCTION	1
1.1 LIPIDOMICS.....	1
1.2 LIPIDS: THE ESSENTIAL METABOLITES.....	3
1.3 OXIDATIVE STRESS AND PHOSPHOLIPIDS.....	4
1.4 BIOLOGICAL ACTIVITIES OF OXIDISED PHOSPHOLIPIDS (OxPL).....	8
1.5 PHOSPHOLIPID AND OXIDISED PHOSPHOLIPID ANALYSIS BY VARIOUS METHODOLOGIES.....	10
1.5.1 <i>Non mass spectrometry (conventional) methodologies</i>	11
1.5.2 <i>Mass Spectrometry based approaches</i>	12
1.5.3 <i>Benefits of Global approach vs a Targeted approach</i>	20
1.5.4 <i>Mass Spectrometric analysis of phospholipids and their oxidised products</i>	21
1.6 DATA HANDLING AND ANALYSIS APPROACHES FOR MASS SPECTROMETRY TECHNIQUE.....	25
1.7 BASIS OF PROJECT.....	29
1.7.1 <i>Aim of the project</i>	30
2 MATERIALS AND METHODS	32
2.1 CHEMICALS AND REAGENTS FOR LIQUID CHROMATOGRAPHY – MASS SPECTROMETRY (LC-MS AND NUCLEAR MAGNETIC SPECTROSCOPY (NMR).....	32
2.1.1 <i>Chemicals</i>	32
2.1.2 <i>Reagents</i>	32
2.1.3 <i>HPLC columns</i>	32
2.2 CHEMICALS AND REAGENTS FOR FOX-2 ASSAY AND TOTAL PHOSPHOLIPID CONTENT ASSAY (AMMONIUM FERROTHIOCYANATE ASSAY AND MALACHITE GREEN ASSAY).....	33
2.3 METHODOLOGY.....	33
2.3.1 <i>Direct infusion mass spectrometry (DIMS) and Liquid chromatography mass spectrometry (LC-MS) method development</i>	33
2.3.2 <i>Non-mass spectrometric assay methods</i>	40
2.3.3 <i>Nuclear magnetic resonance spectroscopy (NMR) analysis of lipid chlorohydrins</i>	41
2.3.4 <i>Oxidised lipidome profiling of clinical samples</i>	42
3 DEVELOPMENT OF LC-MS METHODS USING TARGETED APPROACHES AND OPTIMISATION OF CHROMATOGRAPHIC SEPARATION TO PROVIDE BETTER COVERAGE OF OXIDISED LIPIDOME	44
3.1 BACKGROUND.....	44
3.2 STUDY AIM AND OBJECTIVES.....	52
3.3 RESULT.....	60
3.3.1 <i>Assessment of different methods to generate OxPL species</i>	60
.....	63
3.3.2 <i>Mass spectrometry parameters optimisation for Semi -targeted approaches</i>	68
3.3.3 <i>Assessment of different analytical approaches to determine a suitable cross validation method</i>	71
3.3.4 <i>LC-MS analysis of peroxidation products of SOPC, SLPC and SAPC treated with 10 mM AAPH</i> .	84
3.3.5 <i>Optimisation of chromatographic separation of OxPL</i>	89
3.3.6 <i>Method Validation</i>	97
3.3.7 <i>Evaluation of 2D-LCMS analysis for separation of OxPL</i>	101
3.3.8 <i>Discussion</i>	102
4 DECIPHERING THE OXIDISED LIPIDOME OF ASCITES OF LEAN AND OBESE RATS MODEL OF ACUTE PANCREATITIS	107
4.1 BACKGROUND.....	107
4.2 AIM AND OBJECTIVES.....	108
4.3 RESULTS.....	109
4.4 DISCUSSION.....	122
5 OXIDISED LIPIDOME PROFILING OF ISOLATED COMPONENTS OF RED BLOOD CELL INFECTED WITH MALARIAL PARASITE	125

5.1	BACKGROUND.....	125
5.2	AIM AND OBJECTIVES	127
5.3	RESULTS	127
5.4	DISCUSSION	136
6	OXIDISED LIPIDOME PROFILING OF PLASMA SAMPLES OF DIABETIC PATIENTS USING MASS SPECTROMETRY TECHNOLOGY: A PILOT STUDY	139
6.1	BACKGROUND.....	139
6.2	AIM AND OBJECTIVES.....	140
6.3	RESULTS	141
6.4	DISCUSSION	146
7	BIOLOGICAL EFFECTS OF ANTIFOAMING AGENTS IN RECOMBINANT PROTEIN PRODUCTION	149
7.1	BACKGROUND.....	149
7.2	STUDY GOALS	151
7.3	RESULTS	151
7.3.1	<i>Comparative Lipidomic profiling for P.Pastoris strain expressing GFP or A2aR protein.....</i>	<i>151</i>
7.4	DISCUSSION	166
8	DISCUSSION	169
9	LIST OF REFERENCES	175
1	APPENDIX 1	190
1.1	GRAPHICAL REPRESENTATION OF CHROMATOGRAPHIC PROGRAM AND SOLVENT SYSTEM USED FOR OPTIMISATION OF CHROMATOGRAPHIC SEPARATION AS DETAILED IN CHAPTER 2: SECTION 2.3.1.9.	190
1.2	GRAPHICAL REPRESENTATION OF CHROMATOGRAPHIC PROGRAM FOR EVALUATION OF CHROMATOGRAPHIC SEPARATION USING MONOLITH COLUMN WITH DIFFERENT GRADIENTS (CHAPTER 2 SECTION 2.3.1.9)	192
1.3	GRAPHICAL REPRESENTATION OF CHROMATOGRAPHIC PROGRAM FOR EVALUATION OF CHROMATOGRAPHIC SEPARATION USING 2D-LCMS TECHNOLOGY USING MONOLITH COLUMN AND HILIC COLUMN WITH SOLVENT SYSTEM A AND D (CHAPTER 2 SECTION 2.3.1.9)	193
2	APPENDIX II.....	195
2.1	FULL SPECTRA OF PRECURSOR ION SCAN FOR 184 DA OF CONTROL, UV TREATED AS WELL AS AAPH OXIDISED PHOSPHATIDYLCHOLINE MIXTURE (PC MIX).....	195
2.2	PERMISSION FOR RE-PRINTING THE FIGURE SHOWING PROTON NMR ANALYSIS OF SOPC, SLPC AND SAPC CHLOROHYDRIN SPECIES.....	198
2.3	LIQUID-CHROMATOGRAPHY MASS SPECTROMETRY (LC-MS) ANALYSIS OF CHLOROHYDRIN SPECIES FROM PC MIXTURE ON QTRAP 5500 MASS SPECTROMETER USING TARGETED APPROACHES AND CROSS VALIDATION ON QTOF MS.....	199
2.4	LIQUID-CHROMATOGRAPHY MASS SPECTROMETRY (LC-MS) ANALYSIS OF PEROXIDATION SPECIES FROM PC MIXTURE ON QTRAP 5500 MASS SPECTROMETER USING TARGETED APPROACHES AND CROSS VALIDATION ON QTOF MS.....	201
2.5	EVALUATION OF CHROMATOGRAPHIC SEPARATION OF OXIDISED PHOSPHATIDYLCHOLINES (OXPC) USING DIFFERENT CHROMATOGRAPHIC SYSTEM.....	204
2.1	EVALUATION OF FLOW RATES ON CHROMATOGRAPHIC SEPARATION OF OxPC AND SIGNAL TO NOISE RATIO	204
3	APPENDIX III	206
3.1	LIST OF PUBLICATIONS	206

List of figures

Figure 1.1: Lipidomics is a system level analysis of lipids and their interaction partners.....	2
Figure 1.2: Lipid groups of the lipidome	3
Figure 1.3: Representative chemical structure of several classes of phospholipids	4
Figure 1.4: Oxidative stress and its effect on the physiological process.....	6
Figure 1.5: Schematic representation of phospholipid oxidation.....	7
Figure 1.6: Schematic representation of quadruple MS/MS scans to elucidate structural details of lipids.....	16
Figure 3.1: Representative structures of short chain oxidation products formed by non-enzymatic oxidation of phosphatidylcholine species.....	45
Figure 3.2: Representative structures of long chain oxidation products formed by non-enzymatic oxidation of phosphatidylcholine species.....	45
Figure 3.3: Representative structures of chlorohydrin products formed by 2 electron oxidation of phosphatidylcholine species.....	46
Figure 3.4: Direct infusion mass spectrometry (DIMS) analysis of UV-A oxidation (left panel) and AAPH treated (right panel) of PC mixture using Precursor ion scan for 184 Da	62
Figure 3.5: Direct infusion mass spectrometry (DIMS) analysis of UV-A oxidation (left panel) and AAPH treatment (right panel) of PC mixture using Precursor ion scan for 184 Da	63
Figure 3.6: Direct infusion mass spectrometry (DIMS) analysis of UV-A oxidation (B) and AAPH treatment (D) of PC mixture using Neutral loss scan for 34 Da selective for hydroperoxide species (+ OOH, 32 Da).	63
Figure 3.7: PIS for 184 Da spectra by direct infusion of PC mixture and the three test samples oxidised with different concentration of HOCl (50mM, 100mM, and 150mM). A)	65
Figure 3.8: MS/MS data for PC mix chlorohydrins showing characterization by neutral loss (NL) of 36 and 38 Da, corresponding to loss of H35Cl and H37Cl respectively.	67
Figure 3.9: Direct infusion mass spectrometry (DIMS) analysis of 10 mM AAPH treated phosphatidylcholine mixture using NL 34 scan for optimisation of compound parameters.	68
Figure 3.10: Direct infusion mass spectrometry (DIMS) analysis of 10 mM AAPH treated phosphatidylcholine mixture using NL 34 scan for optimisation of compound parameters..	69
Figure 3.11: Direct infusion mass spectrometry (DIMS) analysis of 10 mM AAPH treated phosphatidylethanolamine (PE) mixture using NL 34 scan for optimisation of compound parameters..	70
Figure 3.12: Direct infusion mass spectrometry (DIMS) analysis of 10 mM AAPH treated phosphatidylserine (PS) mixture using NL 34 scan for optimisation of compound parameters..	70
Figure 3.13: Direct infusion mass spectrometry (DIMS) analysis of 10 mM AAPH treated phosphatidylcholine mixture using PIS 184 Da scan for optimisation of collision induced dissociation parameters:	71
Figure 3.14: : Direct infusion mass spectrometry (DIMS) analysis of 10 mM AAPH treated phosphatidylethanolamine (PE) mixture using NL 141 scan for optimisation of compound parameters.	72
Figure 3.15: Direct infusion mass spectrometry (DIMS) analysis of 10 mM AAPH treated phosphatidylserine (PS) mixture using NL 185 Da scan for optimisation of compound parameters..	72
Figure 3.16: ESI-MS spectra of SOPC, SLPC, and S APC showing abundant peak corresponding to their (M+H) + ions at 788.5, 786.5 and 810.5 respectively	73
Figure 3.17: MS/MS data for phospholipid chlorohydrins showing characterization by neutral loss (NL) of 36 and 38 Da, corresponding to loss of H35Cl and H37Cl respectively. Panels A & B show SOPC mono-chlorohydrin at m/z 840 and 842 respectively for the HO35Cl and HO37Cl products.....	74
Figure 3.18: MSMS fragmentation profile of SOPC mono- chlorohydrin at m/z 840.5 (A) and SLPC bis-chlorohydrin at m/z 890.5 (B).	75
Figure 3.19: 1H-NMR spectra showing the formation of chlorohydrins from SOPC (a), SLPC (b) and S APC (c).	77
Figure 3.20: ESI-MS analysis of SOPC, SLPC, and S APC chlorohydrins in negative mode using ammonium acetate buffer solvent system.	78
Figure 3.21: MS/MS fragmentation spectra of acetate adducts of SOPC, SLPC and S APC and their respective chlorohydrins in negative mode direct infusion MS.	80
Figure 3.22: LC-MS analysis of HOCl treated SOPC,SLPC and S APC samples using monolith column for chromatographic separation and NL 36, NL 38 and IDA based product ion scanning for identification of species on Absciex Qtrap 5500 mass spectrometer (N=3).....	81
Figure 3.23: Overlaid Total ion chromatogram (TIC) of PIS 184 scan (A) and NL 34 scan (B) for control (black) and oxidised S APC sample (grey).	85

Figure 3.24: LC-MS analysis of 10 mM AAPH treated SOPC,SLPC and SAPH samples using monolith column for chromatographic separation and NL 34 Da, PIS 184 Da and IDA based product ion scanning for identification of species on Absciex Qtrap 5500 mass spectrometer (N=3)..	86
Figure 3.25: Evaluation of chromatographic separation of OxPC species using several columns and solvent systems..	90
Figure 3.26: Evaluation of chromatographic separation of OxPC species using monolith column and different solvent systems..	95
Figure 3.27: Evaluation of chromatographic separation of OxPC species using monolith column solvent system A at different flow rates..	96
Figure 3.28: Evaluation of chromatographic separation of OxPC species using monolith column, solvent system A, flow rate of 50 µl/minute using different gradient program ..	96
Figure 3.29: Investigation of repeatability and reproducibility of the method by analysing quality control samples at different time points of the day and at different days (N=3)..	97
Figure 3.30: Evaluation of extraction variability by LCMS analysis of extracted and not extracted set of cocktail of equimolar amount of phospholipid species from different classes.	99
Figure 3.31: Assessment of limit of quantification and linear dynamic range of the method developed using monolith column for chromatographic separation and detection using targeted approaches and validation on QTOF 5600..	101
Figure 3.32: Evaluation of chromatographic separation of OxPC species using monolith and HILIC column alone and in combination by serial coupling and simultaneous gradient analysis.	102
Figure 4.1: Total ion chromatogram (TIC) of total lipid extract of obese and lean rat models of acute pancreatitis.	110
Figure 4.2: Representative strategy used in identification of oxidised species.	111
Figure 4.3: Differential profiling of oxidised phosphatidylcholine (OxPC) species in lean and obese rat model of acute pancreatitis.....	113
Figure 4.4: Differential profiling of oxidised phosphatidylcholine (OxPC) species in lean and obese rat model of acute pancreatitis.....	114
Figure 4.5: Comparative profiling of oxidised phosphatidylcholine (OxPC) species in lean and obese rat model of acute pancreatitis.....	115
Figure 4.6: Investigation of total phospholipid content of total lipid extract of ascites of lean and obese rats with acute pancreatitis.....	117
Figure 4.7: Comparison of several post-acquisition data processing approaches on the profile of native PC species in lean and obese rats' samples.	119
Figure 4.8: Comparison of several post-acquisition data processing approaches on the profile of short chain Ox PC species in lean and obese rats samples..	120
Figure 4.9: Comparison of several post-acquisition data processing approaches on the profile of long chain OxPC species in lean and obese rats' samples.....	121
Figure 5.1: Total ion chromatogram with averaged MS spectra from 4-10 minutes in inset for isolated components of parasitized RBCs. (A-C, Hemozoin, Schizonts and Residual bodies) and uninfected RBC's (D) showing different short chain oxidised phosphatidylcholine species profile as well as variable total phospholipid visible by different peak intensities in the region of 20-28 minutes of the chromatogram where the unmodified species elutes.....	129
Figure 5.2: Total ion chromatogram with averaged MS spectra from 18-22 minutes in inset for isolated components of parasitized RBCs. (A-C, Hemozoin, Schizonts and Residual bodies) and uninfected RBC's (D) showing different long chain oxidised phosphatidylcholine species spectral profile as well as variable total ion chromatogram by different peak intensities in the region of 18-22 minutes of the chromatogram where the long chain oxidised species elutes.....	130
Figure 5.3: Total phospholipid content of isolated components of parasitized RBC's and uninfected RBC determined by Ammonium Ferrothiocyanate assay (AFC).	131
Figure 5.4: Relative fold change analysis of abundance of unmodified PC species in isolated components of infected erythrocytes relative to uninfected RBC... ..	132
Figure 5.5: Relative fold change analysis of abundance of short chain oxidised PC species in isolated components of infected erythrocytes relative to uninfected RBC..	132
Figure 5.6: Relative fold change analysis of abundance of long chain oxidised PC species in isolated components of infected erythrocytes relative to uninfected RBC..	133

Figure 6.1: Total ion chromatogram (TIC) of neutral loss (NL) scan for 34 Da of total lipid extract of plasma of diabetic and healthy volunteers (a&b) and corresponding spectra (c &d)..	142
Figure 6.2: Total ion chromatogram (TIC) of precursor ion scan (PIS scan for 184 Da of total lipid extract of plasma of diabetic and healthy volunteers (a&b) and corresponding spectra representing the elution of short chain oxidation products (4- 14 minutes), long chain oxidation products (18-22 minutes) & native phosphatidylcholine species (22 -26 minutes) respectively ...	143
Figure 6.3: Comparative analysis of abundance of several unmodified and OxPC species a) lyso PCs b) Hydroperoxides c) short chain oxidation products d) hydroxides in lipid extracts of diabetic plasma samples (Red) and healthy volunteers (Blue) (N=14).....	144
Figure 7.1: Comparison of lipid profile of total lipid extract of P.Pastoris strain expressing GFP and A2aR membrane protein calculated using automated approach on Progenesis QI and manual XIC approach.....	152
Figure 7.2: Total ion chromatogram (TIC) of biological replicates of total lipid extract of P.pastoris strain expressing GFP protein (left panel) and A2aR membrane protein (right panel).	154
Figure 7.3: LC-MS mass spectra in the positive ion mode of PC class and PE class from <i>Pichia Pastoris</i> lipid extracts with GFP secreted membrane (left panel) and A2AR secreted membrane (right panel)..	155
Figure 7.4: The extracted ion current (XIC) obtained for ion at m/z 760.5851 (PC 34:1) of choline class (top panel) and m/z 786.6007 (PC 36:2) (bottom panel) shows variability between biological replicates thereby obscuring the subtle change in abundance due to treatment.	156
Figure 7.5: Comparison of different normalisation approaches and its effect on the profile of the representative PC and PE species and relative abundance between GFP and A2aR expressing membrane extract..	158
Figure 7.6: The effect of antifoams on total phospholipid content of P. pastoris..	158
Figure 7.7:Effect of total phospholipid content normalisation on the distribution profile of the representative PC and PE species and relative abundance between GFP and A2aR expressing membrane extract..	159
Figure 7.8: Ratiometric analysis approach to study the distribution of lipids in P.Pastoris membrane extract expressing different proteins: GFP and A2aR.....	160
Figure 7.9: Ratiometric analysis approach to study the effect of J673-A on distribution of lipids in P.Pastoris membrane extract expressing GFP proteins.....	161
Figure 7.10: Ratiometric analysis approach to study the effect of J673-A on distribution of lipids in P.Pastoris membrane extract expressing A2aR protein..	162
Figure 7.11: Ratiometric analysis approach to study the effect of P-2000 on distribution of lipids in P.Pastoris membrane extract expressing GFP proteins.	163
Figure 7.12: Ratiometric analysis approach to study the effect of P-2000 on distribution of lipids in P.Pastoris membrane extract expressing A2aR membrane proteins.	164
Figure 2.1: Direct infusion mass spectrometry of UV treated and AAPH treated PC mixture. The panel shows the different profile of oxidised phosphatidylcholine (OxPC) that are formed through UV exposure and AAPH treatment.	195
Figure 2.2: LC-MS analysis of HOCl treated PC mixture using monolith column for chromatographic separation and NL 36, NL 38 and IDA based product ion scanning for identification of species on Absciex Qtrap 5500 mass spectrometer (N=3). e.....	199
Figure 2.3: Qualitative analysis of all OxPC species identified in control and oxidised PC mixture samples by generating heat map representing colour coded abundance levels of OxPCs..	201
Figure 2.4: Extracted ion chromatogram (XIC) were generated of two representative species for each group; chain shortened products (POVPC, m/z 594.5; PONPC, m/z 650.5), long chain oxidation product (PLPC-OH, m/z 774.5; PLPC-OOH, m/z 790.5) and Native PCs (PLPC, m/z 758.5; SLPC, m/z 786.5) and overlaid to evaluate the elution profile of OxPCs using different column.	204

List of tables

Table 1-1: Specific scan modes for phospholipid classes adapted from (Spickett, Reis et al. 2011).....	21
Table 1-2: Specific ions and losses for oxidised PC adapted from (Spickett, Reis et al. 2011).....	24
Table 3.1: Summary of analytical methods and the level of information that can be obtained using different approaches.....	48
Table 3.2: List of masses of fragment ions of short chain oxidised species observed in product ion scanning.	61
Table 3.3: List of masses of fragment ions of long chain oxidised species observed in product ion scanning.	62
Table 3.4: Automated data analysis using Progenesis QI of high resolution data of chlorohydrin samples of SOPC (a), SLPC (b) and SAPC (c) respectively generated on Absciex 5600 QTOF instrument.	83
Table 3.5: Hydroperoxide quantification using FOX 2 assay. The values are mean± std. dev equivalent to mM eq. of H2O2 concentration	87
Table 3.6: Automated data analysis using Progenesis QI of high resolution data of oxidised samples of SOPC (a), SLPC (b) and SAPC (c) respectively generated on Absciex 5600 QTOF instrument.....	88
Table 3.7: Evaluation and comparison of the effect of different normalisation approaches on the calculated relative standard deviation for technical replicates (N=3)..	98
Table 3.8: Malachite green assay to determine the total phospholipid content of extracted and not-extracted samples.....	100
Table 3.9: Analytical parameters for quantification of OxPLs. Internal standard (13:0PC, 153.97pmoles) was applied on the column together with increasing concentration of calibrants. Equation for calculation was obtained using 1/x weighted linear regression.	101
Table 4-1: Holistic approach for categorising the identification process based on interpretation of MS and MS/MS spectra acquired on low resolution Qtrap 5500 and high resolution QTOF 5600 instrument.	112
Table 4-2: List of all the species identified in total lipid extract of ascites of lean and obese rats with acute pancreatitis.	116
Table 5-1: List of oxidised species of phosphatidylcholine class identified in isolated components of parasitized RBC. Samples were acquired on high resolution QTOF instrument and data mining and statistical analysis performed using Progenesis QI software.	135
Table 6-1: List of oxidised species identified in plasma samples of healthy and diabetic patients using high resolution Q-TOF mass spectrometer..	146
Table 7-1: List of all species belonging to PC, PE and PS class identified in total lipid extract of <i>P.Pastoris</i> ...	153
Table 2.1: Automated data analysis using Progenesis QI of high resolution data of chlorohydrin samples PC mixture generated on Absciex 5600 QTOF instrument.	200
Table 2.2: List of oxidised phosphatidylcholine (OxPC) species with accurate masses, experimental masses, measured retention time and molecular formula.	201
Table 2.3: Effect of flow rates on retention, sensitivity and resolution of representative oxidised species calculated by generating extracted ion chromatogram (XIC) and measuring peak area. The OxPC mixture was separated using monolith column at different flow rates and detection was performed on Q-trap mass spectrometer	205

1 Introduction

1.1 Lipidomics

The revolution that has become known as the field of ‘omics’ has allowed the detailed molecular profiling of complex biological systems to be realized. Although, lipid biochemistry was an active field of research in the 1990s, lipid research gained impetus at the dawn of the 21st century driven by technological advancement with the emergence of lipidomics (a new discipline in the omics collection, which came about mainly as a result of the advent of novel mass spectrometric techniques which have enabled a more rapid and in-depth generation of knowledge about lipid biology and the role of lipids as secondary messengers (Hans & Gross 2001, van Meer 2005, Wenk 2005). In his personal view on AOCS lipid library website, Dr William Christie claimed that the first mention of the terminology “Lipidomics” appeared in an article published in 2001, which defined ‘lipidome’ as, the complete spectrum of lipids in a tissue, organelle, or membrane. In the last decade , publications using the term lipidomics have appeared in increasing numbers (Hans & Gross 2001, Wenk 2005). Lipidomics provides analysis and characterisation of lipids on a system-level and may extend to the identification of their interaction partners. A lipidome, therefore, is the comprehensive and quantitative description of a set of lipid species, and their interaction with other biomolecules (Khalil, Hou et al. 2010, Patti, Yanes et al. 2012, Wu, Shon et al. 2014). Lipidomics could be viewed as a sub-discipline of metabolomics, which is explained in figure 1.1.

Lipidomics can be subdivided into distinct areas such as membrane, organelle, metabolism, and mediator lipidomics and can address the comprehensive quantitative description of lipid metabolism and turn over, the membrane lipid constituents, or the structural characterization and quantification of low abundant bioactive lipid species. Oxidative lipidomics is a relatively new area that represents a sub-set of lipidomics focussing on the characterisation of oxidised lipids and their role in cell signalling and pathogenesis of various diseases. The profiling of an oxidised lipidome can be used to describe the responses of biological systems to environmental or genetic modifications and is considered one of the important links between phenotype and genes (Sparvero, Amoscato et al. 2010).

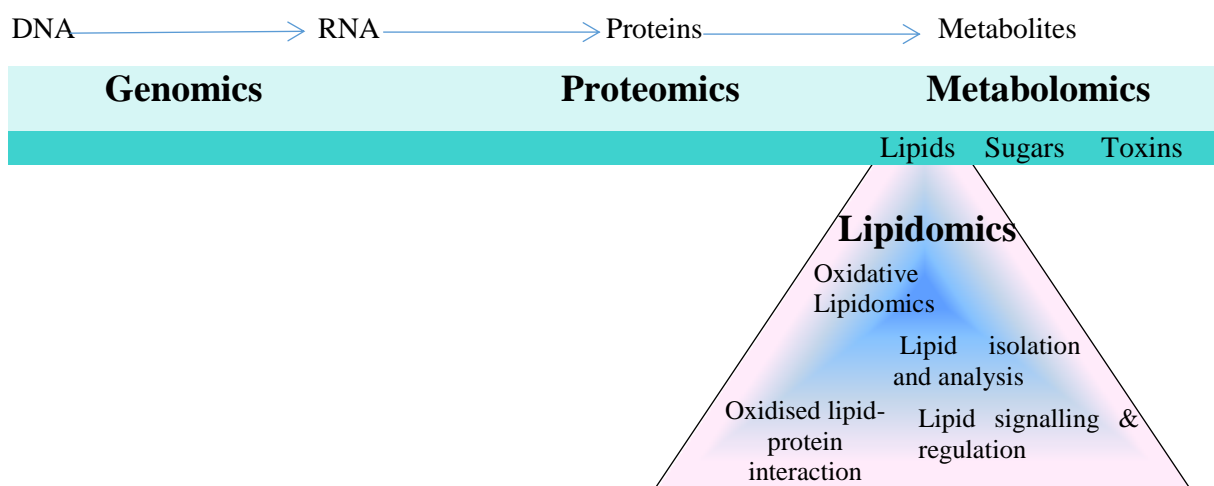


Figure 1.1: Lipidomics is a system level analysis of lipids and their interaction partners. Genes are transcribed and translated into proteins that collectively together with environmental factors; influence the metabolite inventory of a cell, tissue or body fluid. Technological advances now allow qualitative and quantitative measurements at each level on global scales (genomics, proteomics, and metabolomics). Lipidomics is a subgroup within the field of metabolomics. Adapted from (Wenk 2005).

The important role of lipids in cell, tissue and organ (patho) physiology is evident from: i) their unique membrane organizing properties, which provide cells with functionally distinct subcellular membrane compartments (e.g. endoplasmic reticulum, Golgi apparatus, secretory vesicles, plasma membrane, etc.), ii) their functional role in cell signalling (e.g. phospholipase-C and phospholipase-A2 in modulating immunological responses), iii) their endocrine actions (e.g. steroid hormones), and iv) their essential role in production and storage of energy (van Meer 2005, Blanksby and Mitchell 2010). Cells, whether bacterial, fungal or mammalian, are all equipped with metabolic pathways capable of producing a variety of structurally and functionally distinct lipid species by various non-polar fatty acid (FA) or fatty alcohol moieties with different backbone structures (i.e. glycerol phosphate and long chain sphingosine bases) and alternative head groups. In mammalian cell membranes, the total number of molecular lipid species may well be in the thousands. Although this diversity of lipids is very well appreciated and correlates with specific cellular phenomena and disease states, the molecular mechanisms that underpin the diversity are poorly understood due to limited analytical techniques that are capable of measuring the structural details of lipid species in direct comprehensive and quantitative manner. Most of the studies in the pre-2003 era investigated the mechanistic aspects of the lipid metabolism, which in turn was necessary to understand lipid biology. Post 2003, lipidomics emerged as a result of innovation in techniques such as mass spectrometry (MS), nuclear magnetic resonance spectroscopy (NMR), fluorescence spectroscopy, dual polarisation interferometry, and computational methods, coupled with the recognition of the significance of lipids in neuroscience, inflammation and in many metabolic diseases, e.g.,

obesity, atherosclerosis, stroke, hypertension, and diabetes(Sandra and Sandra 2013) (German, Gillies et al. 2007). The foremost objective of lipidomics, and its subsidiary oxidative lipidomics, is to identify the dynamic change in lipid (or oxidised lipid) composition and conformation during development of an organism or when a cell is shifted from an established physiological condition to another condition or pathological state (Spickett and Pitt 2015, Han 2016) . In addition, it includes understanding lipid modification via non-enzymatic oxidation that forms modified compounds, and their interaction with other biologically active molecules and its consequence on cellular homeostasis.

1.2 Lipids: The essential metabolites

While lipids are classified into several major classes based on their chemical composition and functionality (figure 1.2), the focus of the studies in this thesis is a single class of lipids, the phospholipids (PL), which can contain various types of glycerol-alkyl chain linkages such as ester, ether, and vinyl ether bonds, which account for the additional diversity among its class.

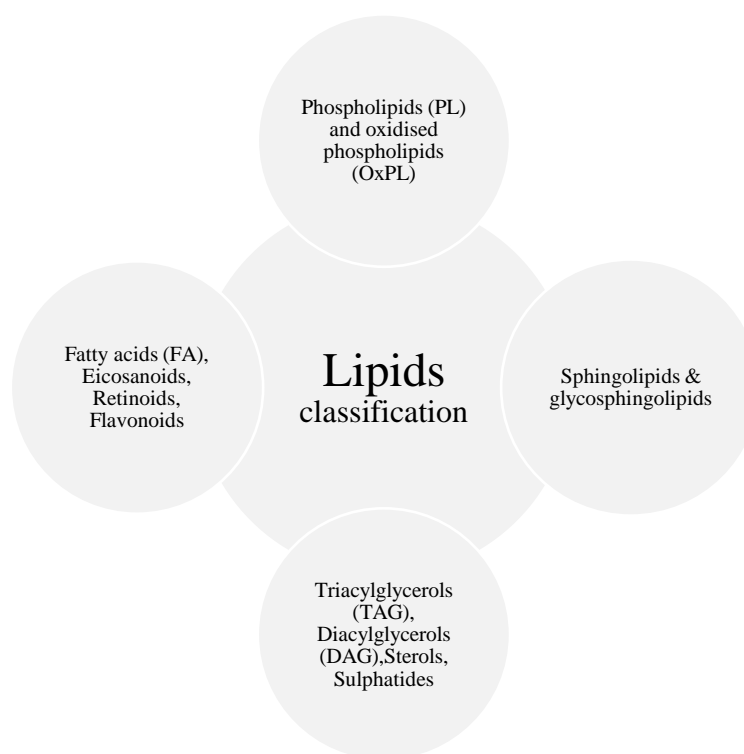


Figure 1.2: Lipid groups of the lipidome (adapted from Fahy, 2009)

The amphiphilic nature of phospholipids comes from replacing one of the fatty acids in a triacylglycerol (TAG) with a polar headgroup. Phosphatidylcholines (PC) are the most abundant phospholipid and the key membrane building block. Approximately 50% of the total phospholipid present in membranes of most animal tissues is PC, a neutral zwitterionic phospholipid, which makes up the majority of the outer leaflet of the plasma membrane (Mouritsen 2011, Subramaniam, Fahy et al. 2011). PC also serves as the biosynthetic precursor for sphingomyelin (SM), phosphatidic acid (PA), lysophosphatidylcholine (LPC), and platelet-activating factor (PAF). A variety of species of phospholipids with different physical and chemical characteristics can be formed, by altering the hydrocarbon chains and the level of saturation at the sn-1 and sn-2 position (first and second carbon position of the glycerol body), as well as the head group moiety at sn-3 chain. Phospholipids are typically classified by their head group structures, examples of which are shown in figure 1.3. The number of possible chain lengths and level of unsaturation of the fatty acids (represented by R₁ and R₂ in the table) creates a plethora of molecular species within each headgroup class. Phospholipids not only serve as components for cellular compartmentalisation but also perform diverse roles in cells from signal transduction to cytoskeleton support. Throughout this thesis, the following nomenclature is used to denote the structure of a phospholipid molecule; 16:0/18:1 PC where PC indicates the headgroup and class of phospholipid (in this case phosphatidylcholine), 16 represents the number of carbon atom fatty acyl chain linked to the glycerol body and the number 0 relates to the number of double bonds in the chain; the number 18:1 specifies the carbon chain length and the levels of unsaturation of the fatty acyl chain linked at sn-2 position.

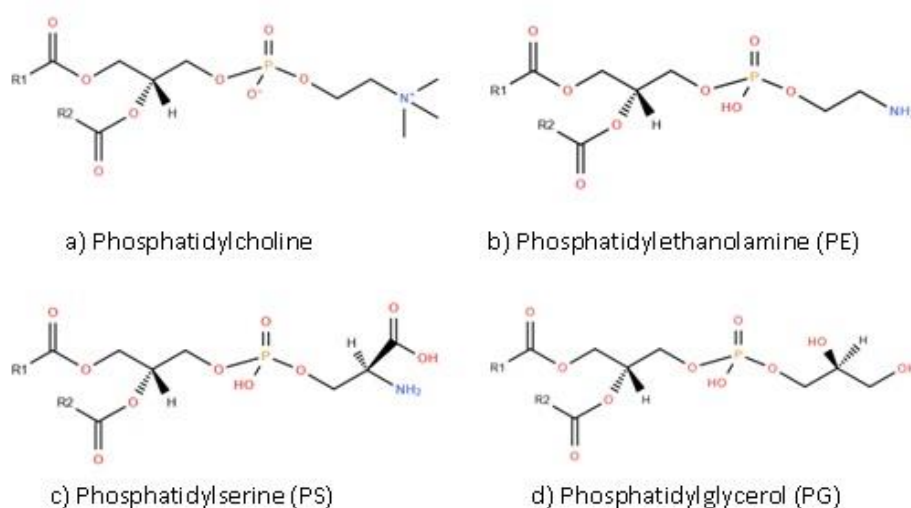


Figure 1.3: Representative chemical structure of several classes of phospholipids

1.3 Oxidative stress and phospholipids

Oxygen is an abundant molecule in biological systems (Harrison, Griending et al. 2003). Despite being a radical, it is less reactive than some other radical species because its two

unpaired electrons are in different molecular orbitals that exhibit parallel spins. Thus, oxygen undergoes univalent reduction to form superoxide ($O_2^{\bullet-}$) by means of enzymes such as the nicotinamide adenine dinucleotide (phosphate) (NADH/NAD(P)H) oxidases and xanthine oxidases (XO) (Fruhirth, Loidl et al. 2007) (Buetler, Krauskopf et al. 2004). The oxidants in aerobic systems can come from endogenous processes such as respiration, metabolism, and phagocytosis or from exogenous sources by inhalation of air pollutants and exposure to oxidants (Reis and Spickett 2012) .

Non- enzymatically, oxygen can also be converted to $O_2^{\bullet-}$ by reacting with redox active compounds such as semiubiquinone of the mitochondrial electron transport chain. Superoxide dismutase (SODs) converts superoxide radicals to hydrogen peroxide (H_2O_2) and oxygen. In biological tissues, $O_2^{\bullet-}$ can also undergo non-enzymatic transformation into H_2O_2 and singlet oxygen (1O_2). H_2O_2 can react with other radicals such as the transition metal Fe^{2+} to produce highly reactive hydroxyl radicals (OH^{\bullet}); this is known as the Fenton reaction (Bonomini, Tengattini et al. 2008). These radicals are capable of destroying biomolecules through oxidation. When Fe^{3+} initially oxidizes $O_2^{\bullet-}$, molecular oxygen and Fe^{2+} are generated; the Fe^{2+} initiates the Fenton reaction and this regenerates Fe^{3+} which perpetuates the production of OH^{\bullet} .

Myeloperoxidase, a haem protein secreted by phagocytes, can amplify the oxidative potential of H_2O_2 . At physiological concentrations of Cl^- , hypochlorous acid ($HOCl$) is the major oxidant generated by the myeloperoxidase- H_2O_2 - Cl^- system, and $HOCl$ can react with $O_2^{\bullet-}$ to produce OH^{\bullet} (Robaszekiewicz, Bartosz et al. 2014). In addition, $HOCl$ can lead to formation of chlorohydrins which are oxidised products formed independent of the free radical mechanism, and has been implicated in several inflammatory disorders and are products of $HOCl$ addition to unsaturated chain of phospholipid (Spickett 2007, Spickett and Fauzi 2011).

In response to growth factors and cytokines, and during normal metabolic turnover such as respiration and phagocytosis, eukaryotic cells produce oxidants. To regulate this, the cells have developed both enzymatic and non-enzymatic mechanisms to protect against oxidants' toxic effects. The enzymatic mechanisms include the actions of enzymes such as SOD, catalase, and glutathione peroxidase. The nonenzymatic antioxidants include glutathione, ascorbate, and α -tocopherol. However, in pathophysiological circumstances, an excess of oxidants can overcome the scavenging capacity of cellular antioxidant systems leading to the pathophysiological state termed "Oxidative stress" (Bochkov 2007, Bochkov, Oskolkova et al. 2010, Birukova, Starosta

et al. 2013) (figure 1.4). The subsequent oxidative stress damages the cell's lipids, membranes, proteins, and DNA.

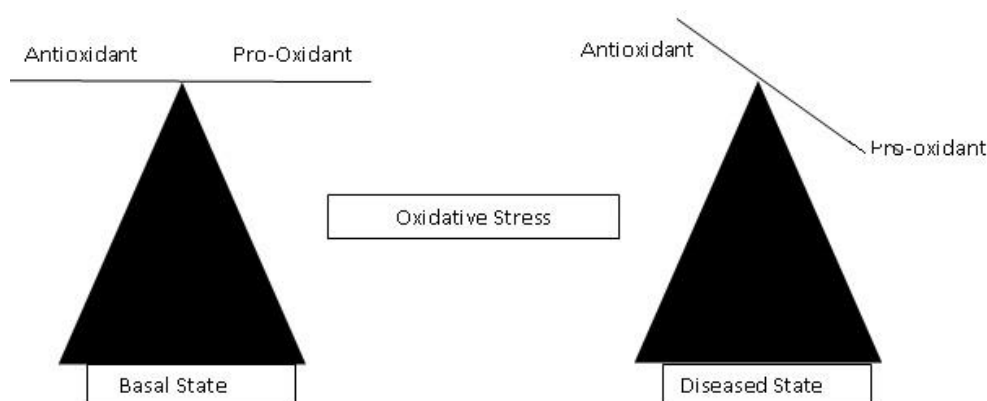


Figure 1.4: Oxidative stress and its effect on the physiological process

Enzymatic oxidation by lipoxygenases and cyclooxygenases (LOX & COX), and non-enzymatic oxidation of phospholipids (PL) containing mono- and polyunsaturated fatty acids (PUFA) can be started by reaction with free radicals or non-radical reactive oxygen species (ROS) and reactive nitrogen species (RNS) (Philippova, Resink et al. 2014) (figure 1.5). The free radical-mediated chain reaction initiated by formation of carbon centred radicals or hydroperoxides of PUFAs, i.e. the peroxidation of PUFAs, is one of the best-understood mechanisms for oxidative modification of biomolecules.

Peroxyl radicals react with bisallylic methylene groups in other PUFA molecules, leading to the transformation of peroxyl radicals to hydroperoxides and generation of new carbon-centered radicals. This initiates additional cycles of peroxidation. PUFA hydroperoxides in turn produce reactive alkoxy and hydroxyl radicals via iron or copper-catalyzed Fenton-like reactions, further propagating the chain reaction (Reis and Spickett 2012, Domingues, Reis et al. 2008). In addition to free radical mechanism, forming hydroperoxides, and hydroxides, PLs can be oxidized by a 2- electron transfer mechanism (electrophilic addition), for example by halogen compounds leading to the formation of chlorohydrins (Arnhold, Osipov et al. 2001, Spickett 2007, Davies 2011, Reis and Spickett 2012, Korotaeva, Samoiloa et al. 2013).

Non-esterified polyunsaturated fatty acids (NE-PUFA), particularly arachidonate and linoleate and PUFA linked to glycerol body as components of phospholipids, are susceptible to oxidation enzymatically. The resulting products include hydroperoxyeicosatetraenoates (H(p)ETEs-PL),

hydroperoxyoctadecadienoates (H(p)ODEs-PL), esterified to phospholipid which are formed in multiple cell types including macrophages, adipocytes, and endothelial cells (Aldrovandi and O'Donnell 2013, Volinsky and Kinnunen 2013). These products formed either enzymatically or non-enzymatically are collectively termed as primary oxidation products. LOX can also directly oxidize LDL although the mechanisms by which this occurs are not fully understood. LOX products may play a role in the beginning stages of atherosclerosis.

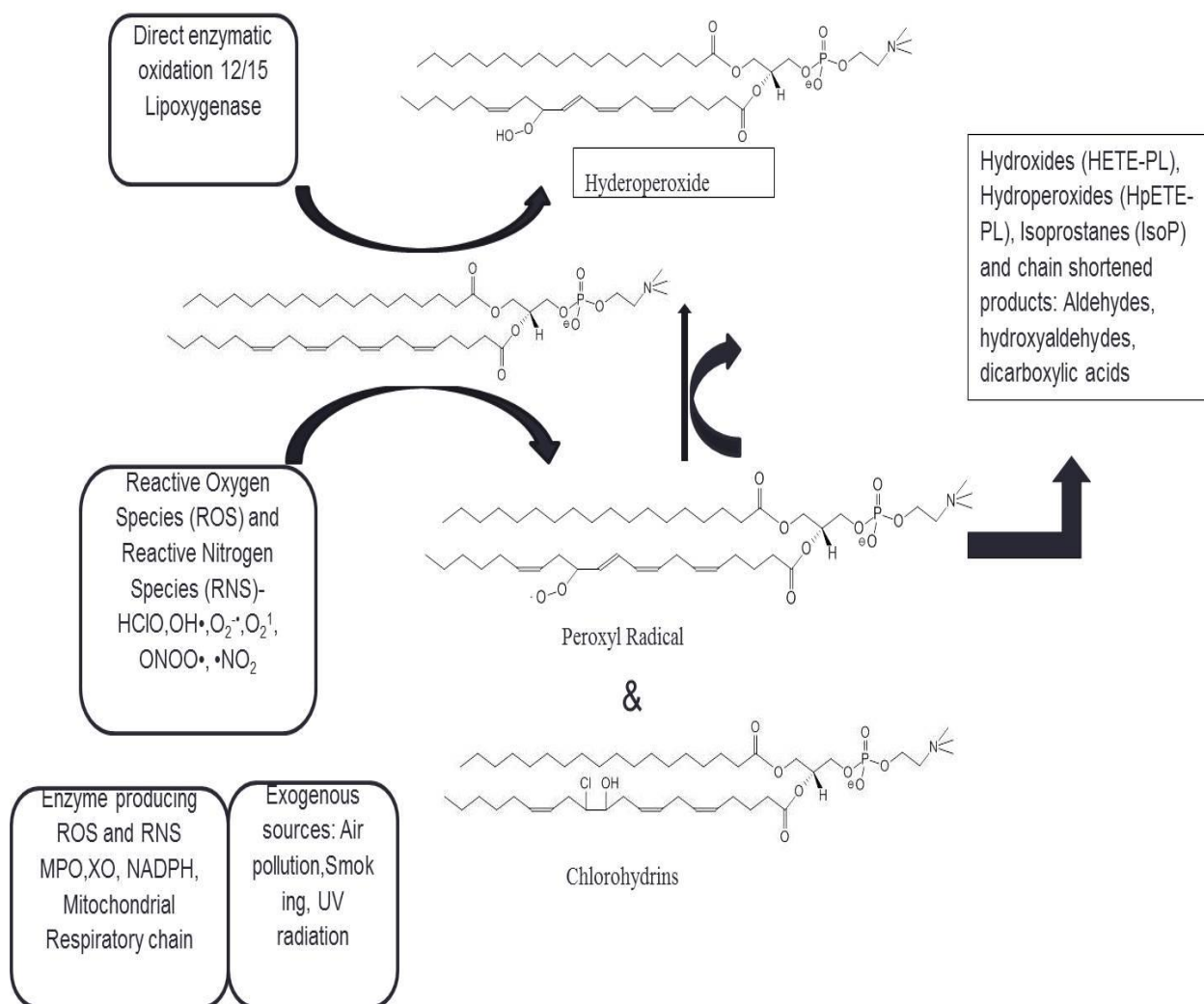


Figure 1.5: Schematic representation of phospholipid oxidation adapted from (Domingues, Reis et al. 2008, Bochkov, Oskolkova et al. 2010, Reis and Spickett 2012)

Peroxidation of PL-esterified PUFAs is initiated by formation of hydroperoxides or peroxy radicals. Further oxidation of primary PL oxidation products into secondary oxidation products proceeds non-enzymatically via three major pathways. First, additional oxidation within the same PUFA generates oxidised phospholipids (OxPLs) with various combinations of functional groups such as hydroperoxides, hydroxides, keto- and epoxy-group. The second pathway involves intramolecular cyclization, rearrangement, and further oxidation. If a bicyclic

endoperoxide is formed as an intermediate product, three groups of products are generated, including isoprostanes, isolevuglandins, and isothromboxanes, while cyclization leading to formation of monocyclic peroxide finally produces isofurans (Bochkov, Oskolkova et al. 2010, Reis and Spickett 2012). Third group of transformations results from several chemical reactions all leading to fragmentation of PUFAs and generation of short residues, having various combinations of hydroxide and carbonyl groups, or terminal furan. Oxidative fragmentation of hydroperoxides occurs via several mechanisms including β -scission, Hock rearrangement, or cyclization of alkoxy radical produced from hydroperoxide (Reis, Domingues et al. 2004, Reis, Domingues et al. 2007).

Several processes play a role in termination of peroxidation chain reaction and detoxification of reactive groups in PL-esterified PUFAs. In addition to scavenging of radicals by antioxidants such as vitamin E, reactive peroxide groups are reduced by specific form of glutathione peroxidase (GPx4) capable of reducing PL-esterified residues, as well as peroxiredoxin VI and glutathione-S- transferase (GST) (Kuhn and O'Donnell 2006). Reactive carbonyl groups in PL residues can be reduced by aldo-keto-reductases from AKR1A and B families. Furthermore, several phospholipase-A forms selectively cleave oxidized residues leading to formation of lyso-PLs and free oxidized fatty acids. Similar activity is shown by Lecithin-Cholesterol acyl transferases (LCAT). Finally, electrophilic PLs can form covalent complexes with amine containing amino acids (Schiff Base and Michael adducts), which may inactivate reactive groups on PLs but on the other hand can damage sensitive proteins (Harrison, Griendling et al. 2003, Hulsmans and Holvoet 2010, Negre-Salvayre, Auge et al. 2010, Aldrovandi and O'Donnell 2013, Volinsky and Kinnunen 2013).

1.4 Biological activities of Oxidised Phospholipids (OxPL)

Processes associated with oxidative stress can result in elevated levels of oxidatively modified or toxic molecules that can cause cellular malfunction, and even cell death. Destruction of membrane lipids by lipid peroxidation compromises the cellular membrane integrity that alters its physiological role and has been correlated with many diseases and normal ageing (Ravandi, Babaei et al. 2004, Fruhwirth, Loidl et al. 2007, Negre-Salvayre, Auge et al. 2010, Greig, Kennedy et al. 2012).

Thus, peroxidation of PL forms variety of biologically active products that can modify the endogenous structures of proteins and other lipids and possibly their function. This leads to the

generation of altered lipids as well as oxidized lipid–protein adducts, giving “modified-self molecules” or so-called “neo-self determinants” that can be recognized by specific innate and adaptive immune responses (Hulsmans and Holvoet 2010, Aldrovandi and O'Donnell 2013). Fragmented oxidised products change their conformation within the cell membrane or lipoprotein outer layer, and protrude into the aqueous phase, thus enabling recognition by cellular receptors (e.g., CD36 immunoglobulins or C- reactive protein). Furthermore, binding of OxPLs to CD36 promotes formation of foam cells characteristic of atherosclerosis (Hulsmans and Holvoet 2010). Oxidized phospholipid components of low-density lipoprotein (Ox-LDL), which are increased in human obesity, can induce endothelial cell activation and pro-atherosclerotic changes in vascular endothelial cells (Ravandi, Babaei et al. 2004, Kuhn and O'Donnell 2006, Haeggstrom and Funk 2011). In addition, it also increases expression of cell adhesion molecules and chemokines involved in monocyte and neutrophil recruitment and binding (Greig, Kennedy et al. 2012). Endothelial cell activation is a phenotypic shift characterised by expression of inflammatory mediators and cell adhesion molecules.

OxPL may lead to endothelial cell activation and formation of foam cells (Kuhn and O'Donnell 2006). Phosphatidylcholine is the most abundant phospholipid product in mammalian cells, and PC oxidation products have been widely studied. PCs that have polyunsaturated fatty acids at the sn-2 position, particularly arachidonate, are especially susceptible to oxidation, and this result in a variety of potential oxidised products. 1-palmitoyl-2-arachidonoyl-sn-glycerophosphatidylcholine (PAPC), which is a major cell membrane constituent is more susceptible to oxidative damage and its oxidation forms biologically active products including 1-palmitoyl, 2-glutaryl phosphatidylcholine (PGPC), 1-palmitoyl, 2-(5,6 epoxyisoprostane-E2),phosphatidylcholine (PEIPC), 1-palmitoyl, 2-oxo-valeroyl phosphatidylcholine (POVPC), and lysophosphatidylcholine (LPC). All of these have been shown to activate endothelial cells and are implicated in atherosclerotic progression (Birukova, Starosta et al. 2013). These same oxidised phospholipids are also deposited in atherosclerotic plaques.. PAPC, POVPC, PGPC, and PEIPC are increased 3-12 fold in circulating modified LDL, and 3-6 fold in vascular lesions in rabbits fed an atherogenic diet (Subbanagounder, Leitinger et al. 2000, Greig, Kennedy et al. 2012)

POVPC increases monocyte chemo attractant protein 1 (MCP-1) expression and monocyte binding to endothelial cell (Niki 2009). A mouse model over-expressing 12/15 LOX, which resulted in elevated production of 12(S)HETE (stereospecific hydroxide product of arachidonate), also had increased MCP-1 and ICAM expression and increased monocyte

binding to the endothelium (Steinberg 2009). PGPC induces monocyte and neutrophil binding and vascular cell adhesion molecule-1 (VCAM-1). PEIPC can cause an increase in MCP-1 in a dose dependent manner in human aortic endothelial cells (HAEC) (Bonomini, Tengattini et al. 2008). LPC also stimulates MCP-1, as well as VCAM-1 and intracellular cell adhesion molecule (ICAM-1) (Pegorier, Stengel et al. 2006). PAPC (unmodified phospholipid) alone does not induce ICAM-1, or VCAM-1, but does stimulate MCP-1 and monocyte binding (Ravandi, Babaei et al. 2004, Niki 2009).

Compare to oxPL, limited reports has been published on the effects of chlorinated lipids on inflammatory cell adhesion (Greig, Kennedy et al. 2012). Chlorohydrin species were identified in human atherosclerotic lesions that led to an increase in the expression of P-selectin on the endothelial cell surface of human coronary artery endothelial cells (HCAECs) (Panassenko, Spalteholz et al. 2003, Messner, Albert et al. 2008, Davies 2011). Sphingomyelin (SM) oxidised by HOCl has been found to activate apoptotic signaling in dopaminergic PC12 neurons by the activation of caspase-3 (Nusshold, Kollrosier et al. 2010). Phospholipid chlorohydrins also depleted ATP levels in human myeloid cells and caused a loss of viability (Dever, Stewart et al. 2003, Dever, Wainwright et al. 2006, Dever, Benson et al. 2008). Chlorinated lipids have also showed an effect on nitric Oxide (NO) bioavailability in endothelial cells (Davies 2011). Treatment with hypochlorite modified LDL of human umbilical cord endothelial cells (HUVECs) caused a decrease in synthesis of cGMP compared with native LDL (Nuszkowski, Gräbner et al. 2001).

1.5 Phospholipid and oxidised phospholipid analysis by various methodologies

By the late 1980s, technological advancements allowed development of newer methods such as electron spin resonance, nuclear magnetic resonance spectroscopy (NMR), infrared spectroscopy, X-ray scattering, differential scanning calorimetry and mass spectrometry to investigate phospholipid structure and the effect of acyl chain unsaturation and substitution position on physical properties of the phospholipid as well as higher-order structural properties. Oxidative damage of biological compounds has been linked to pathogenesis of various inflammatory disorders. Various oxidised phospholipid products have been shown to have wide variety of biological and cell signalling effects as described above, and are considered as markers of oxidative damage (Spickett 2005, Samhan-Arias, Ji et al. 2012). While utilisation of non-mass spectrometry based technologies such as NMR for lipidome analysis is gaining momentum owing to advancement in instrumentation, mass spectrometry is likely be the technology of choice owing to its simplicity in operation compared to NMR, sensitivity and

specificity. In the following section the analysis of lipidome and oxidised lipidome using non-mass spectrometry based techniques and mass spectrometry based techniques will be described.

1.5.1 Non mass spectrometry (conventional) methodologies

In order to gain further insight into the molecular mechanisms that underpin the oxidative damage of biological compounds, the application of analytical methodology capable of measuring the structural details of oxidised lipid species in a direct, comprehensive, and quantitative manner is required. Conventional analytical methods for lipid analysis such as high performance liquid chromatography (HPLC), thin-layer chromatography (TLC), and gas chromatography (GC) with non-mass spectrometry based detection system such as UV or fluorescence. Colorimetric and chemical based assays including targeted analysis using radioactively or fluorescently labelled species are only applicable for the characterization of global perturbations of lipid composition as these methods can detect only a limited number of species or provide information on the lipid class. For example, the thiobarbituric acid activated reactive substances (TBARS) assay is used to measure malodialdehyde and other phospholipid oxidation products containing two carbonyl functional groups. However, this assay is non-specific and also measures non lipid compounds containing aldehydes and thus the result does not truly reflect the extent of lipid oxidation. Various chemical assays and antibody-based assays have been developed to measure products of free radical damage in pathophysiological processes. These assays include measurement of malondialdehyde (MDA), conjugated dienes, short-chain alkanes, lipid hydroperoxides, and ELISA assays involving EO6 antibody, among others (Spickett, Wiswedel et al. 2010). The EO6 antibody is the monoclonal IgM neutral antibody that binds to oxPL as well as OxLDL and protein covalently modified by oxPL. These methods, however, suffer from inherent problems related to sensitivity or specificity, particularly when applied to in vivo situations. In general terms, the capabilities of the different technologies to analyse an oxidised molecule or a mixture of oxPL differ in the amount and type of compounds that can be analysed per run, in the quality of structural information that can be obtained, and sensitivity in measuring lowest amounts accurately in presence of signals from extraneous sources. The discussion below provides overview of non mass spectrometry based techniques used for lipid measurement.

1.5.1.1 Nuclear Magnetic Resonance Spectroscopy (NMR)

^1H or ^{13}C NMR have long been used to investigate metabolites including lipid composition as reviewed by (Emwas 2015). Proton NMR analysis provides a quick and non-destructive

technique for lipidomic analysis with the additional benefit of structural elucidation of compound although it is only used for pure lipid standard compounds or relatively simple mixture (Gross and Han 2011, Khandelwal, Stryker et al. 2014). In a traditional NMR experiment, a sample under a magnetic field is pulsed with radio frequency energy and the Fourier transform of the signals results in a spectra of chemical shift, which is dependent on nuclei environment and presence of functional groups in the vicinity. ^1H -NMR spectra are plots of intensity vs frequency, and for complex mixtures the resonance frequency of several nuclei can overlap that can make interpretation of NMR spectrum difficult. The possibilities of structural elucidation of lipid species and platform resolution have been enhanced with the development of 2D NMR due to the reduction in overlapping peaks. This is achieved by adding extra experimental variables that introduces a second dimension to the resulting spectra and collecting a series of spectra and combining data on a two frequency array representing bond connectivity of the target molecule and or combining proton NMR and ^{31}P NMR for lipidomics analysis (Mahrous, Lee et al. 2008, Clendinen, Stupp et al. 2015) (Li, Yang et al. 2014). Despite the advantages of structural elucidation offered for metabolomic analysis by 2D-NMR or interfacing NMR with chromatographic separation such as liquid chromatography, these technologies has so far not been widely adopted for the analysis of lipidome. This could be because of inherent complexity of lipid mixtures and lack of sensitivity of NMR methods compared to mass spectrometry (Willmann, Leibfritz et al. 2008, Gross and Han 2011). Moreover, liquid chromatography (LC) uses mobile phases typically water, methanol and acetonitrile in a gradient manner that can increase the spectral complexity. Alternatively, one can use fully deuterated solvents, although, this will increase the sample analysis cost owing to the large volume of solvents required for LC separation (Gonnella 2012).

1.5.2 Mass Spectrometry based approaches

Advancement in mass spectrometry technology and chromatographic separation has given an impetus to the development of mass spectrometry based approaches to decipher lipidome and oxidised lipidome in several disease models (Parsons and Spickett 2015). Mass spectrometric methods are less time consuming compared to conventional methods and require less sample amount because of its higher sensitivity and specificity. A mass spectrometer works by monitoring the defined mass range in a narrow atomic mass units (amu) window collectively termed as scanning. The defined mass range, scan speed, and sampling for each mass based on the defined amu window dictates the resolution and sensitivity that can be obtained. While the scanning routines that can be performed as well as sensitivity and resolution that can be achieved are characteristic of analyser geometry and type of mass spectrometer, each mass

spectrometer can be divided into the three major components: ion generation component, mass analyser and detection system (Sauer and Kliem 2010). In order for a molecule to enter the mass analyser and be directed to the detector, it must be first converted to the gaseous phase to obtain a charge thereby converting it to an ionised form that can be separated by mass analysers; this is a pre-requisite of detection by mass spectrometry. It is achieved in the ionisation chamber using different techniques discussed later. The following paragraphs will describe the types of ionisation method and different types of mass analysers.

1.5.2.1 Ionisation techniques

The primary aim of a mass spectrometer is the measurement of the mass to charge ratio of ions generated in the ionisation chamber either by “**Hard ionisation**” techniques such as electron impact ionisation (EI), which is mostly used with gas chromatography mass spectrometry (GCMS), or by “**soft ionisation**” techniques such as electrospray ionisation (ESI) routinely used in liquid chromatography-mass spectrometry (LCMS) based approaches (Willmann, Leibfritz et al. 2008, Sandra and Sandra 2013, Spickett and Pitt 2015). Electron impact ionisation is performed under high vacuum where the electrons emitted from a heated filament are accelerated within an electric field, more often at 70 eV within the source where the sample is introduced leading to formation of charged fragments of analytes. Electrospray ionisation (ESI) is performed at atmospheric pressure and the sample is introduced as a dispersed stream from the ESI probe and charge is imparted to small droplets formed by applying large potential difference of 3 -6 kV. The small droplets are shrunk further through the process of desolvation and high temperature thereby forming gas-phase ions that enters the mass analyser. There are several others ionisation techniques such as chemical ionisation, matrix assisted laser desorption ionisation (MALDI) and others which are of limited relevance to this work and will not be discussed here.

1.5.2.2 Mass analysers

Mass analysers are considered to be the heart of the mass spectrometer where the ionised analytes from the sample are separated based on mass to charge (m/z) ratios. The mechanism via which the separation of ionised analytes occurs in the analyser and the resolution (property of distinguishing between ions having similar masses or different masses) is dependent on the type and geometry of the analyser. **Quadrupoles** are the most common type of analysers and are composed of 4 parallel hyperbolic rods. One pair of opposite rods uses radio frequency (r.f) and the other uses direct current (d.c) to isolate the selected m/z of the analyte and maintain it on

the course to reach the detector. By ramping through different combination of r.f and d.c potential, a full spectrum scan over a mass range is possible (Finnigan 1994). **Time of flight (TOF) analysers** consist of a cylindrical flight tube of defined length maintained at high vacuum. It separates analytes of different m/z based on time taken by the ion to travel the distance across the flight tube, taking into account the principle of ion's velocity in a vacuum in proportion to the mass of ion. Unlike quadrupoles, a strictly defined period is required in TOF, meaning that ions are pulsed into the analyser with a defined timescale set by the user (Guilhaus, Selby et al. 2000). A linear TOF has limited resolution and therefore, to increase resolution reflectors are used, which reflect ions at an angle towards the detector and minimise any kinetic energy difference between ions. **Ion trap analysers (3-D IT)** consist of a cylindrical ring electrode and two end cap electrodes that trap ions within a fixed mass range in 3D space by applying an initial r.f frequency and a fixed d.c voltage. The basic mass analysis process consists of two steps that are performed consecutively in time: injection of ions into the trap by means of an ion injection pulse and a low RF at the ring electrode for trapping the ions, followed by ramping the RF voltage to eject ions consecutively with different m/z values. As too high a number of ions in the trap can adversely affect the mass resolution and accuracy, it led to the development of **2-D ion trap (2D-IT)**, more conventionally called a linear ion trap (LIT). Here, the ions oscillate up and down a linear four rod quadrupole and each end is capped with a reflector to reflect ions back down the quadrupole. To increase ion focussing, analyte ions are subjected to continual collision with helium gas to dampen the internal energy (Schwartz, Senko et al. 2002).

1.5.2.3 Tandem mass spectrometry

To increase sensitivity and resolution further as well as improving the efficiency of mass spectrometer instruments, hybrid type of instruments were developed by combining several analysers together, such as triple quadrupole analysers by serially combining three quadrupoles that can now have the capability to perform MS/MS type-scanning routines collectively defined as **tandem mass spectrometers**. MS/MS is based on the gas phase dissociation of selected ions by increasing their internal energy (Glish 2003). The most common method for activation and dissociation is **collision induced dissociation** in which the ion translational energy is partially converted into ion internal energy by acceleration and collision of the selected ion or all ions with an inert gas such as nitrogen or helium (Johnson and Carlson 2015). Several voltages are applied throughout the course of ion detection cycle that covers the ion generation in the ion source, to the path the ion travels to reach the detector, and these parameters requires optimisation to improve the signal and minimise interference from extraneous sources in all

MS/MS scanning routines. Declustering potential and collision energy (CE) are two such parameters, which are respectively the voltage applied between ion source and mass analyser transmitting ions into vacuum region to dissociate solvent clusters, and the voltage applied to give best MS/MS spectra (Sherwood, Eastham et al. 2009). MS/MS scanning routines (tandem mass spectrometry or MS/MS) on a triple quadrupole MS are the most commonly used approach in the field of targeted lipidomics. MS/MS enables structural elucidation of lipids and their oxidation products, and also increases the overall sensitivity, accuracy and reproducibility of the analysis, as the dwell time (time spent on recording the signal intensity) for the analyte of interest is increased (Schwudke, Oegema et al. 2006). The common selective MS/MS approaches used for identification of a specific group or class of molecules having structural similarity or a common characteristic are **precursor ion scanning (PIS) and neutral loss scanning (NL)** as illustrated in figure 1.6. In PIS, the first quadrupole is in the scanning mode, which scans all the parent ions that are subsequently fragmented in the second quadrupole and the third quadrupole is fixed to monitor the product ion of interest thus, enabling the identification of a class or group of compounds, which on fragmentation yields a common product ion. In the NL scanning, the first quadrupole is in the scanning mode, which scans across a pre-defined mass range of interest; parent ions are fragmented in the second quadrupole and the third quadrupole scans across the pre-defined range but with a specific mass offset that corresponds to the mass of the neutral loss of fragment of interest.

Another frequently used approach for quantification is **selected (or single) reaction monitoring (SRM)**. SRM approach exploits the fragmentation pattern of the analyte of interest and is used in conjunction with chromatographic separation. In this approach, the first quadrupole is in the non-scanning mode and is fixed for the parent ion of interest, which is fragmented in the second quadrupole and the third quadrupole is fixed for the specific product ion, corresponding to the analyte of interest. If more than one analyte is monitored simultaneously, it is called **multiple reaction monitoring (MRM)**.

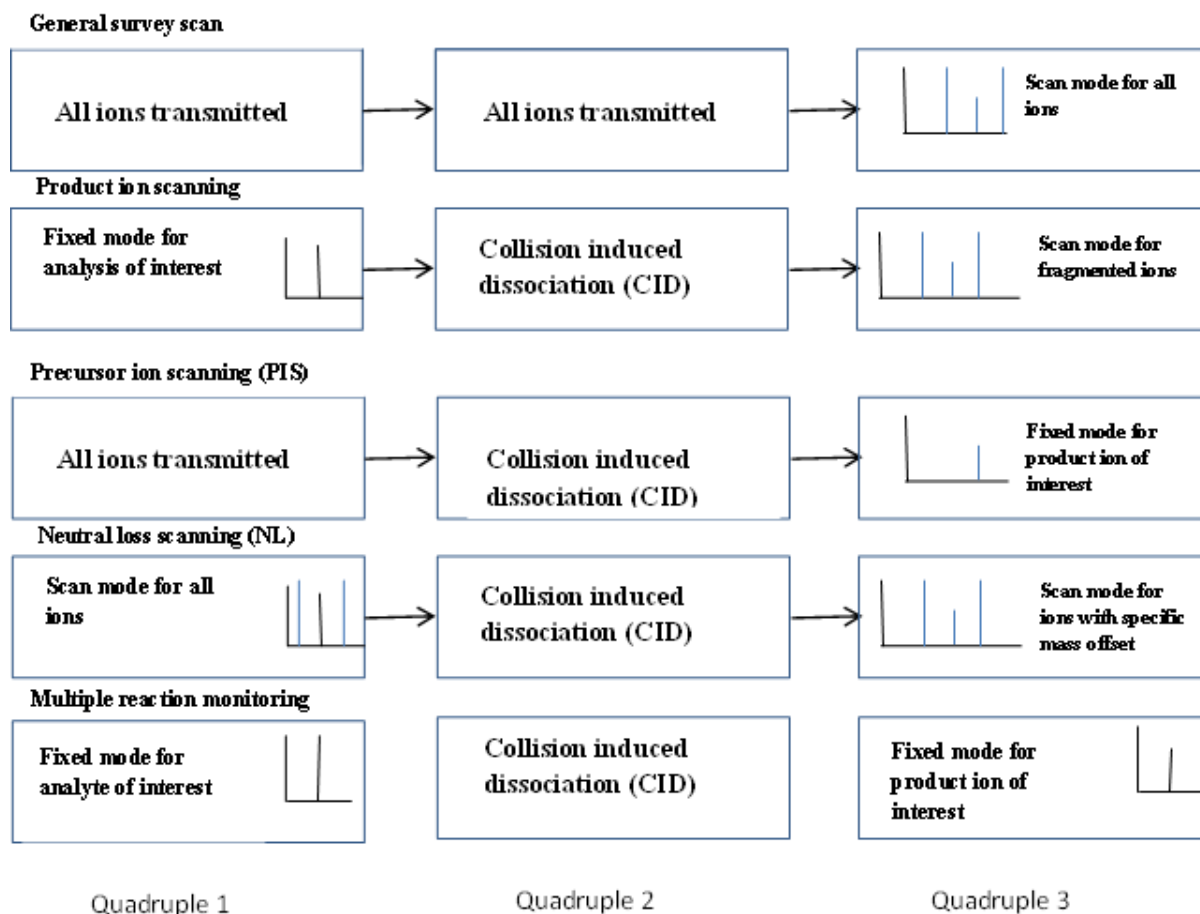


Figure 1.6: Schematic representation of quadrupole MS/MS scans to elucidate structural details of lipids. Adapted from (Blanksby and Mitchell 2010) The top panel shows the general survey scan that allows all ions within the defined mass range to be transmitted through the analysers. The second panel shows the product ion scan where a single ion is allowed through the Q1 analyser, fragmented in Q2 and all the fragments are scanned in Q3. Panel 3 shows precursor ion scan mode where the Q1 is in scanning mode, Q2 fragments all precursors and Q3 is fixed to a single mass i.e it allows only ions that give same fragment ions to pass. Panel 4 is the neutral scan where Q1 and Q3 are both in the scanning mode but with a specific mass offset corresponding to loss of neutral compound on fragmentation. Panel 5 is the multiple (single) reaction-monitoring mode where the Q1 and Q3 are fixed to detect specific precursor giving a specific fragment ion on collision with neutral gas.

In lipidomic approaches, the infusion of crude lipid extracts into the MS and the ionisation via ESI can result in mass spectra with overlapping signals from isobaric species and a high chemical noise from the matrix. Therefore, this selective MS/MS scanning routines supports the identification process, which enables distinguishing between isobaric species. The specific fragmentation pattern by collision-induced dissociation potentially allows identification of each lipid class and species with significantly reduced noise. An early study demonstrated the use of selective scanning routines on tandem mass spectrometers as a powerful tool for the analysis of phospholipids in complex lipid extracts (Brügger, Erben et al. 1997). The selective scanning approach has significantly improved the identification and quantification of modified and unmodified lipid species in both targeted and untargeted lipidomics discussed in section 1.5.3 (Zehethofer and Pinto 2008, Blanksby and Mitchell 2010). The approach used more commonly

to support the identification of the molecular species and distinguish between isobaric species is the product ion scanning. In this approach, the parent ion of interest is selected in the first quadruple, fragmented in the second quadruple, and the product ions or the fragmented pattern is measured in the third quadruple, which further confirms the identification of the molecular entity (Schwudke, Oegema et al. 2006, Zehethofer and Pinto 2008, Sherwood, Eastham et al. 2009, Blanksby and Mitchell 2010).

In the early days of lipidomics, the analysis of complex, high-molecular-weight lipids was carried out by fast atom bombardment (FAB) MS or electron ionisation (EI) MS. FAB and EI have made a major influence on lipid MS, but were limited by sensitivity issues owing to the presence of matrix ions that led to ion suppression, as well as frequent in-source fragmentation that made quantitation very difficult and erroneous. The application of ESI-MS to the analysis of lipids solved the problems of in source fragmentation. In contrast to FAB, ESI is a soft ionization technique (Glish and Vachet 2003). It creates protonated, deprotonated, or adduct ions (e.g. Na^+ , Li^+ , NH_4^+) with minimal fragmentation in source. Additionally, an ESI-MS provides better sensitivity over FAB. Therefore, ESI has given rise to two main approaches for lipid analysis, namely online high-performance liquid chromatography-mass spectrometry (LCMS) and direct infusion ESI-MS commonly referred to as shotgun lipidomics (Isaac, Jeannotte et al. 2007, Khalil, Hou et al. 2010).

1.5.2.4 Direct infusion mass spectrometry approach (shotgun lipidomics approach)

Shotgun lipidomics analysis is a very rapid method making it possible to screen 100-1000s of samples per day. In contrast to the LC-MS approach discussed in the subsequent section, in the shotgun approach the extracted lipid mixture is injected without further purification into the mass spectrometer in the shotgun approach. The terminology “shotgun lipidomics” was first used by Han and Gross in their review article on lipidomics (Han and Gross 2005) (Ekroos 2002, van Meer 2005, Wenk 2005). Later, various reports were published that introduced important innovations in the field of lipidomics. The strategy of in-source separation of different classes of molecules was explained by Hans and Gross. In this process, the environment in the ion source was modulated to favour the ionisation of a particular class/group of lipid species, thus, maximising the ionisation efficiency, which enabled the analysis of less abundant molecule species present in complex matrix by reducing the ion suppression effects of abundant molecules. The ion suppression phenomenon relates to the particular manifestation of the matrix effect, which is associated with the extent of influence on analyte ionisation and affects the detection capability. The problem of the ion suppression effect on the less abundant

molecule species is expected to be more constant. It is lipid class dependent and this effect can be corrected using class specific internal standards to attain the objective of quantification (Koivusalo, Haimi et al. 2001, Khalil, Hou et al. 2010). The parameters that can be adjusted for ion source separation to achieve optimal ionisation are polarity of the electrospray, adduct formation, pH and declustering potential (Han and Gross 2003, Han and Gross 2005, Han, Yang et al. 2006). While this strategy is useful for selective ionisation of different classes of lipids, it may not be possible to analyse very less abundant molecule species like ceramides and free fatty acids and conjugates. Hence, LC-MS based approach was the only other alternative for analyse such low abundant molecules. Alternatively, a sample preparation and enrichment steps like solid phase extraction (SPE) or off line HPLC can be added to the protocol, when using the shotgun approach (Yang, Cheng et al. 2009).

Due to inherent problems in the shotgun approach caused by lack of separation most recent studies involving mass spectrometric analysis utilise chromatographic separation. Similar to the detection method, the chromatographic method chosen influences the sensitivity and class of compounds detected. The two most common hyphenated (separation) platform used in lipid analysis are GCMS and LCMS.

1.5.2.5 Gas Chromatography Mass Spectrometry (GC-MS)

GC is an analytical technique used to separate vaporised compounds without thermal degradation of analytes of interest. GCMS utilises the hard ionisation technique: EI that fragments the molecular ion in the ion source chamber and thereby the molecular ion is hardly observed in the GCMS spectra (Carrasco-Pancorbo, Navas-Iglesias et al. 2009). Compounds are separated using an inert carrier gas such as helium as the mobile phase that flows through a stationary phase bonded to a GC column. A typical GC column is a reverse stationary phase allowing polar compounds to elute before non polar compounds. The elution is dependent upon the temperature gradient of the GC and rate of increment in temperature. The ability to selectively fragment ions and the ability to search mass spectral libraries make identification straightforward and much quicker (Roberts, McCombie et al. 2008, Griffiths, Ogundare et al. 2011). The use of GC-TOFMS compared to low resolution GC-MS increases mass accuracy and therefore confidence in metabolite identification and has been used to good effect in a number of metabolomic analyses, although, GCMS studies in lipidomics field has been limited to fatty acid, sterol and isoprostanes analysis (Navas-Iglesias, Carrasco-Pancorbo et al. 2009). A number of recent advancements have significantly improved GC-MS analysis for metabolomics including 2 dimensional GC separation and linkage to high resolution TOFMS

platforms but never attempted for lipidomics work. However, whilst GC separation is suitable for only thermostable and volatile compounds or compounds rendered thermostable and volatile through transformation by derivatisation reactions (Spickett, Wiswedel et al. 2010, Reis and Spickett 2012, Li, Yang et al. 2014, Spickett and Pitt 2015). These properties limit the analysis to a smaller selection of the molecules than some of the other techniques available. GC-MS has proved to be a reliable and sensitive method for analysis of isoprostanes that are considered as markers of oxidative stress.

1.5.2.6 Liquid chromatography mass spectrometry (LCMS)

Most of the methods developed using shotgun approach either utilise high-resolution mass spectrometers like Orbitrap or Q-TOF to overcome its limitation of overlapping signals for isobaric species thereby allowing exact lipid identification or employ MS/MS scanning routines discussed above with or without coupling chromatographic separation to ESI-MS on a low-resolution mass spectrometer. A combination of reversed phase (RP) HPLC and MS allows detailed analysis of individual molecule species with a high precision in a lipidomic approach by providing distinction (through separation) between polar and non polar species and reducing ion suppression (Mouritsen 2011, Murphy and Axelsen 2011, Sandra and Sandra 2013). Moreover, the identification of individual molecular species can be achieved by introducing the third dimension of retention factor together with m/z value and intensity, which reinforces the identification process even using the low-resolution mass spectrometer. To achieve adequate separation and retention of different lipid and oxidised lipid species, several column chemistries need to be considered as no single column chemistry is capable of covering the entire lipidome/oxidised lipidome. To date reverse phase (RP) column chemistry dominate oxidised lipidomics analysis with hydrophilic interaction liquid chromatography (HILIC) being reserved for lipidomics analysis and separation of lipidome based on lipid class.

The stationary phase of RP columns is nonpolar typically bonded C-18 alkyl chains linked to silica or hybrid hydrocarbon-silica particle. In RP based separation, the polarity of the mobile phase decreases over the LC gradient, thereby supporting separation of analytes based on hydrophobicity. Polar analytes elutes first followed by nonpolar analytes, which are retained more strongly with the non polar stationary phase. The mechanism via which HILIC column separates is opposite to the reverse phase columns although it is completely different to normal phase chromatography. Under HILIC conditions, the unbound stationary phase particle is polar and is adsorbed by the molecules of water and the polarity of the mobile phase increases over the course of the LC gradient allowing more polar compounds eluting with increased polar

mobile phase and non polar compounds eluting early in the run (Koch, Forcisi et al. 2014). Also, the compositions of mobile phases for HILIC column are more compatible with ESI-MS. The theory behind HILIC separation is thought to be based on two observed mechanism that complement each other. It has been observed that the stationary phase particle is layered with immobile water coating that may lead to liquid - liquid extraction between the water layer and the mobile phase. The other mechanism by which the separation is possible is through hydrogen bonding between analytes and immobilised water layer. .

1.5.3 Benefits of Global approach vs a Targeted approach

If the overall lipid composition of the sample is known and the objective of the research is to look at the specific class of lipid species or a pre-defined list of lipids/oxidised lipid species and to ascertain the structural details, a targeted approach using MRM is the approach to be considered. Contrary to the targeted approach, global approach is more suitable if less information is available about the overall composition of the sample as this will enable further developing the hypothesis after understanding the global perturbation on the lipid composition in the diseased state (Han and Gross 2003). Other advantage of this approach is the detection of previously unknown or poorly characterized lipids or the modified lipid species. However, absolute quantification is a challenge due to the complexity of the analysis and lack of adequate standards (Han and Gross 2003).

As mentioned earlier, a targeted approach focuses on specific lipids or lipids classes depending on the prior knowledge about the sample or diseased condition on which the objective or the hypothesis is based. The MS/MS scanning routines such as precursor ion and neutral loss scanning, can be used for semi-targeted analysis of a specific class of lipids without any prior knowledge of the exact lipid composition of the biological sample that needs to be analysed (Ejsing, Duchoslav et al. 2006, Ejsing, Sampaio et al. 2009). This selective scanning routines enables identification of a specific group or class of analytes having a specific characteristic, which increases the sensitivity of the analysis. In addition, this approach enables quantification of hundreds of lipids species with high accuracy and precision. For example, the neutral loss scan for 34 Da will enable identification of all hydroperoxides in a complex biological sample (Adachi, Yoshioka et al. 2005, Hui, Chiba et al. 2010, Reis, Domingues et al. 2013). A targeted approach can be based on either HPLC/MS or shotgun methods, which are discussed above.

1.5.4 Mass Spectrometric analysis of phospholipids and their oxidised products

Collision induced dissociation of phospholipids creates many informative fragments. Perhaps the most useful ones are those deriving from the head group (Table 1.1), since they allow one to do lipid class specific scans (Domingues, Reis et al. 2008). Phosphatidylethanolamines are characterized by loss of 141 Da corresponding to the head group (O'Donnell 2011). Fragmentation at the head group in phosphatidylserines equates to a loss of 185 Da (phosphoserine), but serine can also be lost (– 87 Da). Phosphatidylinositols are characterized by a loss of 241 Da (Spickett and Fauzi 2011).

Table 1.1: Specific scan modes for phospholipid classes adapted from (Spickett, Reis et al. 2011)

Phospholipid Class	Headgroup	Ions formed	Specific scans	Polarity
PC	Phosphocholine	(M+H) ⁺	PIS 184	Positive
PE	Phosphoethanol amine	(M+H) ⁺	NL 141	Positive
PS	Phosphoserine	(M-H) ⁻	NL 87	Negative
PI	Phosphoinositol	(M-H) ⁻	PIS 241	Negative

The most useful ones are those deriving from the head group (table 1.1); since they allow one to do phospholipid class specific scans. In addition, the fragmentations involving the fatty acid ester bond are useful as they provide information on the acyl chains either directly or indirectly based on the lyso-phospholipid fragments (Tyurina, Tyurin et al. 2009, Ozbalci, Sachsenheimer et al. 2013). It is also noteworthy that the intensities of the fragment ions can vary depending which adduct-forming ions (e.g. H⁺, Na⁺, and Li⁺) are present (Han and Gross 1994). Positional isomers are difficult to identify using mass spectrometric methods because they usually produce the same fragment ions. However, the relative abundances of the acyl chain loss ions often differ significantly and can be used for identification (Khalil, Hou et al. 2010). It has been observed that the ester bond of the sn2 fatty acid is more labile. Identification of the double bond positions in the fatty acids of lipids relies on multistage MS (MSⁿ).

PC has a constitutive positive charge at the quaternary nitrogen atom so most of studies are confined to positive ionisation mode analysis. The fragmentation pathway observed in tandem

mass spectra (MS/MS) of PC ions and their oxidised products depends on the selected precursor ion. The MS/MS mass spectra of the $(M+H)^+$ ions are simple and of easy interpretation, while the MS/MS spectra of the $(MNa)^+$ ions show higher number of product ions. The product ion spectrum of $(M+H)^+$ gives an abundant base peak ion at m/z 184.07, which is the peak characteristic of this class of molecules referring to the polar head group (O'Donnell 2011). Other peaks in the product spectra shows loss of fatty acyl chains placed at sn-1 as $(M-R_1COOH$ and $M-R_1C=O)$ and sn-2 position as $(M-R_2COOH$ and $M-R_2C=O)$. The MS/MS spectrum of $(MNa)^+$ shows loss of trimethylamine (59 Da), loss of polar head group (-183 Da), loss of sodiated polar head group (-205 Da), loss of fatty acyl group at sn-1 and sn-2 position as neutral loss of fatty acid and sodiated adduct and the product ion at m/z 147 Da (cyclophosphane group) and acyl product ions (R_1CO^+ and R_2CO^+) (O'Donnell 2011, Reis and Spickett 2012).

However, PC analysis in negative mode provides more information about the fatty acid moieties esterified to the glycerol backbone and is performed using a solvent system containing acetate or formate salts, which gives $(M+Acetate)^-$ or $(M+formate)^-$ ions that on fragmentation gives $(M-CH_3)^-$ ions (Zhang and Salomon 2005, Zhang and Reid 2006). The MS/MS spectra in negative mode provides more information on the fatty acyl chains linked at sn-1 and sn-2 position, although further information regarding the double bond position requires MS^n fragmentation at the expense of sensitivity.

Long chain oxidation products include products resulting from insertion of oxygen atoms or hypohalous acids (HOCl) molecules, giving products with higher molecular weight such as hydroxyl, epoxy, keto, hydroperoxy, polyhydroperoxy and chlorohydrin derivatives (Tyurina, Tyurin et al. 2009, Uppu, Murthy et al. 2010, Spickett and Fauzi 2011, Uchikata, Matsubara et al. 2012). Hydroperoxides of PC are observed based on increment of 32 Da to the mass of the unmodified PC (Spickett, Rennie et al. 2001, Spickett 2005). Main product ions observed correspond to loss of neutral molecule of the polar head (183 Da), confirming that the oxidation product is of PC class. Loss of the fatty acids at the sn-1 and sn-2 positions, forming lysophosphocholines (LPC) ions, allowed identification of the fatty acyl chain that undergoes oxidative modifications (Reis, Domingues et al. 2004, Reis, Domingues et al. 2007). Other fragment ions, not observed in tandem mass spectra of unmodified PC, such as loss of water ($-H_2O$, -18 Da), loss of hydrogen peroxide ($-H_2O_2$, -34 Da) or combined loss of two or three water molecules (-2 or $3 H_2O$, -36 or 48 Da), have been used to infer the presence of hydroxyl, peroxy, and di-hydroxyl or poly-hydroxyl groups on oxidized phosphatidylcholines. Neutral loss scanning of 34 Da is a typical scan for PC hydroperoxides formed during photooxidation of

unsaturated phosphatidylcholine species of fibroblasts (Murphy and Axelsen 2011). Other ions which are observed in the MS/MS spectra is because of charge remote fragmentation of the C-C α -bond near the functional group i.e fragmentation near oxidation position of the fatty acyl chain away from the head group (Domingues, Reis et al. 2008). Recent studies on human atherosclerotic tissue have identified a wider range of oxidized phosphocholines (Ravandi, Babaei et al. 2004). These researchers were able to detect hydroperoxides (C34:2-OOH, m/z 790; C36:2-OOH, m/z 818) and hydroxides (C34:2- 2xOH, m/z 790; C36:2 -OH, m/z 802; C36:4 -2xOH, m/z 814) of PC species that he correlated with different stages of atherosclerotic plaque.

More than a decade ago, Watson et al. first identified three oxidation products of PAPC using ESI-MS at m/z 594, 610 and 828 corresponding to POVPC, PGPC and PEIPC respectively (Greig, Kennedy et al. 2012). Short chain oxidised products of PC were observed in MS/MS spectra in positive and negative mode. However, most of the published work used the ion at m/z 184 for (M+H)⁺ as means of identifying PC class. Other product ions are formed because of cleavage near the terminal group of the short fatty acyl chain. This includes cleavage of the γ bond near the carboxylic acid and α bond near the aldehyde group. The presence of aldehydic and carboxylic acids with hydroxy and keto groups increases the fragmentation observed in ESI tandem mass spectra (Reis, Domingues et al. 2004, Reis and Spickett 2012). This allowed identification of product ions resulting from cleavage of the α -bond near the hydroxy and of the γ -bond near the keto group, and recognition of the substituted carbon atom in the modified acyl chain (Zehethofer and Pinto 2008). In oxPC with a terminal carboxylic group, the MS/MS spectrum show a loss of acyl residue with 14 Da increment in negative mode, which suggests the transfer of a methyl group from the trimethylamine to the COO⁻ group (Domingues, Reis et al. 2008).

Fewer studies have been reported concerning the characterisation of chlorinated PCs formed under oxidative conditions. Analysis of chlorinated fatty acids in free form and bounded with phospholipids was carried out using GC-MS by Winterbourn et.al in 1992 (Winterbourn, van den Berg et al. 1992). Schiller et.al attempted to profile the lipids in LDL and HDL using MALDI-TOF MS and compared the results with ³¹P-NMR (Schiller, Zschornig et al. 2001). While lysophosphocholine were detected with both methods, chlorohydrins of phospholipids were not detected with MALDI-TOF MS. Long chain oxPCs are formed in presence of HOCl, which are identified based on the observation of increment in mass of 52 Da for monochlorohydrin. PC with more than 1 double bond, when oxidised with HOCl, shows

mono, bis, tris and tetrakis chlorohydrins with increment of 52 Da, 104 Da, 156 Da and 208 Da (Arnhold, Osipov et al. 2001, Spickett and Fauzi 2011). The chloride atoms $^{35}\text{Cl}^-$ and $^{37}\text{Cl}^-$ occurs in nature at ratio of 3:1, which led to development of specific neutral loss scanning routines for analysis of chlorinated products in biological samples. Myeloperoxidase-derived HOCl reacts with the vinyl ether bond of plasmalogens yielding α -chlorofatty aldehydes. The α -chlorofatty aldehyde 2-chlorohexadecanal (2-ClHDA) was quantified after conversion to its pentafluorobenzyl oxime derivative using gas chromatography-mass spectrometry and negative-ion chemical ionization detection (Wacker, Albert et al. 2013). In addition, selective scanning routines like neutral loss scans have been established for identification of oxidised and chlorinated PCs as detailed in table 1.2.

Table 1.2: Specific ions and losses for oxidised PC adapted from (Spickett, Reis et al. 2011)

Headgroup	Positive mode	Negative mode
Hydroperoxide	Neutral loss of 34 Da	Neutral loss of 34 Da
Chlorohydrin	Neutral loss of 36 and 38 Da*	Neutral loss of 36 and 38 Da*
POVPC	Neutral loss 98 Da	Neutral loss 98 Da
PGPC	Neutral loss 114 Da	Neutral loss 114 Da
PONPC	Neutral loss 154 Da	Neutral loss 154 Da
PAzPC	Neutral loss 170 Da	Neutral loss 170 Da

* This is the specific and selective scan for ^{37}Cl isotope which constitute 24% of the total Cl⁻ ion.

Multiple reaction monitoring (MRM) which is the most sensitive and quantitative MS/MS scanning routine was used to detect 39 different oxylipins (epoxy eicosatrienoic, oxo- and hydroxy-eicosatetraenoic (HETE-PC) and octadecenoic acids HODE-PC) generated by the action of cyclooxygenase, lipoxygenase and cytochrome P450 enzymes (Morgan, Hammond et al. 2010). Using Qtrap 4000 instrument, a series of HETE-PC were identified by performing MRM scanning in negative mode. More recently a fingerprinting protocol using SRM approach and chromatographic separation using a core shell kinetex column was developed to profile oxidised phosphatidylcholines in UV treated fibroblast (Gruber, Bicker et al. 2012).

1.6 Data handling and analysis approaches for mass spectrometry technique

The (oxidised) lipidome of a biological system may include hundreds of different oxidised species that can vary in abundance by up to 6 orders of magnitude. Therefore, any valid approach to study the oxidised lipidome must be able to provide unbiased analysis that can handle this enormous diversity and multi dimensionality of the data. While the capabilities of mass spectrometry technologies to measure the lipidome is constantly evolving, data analysis approaches still requires optimisation and improvisation to enable handling of wide chemical diversity and range of concentration of all compounds present in biological samples. A necessary requirement of the approach is to interpret very large numbers of chromatographic peaks and mass spectra produced, and to make meaningful comparisons of data obtained from different instruments as well as different biological matrices.

A wide range of mass spectrometric techniques are used in lipidomics, each of them having particular advantages regarding accuracy, precision, comprehensiveness and sample throughput. While the capabilities of mass spectrometry technologies are constantly progressing, a global lipidomic analysis is still constrained by the considerable challenges of covering the wide chemical diversity and range of concentration of all lipids present in an biological sample. In fact, a combination of different technologies may always be necessary for a thorough metabolomic analysis. Based on the analytical platform and the knowledge about its limitations, it is imperative to decide on the data handling process beforehand. Parameters that dictate the accuracy and precision of the mass spectrometry measurement can be broadly categorised into instrument dependent and instrument independent. Mass accuracy is the measurement of the closeness of the measured mass to the true mass of the analyte whereas, precision is the measurement that defines closeness of agreement between the independent results obtained of achieving mass accuracy across multiple runs. An accurate and precise measurement increases the certainty of identification and reduces ambiguity of the detection and quantification process (S L R Ellison & A Williams 2012).

Instrument dependent parameters includes but are not limited to tuning and peak shape, ion abundance, resolving power and calibration. As accurate measurements are often performed in peak profile mode (continuum scanning), the centre of the peak assignment that is finding the centroid on the m/z scale should be accurately assigned, which is influenced by the peak shape, peak symmetry, ion counts unresolved interference and mechanical vibration. Tuning of the instrument that is optimisation of the ionisation conditions, ion transmission and fragmentation, which collectively increases the ion count and improve peak shape is required for accurate

assignment of peaks. Ion abundance is important in the determination of accurate mass both in terms of being too high or too low.

Resolving power of the mass analyzer that is the ability to separate two masses and is different from mass resolution that the former is the performance parameter which is set and the latter describes separation of two mass spectral peaks and is the function of both peak width and the mass being measured. In his report debating about mass resolution and accuracy, Baloch (Baloch, 2004) stated that the usual trade off to gain mass resolution is the sensitivity and it often does not seem convincing until the masses being measured becomes significant as the number of possible corresponding element formulae increases with the mass that makes the identification difficult, if not impossible. Therefore, the required resolving power must be defined by the measurement problem and the level of accuracy required to unambiguously identify the peak (Webb, Bristow et al. 2004). For example, the LTQ Orbitrap instrument has a very high mass resolution and allowed one to resolve PS and PE species that differ by 0.0726 Da (Schwudke et al., 2007). Koulman et al. (2009) were able to resolve lyso PC 18:3 from the sodiated adduct of lyso PC 16:0 that differed by 0.0024 Da using high resolution FTMS instrument.

Mass calibration is one of the most significant parameters that requires consideration in the achievement of accuracy. If the instrument is poorly calibrated then the accuracy of the measurement will be compromised even for high precision measurements. The reference compound for calibration should be selected carefully that will cover the entire mass range as well as is of similar nature to the analyte of interest.

Non-instrument dependent parameters or workflows that influence accuracy and precision of the measurement are dependent on the complexity of sample, the type of hyphenated technique used for measurement as well as the pre-processing and treatment of raw data before the statistical analysis can be performed to infer relationship and comparison (Bro and Smilde 2003). For example, in a hyphenated technique involving chromatographic separation, the signal corresponding to the analyte is transient as oppose to constant during the direct infusion mode and the residence time of the signal must be considered and instrument parameters such as scan speed of the measurement should take into account the width of the transient signal in order to improve the accuracy of measurement and quantification.

The information about the analyte of interest beforehand dictates the types of pre-processing steps involving correction of the signal. For example, in lipidomic and oxidative lipidomic studies, isotopic correction for signal overlap from analytes differing in 2 Da mass (having an extra double bond) is important for accurate quantification as baseline separation of all molecular species is rarely achieved using chromatographic system alone. Moreover, the mass spectrometric response is different for lipid homologues with varying chain length or unsaturation, which further complicates their quantitative analysis (Hans and Gross, 2006). Lipid molecules typically consist of C, H, O, P, N, and also S is present in Sulfatides. Lipids also form adducts with sodium (Na), lithium (Li) and chloride (Cl) ions. ^{13}C is the most relevant isotope for lipids, since they contain many carbons and the abundance of ^{13}C is relatively large (1.109 %) to other elements and correction for this element is sufficient to reduce experimental error to acceptable limits (Hans and Gross, 2006).

One should bear in mind that the isotopic distributions are dependent on isotope abundancies, which differs e.g. in inorganic samples, although for lipidomics studies this rarely is the case. Notably, lipidomics studies often employ specific precursor ion scans. This will introduce bias in the observed isotopic distribution, because it represents only the part of the molecule that reaches the detector. One LC run can produce hundreds or thousands of individual spectra. The goal of the data processing is to reduce complexity through peak assignment, integration and deisotoping, so that a single value (total peak area) can be assigned for each compound. The data is often preprocessed by smoothing for example, by using median or Savitzky-Golay filtering. Baseline correction can be done by modelling approaches.

Before integration, the peak positions and limits have to be known. This can be done by different filtering approaches, for example wavelets or derivatives. Peak assignment is based on mass information and can be guided by other information, like fragmentation data or LC retention times (Shrivastava and Gupta 2011, Subramaniam, Fahy et al. 2011). Good mass accuracy and high resolution obviously helps in the assignment. Deisotoping consists of 1) combining the areas of all the isotope peaks originating from the same compound, and 2) estimating the contributions of different compounds in unresolved peaks. When analyzing biological samples, the mass spectrometer often cannot resolve all the lipid peaks. In the mass spectra produced by instruments with unit resolution, the monoisotopic peak of many lipids overlaps with the second isotope peak of another lipid having one additional double bond. This kind of overlap can be readily corrected for by taking into account the isotopic distributions.

Data handling can be considered as a series of steps involving pre-processing of raw data to extract features; pre-treatment such as scaling and normalisation to address specific properties of the data; and statistical modelling to decipher the subtle biological variation from inherent variability (Yetukuri, Ekroos et al. 2008, Boccard, Veuthey et al. 2010). Data pre-processing constitutes the first step of data handling and its prime objective is to extract all the relevant information from the raw data using noise filtering, data filtering, peak picking and chromatographic alignment algorithms (Shrivastava and Gupta 2011, Subramaniam, Fahy et al. 2011).

While the pre-processing steps such as peak picking and chromatographic alignment are based on software algorithms and mathematical modelling of the chromatographic peak that are not sample specific whereas, data pre-treatment steps involving normalisation and scaling may affect the information content of the data and the appropriate approach should be used with due consideration given to the type of sample and origin (Bro and Smilde 2003, Shurubor, Paolucci et al. 2005, van den Berg, Hoefsloot et al. 2006).

Specific properties of the dataset such as technical variation can limit the interpretability of the lipidomics data, and a normalisation approach is used to remove systemic variation while preserving biological information. Normalisation approaches are often overlooked but in fact, it can have a significant impact on the outcome of the statistical analysis. Due to the large dynamic range of the lipidome each metabolite may be present at concentrations differing in orders of magnitude from each other. This means that abundant metabolites with high variance will skew the analysis of low abundance metabolites (Yetukuri, Ekroos et al. 2008). To resolve this, mass spectrometry data are generally transformed, centred and scaled. While this is very common in the field of metabolomics, surprisingly, these approaches are yet to be used in the field of lipidomics and oxidative lipidomics. The use of centering centres all variance on zero as opposed to the mean intensity. Thus, high and low abundance metabolites are treated equally with the intensity variation being the focus of the statistical analysis (Karpievitch, Taverner et al. 2009, Boccard, Veuthey et al. 2010). The most common form of scaling is a log transformation which not only reduces the impact of very high abundance compounds, but also minimises data skewing by making data normally distributed (van den Berg, Hoefsloot et al. 2006). However, this comes at the price of reduced signal to noise ratio as the noise levels are increased (van den Berg, Hoefsloot et al. 2006). In metabolomic data sets, scaling is also used to reduce the effect of varying fold changes between different metabolites. This is achieved by dividing the variable by a scaling factor and this results in an increased impact of variables with

small variation, which typically would go unnoticed as a result of a few metabolites with a large degree of variation between sample groups.

There are several statistical methods for normalisation: one of the most common is internal standard normalisation, where a known amount of internal standard having chemical similarity to the analyte of interest is added and its peak area is used as scaling factors for more efficient normalisation (Shurubor, Paolucci et al. 2005, Cao, Koulman et al. 2008). Other normalisation approaches are described below: the first is mass spectrometer total intensity normalisation (MSN) and global normalisation (GN). The first MSN normalises all mass spectral peak intensities to the sum peak intensity for the entire chromatogram, effectively giving all chromatograms a uniform sum peak intensity (Chawade, Alexandersson et al. 2014). GN on the other hand normalises to the sum peak intensity of peaks that are present in all samples in the batch with the assumption that most of the ions observed does not change between samples and filtering out outliers effect. Following this normalisation technique, the sum intensity of these common peaks is the same for each chromatogram as opposed to the total peak intensities being equal (Mizuno, Ueda et al. 2016). This eliminates the introduction of any bias due to large peaks associated with uncommon peaks such as those of native lipid species.

1.7 Basis of project

During the last decade liquid chromatography coupled to tandem MS (LC-MS/MS) has become a powerful tool for lipid species analysis. However, existing methods for the analysis of oxidised lipids, show disadvantages like time consuming LC-separation, high sample volumes (low sensitivity), or insufficient validation data. The challenge with the analysis of vast number of different lipid peroxidation products that can be formed at both primary and secondary stages is to establish correlation between concentrations of these oxidised products in biological samples to the pathological state of the disease. Moreover, most of the methods developed for analysis of chlorohydrins and hydroperoxides have used commercially available lipids as model systems. Fewer methodologies were translated to biological samples for identification of hydroperoxides and chlorohydrins. To achieve adequate separation and broad coverage of oxidised lipidome, several column chemistries need to be considered as no single column is capable of including the entire lipidome. As such, the column chemistry that allows for the detection of greatest number of lipid analytes or a combination of methods that provides broader coverage of oxidised lipidome is required.

In addition, existing methodologies while applied to oxPL generated *in-vitro* seemingly does not cover the lipidome in entirety and has limited application in measurement and quantification of oxidised and chlorinated products in biological samples. There are significant challenges to overcome to achieve a sensitive and reliable oxidised phospholipid methodology. These includes the detection of low abundance short chain oxidised species and relatively unstable hydroperoxide species, which have been shown to have different biological properties. To date, these concerns have been muted in favour of speed of analysis, with the aim of being able to run more samples in any given time. This however has the drawback in that only the most abundant species present are analysed, potentially leaving low abundant to go undetected, and thus reducing the coverage of potentially important part of the oxidised lipidome. Hence, there is a need of an improved methodology for detection and quantification of oxidised PC in biological samples, which formed the basis of my project.

1.7.1 Aim of the project

LCMS methods for lipidomic analysis is limited by factors such as long run times, limited back pressures (2000 – 4000 psi) and column particle size greater than 2 μm that all impacts the resolution and peak capacity of the chromatographic separation, meaning that the analyte species are more likely to co-elute leading to ion suppression. This PhD project aimed to develop an improved and robust LC-MS methodology for detection and quantification of wide range of oxidised phospholipids including hydroperoxide and chlorohydrins species. It aims to develop a method by exploiting the specificity and selectivity of the MS/MS scanning routines for hydroperoxides and chlorohydrins, together with the sensitivity of the scans provided by ABSciex QTrap 5500 instrument (QQLIT MS). The QQLIT instrument exhibits no new scan functions; however scan combinations of triple quadrupole mode and trap mode can be performed in the same LC-MS run leading to increased sensitivity and specificity. For example, in this project, precursor ion scan for headgroups (PIS 184 Da) was combined with neutral loss scan for hydroperoxides (NL34) and data dependent enhanced product ion scan (EPI), which utilises the ion trap to provide sensitivity thereby enhancing the structural information. This project also aimed to develop a data handling protocol to minimise any variation caused by sample handling and or normalisation bias. The project further aimed to implement the improved LCMS methodology with data handling protocol to profile oxidised phospholipid in several disease models such as ascites of lean and obese rats induced with acute pancreatitis; isolated components of red blood cells infected with malarial parasite; plasma samples of healthy and diabetic patients. The final aim was to apply the developed method to investigate

the effect of antifoaming agents used in bioreactors on lipid composition during membrane protein production using yeast expression systems.

The work to meet these aims is detailed in 5 chapters of the thesis:

Chapter 3 describes method development and validation that involved optimisation and evaluation of chromatographic separation using several reverse phase and mix mode columns in combination with various solvent systems. It involved formation of oxidised phospholipid mixtures using *invitro* models and identification and annotation based on studying fragmentation spectra, accurate masses and knowledge based on prior literature. The chapter also reports assessment of repeatability and reproducibility by calculating coefficient of variation for inter day quality control and intra-day quality control samples. The chapter further describes the assessment of two-dimensional orthogonal separation using serially coupled reverse phase and HILIC column and analysis of oxidised PC and PE analysis.

Chapter 4 describes implementing the methodology to profile oxidised phospholipids in ascites of lean and obese rat model of acute pancreatitis as well as comparison of different normalisation approaches.

Chapter 5 describes implementation of the methodology to profile oxidised phospholipids in isolated components of RBC infected with malarial parasites, followed by Chapter 6, which describes the implementation of methodology to study the levels of oxidised phosphatidylcholine species in diabetic patients relative to healthy plasma samples.

The work described in chapter 7 involved application of the sensitive lipidomics platform developed using HILIC column to investigate the effects of different antifoaming agents used in bioreactors on lipid composition during membrane protein production using yeast expression system.

2 Materials and Methods

2.1 Chemicals and reagents for liquid chromatography – mass spectrometry (LC-MS and Nuclear Magnetic Spectroscopy (NMR))

2.1.1 Chemicals

L- α phosphocholine mixture (PC mixture from egg yolk), L- α phosphatidylethanolamine mixture (PE mixture from egg yolk) and 1,2-diacyl-sn-glycero-3-phospho-L-serine mixture (PS mixture from bovine brain) was bought from Sigma-Aldrich, Dorset, UK. 2-2'-Azobis (2-methylproprionamide).2HCl (AAPH), a water soluble radical initiator and Sodium Hypochlorite solution (10 – 15 % chlorine) were obtained from Sigma-Aldrich, Dorset, UK. 1-stearoyl-2-oleoyl-sn-glycero-3-phosphocholine (SOPC), 1-stearoyl-2-linoleyl-sn-glycero-3-phosphocholine (SLPC) and 1-stearoyl-2-arachidonyl-sn-glycero-3-phosphocholine (SAPC) were procured from Avanti Polar Lipids, Inc, USA. 1-palmitoyl-2-arachidonyl-sn-glycero-3-phosphoethanolamine (PAPE), 1-O-1'-(Z)-octadecenyl-2-(5Z, 8Z, 11Z, 14Z-eicosatetraenoyl)-sn-glycero-3-phosphoethanolamine (O-18:0, 20:4 PE) and 1-palmitoyl-2-arachidonyl-sn-glycero-3-phosphoserine (PAPS) were procured from Avanti Polar Lipids, Inc, USA. 1-didecanoyl-2-tridecanoyl-sn-glycero-3-phosphoethanolamine(PE (12:0,13:0)), 1-didecanoyl-2-tridecanoyl-sn-glycero-3-phosphoserine (PS (12:0,13:0)) and 1,2-ditridecanoyl-sn-glycero-3-phosphocholine (PC(13:0,13:0)) used as internal standards and were procured from Avanti Polar Lipids, USA. 1-hexadecanoyl-2-azelaoyl-sn-glycero-3-phosphocholine (PAzPC), 1-hexadecanoyl-2-(5'-oxo-valeroyl)-sn-glycero-3-phosphocholine (POVPC) and 1-hexadecanoyl-2-(9'oxononanoyl)-sn-glycero-3-phosphocholine (PONPC) were procured from Avanti Polar Lipids, USA.

2.1.2 Reagents

Deuterated solvents for nuclear magnetic resonance spectroscopy (NMR), namely pyridine-d₅, deuterated chloride, deuterated-methanol, and chloroform, were procured from Goss Scientific, UK. All solvents (methanol, chloroform, water, tetrahydrofuran and hexane) were of HPLC grade and obtained from Thermo Fisher Scientific, UK.

2.1.3 HPLC columns

Pro-swift RP-4H (1x250mm) monolithic column was purchased from Thermo Scientific, UK for LC-MS analysis. The Luna C8 column (150mm X 1 mm), Luna C-18 column (150 X 1 mm)

and C-30 column (150 X 2.1 mm) were purchased from Phenomenex, UK. Mix – mode HILIC column (300 X 2.1 mm) was procured from HiChrom, UK.

2.2 Chemicals and reagents for FOX-2 assay and total phospholipid content assay (ammonium ferrothiocyanate assay and malachite green assay)

Xylenol orange, Hydrogen peroxide (H₂O₂), Ammonium ferrous sulphate hexahydrate ((NH₄)₂FeSO₄.6H₂O), Ferric chloride (FeCl₃.6H₂O), Ammonium molybdenum and Ammonium thiocyanate (NH₄SCN) were bought from Fisher Scientific, UK. Malachite green free base (MLG, purity > 98%) and tween 20 were procured from Sigma – Aldrich, Dorset, UK.

2.3 Methodology

2.3.1 Direct infusion mass spectrometry (DIMS) and Liquid chromatography mass spectrometry (LC-MS) method development

2.3.1.1 Preparation of Vesicles

PC, PE or PS mixture and unmodified individual species of PC, PE or PS class were pre-aliquoted as 100 µg dried weight and reconstituted in 10 µl milli-Q water to make a 10mg/ml suspension. The suspension was vortexed for 1 minute followed by sonication for 30 min. The mixture was further vortexed for 1 minute to form multilamellar lipid vesicles (Akbarzadeh, Rezaei-Sadabady et al. 2013).

2.3.1.2 Oxidative Treatments

2.3.1.2.1 Generation of peroxidation products from PC/PE or PS mixture and individual species of PC, PE or PS class.

1mg/ml lipid vesicles were prepared as described above followed by addition of 100 µl of 10 mM AAPH solution. The reaction mixture was incubated for 24 hr at 37°C. The reaction was stopped by placing the vial on ice and adding 100 µl of ice cold Methanol containing 0.005% BHT. 100 ng of PC (13:0, 13:0) or PE (12:0,13:0) or PS (12:0,13:0) was added to the mixture as internal standard and lipid extraction was carried out using modified Folch method as reported in (Reis, Rudnitskaya et al. 2013). Briefly, the extraction of lipids was performed by addition of 200 µl ice-cold methanol followed by 15 minutes sonication while maintaining cold temperature by addition of ice to the sonication bath. This is followed by addition of 400 µl of

ice cold chloroform and 15 sonication in the water bath at cold temperatures. Subsequently, 150 μ l of ultra-pure water was added and the mixture was vortexed for 2 minutes. Sample was left on ice for 10 minutes with occasional mixing. Sample was centrifuged at 2000g for 5 minutes and the upper (aqueous) phase was removed and re-extracted with addition of 400 μ l of chloroform. The upper phase was discarded and the organic phase was combined to the previous organic layer. The organic layer collected was dried under gentle stream of nitrogen and stored in -20 °C freezer until further analysis.

2.3.1.2.2 UV oxidation of PC mixture

Lipid vesicles were prepared as detailed in section 2.3.1.1 from 4 -100 μ g PC mixture vials and the suspension was transferred to 4 glass petri plates for Control, 30 minute, 60 minute and 90 minute UV treatment respectively. Since superoxide radical are formed by UV radiation which are not effective at causing hydrogen abstraction to form carbon centred radicals, 100 μ l of 10 μ M ferrous sulphate solution was added to aid in formation of carbon centred radicals (Reis & Spickett 2012) . 500 μ L of milli Q water was added to the plates and are placed under the IUUV 250 flood-curing lamp (Intertronics, UK) for specified time period and the reaction was stopped by placing the plates on ice after the UV oxidation and adding 300 μ l of Methanol with 0.005% BHT. Methanol, chloroform mixture (1:1, 200 μ l) was added and the mixture was store dried in -20o C freezer until analysis by direct infusion as detailed in section 2.2.4. The UV IUUV 250 curing lamp was switched on 10 minutes prior to the exposure of lipids and the UV dose was measured using the intensity meter which gives UV intensity values in mW/cm². The UV dose was calculated from the formula: UV Dose (mJ/cm²) = UV intensity x time (in seconds), which was 4000mJ/cm².

2.3.1.2.3 Generation of chlorohydrins products from PC/PE or PS mixture and individual species of PC, PE or PS class

Determine the concentration of sodium hypochlorite solution: The concentration of NaOCl in the stock solution was determined by Perkin-Elmer Lambda 25 UV/Vis Spectrophotometer at 292 nm ($\epsilon_{292} = 350 \text{ M}^{-1}\text{cm}^{-1}$). Briefly, serial dilutions of NaOCl were prepared in 0.1mM NaOH and the absorbance was measured at 292nm. The concentration was calculated using Beer-Lambert's equation: Concentration= Absorbance/Extinction coefficient x dilution factor.

The PC/PE/PS mixture vesicles (10mg/ml) or individual molecular species of PC,PE or PS class were treated with 150 mM of sodium hypochlorite (NaOCl) at pH 6.0 for 30 min to achieve maximum conversion of native lipid to chlorohydrin. Excess hypochlorite was removed by passing the mixture through a reverse phase C18 Sep-pak cartridge (Waters, UK) and washing with an excess of water. The column was pre-conditioned with methanol (1 ml) and equilibrated with water (2 ml) prior to loading the sample and lipids were extracted with 100% methanol (0.5 ml) and 1:1 methanol/chloroform (1.5 ml). The organic solvent was dried under nitrogen and PC mixture chlorohydrins (PC Mix-CIOH) were stored in -200 C freezer until further analysis on a mass spectrometer.

2.3.1.3 Lipid extraction after treatment

After the oxidative treatment, the oxidised PC/PE or PS mixture (OxPC or OxPE or OxPS) was supplemented with 100 ng of (13:0/13:0) PC or (12:0/13:0) PE or (12:0/13:0) PS respectively as internal standard by adding 100 µl of 1 µg/ml (13:0/13:0) PC or (12:0/13:0) PE or (12:0/13:0) PS in methanol with BHT, followed by adding 100 µl of methanol containing 0.005% BHT to make total volume of methanol as 200 µl. The mixture was sonicated for 15 minutes followed by adding 400 µl of chloroform and 150 µl LC-MS grade water. The mixture was vortexed and sonicated for 15 minutes followed by centrifugation at 14500g for 2 minutes. The top aqueous layer was collected and re-extracted with 400 µl of chloroform as above. The upper phase was discarded and both organic phases were combined, dried under nitrogen stream and stored at -70°C.

2.3.1.4 Optimisation of mass spectrometry parameters for precursor ion scans (PIS), neutral loss scans (NL) by direct infusion mass spectrometry

The instrument parameters were optimised to achieve better sensitivity and the detailed description about the method is written in section 3.3.1.2 of chapter 3.

2.3.1.5 LC-MS analysis of peroxidation and chlorohydrins products of PC, PE or PS mixture using targeted approaches on ABsciex Qtrap 5500 mass spectrometer.

PC,PE or PS mixture oxidation products were separated by reverse phase chromatography on an HPLC system (Dionex ultimate 3000 system) controlled by Chromoleon software, fitted with the Proswift RP-4H column (1mm x 250mm) kept at room temperature in the column compartment. The eluent used was (A) water with 0.1% formic acid and 5mM ammonium

formate and (B) methanol with 0.1% formic acid and 5mM ammonium formate. The run time for the entire LC-MS was 50 minutes and the chromatographic elution was programmed using Dionex chromatographic management system where the mobile phase at 0 – 4 min was fixed at isocratic hold of 70% B followed by 3 step gradient increase to 80% B at 8 minutes, 90% B at 15 and 100% B at 20 minutes. The gradient remained constant until 38 minutes and decreased back to 70%B until 50 minutes. The flow of the mobile phase was set to 50 μ l/minute. The mass spectrometry detection using targeted scanning routines was performed on an Agilent 5500 QTrap instrument and the validation of data analysis was performed on a high resolution Agilent Q-TOF instrument using accurate masses.

Eluting Oxidised PC mixture (OxPC) was detected on a Q-Trap Agilent 5500 mass spectrometer controlled with Analyst software. The targeted approaches for detection of OxPC used were Neutral loss scanning (NL) of 34 Da for mass range of 700 Da – 1000 Da and precursor ion scanning (PIS) of 184 Da for mass range 400 Da -1000 Da. For PE and PS mixture, targeted approaches for detection of OxPE and OxPS species were neutral loss scan of 141 Da and neutral loss scan of 185 Da respectively. The declustering potential was set to 50 V for all scans; collision energy for NL scan for 34 Da set to 35 eV and PIS for 184 Da scan set to 45 eV. Collision energy for NL scan for 141 Da to identify OxPE species and NL 34 scan for PE hydroperoxides were set to 32 eV and 23 eV respectively. Collision energy for NL scan for 185 Da to identify OxPS species and NL 34 scan for PS hydroperoxides were set to 35 eV and 23 eV respectively. Information dependent data acquisition (IDA) was used to collect MS/MS data based on following criteria: 1 most intense ion with +1 charge and minimum intensity of 1000 cps was chosen for analysis, using dynamic exclusion for 20 seconds after 2 occurrences and a fixed collision energy setting of 47 eV. Other source parameters were adjusted to give optimal response from the direct infusion of a dilute solution of standards.

For analysis of chlorohydrin species belonging to PC,PE and PS class; neutral scanning of 36 Da for ^{35}Cl isotope and 38 Da for ^{37}Cl isotope was performed to confirm the detection of chlorohydrins. Collision energy used for NL 36 and 38 Da respectively was optimised at 35 eV with mass range scanned from m/z 700 – 1000 and setting the resolution at Q1 and Q3 at low and unit respectively.

2.3.1.6 Data validation by LC-MS analysis of peroxidation and chlorohydrins products of PC, PE or PS mixture using high resolution TOF-MS scan on ABsciex Q-TOF 5600 mass spectrometer

For analysis of OxPC, OxPE and OxPS samples on high resolution Q-TOF mass spectrometry, similar chromatographic elution program was used and the Q-TOF MS survey scan was collected in positive mode from 400 Da – 1200 Da using high resolution and accumulation time of 250 ms. IDA was used to collect MS/MS data for 4 most intense ions with intensity greater than 200 cps, fixed collision energy of 45 eV and dynamic exclusion activated after 2 occurrences for 20 seconds. The experiment was repeated 3 times with each experiment performed in triplicates.

2.3.1.7 Manual Data analysis

Data analysis was performed manually using Peakview 2.0 software by calculating peak area through generating Extracted ion chromatograms (XIC) for individual masses of different oxidised species and native species at fixed peak width setting of 0.5 Da. The identification of the species was performed by comparing the MS/MS spectra at each m/z to the published literature as well as the MS/MS spectra of the standard preparations. The peak area was normalised using the peak area of the internal standard and the mean value of three technical replicates was calculated and used for relative quantification.

2.3.1.8 Data validation by automated data analysis on Progenesis QI

The LC-MS run acquired with the 5600 Triple TOF were loaded as .wiff files onto the software Progenesis QI for Lipidomics (Non Linear Dynamics, Newcastle upon Tyne, UK), used for the label-free quantification of phospholipids belonging to the PC,PE and PS class and the oxidation products formed via non-enzymatic oxidation of these classes. For each LC-MS run, elution profile and isotope pattern of the analysed unmodified and oxidised phospholipid classes are integrated in a 2D map where m/z is plotted against retention time. Each detected ion that produces a peak across the mass spectrum represents a feature that can be determined by the feature-finding algorithm. 2D maps generated by different LC-MS runs are then aligned for comparison so that features corresponding to the same species are assigned to each other. Finally, the abundance of a given feature is measured summing the peak intensities in the feature region and compared across multiple aligned 2D maps corresponding to different runs or samples. The alignment was performed by loading LC-MS runs corresponding to control and

in-vitro oxidised mixture of different classes in triplicates. The alignment reference was chosen by letting the software automatically assess every run in the each of the single run experiment for suitability. After manual validation of the alignments, additional vectors were added where necessary. The feature normalization was set to normalize to all compounds or set of housekeeping internal standards.

The automatic sensitivity parameter of the peak picking algorithm was set to default. The maximum allowable ion charge was set at 1. The experimental design setup was set as Between-subject Design. The identification of native and oxidised species for PC, PE and PS classes were performed manually by studying the MS/MS fragmentation spectra and observing experimental masses against theoretical masses. Furthermore, identification is confirmed by searching against the in-house built sdf database consisting of all the PC, PE and PS species from the lipidmap database and oxidised species structures drawn manually using Knowitall software (BioRad), with mass tolerance set at 5 ppm and performing theoretical fragmentation. Relative quantification and statistics is performed by the in-built feature in the Progenesis QI software. The conceptual workflow in the Progenesis QI automated data analysis is further explained in chapter 3, section 3.3.1.3.

2.3.1.9 Optimisation of chromatographic separation using several reverse phase columns and eluent systems

The steps taken to optimise chromatographic separation by modulating the mobile phases and testing several columns is detailed in methodology section 3.3.1.2 of chapter 3.

2.3.1.10 Method validation

To validate the method to confirm its suitability for application to profile the oxidised lipidome of biological samples, several approaches were considered.

1. Repeatability and reproducibility of the method: Quality control samples were prepared by in-vitro oxidation of PC, PE and PS mixture in triplicates 2.3.1.3 and the samples were analysed on Qtrap ABSciex 5500 mass spectrometer using targeted approaches and monolith column (section 2.3.1.9) for separation at different times of the day to investigate the repeatability, and on different days to assess the reproducibility. Peak area for all oxidised species and native species were calculated, normalised with the internal standard and the relative standard deviation was calculated for intraday and inter day samples.

2. Assessment of sample loss during sample preparation steps involving lipid extraction:

Two equimolar mixture of different phospholipid classes (PC, PE and PS) and commercially available oxidised phospholipid species (PAzPC, PGPC, POVPC) were prepared in triplicates and one of the set was processed through the extraction protocol 2.3.1.3 followed by preparation of samples for mass spectrometric analysis on Qtrap 5500 MS using targeted approaches with monolith column for separation and normalised peak area for different species were calculated and compared to assess the loss of individual species or cluster of species belonging to a single class during sample preparation. Subsequently, the total phospholipid content was investigated in both sets by performing phosphorous release assay involving malachite green detailed below. Briefly, the samples from each set were dried and digested by adding perchloric acid (200 μ l) and heated at 160°C for 30 minutes to release the inorganic phosphate. Subsequently, 2 ml of working solution that contains 0.4 % malachite green in water, 4.2 % ammonium molybdate in 5 M HCl and 1.5 % tween 20 was added to the sample. The absorbance reading at 660 nm was reported and the total inorganic phosphate content was extrapolated from the calibration graph prepared using potassium dihydrogen phosphate.

3. Assessment of limit of quantification and the linear dynamic range:

Different concentration of commercially available oxidised PC species (PAzPC, PONPC, POVPC and PGPC) were prepared covering the range over six orders of magnitude and analysed on Absciex Qtrap 5500 mass spectrometer using targeted approaches involving precursor ion scan for 184 Da, coupled with monolith column for separation. Subsequently, the samples were re-analysed on a high resolution Absciex 5600 Q-TOF mass spectrometer coupled to monolith column for separation, involving general TOF-MS survey scan and information dependent acquisition (IDA) based product ion scan to compare the instrument response and linear dynamic range. The normalised peak area for different concentration of PGPC, PONPC, POVPC and PAzPC were calculated and plotted against the respective concentration and linearity of the response was calculated using weighted linear regression model with residual analysis to confirm the suitability of the model.

2.3.2 Non-mass spectrometric assay methods

2.3.2.1 *Ferrous ion oxidation xylenol orange (FOX-2) assay*

Ferrous ion oxidation xylenol orange-2 (FOX-2) method of hydroperoxide estimation is based upon oxidation of Fe^{2+} to Fe^{3+} by sample oxidising agents which then binds with reagent xylenol orange (XO) to give a colour complex having absorption maximum at 560 nm as described by Wolf et al. The Fox-2 reagent was prepared as follows: 250 μM of ammonium ferrous sulphate (6.9 mg) was dissolved in 25 μM of sulphuric acid (10 ml) designated as solution B and 4.4 mM of BHT (98 mg), 100 mM xylenol orange (7.6 mg) was dissolved in 90 ml of methanol designated as solution A and 1 part of solution B was mixed 9 parts of solution A to make the working FOX-2 reagent with final concentration of ferrous sulphate as 250 mM, 25 mM of sulphuric acid and 100 mM xylenol orange. Standards were prepared using different concentrations of hydrogen peroxide (0.01 mM to 0.4 mM) from the stock 30 % hydroperoxide solution, where the concentration was pre-determined by titration with potassium permanganate. All the other reagents were at least of reagent grade. Double distilled water was used throughout the experiment. Glassware were cleaned with warm concentrated nitric acid and thoroughly rinsed with double distilled water before an experiment. A Perkin-Elmer Lambda 25 UV/Vis Spectrophotometer and 1 ml quartz cuvette were used throughout the experiment.

Aliquots of 100 μg of invitro oxidised PC, PE and PS mixture and control in 50 μl 1:1 methanol chloroform mixture were added with 950 μl of working solution of FOX 2 reagent and left to react for 30 minutes at room temperature in the dark and the absorbance of the samples were read at 560 nm against the H_2O_2 standards.

2.3.2.2 *Phosphorous release assay using malachite green*

The digestion of phospholipids followed by estimation of the released inorganic phosphorous based on interaction with phosphomolybdenum and malachite green as described by (Zhou and Arthur 1992) was used for determination of phospholipid content in *invitro* oxidised samples. A stock solution of malachite green (0.4 %) was prepared by vigorously mixing the required amount in distil water using magnetic stirrer for 30 minutes. Separately, 4.2 % of ammonium molybdate in 5 M HCl was prepared and one volume of this solution was mixed with 3 volumes of malachite green suspension. This mixture was vigorously stirred and filtered through whatman filter paper. The working solution of malachite green was prepared fresh by adding

0.045 % tween -20 to the above mentioned mixture of malachite green and ammonium molybdate with vigorous stirring for 30 minutes on a magnetic stirrer.

Dried extract of invitro oxidised samples of PC, PE and PS mixture and control samples were reacted with concentrated perchloric acid and placed on a multi block heater pre-heated to 160 °C for 30 minutes to release inorganic phosphate. The tubes were cooled down and 2ml of working solution was added to each tube and the tubes were allowed to stand for 20 minutes. Absorbance was measured at 660 nm on a Perkin- elmer lambda 25 UV/vis spectrophotometer against the standards prepared using potassium dihydrogen phosphate.

2.3.2.3 Ammonium ferrothiocyanate assay for total phospholipid content

This colorimetric assay is based on the formation of complex between phospholipids and ammonium ferrothiocyanate and was performed for determination of total phospholipids in clinical samples (Stewart 1980). Working solution was prepared by adding 2.7 g of ferric chloride and 3 g of ammonium thiocyanate in 100 ml water. Dried lipid extracts were reconstituted in 2 ml chloroform and 1 ml of working reagent is added. The samples were vortexed for 1 minute and centrifuged at 14500 g for 5 minutes and the bottom coloured layer were collected in clean glass tubes using Pasteur pipettes and the absorbance was measured at 488 nm. The concentration was determined by comparing the absorbance reading against standard phospholipid solution.

2.3.3 Nuclear magnetic resonance spectroscopy (NMR) analysis of lipid chlorohydrins

The NMR analysis was performed on 270MHz Bruker NMR instrument for only individual species of PC class. Deuterated solvent was used for chlorohydrin analysis to acquire highly resolution spectra while preventing any interference from proton coupling. The solvent system used was 1:1:2:10 mixture of pyridine-d₅: deuterated chloride in D₂O: methanol-d₄: chloroform-d adapted from (Edzes, Teerlink et al. 1992). Spectra were acquired in the Fourier transform mode with 5000 data points, 90⁰ pulses. The parameters optimised for ¹H-NMR analysis of chlorohydrins were the relaxing time, which was set to three seconds and the number of scans acquired were 5000 to achieve optimum sensitivity. The acquired NMR spectra was corrected for phase and baseline distortions by applying a simple polynomial curve fit and referenced to Trimethylsilane (TMS) peak (δ 0.0). The data analysis of chlorohydrins was

executed on Mestrenova version 1.0 software where the control and modified lipid spectra were overlaid for comparison after pre-processing the spectra.

2.3.4 Oxidised lipidome profiling of clinical samples

2.3.4.1 *Lean and obese rat model of acute pancreatitis*

The ascites of lean and obese rat (7 each) induced with acute pancreatitis were received from University of Valencia, Spain and stored in – 80 °C. Total lipids were extracted using modified Folch method as described in section 1.3.1.3 from 500 µl of ascites of lean and obese rats and the dried lipid extracts were reconstituted in 1:1 methanol: chloroform mixture before preparing 5-fold dilution with starting solvent (70% Methanol with 5mM ammonium formate and 0.1 % formic acid) and analysis was performed on Qtrap 5500 followed by Q-TOF MS using monolith column for separation. Manual data analysis was performed on data generated on low resolution Absciex Qtrap 5500 MS using targeted approaches for PC, PE and PS class oxidation products and data validation was performed on high resolution QTOF ABsciex 5600 MS with automated data analysis using Progenesis QI for lipidomics software.

2.3.4.2 *Isolated components of malarial parasite*

The isolated components of malarial parasite (hemozoin, residual bodies, mature Schizonts & uninfected RBC) were received from University of Turin, Italy and stored in – 80 °C. Total lipids were extracted using modified Folch method as described in section 1.3.1.3 from 40 µl of each sample and the dried lipid extracts were reconstituted in 1:1 methanol: chloroform mixture before preparing 5-fold dilution with starting solvent (70% Methanol with 5mM ammonium formate and 0.1 % formic acid) and analysis manual data was performed for data generated on Qtrap 5500 followed by cross validation analysis of data generated on Q-TOF MS using monolith column for separation. Manual data analysis was performed using peakview software and calculating peak area of each identified species by generating XIC with peak width set at 0.5 Da as detailed in section 2.3.1.7. Cross data validation was performed with automated data analysis using Progenesis QI for lipidomics software as detailed in section 2.3.1.8.

2.3.4.3 Diabetic plasma samples

This work was done in collaboration with Dr James Brown group at Aston University who provided us the plasma samples of healthy and diabetic patients. The plasma samples of diabetic patients (N=7) and healthy volunteers (N=7) were collected after Aston University ethics committee approval by Dr Brown research group. Plasma sample (40 μ l) was used for lipid extraction using the method described in section 2.3.1.1 using 100 ng of (13:0/13:0) PC as internal standard. The dried lipid extract was reconstituted in 1:1 methanol:chloroform mixture before preparing 10-fold dilution with starting solvent (70% Methanol with 5mM ammonium formate and 0.1 % formic acid) and analysis was performed on Qtrap 5500 for PC, PE and PS class oxidation products followed by cross validation of data acquisition and analysis using Q-TOF MS and monolith column for chromatographic separation. Manual data analysis was performed on data generated on low resolution Absciex Qtrap 5500 MS using targeted approaches and data validation was performed on high resolution QTOF ABsciex 5600 MS with automated data analysis using Progenesis QI for lipidomics software as detailed in section 2.3.1.7 and 2.3.1.8.

2.3.4.4 Lipidomic analysis of total lipid extract of yeast expressing recombinant protein treated with different concentration of antifoaming agents.

This work was done in collaboration with Prof Roslyn Bill group at Aston University who provided us the total lipid extract of yeast producing different proteins treated with different concentration of antifoaming agents.

Two different antifoaming agents: P-2000 and J673-A at 0.5 % and 1 % concentration were investigated for the effect on lipid composition of the *P.Pastoris* strain producing GFP protein and A2aR membrane protein. The dried lipid extract was reconstituted in 1:1 methanol:chloroform mixture before preparing 10-fold dilution with starting solvent (70% Methanol with 5mM ammonium formate and 0.1 % formic acid) and analysis was performed on QTOF 5600 for species PC, PE and PS class using HILIC column and solvent system D for chromatographic separation as detailed in 2.3.1.6 and 2.3.1. 9 section. Manual data analysis was performed on data generated on high resolution QTOF ABsciex 5600 MS using targeted approaches and data validation was performed with automated data analysis using Progenesis QI for lipidomics software as detailed in section 2.3.1.7 and 2.3.1.8.

3 Development of LC-MS methods using targeted approaches and optimisation of chromatographic separation to provide better coverage of oxidised lipidome

3.1 Background

Global oxidised lipidome analysis of biological samples offers great potential for detection of biomarkers of disease. A single species belonging to the glycerophospholipid group bearing an unsaturated fatty acyl chain can give rise to over 50 different modified species. The species formed through oxidation can further be categorised based on the nature of oxidant, extent of oxidation and concentration of oxidant and other aiding compounds (Reis and Spickett 2012). For instance, oxidation through the action of myeloperoxidase in presence of chloride ions will predominantly give rise to **chlorohydrin** species (Jerlich, Pitt et al. 2000, Arnhold, Osipov et al. 2001), whereas oxidation through Fenton type reaction will form peroxidation species that can be grouped or classified into “**long chain oxidation products**” (where the mass of the modified compound is greater than the parent mass depending on the number of oxygen atoms attached to the species) and “**short chain oxidation products**” (formed after oxidative cleavage of long chain oxidation products) (Arnhold, Osipov et al. 2001, Dever, Benson et al. 2008, Gruber, Bicker et al. 2012). Examples of these oxidised and chlorohydrin species are shown in figure 3.1, 3.2 and 3.3 respectively. The nomenclature was established with the terminology in the parentheses corresponded to the aldehyde or carboxylate bearing truncated acyl chain at sn-2 position followed by the first letter of the fatty acyl chain linked at sn-1 position and last 2 letters belonged to the phospholipid class. For instance, the (oxonanonyl) SPC corresponds to the stearyl fatty acyl chain bearing phosphatidylcholine class species with nine carbon terminal aldehyde chain at sn-2 position.

Similarly, for long chain species the nomenclature system was established as follows: the first two letters corresponded to the fatty acyl chain linked at sn-1 and sn-2 positions followed by the class specific information. Based on level of oxidation and type of oxidised species the name of the species was associated with OOH, OH, O or ClOH that corresponded to hydroperoxide, hydroxide, keto or chlorohydrin species respectively, with di, tri or tetra as prefix to define the level of oxidation.

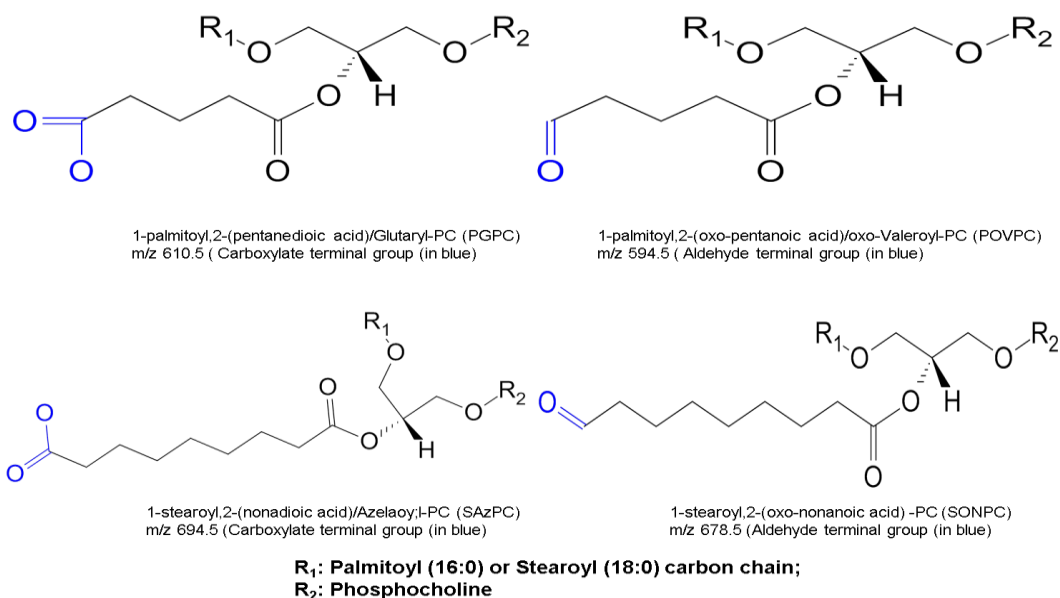


Figure 3.1: Representative structures of short chain oxidation products formed by non-enzymatic oxidation of phosphatidylcholine species

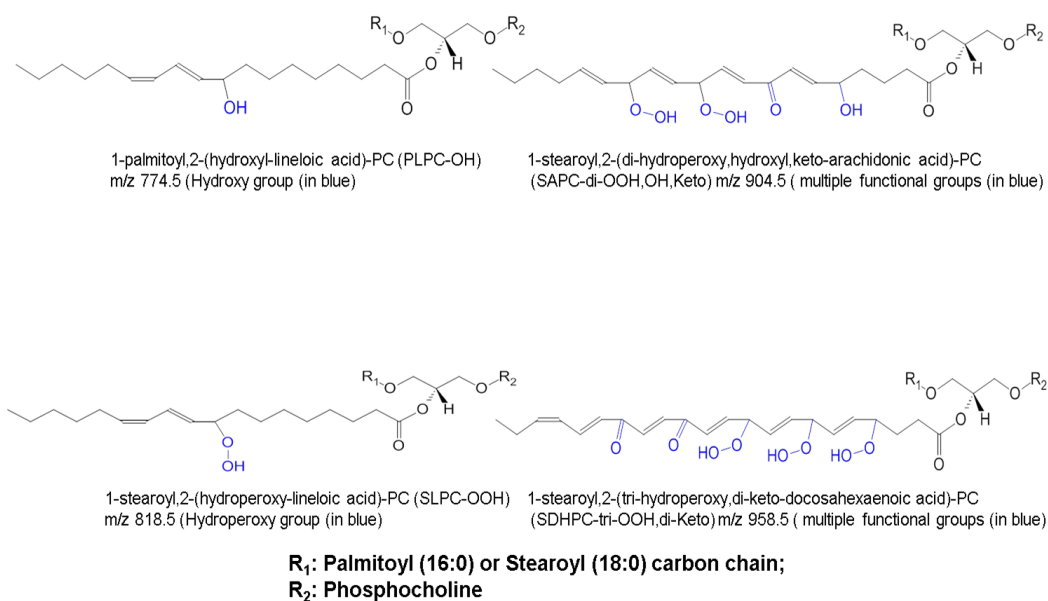


Figure 3.2: Representative structures of long chain oxidation products formed by non-enzymatic oxidation of phosphatidylcholine species

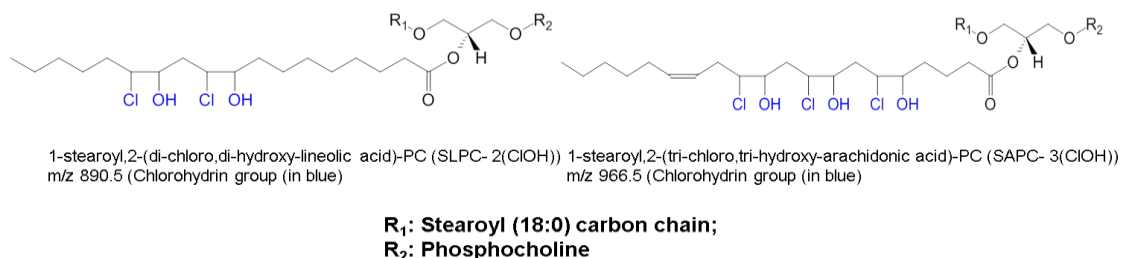


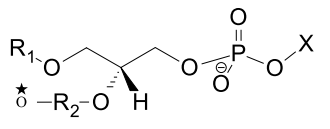
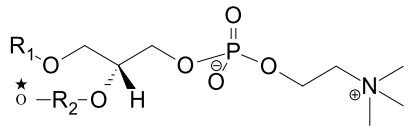
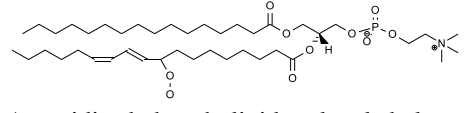
Figure 3.3: Representative structures of chlorohydrin products formed by 2 electron oxidation of phosphatidylcholine species

In lieu of the extreme diversity of phospholipid species due to the fact that more than 1000 of species that can be formed by combination of different headgroups and fatty acyl chains, the number of oxidised species that are generated in response to reactive oxygen species can be overwhelming. In addition, they can exist as many different derivatives and isomers *in vivo*. This can lead to formation of hundreds of different modified species from the lipidome of mammalian membrane, adding to the complexity and difficulty in characterisation and quantification of these species in biological samples (Nakanishi, Iida et al. 2009). These oxidised phospholipid species (OxPL) can have non- identical biological activities (Bochkov, Oskolkova et al. 2010, Aldrovandi and O'Donnell 2013, Spickett and Pitt 2015). To understand the biological importance of oxidised phospholipids (OxPL) along with their role as a disease biomarker, information on the precise concentration of all oxidised species in biological samples must be obtained (Gruber, Bicker et al. 2012). Moreover, it is important to measure simultaneously all long chain oxidation products including hydroperoxides and hydroxides, and short chain oxidation products including saturated and unsaturated aldehydes and di-carboxylic acids derivatives. This is required to investigate the dynamic assessment of oxidised phospholipids in a disease state, and to examine their relevance to function and disease *in-vivo* (Uchikata, Matsubara et al. 2012).

The analytical technologies to measure the abundance and identification of oxPL species have evolved over the years. In the pre- 2000 era, methods involving mass spectrometry measurements were limited and general methodology to analyse oxPL species were used such as UV spectrophotometric assays & fluorescence based assays like FOX2 assay, isoluminol assay and DNPH assay that provided only global measure of oxidative stress without giving any information on the molecular level (Zhang, Cazars et al. 1995, Konishi, Iwasa et al. 2006). Although, these methods provide useful initial insights about potential oxidative state, they suffer from inherent problems related to sensitivity and specificity of detecting individual molecular species, when applied to situations *in-vivo* (Tyurina, Tyurin et al. 2009).

On the other hand, mass spectrometry coupled with liquid chromatography as a technique to measure oxidised phospholipids has gain popularity because it measures mass –to charge ratio (m/z) of compounds and can distinguish or separate different molecular species based on their masses and functional chemistry, therefore, can selectively identify several different species in complex mixture simultaneously. The last decade has seen surge in more sophisticated methods involving use of liquid chromatography coupled with mass spectrometry (LC-MS), supporting the significance of OxPL in health and disease (Spickett 2001, Sparvero, Amoscato et al. 2010, Spickett, Wiswedel et al. 2010, Spickett, Reis et al. 2011, Stutts, Menger et al. 2013). Table 3.1 illustrates the limitation of methods based on the level of structural information that can be obtained. While the mass spectrometry based scanning approaches such as PIS and NL used alone can provide limited information, their strength and specificity in identifying a range of species is increased when used in combination. Similarly, shotgun approaches like direct infusion mass spectrometry (DIMS) provides qualitative information when used alone and requires combination of several different scanning methods to improve the information content of the method.

Table 3.1: Summary of analytical methods and the level of information that can be obtained using different approaches

Increasing level of structural information obtained	Representative example about information obtained	Method description	Limitations	Publications using this methods
	 <p>An oxidised phospholipid molecule</p>	UV, Fluorescence based methods like FOX-2 Assay, DNPH assay, TBARS assay	No information at molecular level	(Breusing, Grune et al. 2010),(Zhang, Cazars et al. 1995, Wu, Svenungsson et al. 1999, Grintzalis, Zisimopoulos et al. 2013)
	 <p>An oxidised phospholipid molecule belong to phosphatidylcholine class</p>	Direct infusion mass spectrometry (DIMS), Precursor ion scan (PIS) or high resolution (HR) – LCMS (All used alone)	Only Class specific information obtained, application to complex samples challenging	(Spickett, Pitt et al. 1998, Spickett, Rennie et al. 2001, Ekroos 2002, Wang, Xie et al. 2004, Christer S. Ejsing 2006)
	 <p>An oxidised phospholipid molecule belong to phosphatidylcholine class with further information on fatty acyl chains</p>	LC-MS/MS approaches based on Precursorion scanning (PIS) in combination with neutral loss scanning (NL) and product ion scanning (EPI) and HR-LCMS/MS method	Information on exact location of the oxidation not possible	(Yin, Cox et al. 2009, Gruber, Bicker et al. 2012, Lee, Lim et al. 2013, Reis, Domingues et al. 2013)

Moreover, the type of scanning approaches that one can perform on a mass spectrometer depends on the type of mass analysers. For instance, selective scanning approaches like precursor ion scanning (PIS) and neutral loss scanning (NL) can be performed on triple quadruple mass spectrometers whereas MS^n based approaches to elucidate structural information to the highest level can be performed on instruments with ion trap analysers. Due to extreme chemical diversity of the oxidised lipidome together with the range of concentrations of these species in biological samples, complementary analytical approaches are required to monitor it completely (Domingues, Reis et al. 2008, Spickett and Pitt 2015). It is analytically impractical to measure oxidised species of all classes in a single run because of variation in the charge of the polar head group and extreme diversity of oxidised phospholipid species OxPL).

Moreover, sensitivity is the major concern, because currently no method is available to selectively enrich or amplify these species to improve their detection (Mousavi, Bojko et al. 2015, Ulmer 2015). Therefore, the strength of the mass spectrometric analysis can be exploited by enhancing the selectivity of the methods.

Selectivity of the analysis can be improved by using semi-targeted approaches like PIS and NL, which decrease the contribution of the background ions to the measured signals, producing a net gain in sensitivity and signal to noise ratio, and further structural information can be obtained using MSⁿ approaches to gain confidence in the identification (Blanksby and Mitchell 2010, Spickett, Reis et al. 2011). This was made possible by development of hybrid instruments by manufacturing companies like Absciex Inc., which developed the Qtrap 5500, an instrument that consists of three quadruples and a linear ion trap mass analyser (QQQLIT). This enabled the enhanced performance of selective scanning approaches like PIS and NL, and MSⁿ approaches together, thereby improving the detection range.

Although semi-targeted scanning approaches like PIS 184 Da, NL 141 Da and NL 185 Da for selective identification of phosphatidylcholine class, phosphatidylethanolamine class (PE) and phosphatidylserine class (PS) respectively were reported earlier, these scanning approaches have not been used extensively for analysis of OxPL species (Murphy and Axelsen 2011, Murphy and Gaskell 2011, O'Donnell 2011, Reis and Spickett 2012). Moreover, NL 34 Da, NL 36 Da and NL 38 Da scanning methods for identification of hydroperoxide and chlorohydrin species respectively, reported by several research groups were not widely exploited for development of mass spectrometry methods (Spickett, Reis et al. 2011, Reis, Domingues et al. 2013).

Moreover, advancement in the mass spectrometry field has led to development of sophisticated instruments that can theoretically handle the diversity of OxPL. Examples of such instruments are 3rd generation Orbitrap mass spectrometers and imaging mass spectrometers. However, such sophisticated instruments are very expensive therefore, are limited to small number of institutes whereas, most common bench top instruments like Qtrap, triple quadruple or QTOF based instruments can be found in several mass spectrometry laboratories. Therefore, the primary aim of this project was to develop methods that can be utilised by wider research communities using semi targeted scanning approaches. Our study focused on the detection of oxidised phosphatidylcholines (OxPCs), oxidised phosphatidylethanolamines (OxPE) and oxidised

phosphatidylserines (OxPS), which represent three important classes demonstrating a variety of biological activities but insufficiently characterised in several inflammatory diseases. Targeted approaches like precursor ion scanning (PIS) and neutral loss scanning (NL) were developed based on the knowledge of common fragmentation patterns of a small group of molecular species bearing a common structural motif, have been reported earlier but have not been extensively used to measure OxPC species in biological samples

While mass spectrometer instruments can separate and identify species that have different molecular masses, there are limitations in separation of isomeric and isobaric species (Sandra, Pereira Ados et al. 2010). Moreover, isobaric and isomeric species are not uncommon in oxidative Lipidomics and therefore, to handle the diversity of OxPL species that can be formed, it is often required to couple chromatographic separation with mass spectrometry detection (van Meer 2005, Peterson and Cummings 2006, Wörmer, Lipp et al. 2013).

Various reports describe the combination of either reverse phased and or normal- phase LC coupled with mass spectrometry in multi-dimensional set ups to detect and measure long chain oxidation products(Hui, Chiba et al. 2010, Morgan, Hammond et al. 2010, Thomas, Morgan et al. 2010, Strassburg, Huijbrechts et al. 2012). Most of the methods developed so far relied on mass spectrometric and chromatographic development (Fu, Xu et al. 2014, Groessl, Graf et al. 2015) or focused on high throughput analysis (fast HPLC) at the expense of detection of low abundant oxidation products (Gruber, Bicker et al. 2012). Most of the current methods published so far, have been either confined to a small number of molecular species based on Multiple Reaction monitoring (MRM) based approach or have used high resolution mass spectrometry coupled with liquid chromatography to detect specified oxidised phospholipid species, solely based on accurate masses and/or tandem mass spectrometry (MS-MS) to obtain structural information(Adachi, Asano et al. 2006, Uchikata, Matsubara et al. 2012, Uchikata, Matsubara et al. 2012). The MRM and high resolution based methods are highly sensitive and focused methods and are ideal for observing and quantifying certain pre-determined species. Nevertheless, further improved methods that are capable of quantifying multiple oxidised species in biological samples belonging to different phospholipid class are still required.

To date, there is no report of systematic evaluation of chromatographic separation for OxPL species. The resolution parameter that dictates the chromatographic separation is dependent on three other parameters: efficiency, selectivity, and capacity; the maximum improvement in

resolution is related to altering the selectivity parameter, which is the factor that is dependent upon the chemistry of the analyte, mobile and stationary phases (Zhou, Song et al. 2005, Weng 2014). All of these factors may be altered to optimise the chromatographic separation. In this project, one of the primary objectives was to perform systematic evaluation of chromatographic separation by testing several stationary and mobile phase systems to achieve best separation of OxPL species. We also investigated the two dimensional separation by serially coupling two columns that provides orthogonal selectivity. The set up was adapted from (Haggarty, Oppermann et al. 2015) by coupling the HILIC column and reverse phase column.

The number and chemical composition of OxPL species that need to be identified and measured shapes the experimental design and choice of instrumentation. When the objective is to identify and measure as many OxPL species as possible and compare between samples without bias, an appropriate validation approach needs to be identified in advance to confirm the findings and minimise the number of false positive identifications and measurement. Moreover, when the method analyses low abundant OxPL species belonging to different classes and high abundant phospholipid species together, it becomes inevitable to have an efficient validation approach that is equally specific and sensitive for analytes of interest to confirm the identifications and findings. An ideal approach should be a non-mass spectrometric approach. In this project, we tried different approaches like $^1\text{H-NMR}$ for chlorohydrin species, UV spectroscopy for hydroperoxide species. However, it was realised that only a separate mass spectrometric approach can complement a mass spectrometry methodology. Therefore, validation of our findings was done by transferring the method to a high resolution Q-TOF mass spectrometer with added layer of identification based on high resolving power.

Moreover, peak identification and integration across multiple samples manually can introduce bias that can further add to systemic error, which affects the accuracy and reproducibility of the experiment (Vogesser and Seger 2010). Furthermore, missing values and overlapping peaks can complicate the manual data handling process and can substantially skew the statistical analysis. Therefore, automated data analysis using Progenesis QI software was performed to validate manual data analysis. Annotation of species was performed by searching against the in-house built data base of all possible OxPL species in sdf format to enable theoretical fragmentation search with mass tolerance less than 5 ppm.

The multiple steps involved in sample preparation, varied composition of analyte solution due to the use of gradients or presence of co-eluent during chromatographic separation, minor alteration in ionisation conditions and instrumentation may contribute to differential ionisation conditions from run to run and affect the ion intensity measurement process (Kofeler, Fauland et al. 2012) (Sandra, Pereira Ados et al. 2010, Weng 2014). Moreover, the variation in sampling of biological samples can be substantial and add to the total uninduced variation, thereby affecting the extraction of biological information from the data analysis (Sysi-Aho, Katajamaa et al. 2007) (Veselkov, Vingara et al. 2011, Yang and Han 2011). In this study, different normalisation approaches like addition of internal standard, global normalisation, total ion intensity and total phospholipid content were tested to pre-estimate the propagated error and minimise systemic variation. Moreover, to confirm the accuracy and reproducibility of the method, inter- day, intra-day and extraction variability were tested. The linear dynamic range was assessed by examining the responses of several commercially available OxPLs at different concentrations.

3.2 Study aim and objectives

In summary, the aim of this chapter is 3 fold:

- The development of an improved LC-MS method using targeted approaches like precursor ion scanning and neutral loss scanning and optimisation of chromatographic separation of OxPL to provide better coverage of the oxidised lipidome.
- Development and testing of several data processing approaches to reduce unnecessary variation caused by systemic errors propagated during sample preparation and handling.
- Cross validation of LC-MS data analysis through testing several analytical platforms like NMR, high resolution LCMS and automated data analysis using Progenesis QI software.

To meet these aims, following steps were undertaken:

- Assessment of different methods to generate OxPL species.
- Tuning of MS parameters such as collision energy and declustering potential to improve the signal to noise ratio and achieving optimum sensitivity.
- Evaluation of several reverse phase columns and solvent systems outlined in the appendix to achieve best separation.
- Cross validation of the method using different analytical approaches like NMR and high resolution Q-TOF mass spectrometry analysis.
- Assessment of reproducibility and repeatability of the method by testing several normalisation approaches and determining inter –day and intra- day repeatability.

3.3 Methodology

3.3.1.1 Optimisation of mass spectrometry parameters for precursor ion scans (PIS), neutral loss scans (NL) by direct infusion mass spectrometry

Commercially available standard phospholipids (SOPC, SLPC, SAPC, PAPE and PAPS) and/or PC/PE or PS mixtures and their corresponding oxidation products and chlorohydrins were analysed by electrospray mass spectrometry (ESI-MS) in positive mode. All analysis was performed on ABSciex 5500 QTrap Mass spectrometer (QQQLIT) with parameter tuning and optimisation performed using Analyst 1.5.1 software. The parameters optimised for analysis of phospholipids and their oxidation products are stated below. The ion spray voltage optimised for positive mode analysis was 5500 V. Other source parameters that were optimised for analysis of oxidised phospholipids were the source temperature that was fixed at 150°C and the nebulisation gas flow rate (GS1) at 13 L. Moreover, other parameters like declustering potential (Hajjar and Gotto) was optimised to 50 V and collision gas was kept high and was fixed at 10 for general scanning and was ramped from 10 - 47 for MS/MS experiments (neutral loss, precursor ion and product ion scanning) to identify optimal collision energy. Syringe parameters were fixed by selecting the syringe code corresponding to 500µl syringe and flow

rate at 10 μl / minute for direct infusion. The resolution was set to unit for general enhanced mass spectral scanning (EMS) and enhanced product ion scanning (EPI). For MS/MS spectra in precursor ion scanning, the resolution was set to unit for both Q1 and Q3 analyser, and Q1 at low and Q3 at unit resolution for neutral loss scanning (NL). The filling of the ion trap was set to dynamic and the m/z range scanning for positive mode was 490- 1000. The scan rate was set to 10,000 scans per second for general mass scanning and 200Da/ seconds for MS/MS scanning routines. The solvent system used for analysis of oxidised phospholipids in positive mode was ternary mixture consisting of methanol, water and formic acid at the ratio of 90:9.9:0.1. The modified lipid aliquots were diluted to 100 fold prior to MS analysis by direct infusion.

In analysis of lipid chlorohydrins by direct infusion in positive mode, the native phospholipids were identified as $(\text{M}+\text{H})^+$ peak of m/z 788.5 for SOPC, 786.5 for SLPC and 810.5 for SAPC respectively. The increment of 52 Da (monochlorohydrin) to the mass of native phospholipid corresponding to addition of ClOH group, that is proportional to the number of double bonds in the unsaturated fatty acid chain esterified at sn-2 position, was detected for chlorohydrins. Moreover, neutral scanning of 36 Da for ^{35}Cl isotope and 38 Da for ^{37}Cl isotope was performed to confirm the detection of chlorohydrins. The precursor ion scanning at m/z 184.07 Da was performed to characterise all ions having phosphocholine as their head group.

For UV treated and AAPH oxidised samples, along with EMS scan and PIS scan of 184 to characterise phosphatidylcholines, neutral loss scan of 34 Da was performed to detect hydroperoxides. In EMS scan, the hydroperoxides peaks were detected with increment of 32 Da corresponding to monohydroperoxides and hydroxides were monitored with increment of 16 Da corresponding to mono-hydroxides. For PE class mixture and individual PE species neutral loss scan of 141 Da was optimised to selectively identify all oxidation and native PE species. For PS class mixture and individual PS species, neutral loss scan of 185 Da in positive mode and neutral loss scan of 87 Da in negative mode was optimised and compared to achieve better signal to noise ratio. The solvent used for negative mode was the mixture containing methanol and 10mM ammonium acetate in the ratio of 90:10. The ion spray voltage optimised for negative mode analysis was 4500 V. Other source parameters that were optimised for analysis of oxidised phospholipids were the source temperature that was fixed at 150°C and the nebulisation gas flow rate (GS1) at 13 L. Moreover, other parameters like declustering potential (Hajjar and Gotto) was optimised to 50 V and collision gas was kept high and was fixed at 10 for general scanning and was ramped from 10 - 47 for MS/MS experiments (neutral loss,

precursor ion and product ion scanning). For MS/MS spectra in neutral loss scanning mode, the resolution was set to low for Q1 and unit for Q3. The filling of the ion trap was set to dynamic and the m/z range scanning for negative mode was m/z 200 – 1000. Also, secondary (fragmented) oxidised products like lysophosphocholines (LPC) at m/z 496.5 and 524.5, corresponding to palmitoyl-LPC and stearoyl-LPC respectively where the fatty acid esterified at sn-2 position is lost is detected along with other lipid species specific oxidation products like 1-palmitoyl-2-glutaryl-sn-glycero-3-phosphocholine (PGPC) at m/z 610.5 and 1-palmitoyl-2-(5'-oxo-valeroyl)-sn-glycero-3-phosphocholine (POVPC) 594.5 for PAPC. In addition, other products for linoleyl PC oxidation products at m/z 650 and 666, corresponding to PONPC and PAzPC were also detected in positive mode analysis of oxidised phospholipids.

3.3.1.2 Optimisation of chromatographic separation using several reverse phase columns and eluent systems

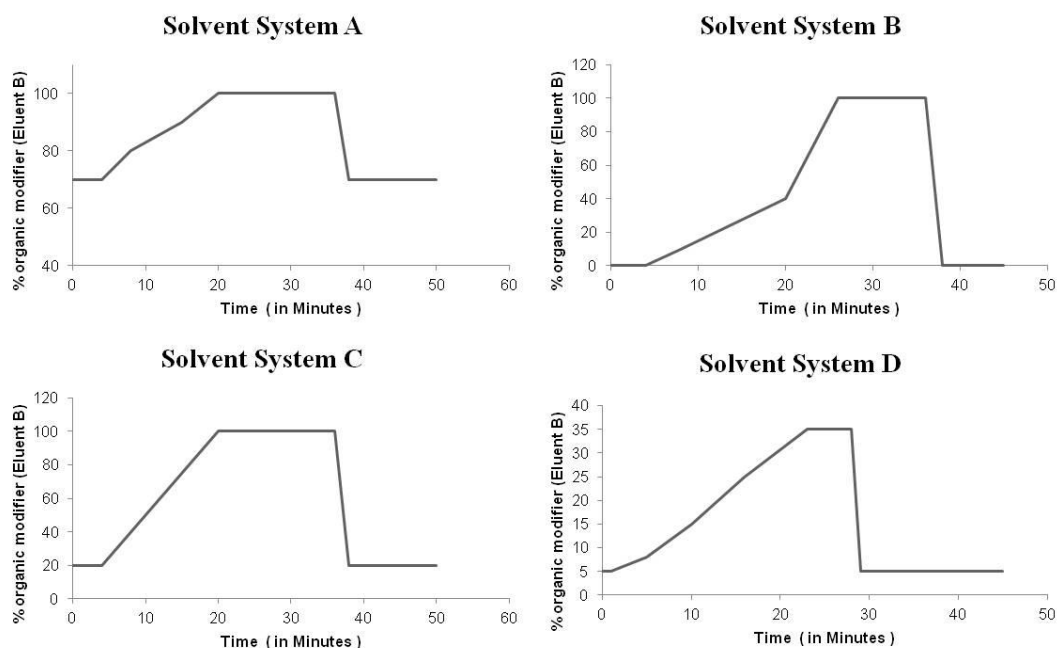


Figure 3.4: The figure shows graphical representation of the chromatographic gradient programs that were evaluated to achieve better separation. Solvent system A consists of LC-MS grade water with 5 mM ammonium formate and 0.1 % formic acid as eluent A and Methanol with 5 mM ammonium formate and 0.1 % formic acid as eluent B; Solvent system B consists of ternary mixture of methanol, hexane and 0.1 M ammonium acetate (71:5:7) as eluent A and methanol, hexane mixture (95:5) as eluent B; Solvent system C consists of ternary mixture of tetrahydrofuran (THF), methanol and 10 mM ammonium acetate (30:20:50) as eluent A and THF, methanol and 10mM ammonium acetate (70:20:10) as eluent B; Solvent system D consists of 20 % isopropyl alcohol (IPA) in Acetonitrile (ACN) as eluent A and 20 % IPA in 20 mM ammonium formate as eluent B.

Conventional reverse phase columns like C-8 Luna column (150 x 1mm), C- 18 Luna column (150 x 1mm), C-30 Luna column (150 x 2.1mm) and Proswift –RP 4H polystyrene – divinyl benzene coated monolith column (1 x 250mm); and mix mode Hichrom amino based HILIC column (150 X 3.1mm) were evaluated using combination of different eluent systems, while maintaining the linear flow rate and using mass spectrometry for detection.

The solvent systems that were used to achieve best separation were: **Solvent system A** consisting of LC-MS grade water with 5 mM ammonium formate and 0.1 % formic acid as eluent A and Methanol with 5 mM ammonium formate and 0.1 % formic acid as eluent B; **Solvent system B** consisting of ternary mixture of methanol, hexane and 0.1 M ammonium acetate (71:5:7) as eluent A and methanol, hexane mixture (95:5) as eluent B; **Solvent system C** consisting of ternary mixture of tetrahydrofuran (THF), methanol and 10 mM ammonium acetate (30:20:50) as eluent A and THF, methanol and 10mM ammonium acetate (70:20:10) as eluent B; **Solvent system D** consisting of 20 % isopropyl alcohol (IPA) in Acetonitrile (ACN) as eluent A and 20 % IPA in 20 mM ammonium formate as eluent B. The figure 3.4 shows the gradient program for each solvent system used for chromatographic evaluation.

Gradient run for solvent system A consisted of a 50 minute run with 0 – 4 minute isocratic hold at 70 % B, followed by 3 step gradient increase to 80 % B at 8 minutes, 90 % B at 15 and 100 % B at 20 minutes. The gradient remained constant until 38 minutes and decreased back to 70 % B until 50 minutes. Gradient run for solvent system B was a 45 minute run with 0 – 4 minute at 100 % A followed by 3 step gradient increase to 10 % B at 8 minutes, 40 % B at 20 minutes and 100 % B at 26 minutes with isocratic hold at 100 B until 36 minutes and equilibration to 100 % A from 38 – 45 minutes. Gradient run for solvent system C consisted of a 50 minute run starting at 20 % B at 4 minutes and increasing to 100 % B at 20 minutes, followed by isocratic hold at 100 % B until 36 minutes and back to starting condition at 38 minutes. Gradient program for solvent D consisted of a 45 minute run under HILIC conditions only used for the silica based HILIC column from Hichrom, UK with multi step gradient as follows: 0 – 1 minute held at 5 % B, 1 – 5 minutes to 8 % B, 5 – 10 minutes to 15 % B, 10 – 13 minutes held at 15 % B, 13 – 23 minutes to 35 % B, 23 – 28 minutes held at 35 % B and back to starting conditions at 29 minutes until 45 minutes.

Mass spectrometric parameters were similar for all solvent systems as outlined in section 1.3.1.5 expect for solvent system D under HILIC conditions. The mass spectrometric detection

for solvent system D under HILIC conditions at 300 $\mu\text{l}/\text{minute}$ was as follows: The source temperature was set at 350 $^{\circ}\text{C}$; the spray voltage was 5500V; the declustering potential was set to 50 V for all scans; nitrogen was used as the curtain gas and nebulising gas with flow rates set to 35 AU and 26 AU respectively. Survey scan MS data were acquired by electrospray ionization in positive mode from 400-1200 Da in high resolution mode for 500 ms. Information dependent data acquisition (IDA) was used to collect MS/MS data based on following criteria: the 4 most intense ions with +1 charge and a minimum intensity of 250 cps were chosen for analysis, using dynamic exclusion for 20 seconds after 2 occurrences and a fixed collision energy setting of 47 eV. Each chromatographic program and solvent system is further outlined in Appendix 1.

Chromatographic separation was also evaluated for monolith column by running the gradient outlined for solvent system A at different flow rates: 50 $\mu\text{l}/\text{minute}$, 100 $\mu\text{l}/\text{minute}$ and 200 $\mu\text{l}/\text{minute}$ and the sensitivity and elution profile was evaluated. Furthermore, different gradient program were evaluated for monolith column with solvent system A. The 3 step gradient program as outlined in section 2.3.1.5 was evaluated against a 16 minute steep gradient (70 % B at 4 minutes to 100 % B at 20 minutes) and 26 minute shallow gradient (70 % B at 4 minutes to 100 % B at 30 minutes) and the separation profile of OxPC species was evaluated. The chromatographic program for 16 minute steep gradient and 26 minute shallow gradient is graphically represented in appendix 1.

For optimisation of two dimensional LCMS work serial coupling of monolith column and HILIC column was set up and solvent A and solvent system D were used as mobile phases. The technique was adapted from the published work used for polar metabolites (Louw, Pereira et al. 2008, Haggarty, Oppermann et al. 2015). For the first separation monolith column (Proswift RP-4H, 1x 250mm) was used using solvent system A as mobile phases and the 2nd separation was performed using HILIC column (ACE Silica, 150 x 3.1mm) column in combination of solvent system D as mobile phases.

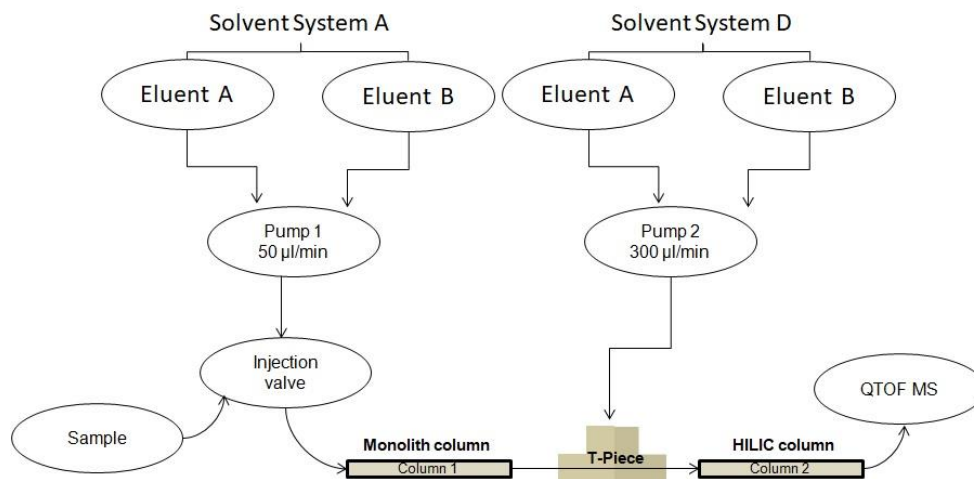


Figure 3.5: Schematic representation of the setup for 2D- orthogonal reversephase-HILIC chromatography interfaced with QTOF MS.

The two columns were coupled in series using a T-piece with third port connected to the 2nd binary pump. The scheme of the chromatographic program is explained in appendix 1 and in figure 3.5. The two different gradient program using solvent system A for monolith column and solvent system D for HILIC column are as below:

For reverse phase separation gradient run for solvent system A, the program consisted of a 50 minute run with 0 – 4 minute isocratic hold at 70 % B, followed by 3 step gradient increase to 80 % B at 8 minutes, 90 % B at 15 and 100 % B at 20 minutes. The gradient remained constant until 38 minutes and decreased back to 70 % B until 50 minutes. For HILIC separation gradient consisted of multi-step increment as follows: 0 – 1 minute held at 5 % B, 1 – 5 minutes to 8 % B, 5 – 10 minutes to 15 % B, 10 – 13 minutes held at 15 % B, 13 – 23 minutes to 35 % B, 23 – 28 minutes held at 35 % B and back to starting conditions at 29 minutes until 45 minutes.

For the modified gradient program for HILIC column used for 2D-LCMS work the gradient was as follows: 0 – 1 minute held at 5 % B, 1 – 5 minutes to 8 % B, 5 – 10 minutes to 15 % B, 10 – 15 minutes to 17.5 % B, 15 – 20 minutes to 20 % B, 20 – 30 minutes to 30 % B, 30 – 35 minutes to 35 % B, 35 – 40 minutes held at 35 % B and back to starting conditions at 41 minutes until 50 minutes.

3.3.1.3 Conceptual framework for the automated data analysis workflow using Progenesis QI software

Untargeted mass spectrometry analysis generates a huge amount of data. While processing the data is crucial for subsequent comparative analysis, the outcome of the data processing strongly depends on parameter settings and if not chosen carefully, can easily lead to biased results (Libiseller, Dvorzak et al., 2015). The workflow in Progenesis QI is designed to provide accurate measurement of the analytes to allow comparative analysis.

After the raw data files are uploaded, the feature detection algorithm, which is based on the combination of determining the boundaries, that is centre and intensities of the two dimensional signal of the LCMS raw data is applied to extract features defined by the matrices of m/z and retention time of ions. This is done by combining the density based detection approach (an alternative to common binning approach) introduced by Stolt et al. and wavelet based approach. Based on the information provided by the user about possible adducts that can be formed with the analyte, the software implements the deconvolution step, which will group the ion as a single compound representing the cluster of an analyte with different adduct forms.

In parallel, all the raw data files are represented by an ion intensity map, the map of sample's MS signals separated by m/z and time, which provides an immediate visual quality check, highlighting any problems experienced in sample acquisition. These ion maps are further used for chromatographic alignment that produces an aggregate run representative of the compounds/analytes in all samples and uses these aggregates for peak picking and these can be used to manually correct for chromatographic drift by placing landmarks in the chromatographic run called alignment vectors.

The next step of data preprocessing is peak picking also known as feature extraction that requires correction for isotopes. To ensure consistent peak picking and matching across all data files, an aggregate data set is created from the aligned runs. This contains all peak information from all sample files, allowing the detection of a single map of compound ions. This map is then applied to each sample, giving 100% matching of peaks with no missing values, so you can generate reliable results using valid multivariate statistical analysis.

After detection, the ion abundance measurements are normalised so that the comparisons can be made between the runs and find compounds of biological interest. Once the detected compounds are listed, the identification can be carried out based not only on neutral mass and retention time (if data was available) but also collisional cross-sectional area (CCS) and MS/MS fragmentation data. Compounds which have more than one possible identification can be reviewed so the results can be narrowed down and the correct identification can be selected by observing the measured isotope distribution compared to the theoretical. This isotope distribution match contributes to the overall compound identification score.

3.4 Result

3.4.1 Assessment of different methods to generate OxPL species

Commercially available egg yolk lecithin (crude phosphatidylcholine mixture) was subjected to oxidation using different methods: exposure to UV light, treatment with the azo initiator: 2, 2'-Azobis (2amidinopropane) dihydrochloride (AAPH), or reaction with hypochlorous acid (HOCl).

The figures 3.6 and 3.7 show the different profiles of OxPL formed when PC mixture is exposed to UV radiation or 10 mM AAPH treatment. Figure 3.6 show the zoomed spectra of the PIS scan for 184 Da of control samples as well as UV treated and AAPH oxidised samples in the m/z 480 – 750 range. The complete spectra is shown in the appendix II. Several peaks in the mass range of m/z 500 – 700 were observed in the treated samples that were absent in control samples.

The top panels of figure 3.6 show the spectra of control samples whereas the bottom panels show spectra of the treated sample, showing a 10-fold decrease in intensity of unmodified lipids. The peaks observed in the m/z 500-700 range are collectively termed “**short chain oxidation products**”, which are secondary oxidation products and have masses smaller than the unmodified phospholipid species. The peaks at m/z 594.5, (oxo-valeroyl)PPC; 610.5, (Glutaryl)PPC; 622.5, (oxo-valeroyl)SPC; 638.5, (Glutaryl)SPC; 650.5, (oxo-nanonyl)PPC ; 666.5, (azelaoyl)PPC; 678.5, (oxo-nanonyl)SPC and 694.5, (azelaoyl)SPC were observed and their respective identification were confirmed by studying the fragmentation spectra and comparing them to the published literature. The table 3.2 shows the common fragment masses observed for short chain oxidised species in the product ion spectra in addition to the fragment mass of 184 Da that corresponded to the phosphocholine fragment.

Table 3.2: List of masses of fragment ions of short chain oxidised species observed in product ion scanning.

Compound name	m/z	M-R2CO	M-R2COOH	M-R1CO	M-R1COOH	M-phosphocholine	M-R1COOH-phosphocholine
(oxo-valeroyl)PPC	594.38	496.34	478.33	356.15	338.14	411.31	155.07
(Glutaryl)PPC	610.37	496.34	478.33	372.14	354.13	427.31	171.07
(oxo-valeroyl)SPC	622.41	524.51	506.24	356.18	338.17	439.34	155.10
(Glutaryl)SPC	638.52	524.51	506.24	372.29	354.28	455.45	171.21
(oxo-nanonyl)PPC	650.44	496.34	478.33	412.21	394.20	467.37	211.13
(azelaoyl)PPC	666.43	496.34	478.33	428.20	410.19	483.37	227.13
(oxo-nanonyl)SPC	678.52	524.51	506.24	412.29	394.28	495.45	211.21
(azelaoyl)SPC	694.52	524.51	506.24	428.29	410.28	511.45	227.21

Figure 3.7 shows the zoomed spectra of the PIS scan for 184 Da of control samples as well as UV treated and AAPH oxidised samples in the m/z 700 – 1000 range. Several peaks in the mass range of m/z 700 – 1000 were observed in the treated samples that were absent in control samples. The peaks observed in the m/z 700- 1000 range are collectively termed as “**long chain oxidation products**”, which are primary oxidation products and have masses larger than the unmodified phospholipid species. The peaks at m/z 774.5 and 802.5 respectively correspond to hydroxide species of PLPC (phosphatidylcholine class species bearing palmitoyl and lineoyl fatty acyl chain) and SLPC respectively with increment of 16 Da in mass with addition of 1 atom of oxygen. The assignment of m/z values to corresponding oxidised species was done by performing product ion scanning for each observed oxidised species and also comparing the observed fragment spectrum to published literature. For example, a peak at m/z 818.5 was observed in both UV treated as well as AAPH oxidised samples that can be assigned to either the di-hydroxide peak of SLPC with increment of 32 Da at m/z 818.5 or an hydroperoxide derivative of SLPC. The peak in UV treated samples was assigned to a di-hydroxide peak (2-OH, +32 Da: SLPC di (OH)) of SLPC instead of a hydroperoxide peak (OOH, +32 Da: SLPC-OOH) by observing the neutral loss scan for 34 Da, which is selective scanning method for hydroperoxide species. Moreover, the fragment ion with loss of 34 Da was absent in product ion spectra. Similarly, the peak at m/z 818.5 was assigned to the hydroperoxide species in AAPH treated sample that was confirmed by performing MS/MS scan and neutral loss for 34 Da scan as shown in figure 3.8. Moreover, higher levels of oxidation products bearing more than 4 oxygen atoms were only apparent in AAPH treated sample at m/z 904.5, 958.5 that corresponds to dihydroperoxide-hydroxyl-keto species of highly susceptible poly-unsaturated bearing native species: 18:0/20:4 PC (m/z 810.5), which is abundantly present in mammalian cellular membrane and trihydroperoxide-diketo species of ω 3 fatty acid bearing species: 18:0/22:6 PC (m/z 834.5). The table 3.3 shows the common fragment masses observed for long

chain oxidised species in the product ion spectra in addition to the fragment mass of 184 Da that corresponded to the phosphocholine fragment.

Table 3.3: List of masses of fragment ions of long chain oxidised species observed in product ion scanning.

Compound name	m/z	M-R2CO	M-R2COOH	M-R1CO	M-R1COOH	M-phosphocholine	M-R1COOH-phosphocholine
PLPC-OH	774.52	496.34	478.33	536.29	518.28	591.45	335.21
POPC-OH	776.54	496.34	478.33	538.31	520.30	593.47	337.23
PLPC-OOH	790.50	496.34	478.33	552.27	534.26	607.43	351.19
SLPC-OH	800.50	524.51	506.24	534.27	516.26	617.43	333.19
SOPC-OH	802.50	524.51	506.24	536.27	518.26	619.43	335.19
SLPC-OOH	818.52	524.51	506.24	552.29	534.28	635.45	351.21
SLPC-OOH(OH)	834.56	524.51	506.24	568.33	550.32	651.49	367.25
SAPC(O)OHdi(OOH)	904.50	524.51	506.24	638.27	620.26	721.43	437.19
SDHPCdi(O)3(OOH)	958.52	524.51	506.24	692.29	674.28	775.45	491.21

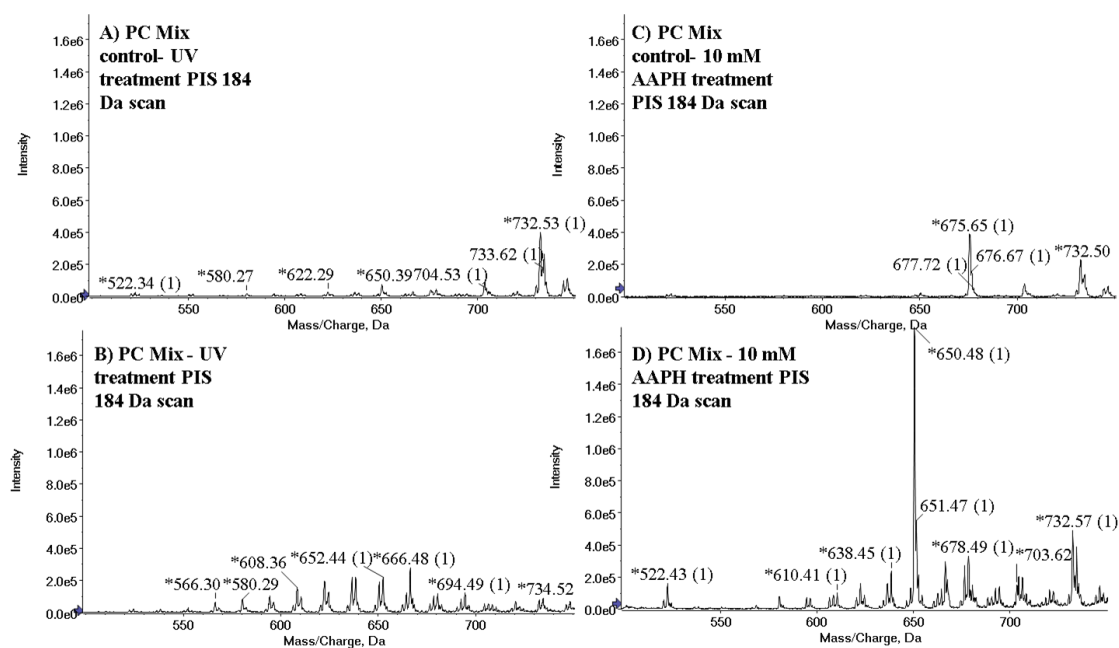


Figure 3.6: Direct infusion mass spectrometry (DIMS) analysis of UV-A oxidation (left panel) and AAPH treated (right panel) of PC mixture using Precursor ion scan for 184 Da (A) shows PIS scan of control-1 sample for UV-A treatment (B) is the PIS scan of UV-A treated sample (C) show PIS scan of control sample for 10 mM AAPH treatment and (D) shows the PIS scan of 10 mM AAPH treated sample respectively. Secondary fragmented product ions are observed in 500-600 m/z range

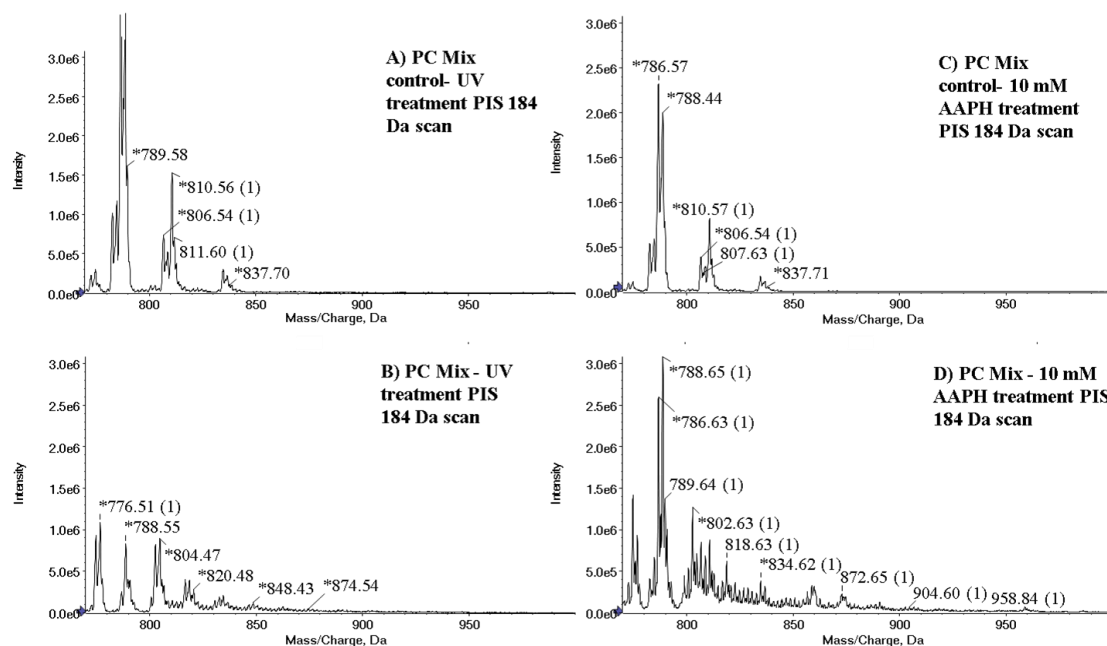


Figure 3.7: Direct infusion mass spectrometry (DIMS) analysis of UV-A oxidation (left panel) and AAPH treatment (right panel) of PC mixture using Precursor ion scan for 184 Da (A) shows PIS scan of control-1 sample for UV-A treatment (B) is the PIS scan of UV-A treated sample (C) shows PIS scan of control sample for 10 mM AAPH treatment and (D) shows the PIS scan of 10 mM AAPH treated sample respectively. No hydroperoxides peaks are apparent in UV treated samples, which may have been decomposed to hydroxides that are more stable. For example, peak at m/z 774.5 and 802.5 which are hydroxides of PLPC and SLPC respectively. Higher masses of oxidation products at m/z 872.5, 904.5 and 958.5 are only apparent in 10 mM AAPH treated sample.

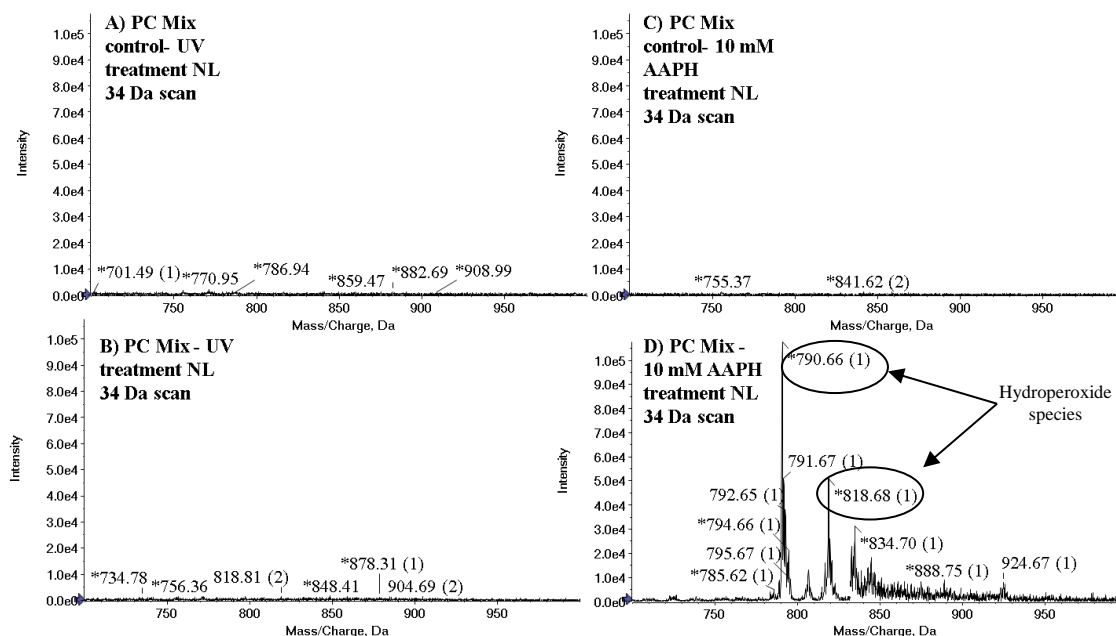


Figure 3.8: Direct infusion mass spectrometry (DIMS) analysis of UV-A oxidation (B) and AAPH treatment (D) of PC mixture using Neutral loss scan for 34 Da selective for hydroperoxide species (+ OOH, 32 Da). The AAPH treated spectra shows the peaks at m/z 790.5 and 818.5 that corresponds to hydroperoxide species of PLPC (m/z 758.5) and SLPC (m/z 786.5) and the spectra for UV treated sample does not shows any hydroperoxide species.

PC mixture oxidation with 50 mM, 100mM and 150 mM of HOCl predominantly generated chlorohydrin species. Figure 3.9 shows the MS spectra for PIS 184 Da of control and three treatment samples. The control group showed (M+H)⁺ ion peaks for unmodified phosphatidylcholine class species. The peaks at m/z 732.5 (16:0,16:1 PC), 758.5 (16:0, 18:2 PC) , 760.5 (16:0, 18:1 PC), 786.5 (18:0, 18:2 PC), 788.5 (18:0, 18:1 PC) , 806.5 (16:0, 22:6 PC), 810.5 (18:0, 20:4 PC) and 834.5 (18:0, 22:6 PC) were observed in the control sample that got modified to chlorohydrin species on treatment with hypochlorous acid as observed with disappearance of these peaks in the treated samples. The treatment group panel spectra showed emergence of new peaks with mass shift in multiples of 52 Da to the mass of native phospholipids. For instance, a peak at m/z 812.5 corresponds to monochlorohydrin of 16:0, 18:1 PC (m/z 760.5). SOPC (18:0, 18:1 PC) have a single double bond hence, only a monochlorohydrin is formed at an increment of 52 Da at m/z 840.5. The bischlorohydrin species of SLPC (18:0, 18:2 PC) was observed at m/z 890.5 with increment of 104 Da corresponding to addition of two ClOH moieties to the SLPC molecule. SLPC has 2 double bonds, and therefore there are 2 possibilities: a mono-chlorohydrin with a double bond remaining and/or di-chlorohydrin at increment of 104 Da. However, only peak at m/z 890.5 corresponding to addition of 2 ClOH moieties is apparent while a mono-chlorohydrin is not observed at m/z 838.5. For S APC (18:0, 20:4 PC, m/z 810.5) having four double bonds, there is a possibility of forming mono, bis, tris and tetra chlorohydrin with increment of 52 Da, 104 Da, 156 Da and 208 Da respectively. However, a peak at m/z 966.5 corresponding to tris-chlorohydrin is observed. Since the mass range of the Qtrap instrument for scanning is 50-1000, tetra-chlorohydrin of S APC was not observed because of the mass (1018.5 Da) which is beyond the scanning range of the Qtrap instrument. The abundance of ³⁵Cl to ³⁷Cl isotope of chlorine atom in nature is at the ratio of 3:1. Therefore, a (M+2) peak at intensity approximately at one-third of the (M+H)⁺ peak is observed for all molecules containing chloride atom that

supports the identification of chlorohydrins.

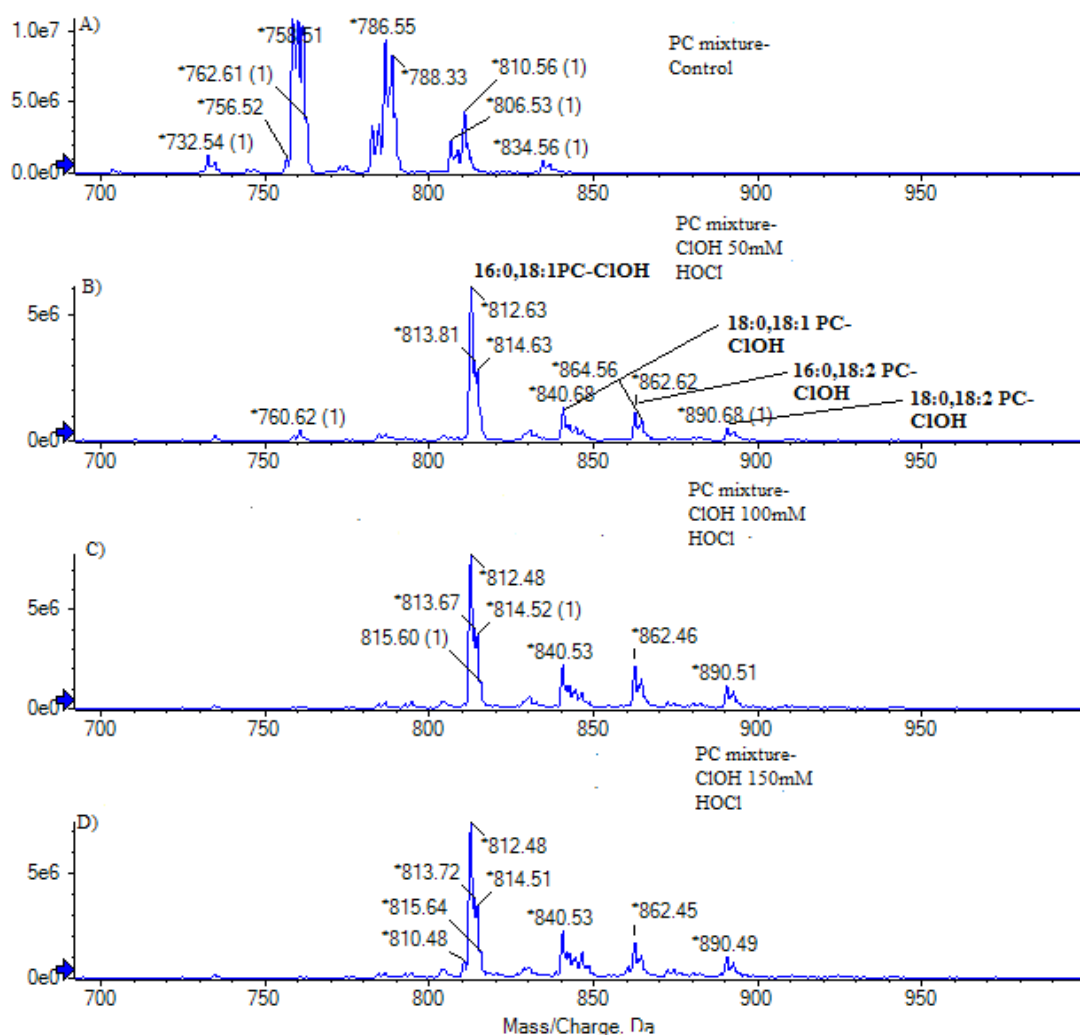


Figure 3.9: PIS for 184 Da spectra by direct infusion of PC mixture and the three test samples oxidised with different concentration of HOCl (50mM, 100mM, and 150mM). A) Control group showing peaks corresponding to 8 different PC molecular species viz. PPPC,POPC,PLPC,SOPC,SLPC,PDPC,SAPC and SDPC respectively. B, C, D) showing mass shift in multiples of 52 Da corresponding to monochlorohydrin formation (52 Da) and 104 Da (bis-chlorohydrin) corresponding to bischlorohydrin formation from PC species having unsaturated fatty acid at sn-2 position with 2 double bonds.

Neutral loss of 36 Da and 38 Da are the selective MS/MS scanning approaches that support identification of chlorohydrins containing ^{35}Cl and ^{37}Cl respectively. In neutral loss scanning, the Q1 analyser and Q3 analyser are set to the scanning mode but with a specific mass offset, which on collision with inert gas in Q2 analyser, only allows those ions to pass through the Q3 analyser that loses neutral masses proportional to the mass offset. Hence, chlorohydrin molecules with ^{35}Cl isotope loses H^{35}Cl on collision with inert gases proportional to 36 Da and chlorohydrin molecules with ^{37}Cl isotope loses H^{37}Cl on collision with inert gases proportional

to 38 Da. The neutral loss scanning for 36 Da and 38 Da was used to support the identification of chlorohydrins as shown in figure 3.10. The peaks in NL 36 scan at m/z 812.6, 862.6, 890.6 and 966.6 corresponded to chlorohydrins with ^{35}Cl and likewise, peaks at m/z 814.6, 864.6, 892.6 and 968.6 corresponds to chlorohydrins with ^{37}Cl . The neutral loss scanning for control sample did not showed any of this peaks thus, supporting the identification.

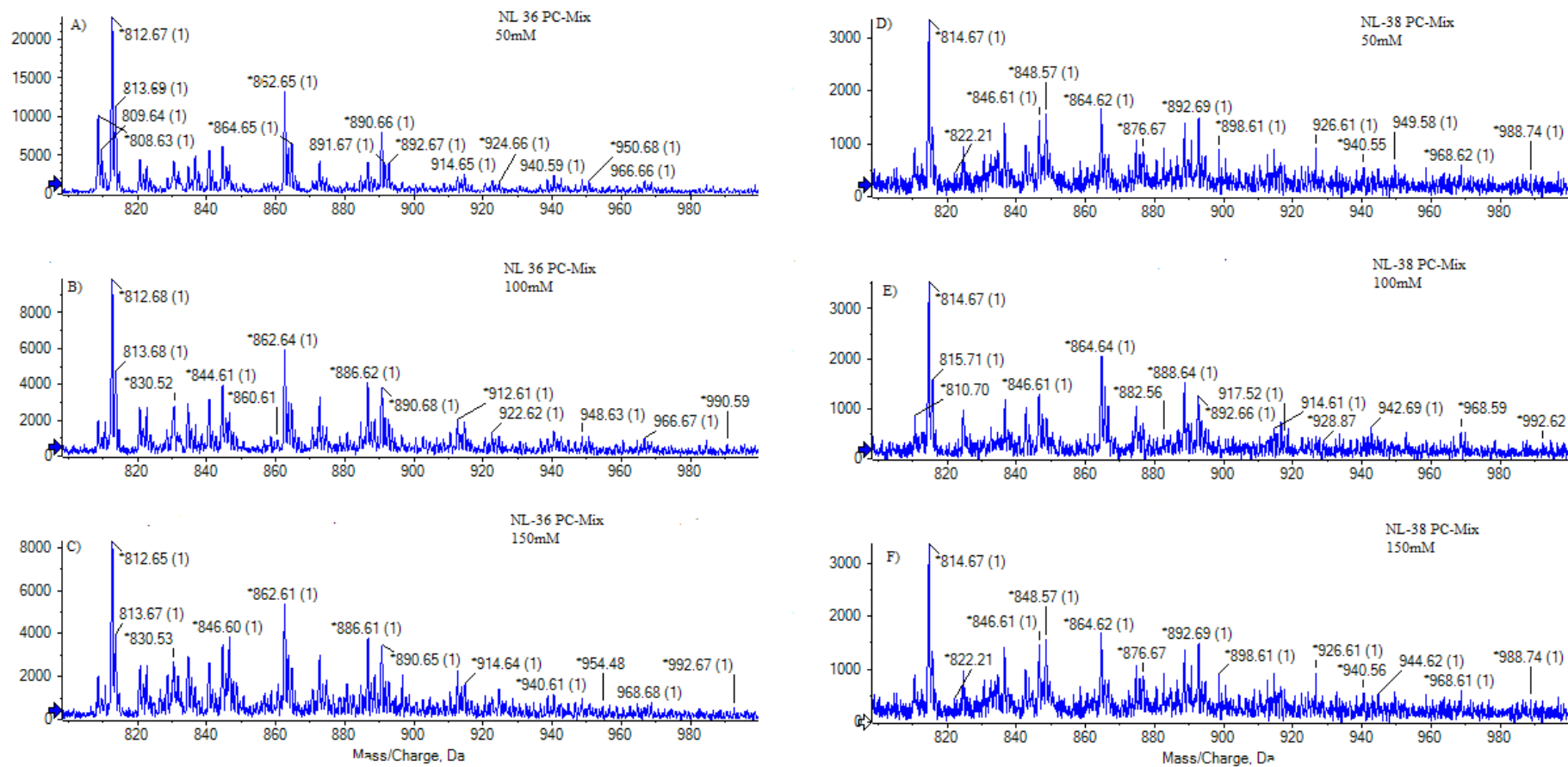


Figure 3.10: MS/MS data for PC mix chlorohydrins showing characterization by neutral loss (NL) of 36 and 38 Da, corresponding to loss of H35Cl and H37Cl respectively. Panels A & D show PC mix ClOH peaks at m/z 812.6, 862.6, 890.6, and 966.6 for HO35Cl and m/z 814.6, 864.6, 892.6, and 968.6 for the and HO37Cl products. Similarly, panel (B&E) and (C & F) are showing similar spectra for 100mM oxidised test sample and 150mM oxidised test sample respectively

3.4.2 Mass spectrometry parameters optimisation for Semi -targeted approaches

The first step in method development is optimising the instrument source and compound parameters to maximise ionisation efficiency, ion transmission and focussing. The parameters critical for semi- targeted approaches like precursor ion scanning (PIS) and neutral loss scanning (NL) are the collision energy (CE), declustering potential, step size, mass range and quadrupole 1 resolution (Q1-R) to improve the duty cycle and % transmission, which are associated with sensitivity gain.

3.4.2.1 Neutral loss of 34 Da to detect hydroperoxide species

Hydroperoxide are the primary oxidation products formed by addition of OOH moiety (+32 Da) to the unsaturated phospholipid species. On collision induced activation (CAD), the species tend to lose a functional group bearing 34 Da mass. This information can be used to selective identify all hydroperoxide species present in a mixture. The figure 3.11 shows the representative spectrum for NL 34 scan acquired at different CE and the graph with the plot of peak height and CE for PLPC-OOH and SLPC-OOH respectively. The peaks at m/z 790.5 and 818.5 are the monohydroperoxide species of PLPC and SLPC respectively.

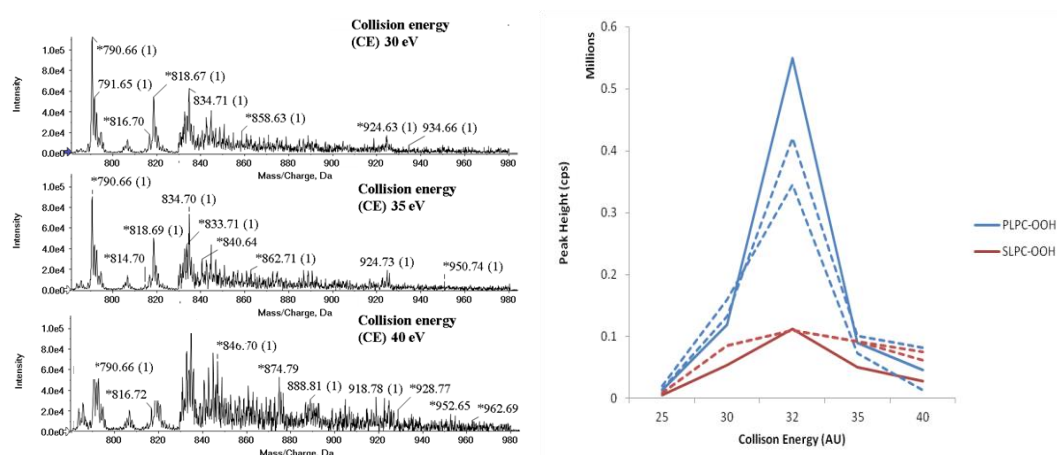


Figure 3.11: Direct infusion mass spectrometry (DIMS) analysis of 10 mM AAPH treated phosphatidylcholine mixture using NL 34 scan for optimisation of compound parameters. Hydroperoxides peaks at increment of 32 Da are observed at m/z 790.5 (758.5 + 32 Da) and 818.5 (786.5 + 32 Da) in 10 mM AAPH treated samples. The 3 panel in the left shows the raw mass spectra . The figure (right hand) shows the plot of peak height and CE for PLPC-OOH and SLPC-OOH respectively with solid and dotted lines representing experimental repeats.

As the CE is ramped from 30 eV to 32eV marked improvement in sensitivity is observed as represented by the peak height of PLPC-OOH and SLPC-OOH in figure 3.11. The dotted and

the solid line represents the experimental repeats. However, as the CE is gradually increased to 40 eV, drop in sensitivity is observed. This suggested that the optimum CE for this scan for hydroperoxide of PC species to be between 30 -35 eV.

Similarly, gain in sensitivity was optimised by changing the Q1 resolution and step size for oxidised PC mixture, keeping the CE constant at 35 eV. The figure 3.12 A & B (and figure 2.2, appendix II) shows the graphical plot of peak height and resolution parameter (A) and step size (B) respectively with oxidised PC mixture acquired using NL 34 scan by direct infusion on a Qtrap 5500 mass spectrometer. The peak height of two analytes: PLPC-OOH and SLPC-OOH is plotted at different MS parameter with solid and dotted lines representing experimental repeats. The data suggests that the step size set to 0.1 Da and low Q1 resolution provided maximal ion counts.

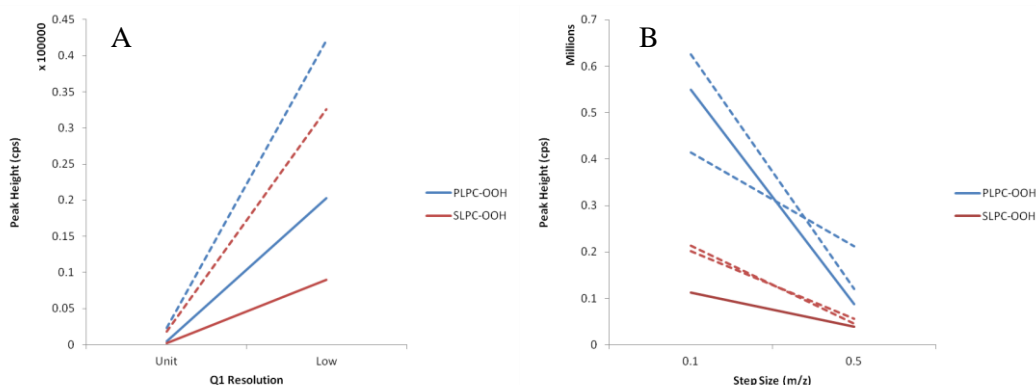


Figure 3.12: Direct infusion mass spectrometry (DIMS) analysis of 10 mM AAPH treated phosphatidylcholine mixture using NL 34 scan for optimisation of compound parameters. Hydroperoxides peaks at increment of 32 Da are observed at m/z 790.5 ($758.5 + 32$ Da) and 818.5 ($786.5 + 32$ Da) in 10 mM AAPH treated samples. The panel shows that the scan with step size of 0.1 and low Q1 resolution maximised ion intensity.

Similarly, NL scan for 34 Da to selectively identify hydroperoxide species of phosphatidylethanolamine (PE) mixture and phosphatidylserine (PS) species was performed. The spectra are shown in appendix II. The figure 3.13 and 3.14 shows the optimisation of CE parameter for NL 34 scan for hydroperoxide species of PE mixture and PS mixture respectively. The peak at m/z 748.5 and 776.5 are the monohydroperoxide species of PLPE-OOH (16:0/18:2 PE) and SLPE-OOH (18:0/18:2 PE) respectively and the CE between 23 eV and 25 eV provides best gain in sensitivity. Likewise, the peak at m/z 822.5 in figure 3.14 relates to the monohydroperoxide species of SOPS (18:0/18:1 PS) and the signal to noise ratio for this species was improved at CE 25 eV.

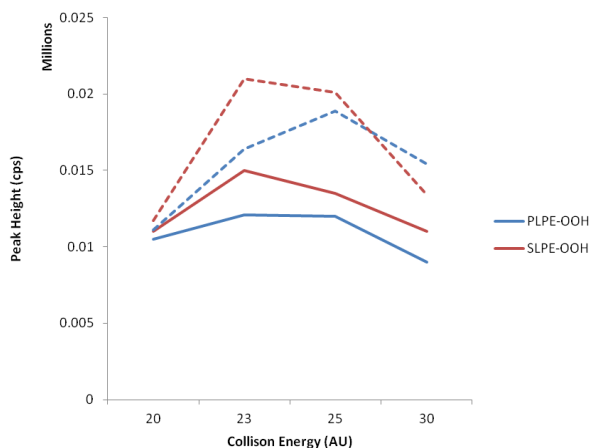


Figure 3.13: Direct infusion mass spectrometry (DIMS) analysis of 10 mM AAPH treated phosphatidylethanolamine (PE) mixture using NL 34 scan for optimisation of compound parameters. Hydroperoxides peaks at increment of 32 Da are observed at m/z 748.5 ($716.5 + 32\text{Da}$) and 776.5 ($744.5 + 32\text{Da}$) in 10 mM AAPH treated samples. The solid and dotted lines represents experimental repeats.

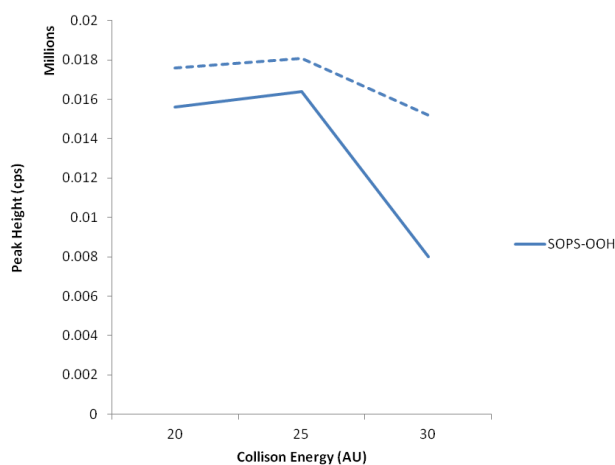


Figure 3.14: Direct infusion mass spectrometry (DIMS) analysis of 10 mM AAPH treated phosphatidylserine (PS) mixture using NL 34 scan for optimisation of compound parameters. Hydroperoxides peaks at increment of 32 Da are observed at m/z 822.5 ($790.5 + 32\text{Da}$) in 10 mM AAPH treated samples. The 3 panel shows that the scan with CE set between 20 -25 eV provided better sensitivity. The solid and dotted lines represents experimental repeats.

3.4.2.2 Head group based scanning approaches

3.4.2.2.1 A) Precursor ion Scan for 184 Da

The signature fragmentation specific to lipid classes have been known since a decade and can be used to selectively identify all species belonging to a specific phospholipid class. Precursor ion scanning of 184 Da is selective for identification of all species belonging to a PC class. To improve the ion count, the CE and declustering potential (DP) were optimised as shown in figure 3.15. The ramping of CE from 10 – 50 eV and DP from 20 – 100 eV was performed and the peak height of representative species were observed. The species were the 16:0 lyso PC (m/z 496.5), POVPC (m/z 594.5), PONPC (m/z 650.5), PLPC-OH (m/z 774.5), SLPC-OOH (m/z 818.5), PLPC (m/z 758.5) and POPC (m/z 760.5). The data suggested that the ion counts were maximal around 40 -45 eV for the CE and no effect of the declustering potential ramping was observed. The representative spectra can be found in the section 2.2 of appendix II.

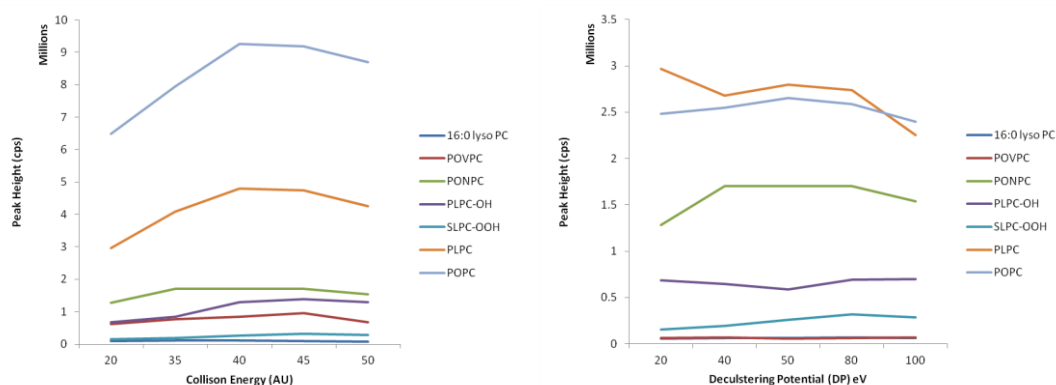


Figure 3.15: Direct infusion mass spectrometry (DIMS) analysis of 10 mM AAPH treated phosphatidylcholine mixture using PIS 184 Da scan for optimisation of collision induced dissociation parameters: Collision Energy (CE) and Declustering Potential (DP) . Peak heights for representative species of PC class were measured at different CE and DP. The peak height profile at different values of DP did not showed any significant difference whereas the ion counts that constituted the peak height of representative species showed improvement at CE range of 40 – 45 eV.

3.4.3 Assessment of different analytical approaches to determine a suitable cross validation method

Individual phosphatidylcholine species like SOPC (18:0/18:1), SLPC (18:0/18:2) and SAPC (18:0/20:4) were oxidised with molar equivalent molar concentrations of hypochlorous acid (HOCl) and analysed using several approaches like Nuclear Magnetic Resonance (NMR) spectroscopy, negative mode mass spectrometry and high resolution mass spectrometry on Q-

TOF instrument to determine a suitable cross validation approach that can be used for all subsequent experiments to confirm the identification and comparative profiling.

3.4.3.1 Direct infusion mass spectrometry in positive mode to confirm the generation of chlorohydrin species

With the objective of developing a better methodology for analysis of chlorohydrins, simple in-vitro model systems like standard phospholipids that are commercially available and are found naturally in mammalian cell membranes were oxidised with molar equivalent concentration of hypochlorous acid to generate chlorohydrins. The analysis was performed in positive ion mode by direct infusion of the diluted solution of the unmodified and chlorohydrin lipids.

Analysis of 3 model system of standard lipids namely SOPC, SLPC and SAPC gave abundant peak in MS spectra corresponding to $(M+H)^+$ ions at m/z 788.5, 786.5 and 810.5 as shown in figure 3.16. The chlorohydrin peaks in the test spectra were observed at increment of 52 Da corresponding to addition of a single HOCl moiety. SOPC have a single double bond hence, only a monochlorohydrin is formed at an increment of 52 Da at m/z 840.5. The chlorohydrin of SLPC was observed at m/z 890.5 that corresponded to the addition of two HOCl groups with increment of 104 Da to the native mass. For SAPC having four double bonds, there is a possibility of forming mono, bis, tris and tetra chlorohydrin with increment of 52 Da, 104 Da, 156 Da and 208 Da respectively. However, as observed in the spectra of SAPC-CIOH in the figure 1-16, only a peak at m/z 966.5 corresponding to tris-chlorohydrin is apparent.

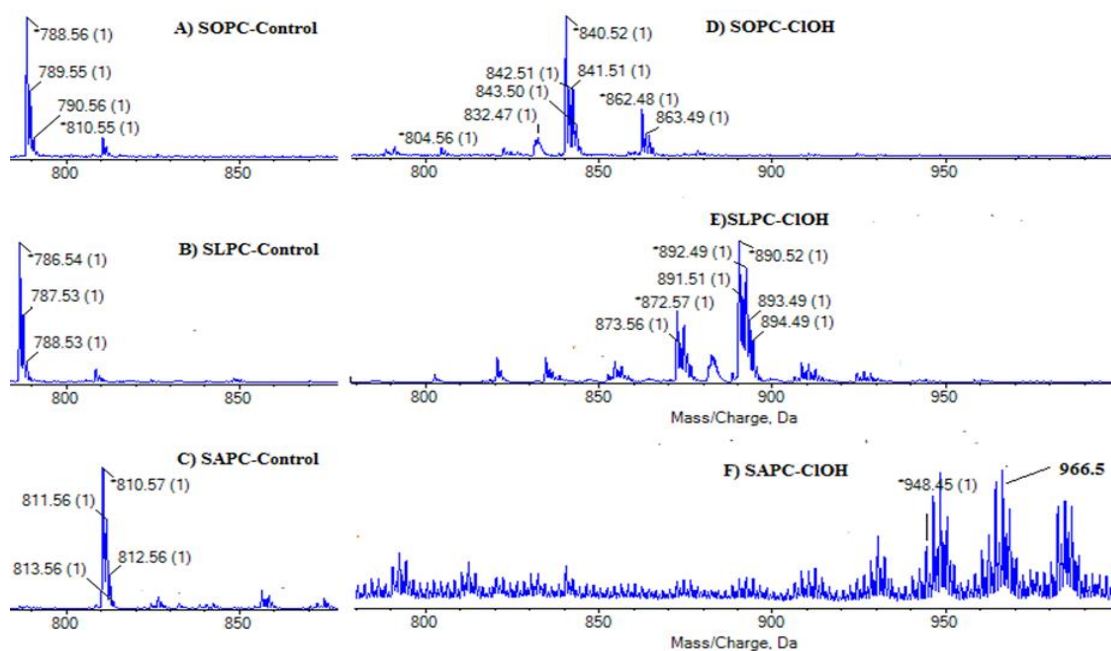


Figure 3.16: ESI-MS spectra of SOPC, SLPC, and SAPC showing abundant peak corresponding to their $(M+H)^+$ ions at 788.5, 786.5 and 810.5 respectively, B) showing their chlorohydrins at increment in multiples of 52Da (per addition of chlorohydrin moiety). SOPC-C1OH (+52Da) at m/z 840.5, SLPC-diC1OH (+104Da) at m/z 890.5 and SAPC-trisC1OH (+156Da) at m/z 966.5. This experiment was carried by direct infusion of the 1000 fold diluted lipid extract at $5\mu\text{l}/\text{minute}$ on AbSciex 5500 QTrap instrument.

Neutral loss of 36 Da and neutral loss 38 Da were performed to confirm the formation of chlorohydrins as observed in figure 3.17. As observed in figure 3.17, the neutral loss for 36 Da for SOPC-C1OH, SLPC-C1OH and SAPC-C1OH samples showed corresponding chlorohydrin peaks at m/z 840.5, 890.5 and 966.5 respectively. Other peaks observed at m/z 822.5 in SOPC-C1OH spectra, m/z 872.5 in SLPC-C1OH spectra and at m/z 948.5 in SAPC-C1OH are the dehydrated peak of the chlorohydrin molecules with loss of water molecule (- 18 Da). Other spectra in figure 3.17 (B, D and F) for the neutral loss of 38 Da, showed the $M+2$ peak corresponding to the loss of H^{37}Cl molecule at m/z 842.5, 892.5 and 968.5 respectively in SOPC-C1OH, SLPC-C1OH and SAPC-C1OH spectra.

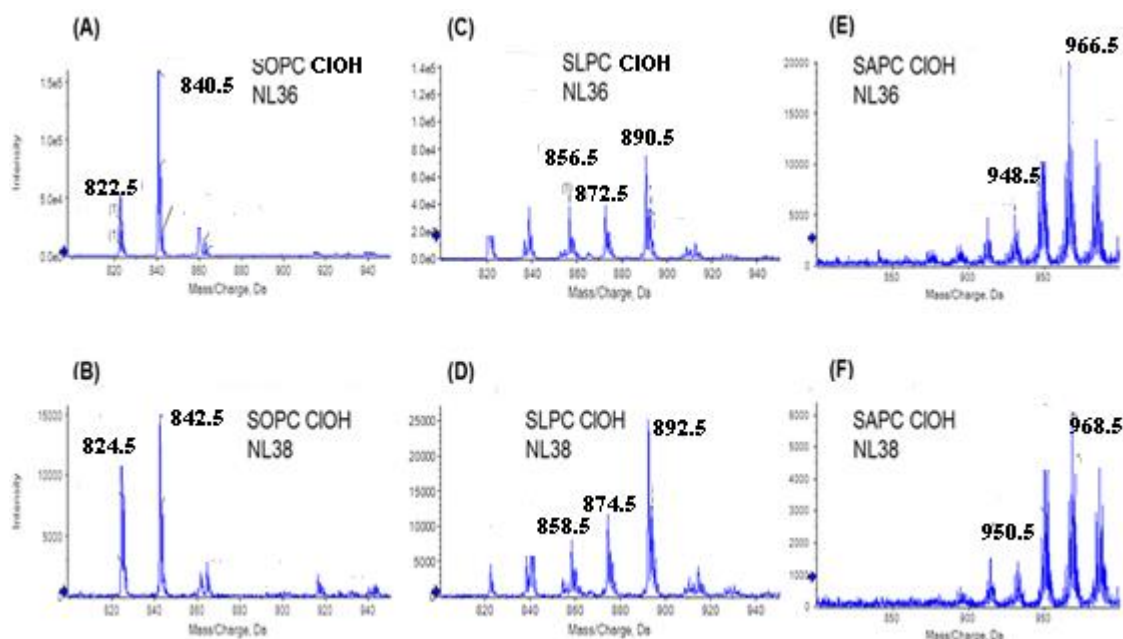


Figure 3.17: MS/MS data for phospholipid chlorohydrins showing characterization by neutral loss (NL) of 36 and 38 Da, corresponding to loss of H₃₅Cl and H₃₇Cl respectively. Panels A & B show SOPC mono-chlorohydrin at m/z 840 and 842 respectively for the HO₃₅Cl and HO₃₇Cl products. Panels C & D show SLPC chlorohydrins with the bis-chlorohydrins at m/z 890 and 892. Panels E & F show multiple SAPC chlorohydrins, although the tetra-chlorohydrin cannot be observed as the top instrument m/z is 1000. All chlorohydrins show the presence of dehydration products under the fragmentation conditions used, as described previously. No significant formation of lysolipids was observed with SOPC and SLPC, but a small amount (~10%) of lysolipid at m/z 524 did occur. MS analysis was carried out using direct infusion onto an ABSciex 5500QTrap, essentially as described previously.

These identifications were confirmed by performing product ion scanning of individual species. The MS/MS fragmentation spectra of chlorohydrin peaks at m/z 840.5 (SOPC-CIOH) and m/z 890.5 (SLPC-2(CIOH)) showed the lysolipid peaks (m/z 506 and 524) retaining the stearate at sn-1 position, which corresponded to the dehydrated 18:0 lysoPC and the 18:0 lysoPC respectively (figure 3.18). Also, it showed the lysolipid peak retaining the chlorohydrin modified chain at m/z 556 and 574 for the SOPC-CIOH MS/MS spectra (m/z 840.5) and at m/z 606.5 and 624.5 for the SLPC-CIOH spectra (m/z 890.5). Also, both parent ions showed characteristic loss of water (18 Da) and HCl (36 Da) respectively at 822.5 and 804.5 for the SLPC-CIOH parent ion and at 854.5 and 872.5 respectively. These fragmentation spectra that strengthened the identification of the chlorohydrin formation, showing the lysolipid peaks retaining the chlorohydrin modified chain, has not been reported yet and was a novel finding.

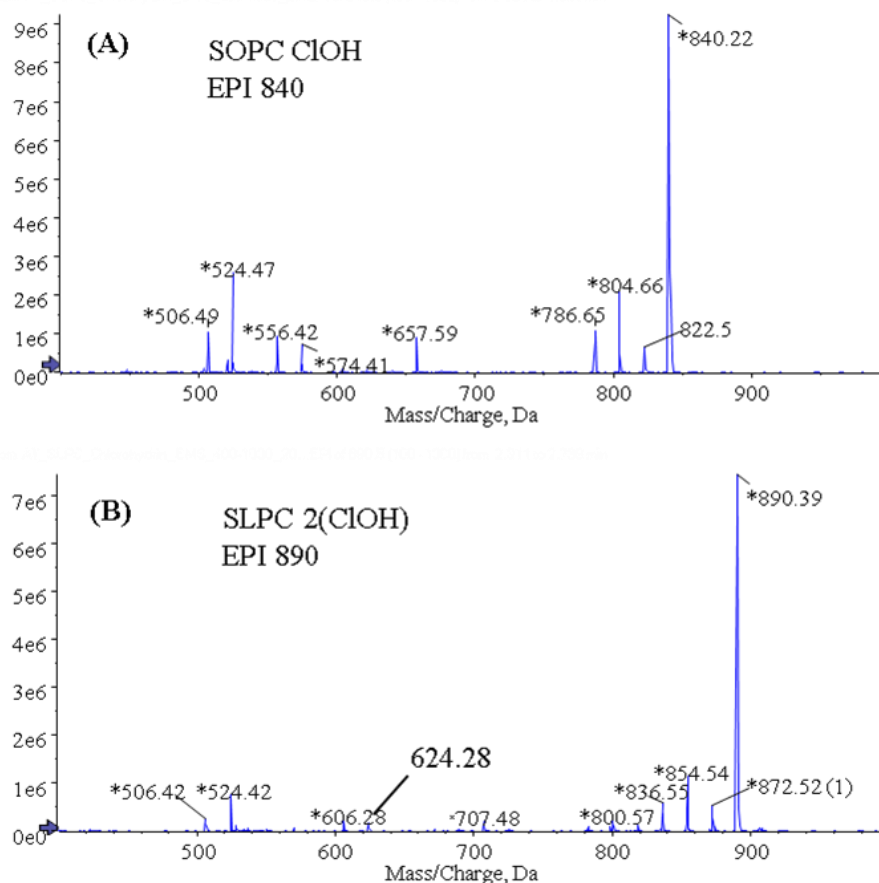


Figure 3.18: MSMS fragmentation profile of SOPC mono- chlorohydrin at m/z 840.5 (A) and SLPC bis-chlorohydrin at m/z 890.5 (B). SOPC chlorohydrin shows fragment ions at m/z 524 and 506, corresponding to the lysolipid retaining stearate, and peaks at m/z 574 and 556 for lysolipid retaining the chlorohydrin modified chain. SLPC chlorohydrin shows the same fragment ions for the lysolipid retaining stearate, and peaks at m/z 624 and 606 for lysolipid retaining the bis-chlorohydrin modified chain. Both parent ions also show characteristic loss of water (18 Da) and HCl (36 Da). MS analysis was carried out using direct infusion onto an ABSciex 5500QTrap, essentially as described previously.

3.4.3.2 ^1H -Nuclear Magnetic Spectroscopy (NMR) of chlorohydrins

NMR analysis of SOPC, SLPC, and SAPC chlorohydrins was performed to confirm and validate the mass spectrometric results of formation of chlorohydrins. The proton attached to allylic carbon (adjacent to the olefinic carbon) and bisallylic carbon (carbon atom conjugating two-olefinic carbon atom) have electron deficient environments due to the double bond in the vicinity and are deshielded, and are observed downfield in the NMR spectra along with the vinylic protons. Formation of chlorohydrins was confirmed by loss of signals due to these protons in the downfield region, which were apparent in the unmodified lipids (figure 3.19).

For instance, in SAPC-control (red spectrum in figure 3.19, c), the peak at 5.3ppm related to the vinyl proton, peak at 2.8 ppm corresponded to the bisallylic proton and peak at 2.04 ppm observed was due to the allylic protons which were absent in the SAPC-CIOH spectra (green spectra, 3.19, c). Moreover, additional peak appeared around 1.8ppm and 3.8ppm that corresponded to the formation of new bonds near these protons.

This experiment was performed on a 250 Mhz Bruker NMR instrument and owing to low magnetic strength of the instrument, either the number of scans had to be quadrupled or the loading amount had to be doubled to achieve better signal to noise ratio and integration of these peaks. Moreover, these were relatively simple samples and the instrument could not have been able to handle complex biological samples where the amount of chlorohydrins can differ in orders of magnitude and can be very low, and therefore, other approaches were investigated.



Figure 3.19: $^1\text{H-NMR}$ spectra showing the formation of chlorohydrins from SOPC (a), SLPC (b) and SAPC (c). In each panel, native lipid is the bottom, red spectrum and chlorohydrin is the top, blue spectrum. In the native spectra, the multiplet labelled (1) at 5.3 ppm corresponds to the vinyl protons ($\text{CH}=\text{CH}$), the multiplet (2) at 2.8 ppm is bis-allylic protons ($=\text{CCH}_2\text{C}=\text{C}$) which is absent in SOPC, and the multiplet (3) at 2.04 ppm corresponds to allylic protons ($\text{CH}_2\text{C}=\text{C}$). These signals all disappear on formation of chlorohydrins indicating the loss of the double bonds, and other signals corresponding to CHs and CH_2 s adjacent to the substituted carbons appear (4 & 5). Phospholipids were prepared in 1:1:2:10 pyridine- d_5 : DCI in D_2O : methanol- d_4 : chloroform- d ; spectra were acquired at 270 MHz and referenced to tetramethylsilane (TMS) at 0 ppm. (Printed with permission from Elsevier-permission letter can be viewed in the Appendix II section of the thesis)

3.4.3.3 Negative mode analysis of chlorohydrin species

The SOPC-CIOH, SLPC-CIOH and SAPC-CIOH and their native lipid species were also analysed in negative mode using an ammonium acetate solvent system (methanol: 10mM ammonium acetate (90:10)) that formed $(M+\text{acetate})^-$ adduct with increment of 58 Da to the neutral mass. Also, $(M-\text{methyl})^-$ ion corresponding to loss of 15 Da mass was observed in the general survey spectra (figure 3.20). The peak at m/z 846.5 and 772.5 corresponding to the acetate adduct and $(M-15)^-$ ion, observed for the SOPC-control spectra. Likewise, the spectra for SLPC showed peak at m/z 844.5 and 770.5 that are related to acetate adduct and the peak with loss of methylene respectively. The SAPC-control spectra also showed the similar peaks at m/z 868.5 and 795.5 respectively. Similarly, the spectra of the chlorohydrins in negative mode showed similar peaks as acetate adduct and with loss of methylene (-15 Da).

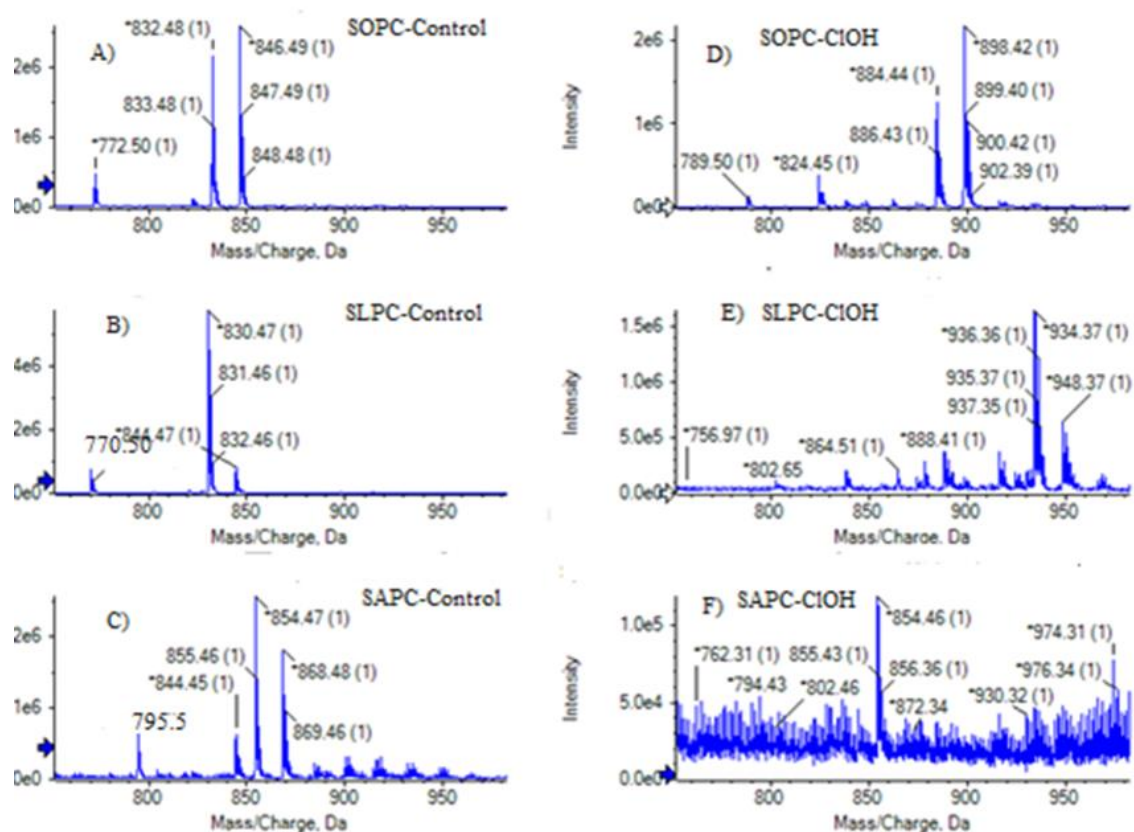


Figure 3.20: ESI-MS analysis of SOPC, SLPC, and SAPC chlorohydrins in negative mode using ammonium acetate buffer solvent system. All peaks are observed as $(M+\text{acetate})^-$ ion (+58Da). A-C) shows SOPC, SLPC and SAPC control at m/z 846.5, 844.5, and 868.5 respectively. Also, $(M-15)^-$ peak is observed at m/z 772.5, 770.5, and 795.5 respectively. D-F) spectra of SOPC-CIOH and SLPC-CIOH at m/z 898.5 and 948.5 respectively. However, the top limit of the Qtrap spectrometer is 1000 m/z , it is not possible to observe ion for tris-chlorohydrin of SAPC with acetate adduct at m/z 1024.5

The fragmentation profile of the acetate adducts in negative mode showed peaks corresponding to the fatty acid anions corresponding to the saturated chain at sn-1 position (stearate anion) and unsaturated fatty acid at sn-2 anion for control samples (figure 3.21). For example, the EPI scan of m/z 846.5 showed abundant ion at m/z 283.3 and 281.3 corresponding to stearic acid at sn-1 position and oleic acid at sn-2 position. The EPI scan of m/z 844.5 (SLPC-control) showed fatty acid ion peaks at m/z 283.4 (stearate ion) and 279.4 (linoleate ion) and for the SAPC-control (m/z 868.5), the fatty acid anion peaks were observed at m/z 283.4 and 303.4 corresponding to stearate and arachidonate anion respectively. Moreover, the peak at m/z 259.4 was observed in the fragmentation spectra of SAPC-control showing characteristic loss of CO₂ (44 Da) from the arachidonate anion.

The SOPC-CIOH fragmentation spectra of m/z 898.5 showed abundant ion at m/z 283.3 corresponding to the stearic acid anion, and at m/z 297.42 that showed the fatty acid anion retaining the chlorohydrin modified chain with loss of HCl (36 Da). Similarly, SLPC-CIOH fragmentation spectra of parent ion 948.5, showed fatty acid anion peak at m/z 283.4 (stearate ion) and chlorohydrin modified chain at m/z 311.4 with loss of two molecules of HCl (72 Da) proportional to the number of chlorohydrin moieties added to the unsaturated fatty acid chain at sn-2 position with loss of double bond. Likewise, SAPC-CIOH fragmentation spectra of parent ion m/z 1024.5 showed fatty acid anion peak at 283.4 (stearate ion) and at m/z 351.5 corresponding to the chlorohydrin modified chain with loss of three molecules of HCl (108 Da) that is proportional to the number of chlorohydrin moieties added on reaction with HOCl (figure 3.21).

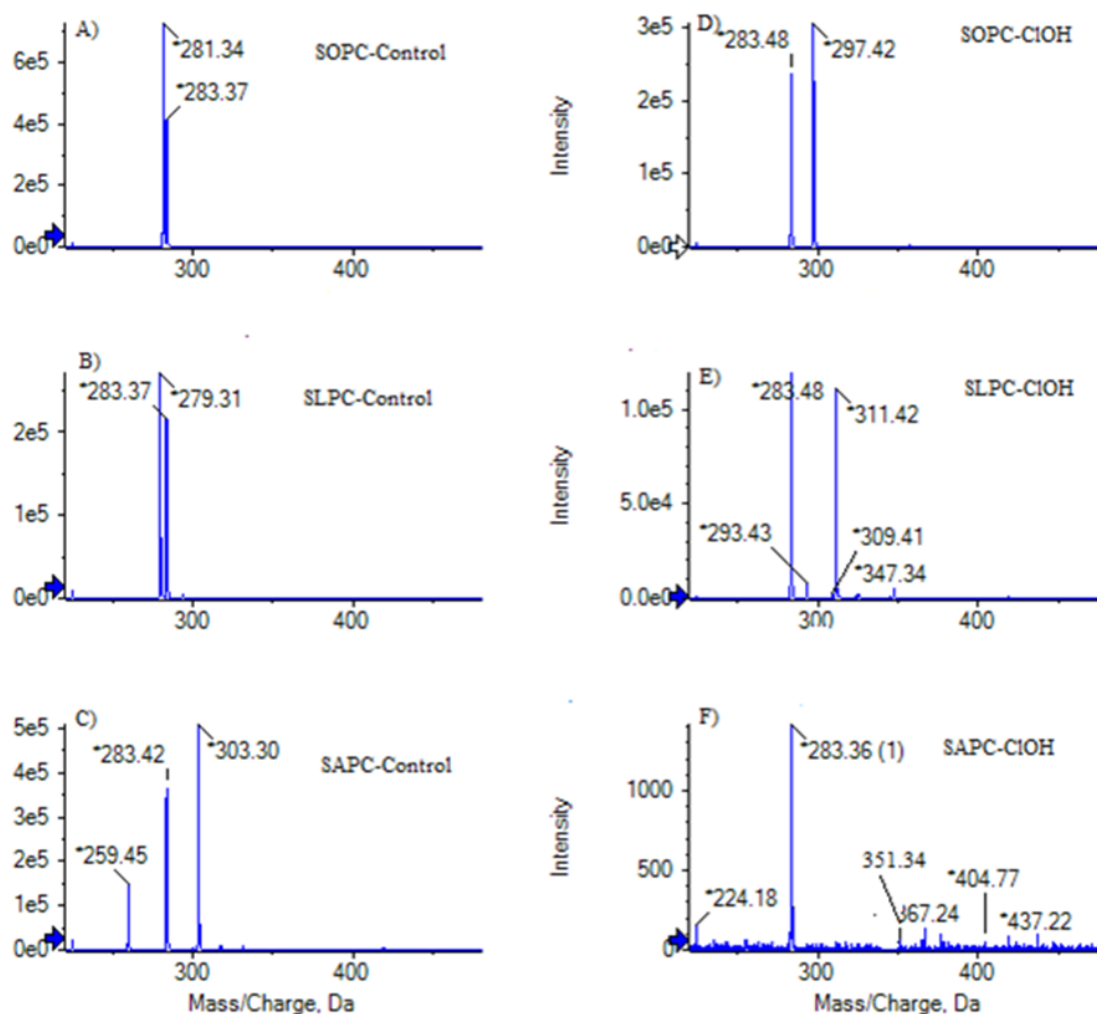


Figure 3.21: MS/MS fragmentation spectra of acetate adducts of SOPC, SLPC and SAPC and their respective chlorohydrins in negative mode direct infusion MS. A-C) shows EPI scanning spectra for control samples in m/z range 200-450 providing information about the fatty acid esterified at sn-1 and sn-2 position. D-F) EPI scanning of SOPC, SLPC, and SAPC chlorohydrins supported the formation of chlorohydrins. The experiment was performed on ABSciex 5500 Qtrap instrument.

3.4.3.4 *Liquid-chromatography mass spectrometry (LC-MS) analysis of chlorohydrin species on Qtrap 5500 mass spectrometer using targeted approaches*

The data so far was qualitative in nature and did not address the quantification and comparison of these species in different species. Therefore, we commenced on adding another layer of parameter profiling: retention time to assist in identification and quantification.

LC-MS analysis of SOPC, SLPC and SAPC control and chlorohydrin species was performed by coupling the Dionex 3000 UHPLC system to the Qtrap 500 MS with management of the instruments performed using Chromleon and Analyst softwares. The Dionex monolith column (Proswift RP -4H, 1x 250 mm) with phenyl surface chemistry linked to divinyl

benzene polystyrene polymer base was tested for reverse phase chromatographic separation along with binary solvent system involving methanol and water with buffering provided by 5mM Ammonium formate and 0.1 % formic acid. An odd chain based phosphatidylcholine species (13:0 PC) was used as an internal standard to correct for technical variation. The figure 3.22 shows the average relative abundance level and retention time of native, chlorohydrin and oxidised species (N=3) in the form of heat map in control and HOCl treated SOPC, SLPC and SACP samples.

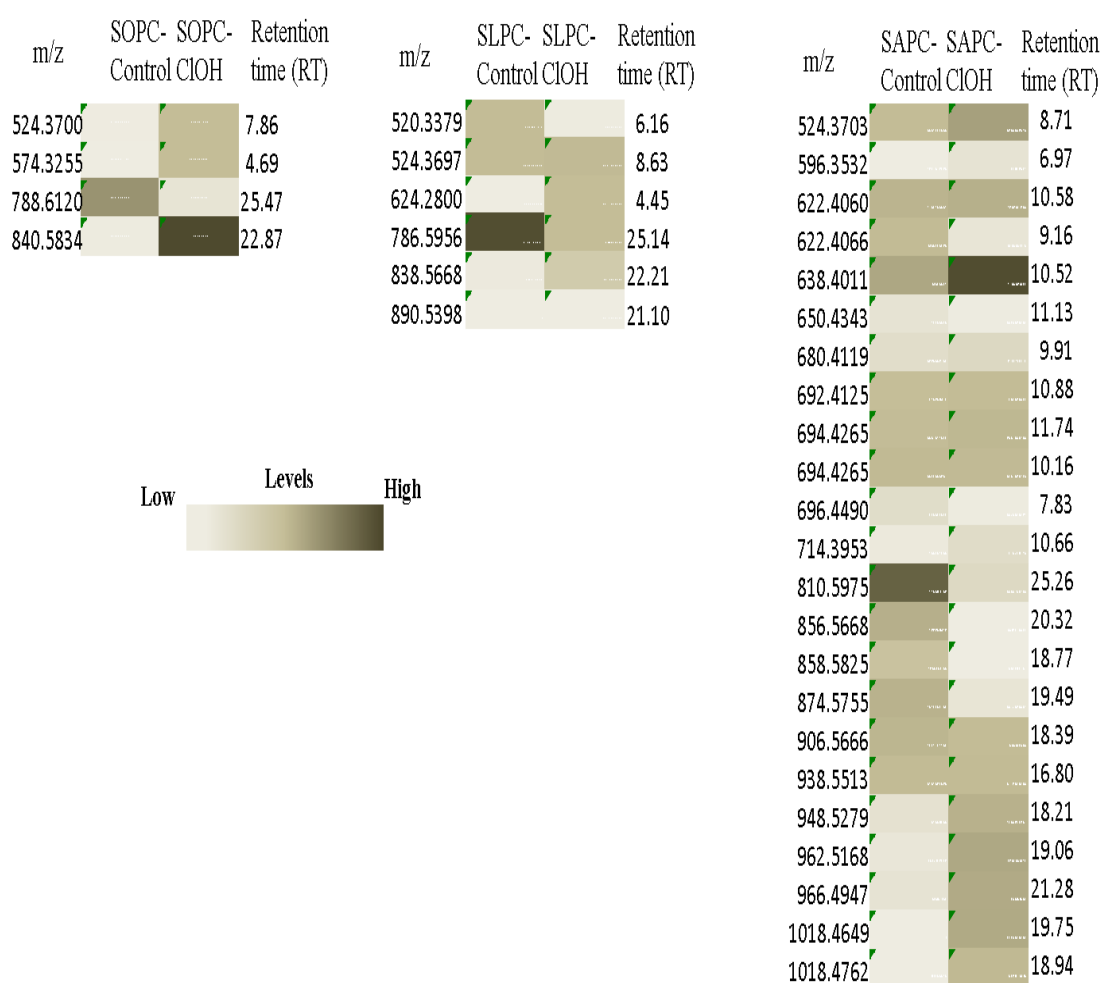


Figure 3.22: LC-MS analysis of HOCl treated SOPC,SLPC and SACP samples using monolith column for chromatographic separation and NL 36, NL 38 and IDA based product ion scanning for identification of species on Absciex Qtrap 5500 mass spectrometer (N=3). The individual peak areas were calculated by generating extracted ion chromatogram (XIC) for individual species, normalised using peak area of internal standard (13:0 /PC) added before extraction step and represented as heat map where light colour corresponds to low abundance level and dark colour corresponds to relative high abundance.

The abundance level is proportional to colour intensity and the data displaying the average normalised peak area of three replicates suggests relatively higher levels of chlorohydrin species in treated samples compared to control samples. Moreover, as the complexity of the model system defined by the level of unsaturation increases from SOPC to SAPC, the number of species identified increases along with some oxidised species identified in samples with polyunsaturated species (SAPC), which could be due to adventitious oxidation because of exposure to air during handling. Moreover, the lysophospholipid species, which are species that lost either fatty acyl chain and may retain the oxidised/chlorinated moieties, were also observed. For example, the peak observed at m/z 574.32 is the lyso species that has lost the fatty acyl chain (18:0 carbon chain), which was esterified at sn-1 position, and have retained the chlorohydrin group. Moreover, some peroxidised species in the form of secondary fragmented products and long chain oxidation products were observed in treated SAPC samples along with chlorohydrin species. This may be due to the adventitious oxidation due to exposure to air and/or peroxidation in response to hypochlorous acid. However, the predominantly species that are formed by treatment with hypochlorous acid is the chlorohydrin species. The peak area for individual species was calculated in all the replicates by generating the extracted ion chromatogram (XIC), corrected for technical variation using the peak area of internal standard that was added to each sample in equal amount prior to extraction and statistical analysis was performed using averaged peak area for all species on graph prism by comparing the corrected peak area values across samples.

3.4.3.5 High resolution LC-MS analysis of chlorohydrin species on Absciex 5600 Q-TOF mass spectrometer and data analysis using Progenesis QI

The same method was transferred onto the high resolution QTOF mass spectrometer and the parameters for general TOF MS survey scan were optimised like the accumulation time was set to 500 ms for QTOF scan and 250 ms for MS/MS scans. All other parameters were similar to that optimised for Qtrap 5500 MS. For data analysis, mass tolerance was set to 5 ppm to confirm high accuracy in identification. Data analysis was performed using Progenesis QI software by performing chromatographic alignment, peak picking using co-detection algorithm to minimise the effect of missing values, deconvolution of all adducts and identification based on search and matching of MS and MS/MS profile against in house built database that consisted of structures of all possible chlorohydrin and oxidised species and native species present in eukaryotes. The table 3.4, summarise the findings of automated data analysis of SOPC, SLPC

and SACP samples treated with molar equivalents of hypochlorous acid, generated on high resolution QTOF instrument.

Table 3.4: Automated data analysis using Progenesis QI of high resolution data of chlorohydrin samples of SOPC (a), SLPC (b) and SACP (c) respectively generated on Absciex 5600 QTOF instrument. The table shows the retention time, statistical analysis p-value post ANOVA, accepted identification, mass error and the sample where high levels was found.

a) SOPC						
Experimental m/z	Retention time (RT)	ANOVA (p)	Accepted compound ID	Formula	Mass Error (ppm)	Highest Mean
524.3700	7.86	3.0E-05	PC(18:0/0:0)	C26H54NO7P	-2.05	treated
574.3255	4.69	3.5E-07	PC(0:0/18:1-CIOH)	C26H53NO8PCI	-2.60	treated
788.6120	25.47	1.4E-07	SOPC	C44H86NO8P	-5.56	control
840.5834	22.87	4.8E-08	SOPC-CIOH	C44H87CINO9P	-5.44	treated
b) SLPC						
520.3379	6.16	7.6E-07	PC(18:2(9Z,12Z)/0:0)	C26H50NO7P	-3.58	control
524.3697	8.63	1.2E-01	PC(18:0/0:0)	C26H54NO7P	-2.65	treated
624.2800	4.45	3.9E-07	PC(0:0/18:2-diCIOH)	C26H52NO9PCI2	-4.70	treated
786.5956	25.14	4.0E-06	SLPC	C44H84NO8P	-6.52	control
838.5668	22.21	6.0E-05	SLPC-CIOH	C44H85CINO9P	-6.58	treated
890.5398	21.10	3.1E-04	SLPC-diCIOH	C44H86C12NO10P	-4.60	treated
c) SACP						
524.3703	8.71	5.7E-05	PC(18:0/0:0)	C26H54NO7P	-1.47	treated
596.3532	6.97	5.9E-03	Unknown			
622.4060	10.58	3.9E-01	SOVPC	C31H60NO9P	-2.99	treated
638.4011	10.52	6.1E-06	SGPC	C31H60NO10P	-2.54	treated
650.4343	11.13	1.9E-01	(7'-oxo heptanoic acid) SPC	C33H64NO9P	-7.43	treated
680.4119	9.91	2.9E-01	Unknown			
692.4125	10.88	1.5E-01	(5'-oxo,6-octenedioicacid) SPC	C34H62NO11P	-1.25	treated
694.4265	11.74	7.5E-02	(5'-hydroxy,6-octenedioicacid) SPC	C34H64NO11P	-3.59	treated
696.4490	7.83	1.8E-02	Unknown			
810.5975	25.26	4.5E-08	SAPC	C46H84NO8P	-3.98	control
856.5668	20.32	3.3E-06	SEIPC	C46H82NO11P	-3.59	
858.5825	18.77	1.9E-05	D2isoprostane-SPC	C46H84NO11P	-3.45	control
874.5755	19.49	2.3E-06	SAPC-diOOH	C46H84NO12P	-5.60	control
906.5666	18.39	4.3E-05	SAPC-triOOH	C46H84NO14P	-4.00	treated
938.5513	16.80	2.2E-01	SAPC-tetraOOH	C46H84NO16P	-9.30	treated
948.5279	18.21	2.0E-06	Unknown			
962.5168	19.06	8.5E-07	Unknown			
966.4947	21.28	5.2E-08	SAPC-triCIOH	C46H87NO11PCI3	-2.50	treated
1018.4649	19.75	2.9E-11	SAPC-tetraCIOH	C46H88NO12PCI4	-2.30	treated

¹ Nomenclature PC phosphatidylcholine; Letter S, O, L and A corresponds to Stearoyl, Oleoyl, Linoleoyl and Arachidonyl fatty acyl chain; numerical type nomenclature is used for lysophospholipids that lost 1 fatty acyl chain. For example: in PC (18:0/0:0), first two digit corresponds to the number of carbon fatty acyl chain; the next digit corresponds to the number of double bonds and similarly the other digits post hyphen corresponds to the similar chain at sn-2 position; SEIPC corresponds to eoxyisoprostane compound with stearoyl chain and other higher hydroperoxides and chlorohydrin species are designated with OOH and CIOH with di, tri and tetra

corresponding to number of these functional groups associated with the structure. Please see abbreviation section for more details.

Similar results were obtained when relatively complex mixture of PC species was treated with HOCl. The data can be viewed in the appendix II section.

3.4.4 LC-MS analysis of peroxidation products of SOPC, SLPC and SAPC treated with 10 mM AAPH

3.4.4.1 Semi-targeted approach analysis on Qtrap 5500

Non- enzymatic oxidation of SOPC, SLPC and SAPC using 10 mM AAPH and incubation for 24 hrs formed variety of oxidised species. The chromatographic separation using monolith column, and detection on Q-trap mass spectrometer using targeted approaches like PIS for 184 Da for all oxidised and native species of phosphatidylcholine class, and NL 34 scan for detection of hydroperoxides in conjunction with IDA based MS/MS scans for structural information, enabled identification of more than 100 oxidised species. The figure 3.23 (A & B) and 3.24 illustrates the formation and up regulation of short chain oxidation products that eluted between 5-14 minutes, and long chain oxidation products eluting between 18-22 minutes, in oxidised sample, compared to control sample. The figure 3.23 illustrates the unequivocal identification of hydroperoxide species that can be achieved by NL 34 scanning. Multiple peaks may represent isobaric compounds with different chemical composition or may correspond to multiple positional isomers of the same OxPC, which elutes as clusters of poorly separated peaks. As an example illustrated in figure 3.23 (C & D), the native di-unsaturated phosphatidylcholine: 1-plamitoyl, 2-linoleoyl-phosphatidylcholine (PLPC, m/z 758.5) after oxidation forms a di-hydroxide species, m/z 790.5 (by addition of 2(OH)), and a monohydroperoxide species, m/z 790.5 (by addition of OOH). The native phospahtidylcholine species (di-stearoyl-phosphatidylcholine, m/z 790.5) is also isobaric to the above mentioned oxidation species and these all species were observed in the PIS 184 scan. While the XIC for m/z 790.5 from PIS 184 scan showed 3 chromatographic peaks at 17.5 minutes, 19.5 minutes and 25.5 minutes, the XIC for m/z 790.5 in NL 34 scan showed a single peak at 19.5 minutes. Thus, NL 34 scans can be used to identify all hydroperoxide species. Without the chromatographic separation, the resolution requirement to separate these two isobaric peaks at m/z 790.5608 (PLPC-2(OH)) and 790.5563 (PLPC-OOH) would be 100,000, which would had been possible only on fourier transform- ion cyclotron instruments.

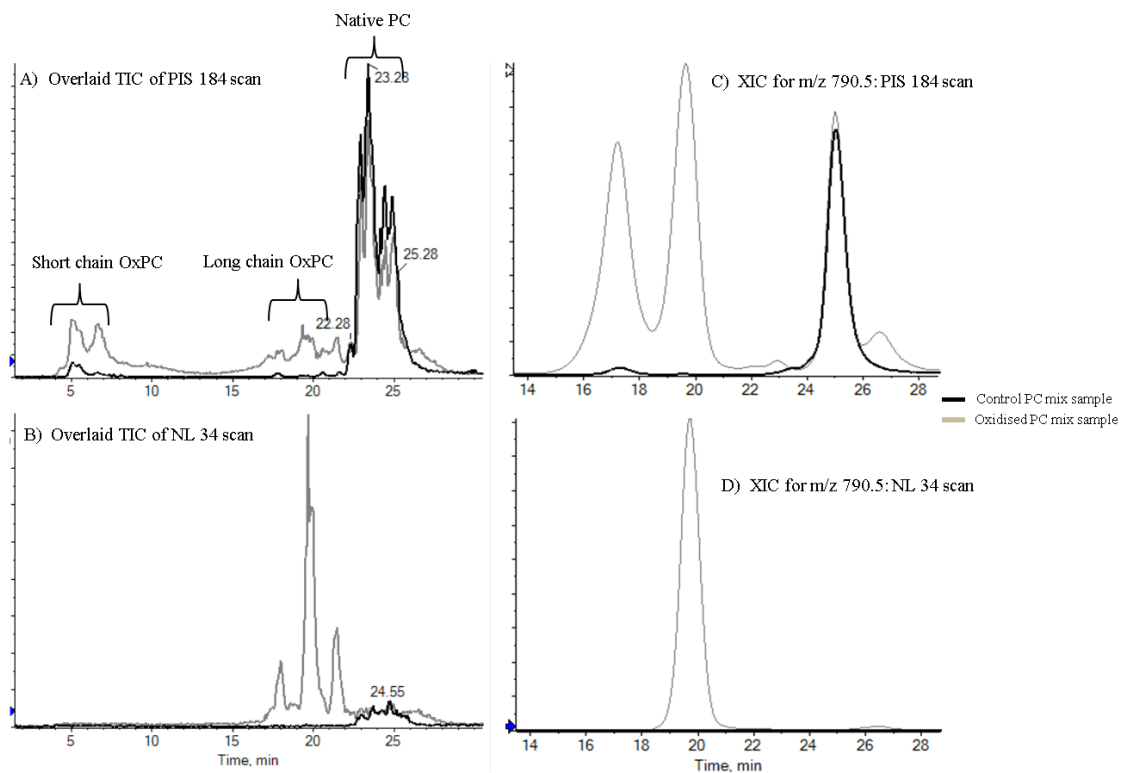


Figure 3.23: Overlaid Total ion chromatogram (TIC) of PIS 184 scan (A) and NL 34 scan (B) for control (black) and oxidised PC mix sample (grey). It illustrates formation and early elution of short chain and long chain oxidised PC species compared to native PC species. The figure (C & D) are overlaid XIC for m/z 790.5 from PIS 184 scan (C) and NL 34 scan (D) that illustrates the unequivocal identification of hydroperoxide species by NL 34 scan. This experiment was performed using monolith column for separation and Qtrap MS with targeted approaches for detection.

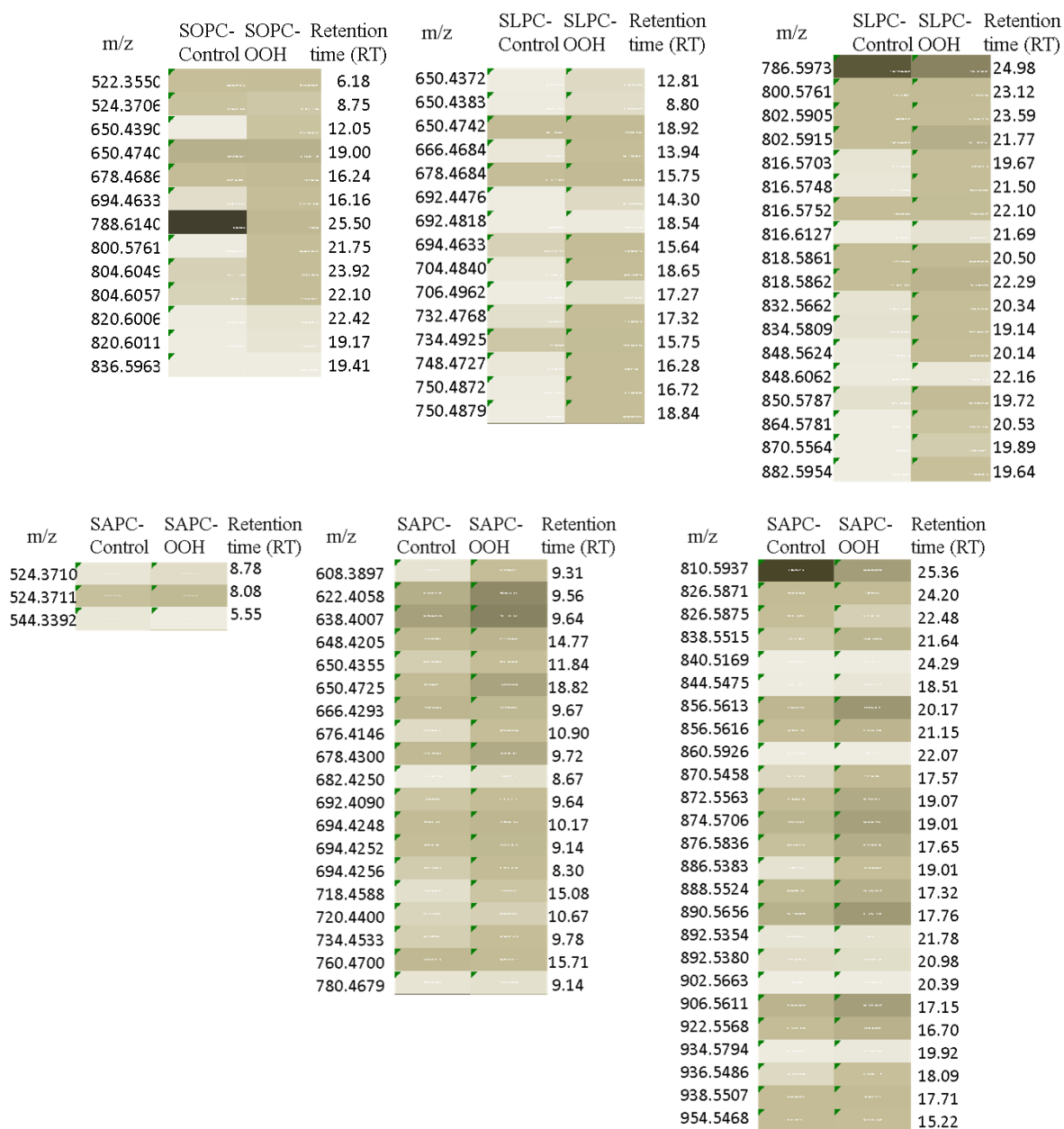


Figure 3.24: LC-MS analysis of 10 mM AAPH treated SOPC,SLPC and SACP samples using monolith column for chromatographic separation and NL 34 Da, PIS 184 Da and IDA based product ion scanning for identification of species on Absciex Qtrap 5500 mass spectrometer (N=3). The individual peak areas were calculated by generating extracted ion chromatogram (XIC) for individual species, normalised using peak area of internal standard (13:0 /PC) added before extraction step and represented as heat map where light colour corresponds to low abundance level and dark colour corresponds to relative high abundance.

As expected, due to oxidative fragmentation of oxidised fatty acid residue or addition of oxygen, the OxPC species eluted from the reverse-phased monolithic column significantly earlier as compared to the native phospholipids. We were able to detect more than 100 different oxidised species using our method based on targeted approaches, which were up regulated in the oxidised sample, compared to control sample (figure 3.24). The XIC's were generated for the nominal masses of all previously identified OxPC species and peak area was measured. The experiment was repeated three times, measured peak area was averaged and normalised to the

peak area of the internal standard and heat map was generated for mean peak area of all species in control and oxidised sample, representing colour coded abundance. The list consisted of 5 different categories of oxidised PCs consisting of lyso-products, short chain oxidation products encompassing fragmented ω -terminal, fragmented α - β unsaturated aldehydes and dicarboxylic acids, non-fragmented prostane ring species, long chain oxidation products (hydroperoxides, hydroxides) and native PCs.

3.4.4.2 Confirmation of presence of hydroperoxides using FOX 2 assay

The UV spectrophotometric assay based on the principle of detection of ferric ion-xylene orange complex that is formed when the ferrous ions present in reagent is converted to ferric ion in presence of hydroperoxides. This method was utilized to validate the level of hydroperoxide species in in-vitro oxidised samples. The table 3.5 summarises the concentration of the total hydroperoxide in control and treated samples and the values represents the mean \pm standard deviation mM equivalent to H_2O_2 . The oxidised samples showed higher levels of hydroperoxides compared to the control samples.

Table 3.5: Hydroperoxide quantification using FOX 2 assay. The values are mean \pm std. dev equivalent to mM eq. of H_2O_2 concentration

Sample	Concentration of Hydroperoxides (eq. to mM of H_2O_2)
SOPC control	-0.07 \pm 0.011
SLPC control	-0.07 \pm 0.002
SAPC control	-0.06 \pm 0.004
PC mixture control	-0.06 \pm 0.004
SOPC oxidised	0.01 \pm 0.006
SLPC oxidised	0.06 \pm 0.009
SAPC oxidised	0.01 \pm 0.006
PC mixture oxidised	0.15 \pm 0.005

3.4.4.3 High resolution LC-MS analysis on QTOF 5600

Based on previously identified and functionally characterised types of oxidation products, we measured exact masses, molecular formula, and retention time using current chromatographic condition for monolith column and detection on high resolution Q-TOF mass spectrometer was performed to validate our identification. Automated data analysis using Progenesis QI software was used to confirm and validate the manual data analysis. The table 3.6 summarise the findings

of automated data analysis of high resolution data of SOPC, SLPC and SAPC samples treated with 10 mM of AAPH.

Table 3.6: Automated data analysis using Progenesis QI of high resolution data of oxidised samples of SOPC (a) ,SLPC (b) and SAPC (c) respectively generated on Absciex 5600 QTOF instrument. The table shows the retention time, statistical analysis p-value post ANOVA, accepted identification, mass error and the sample where high levels was found

a) SOPC						
Experimental m/z	Retention time (RT)	ANOVA (p)	Accepted compound ID	Formula	Mass Error (ppm)	Highest Mean
522.3550	6.18	0.494	PC(0:0/18:1(9Z))	C26H52NO7P	-0.73	control
524.3706	8.75	0.549	PC(18:0/0:0)	C26H54NO7P	-0.95	treated
650.4390	12.05	0.001	S-7KPC	C33H64NO9P	-0.29	treated
678.4686	16.24	0.000	SONPC	C35H68NO9P	-2.74	treated
694.4633	16.16	0.000	SAzPC	C36H69NO10P	-2.74	treated
788.6140	25.50	0.007	SOPC	C44H86NO8P	-3.05	treated
804.6049	23.92	0.000	SOPC-OH	C44H86NO9P	-8.00	control
804.6057	22.10	0.000	SOPC-OH	C44H86NO9P	-7.02	treated
820.6006	22.42	0.002	SOPC-OOH	C44H86NO10P	-6.85	treated
820.6011	19.17	0.002	SOPC-OOH	C44H86NO8P	-6.46	treated
836.5963	19.41	0.000	SOPC-OOH-OH	C44H86NO9P	-6.02	treated
b) SLPC						
520.3398	5.73	0.162	PC(18:2(9Z,12Z)/0:0)	C26H50NO7P	0.12	
524.3712	8.26	0.071	PC(18:0/0:0)	C26H54NO7P	0.31	
536.3345	4.67	0.000	PC(18:2(OH)/0:0)	C26H50NO8P	-0.30	treated
552.3293	4.56	0.000	PC(18:2(OOH)/0:0)	C26H50NO9P	-0.50	treated
650.4383	8.80	0.000	S-7KPC	C33H64NO9P	-1.27	treated
650.4742	18.92	0.266	13-0PC-internal standard	C34H68NO8P	-2.04	
666.4684	13.94	0.000	Unknown			
678.4684	15.75	0.000	SONPC	C35H68NO9P	-3.00	treated
692.4476	14.30	0.000	Unknown			
692.4818	18.54	0.000	Unknown			
694.4633	15.64	0.000	SAzPC	C35H68NO10P	-3.01	treated
704.4840	18.65	0.000	Unknown			
706.4962	17.27	0.000	Unknown			
732.4768	17.32	0.000	KODA-PC-Stearoyl	C38H70NO10P	-5.75	treated
734.4925	15.75	0.000	HODA-PC-Stearoyl	C38H72NO10P	-5.63	treated
748.4727	16.28	0.000	KDdiA-PC-Stearoyl	C38H70NO11P	-4.27	treated
750.4872	16.72	0.000	HDdiA-PC-Stearoyl	C38H72NO11P	-4.95	treated
750.4879	18.84	0.000	HDdiA-PC-Stearoyl	C38H72NO11P	-4.90	treated
786.5973	24.98	0.000	PC(18:2(9Z,12Z)/18:0)	C44H84NO8P	-4.37	control
800.5761	23.12	0.000	SLPC=O	C44H82NO9P	-4.88	treated
802.5905	23.59	0.000	SLPC-OH	C44H84NO9P	-6.38	treated
802.5915	21.77	0.000	SLPC-OH	C44H84NO9P	-5.17	treated
816.5703	19.67	0.000	SLPC, epoxy, keto	C44H82NO10P	-5.60	treated
818.5861	20.50	0.000	SLPC-2(OH)	C44H84NO10P	-5.43	treated
818.5862	22.29	0.000	SLPC-OOH	C44H84NO10P	-5.32	treated
832.5662	20.34	0.000	SLPC-OOH, keto	C44H82NO11P	-4.40	treated
834.5809	19.14	0.000	SLPC-OOH, OH	C44H84NO11P	-5.50	treated
848.5624	20.14	0.000	Unknown			
848.6062	22.16	0.036	Unknown			
850.5787	19.72	0.000	SLPC diOOH	C44H84NO12P	-2.00	treated
864.5781	20.53	0.000	SLPC-diOOH ,keto	C44H82NO13P	21.30	treated
870.5564	19.89	0.000	Unknown	-	-	
882.5954	19.64	0.000	SLPC-diOOH ,OH,OH	C44H84NO14P	28.50	treated
c) SAPC						
524.3710	8.78	0.0192	PC(18:0/0:0)	C26H54NO7P	-0.11	treated
544.3392	5.55	0.0061	PC(0:0/20:4(5Z,8Z,11Z,14Z))	C28H50NO7P	-1.00	treated
608.3897	9.31	0.0000	Unknown			
622.4058	9.56	0.0000	SOVPC	C31H60NO9P	-3.27	treated
638.4007	9.64	0.0001	SGPC	C31H60NO10P	-3.23	treated
648.4205	14.77	0.0000	7-Keto,5-heptaenoyl-SPC	C33H62NO9P	-4.60	treated

650.4355	11.84	0.0005	7-OH,5-heptaenoyl-SPC	C33H64NO9P	-5.60	treated
666.4293	9.67	0.0057	7-OOH,5-heptaenoyl-SPC	C34H68NO9P	-6.70	treated
676.4146	10.90	0.0000	KOOA-PC-stearoyl	C34H62NO10P	-5.63	treated
678.4300	9.72	0.0000	HOOA-SPC	C34H64NO10P	-6.00	treated
682.4250	8.67	0.0001	Unknown			
692.4090	9.64	0.0010	KODiA-PC-stearoyl	C34H62NO11P	-6.22	treated
694.4248	10.17	0.0014	HODiA-PC-Stearoyl	C34H64NO11P	-6.01	treated
718.4588	15.08	0.0012	5-OH-6,8-undecedi-enoyl-SPC	C37H68NO10P	-9.10	treated
720.4400	10.67	0.0990	Unknown			
734.4533	9.78	0.0004	5-OH-6,8-undecediendi-oyl-SPC	C37H68NO11P	-9.50	treated
760.4700	15.71	0.0004	10-OH-5,8,11-tridecatri-enoyl-SPC	C39H70NO11P	-7.80	treated
780.4679	9.14	0.0015	Unknown			
810.5937	25.36	0.0002	SAPC	C46H84NO8P	-8.70	control
826.5875	22.48	0.0004	SAPC-OH	C46H84NO9P	-10.30	treated
838.5515	21.64	0.0000	SECPC	C46H80NO10P	-9.30	treated
840.5169	24.29	0.0107	SAPC-OH,keto	C46H82NO10P	-9.00	treated
844.5475	18.51	0.0001	Unknown			
856.5613	20.17	0.0000	SEIPC	C46H82NO11P	-9.60	treated
856.5616	21.15	0.0000	SEIPC	C46H82NO11P	-9.60	treated
860.5926	22.07	0.3497	F2isoprostane-Stearoyl	C46H86NO11P	-9.88	treated
870.5458	17.57	0.0000	SAPC-OOH,di-keto	C46H80NO12P	-3.80	treated
872.5563	19.07	0.0000	SAPC-OOH,keto,hydroxy	C46H82NO12P	-9.70	treated
874.5706	19.01	0.0000	SAPC-diOOH	C46H84NO12P	-10.30	treated
876.5836	17.65	0.0000	Isofuran-SPC	C46H86NO12P	-14.20	treated
886.5383	19.01	0.0000	Unknown			
888.5524	17.32	0.0000	SAPC-diOOH,keto	C46H82NO13P	-8.20	treated
890.5656	17.76	0.0000	SAPC-diOOH,OH	C46H84NO13P	-10.90	treated
892.5354	21.78	0.0051	Unknown			
892.5380	20.98	0.7132	Unknown			
902.5663	20.39	0.0005	Unknown			
906.5611	17.15	0.0000	SAPC-triOOH	C46H84NO14P	-10.10	
922.5568	16.70	0.0000	SAPC-triOOH,OH	C46H84NO15P	-9.00	
934.5794	19.92	0.0001	Unknown			
936.5486	18.09	0.0000	SAPC-triOOH,OH,Keto	C46H84NO16P	4.50	
938.5507	17.71	0.0005	SAPC-tetraOOH	C46H84NO16P	-10.00	
954.5468	15.22	0.0017	SAPC-tetraOOH,OH	C46H84NO17P	-8.60	

Similar result was obtained when PC mixture was used as a model to study phospholipid oxidation. The data is shown in the appendix II section.

3.4.5 Optimisation of chromatographic separation of OxPL

3.4.5.1 *Altering the stationary phase and mobile phase to achieve better selectivity*

The chromatographic separation of OxPC species was evaluated using several columns like C-8 Luna column (150 x 1mm), C-18 Luna column (150 x 1mm), C-30 Luna column (150 x 2.1mm) and Proswift –RP 4H polystyrene – divinyl benzene coated monolith column (1 x 250mm); and mix mode Hichrom amino based HILIC column (150 X 3.1mm) using different solvent systems. The detailed description of chromatographic system is provided in the appendix section. Extracted ion chromatogram (XIC) of five representative species of short chain oxidation products, long chain oxidation products and native PCs separated on different columns and solvent system was obtained and the median time point with inter-quartile range of the elution for each group was calculated and graphically represented to evaluate the separation (N=3) (figure 3.25). The data illustrates that the polystyrene-divinylbenzene coated

monolith column provided robust separation of short chain oxidation products from long chain oxidation products and unmodified PCs and PEs, compared to other tested columns and solvent systems.

While the C-18 column with Hexane-methanol solvent system (Solvent system B) also provided better separation, reproducibility was an issue owing to volatile nature of the solvent system. Moreover, dispersibility of separation within each group represented by the inter-quartile range, which is defined by the separation of different species belonging to the same group, was observed to be better with monolith column, compared to other conventional reverse phase columns. While the HILIC column separated different phospholipid classes more effectively, different classes of oxidised species within phospholipid class were not separated effectively using a HILIC column. The overlaid extracted ion chromatogram (XIC) of representative species grouped into chain shortened products, long chain oxidation products and native PC's showing elution profile for different chromatographic separation system is shown in section 2.6 of appendix II.

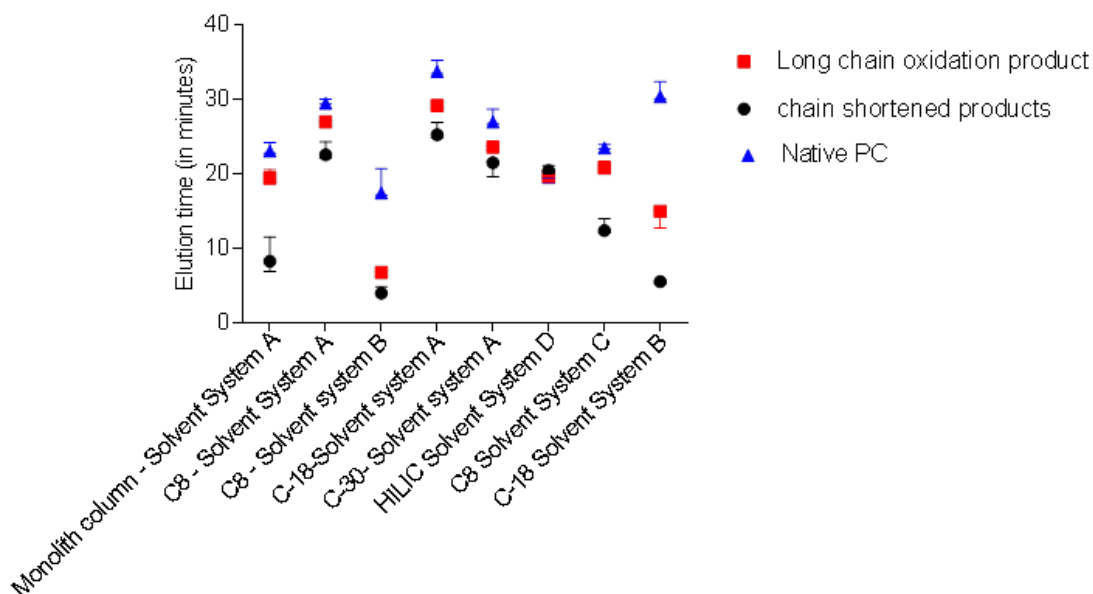


Figure 3.25: Evaluation of chromatographic separation of OxPC species using several columns and solvent systems. Extracted ion chromatogram (XIC) was generated of five representative species for each group; chain shortened products (POVPC, m/z 594.5; PONPC, m/z 650.5; SONPC, m/z 678.5; SAzPC, m/z 694.5 and KODA-PC, m/z 704.5), long chain oxidation product (PLPC-OH, m/z 774.5; PLPC-OOH, m/z 790.5; SEIPC, m/z 856.5; SLPC (2OOH), m/z 850.5 and SLPC-OOH, m/z 818.5) and Native PCs (DPPC, m/z 734.5; PLPC, m/z 758.5; SLPC, m/z 786.5; PAPC, m/z 782.5 and SDHPC, m/z 834.5) and the median elution time with inter-quartile range for each group was used to plot the data. Different solvent systems were also used to optimise the separation of different species. **Solvent system B** represents the ternary solvent system consisting of Methanol:Hexane:0.1M ammonium acetate (71:5:7) as eluent A and methanol: hexane (95:5) as eluent B. **Solvent system D** indicates solvent system for HILIC column: eluent A- 20% Isopropyl alcohol (IPA) in Acetonitrile (ACN) and eluent B- 20

% IPA in ammonium formate (20mM); **Solvent system C** indicates another solvent system consisting of eluent A as Tetrahydrofuran (THF):methanol:water (30:20:50) and eluent B as THF: methanol: water (70:20:10) with 10mM ammonium acetate and **Solvent system A** consist of water with 0.1% formic acid and 5 mM formate as eluent A and methanol with formic acid and 5mM formate as eluent B.

Further evaluation was performed by measuring the chromatographic peak width at half height (Full width at half maximum (FWHM) and selectivity factor (α) for each representative species of the short chain oxidation product, long chain oxidation product and native PC species. The formula for calculating the selectivity factor is the ratio of retention time of the parent analyte to the retention time of the product analyte.

The table 3.7 summarises the FWHM for all the representative analytes of each oxidised product category measured for the chromatographic system under evaluation. The measurement indicates that the chromatographic peaks for chromatographic system involving monolith column and solvent system A were broader compared to other silica based columns such as C8 and C18 in combination with the solvent system B. This may affect the chromatographic resolution adversely. However, the chromatographic resolution is majorly influenced by the selectivity that is the elution profile of the analyte of interest relative to other analytes.

To further evaluate the chromatographic performance the ratio of retention time of short chain oxidation product and long chain oxidation product to their precursor native species was calculated to investigate the relative retention difference between parent and product analytes. The table 3.8 lists the selectivity factor calculated for the representative short chain and long chain oxidation products. The calculation suggests that monolith column provided selectivity better than C8, C18 and C30 column when solvent system A or C was used but the opposite effect was observed when solvent system B was used in combination with silica based columns.

Moreover, when the inter-day repeatability was investigated for the chromatographic system involving solvent system B and C18 column, substantial drift in retention time was observed and therefore, it was concluded that monolith column provided robust separation when compared to other chromatographic system. The figure 3.26 shows the overlaid total ion chromatogram (TIC) of precursor ion scan of the same sample acquired on day 1 and day 3 using the C18 and solvent B chromatographic system. Significant difference in the elution time of peaks is observed suggesting the change in organic strength of the mobile phase over period

of time. These can adversely affect the chromatographic alignment and peak picking & identification process during comparative analysis.

Table 3.7: Evaluation of the efficiency of several chromatographic systems by calculating the peak width at half height (FWHM) for representative analytes of the oxidised products.

	chain shortened product					Long chain oxidation product						Native PC						
	PONPC	SONPC	POVPC	SAzPC	KODA-PC	Average	PLPC-OH	PLPC-OOH	SEIPC	SLPC2-OOH	SLPC-OOH	Average	PLPC	SLPC	PAPC	PPPC	SDHPC	Average
Monolith column - Solvent System A	0.72	0.37	0.6	0.72	1.08	0.71	0.66	0.67	0.57	0.72	0.47	0.618	0.73	0.58	0.37	0.65	0.64	0.594
C8 - Solvent System A	0.4	0.7	0.5	0.5	0.7	0.56	0.6	0.5	0.6	0.54	1.4	0.728	0.2	0.3	0.4	0.3	0.6	0.36
C8 - Solvent system B	0.28	0.22	0.2	0.2	0.33	0.246	0.36	0.6	0.46	0.56	0.3	0.456	0.3	0.37	0.3	0.29	0.3	0.312
C-18	0.23	0.23	0.2	0.22	0.2	0.216	0.32	0.34	0.27	0.45	0.32	0.34	0.36	0.4	0.3	0.28	0.32	0.332
C-30	0.3	0.3	0.3	0.3	0.4	0.32	0.7	0.6	0.4	0.5	0.4	0.52	0.4	0.4	0.3	0.4	0.5	0.4
HILIC Solvent System D	0.31	0.3	0.3	0.35	0.4	0.332	0.35	0.36	0.45	0.52	0.45	0.426	0.26	0.36	0.3	0.27	0.32	0.302
C8 Solvent System C	0.6	0.7	0.4	0.7	0.4	0.56	0.8	1.1	0.6	0.9	0.9	0.86	0.5	0.4	0.5	0.4	0.5	0.46
C-18 Solvent System B	0.3	0.56	0.25	0.3	0.53	0.388	0.67	0.32	0.3	0.57	0.46	0.464	0.35	0.47	0.31	0.36	0.3	0.358

Table 3.8: Evaluation of the efficiency of several chromatographic systems by calculating the selectivity factor (α) for representative analytes of the oxidised products.

	chain shortened product					Long chain oxidation product						
	PONPC	SONPC	POVPC	SAzPC	KODA-PC	Average α	PLPC-OH	PLPC-OOH	SEIPC	SLPC(2OOH)	SLPC-OOH	Average α
Monolith column - Solvent System A	3.28	2.05	4.35	2.02	3.03	2.94	1.11	1.17	1.29	1.30	1.15	1.20
C8 - Solvent System A	1.31	1.23	1.43	1.21	1.36	1.31	1.09	1.09	1.15	1.12	1.09	1.11
C8 - Solvent system B	4.40	4.52	4.60	4.42	3.93	4.37	2.57	2.57	3.49	2.93	2.50	2.81
C-18	1.34	1.33	1.43	1.24	1.42	1.35	1.15	1.16	1.25	1.17	1.19	1.19
C-30	1.37	1.35	1.51	1.25	1.29	1.35	1.13	1.14	1.26	1.16	1.24	1.19
HILIC Solvent System D	0.96	0.92	0.95	0.93	0.96	0.94	0.99	1.00	0.99	0.98	0.98	0.99
C8 Solvent System C	1.89	1.71	1.94	1.68	1.82	1.81	1.08	1.13	1.19	1.13	1.10	1.12
C-18 Solvent System B	5.52	4.38	6.27	5.43	6.27	5.57	2.02	2.04	2.58	2.66	1.61	2.18

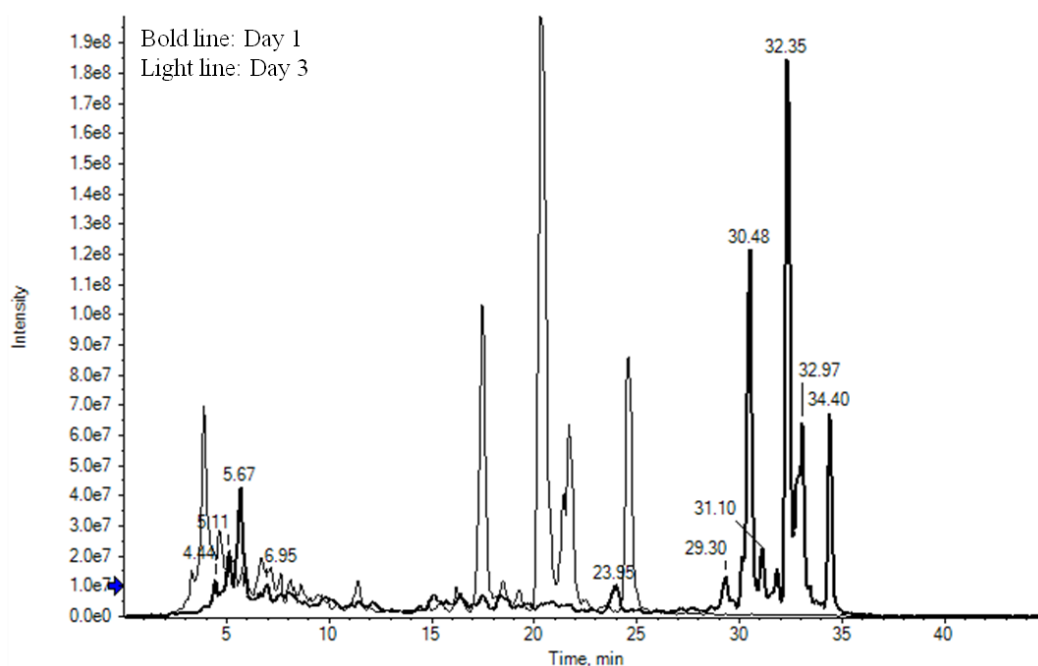


Figure 3.26: Overlaid chromatographic run of oxidised PC mixture acquired on day 1 and day 3 that were analysed using C18 column and solvent system B using precursor ion scan 184 Da. The bold line profile shows the day 1 run and the light line shows the day 3 run of the same sample.

3.4.5.2 Testing different solvent system with monolith column to achieve best separation

Once the stationary phase that provided better separation was determined, other solvent systems were tested to further refine the separation. The figure 3.27 shows that the monolith column with solvent system-A provided better separation compared to other solvent systems. Three representative species for each group was selected and median elution time with inter quartile range was calculated to evaluate the separation.

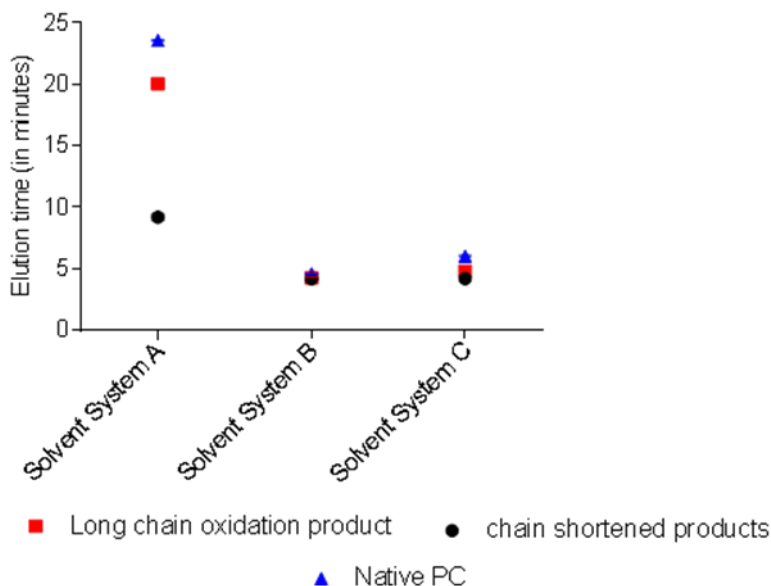


Figure 3.27: Evaluation of chromatographic separation of OxPC species using monolith column and different solvent systems. Extracted ion chromatogram (XIC) was generated of three representative species for each group: chain shortened, long chain oxidation product and Native PCs and the median elution time with inter-quartile range for each group was used to plot the data. Different solvent systems were also used to optimise the separation of different species. **Solvent system B** represents the ternary solvent system consisting of Methanol:Hexane:0.1M ammonium acetate (71:5:7) as eluent A and methanol: hexane (95:5) as eluent B. **Solvent system C** indicates another solvent system consisting of eluent A as Tetrahydrofuran (THF):methanol:water (30:20:50) and eluent B as THF: methanol: water (70:20:10) with 10mM ammonium acetate and **Solvent system A** consist of water with 0.1% formic acid and 5 mM formate as eluent A and methanol with formic acid and 5mM formate as eluent B.

3.4.5.3 Optimisation of flow rate and gradient system

The optimum separation of analytes is dependent on longitudinal diffusion, resistance to mass transfer and eddy diffusion, which again is associated with running samples at optimal linear velocity. Therefore, an oxidised PC sample was run at different flow rates on monolith column with solvent system A to determine optimal flow rate for better separation.

The experiment was repeated three times and the median elution time of three representative species for each group of short chain oxidation products, long chain oxidation products and native PCs was calculated along with the normalised peak area that is associated with sensitivity to determine optima flow rate for separation. The figure 3.28 shows that the flow rate at 50 $\mu\text{l}/\text{minute}$ was optimal for best separation and sensitivity. The table in appendix II enlists all the species with calculated peak area that were used in the evaluation.

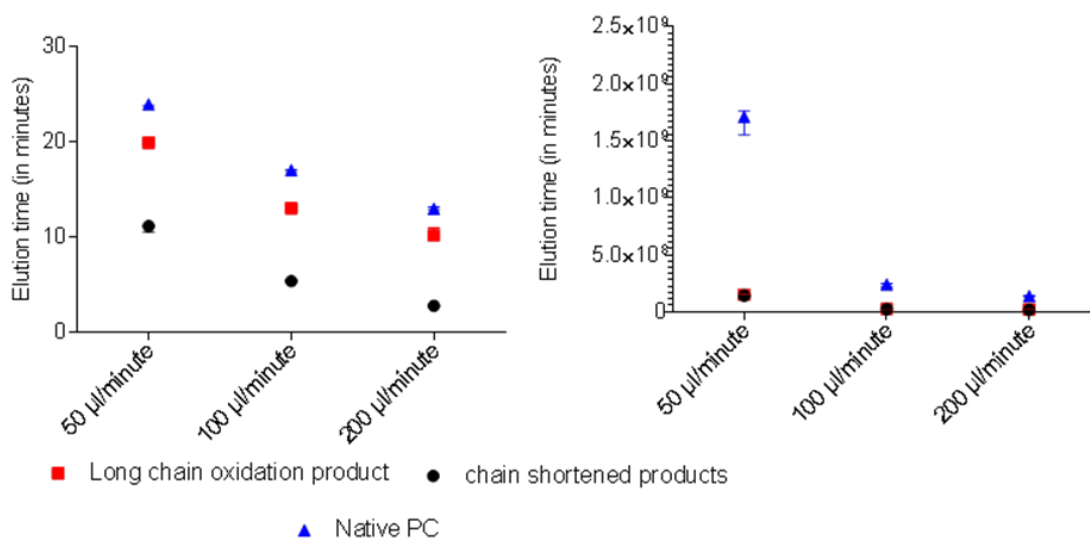


Figure 3.28: Evaluation of chromatographic separation of OxPC species using monolith column solvent system A at different flow rates. Extracted ion chromatogram (XIC) was generated of three representative species for each group: chain shortened, long chain oxidation product and Native PCs and the median elution time with inter-quartile range for each group and normalised peak area was used to plot the data.

Finally, the gradient was optimised for monolith column and solvent system A at 50 µl/ minute flow rate.

Three different gradients: a short gradient running from 70 % B to 100 % B in 16 minutes; a long gradient running from 70 % B to 100 % B in 26 minutes and a program consisting of three step gradients from 70 % B to 100 % B in 16 minutes was evaluated for optimal separation. The details of the gradient program are provided in the appendix section. The figure 3.29 shows the evaluation of elution profile of representative species within each group of short chain oxidation product, long chain oxidation product and native PCs analysed at different chromatographic gradient program.

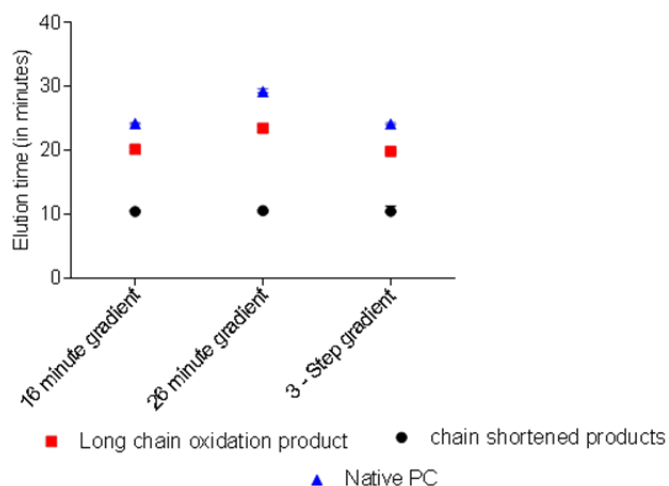


Figure 3.29: Evaluation of chromatographic separation of OxPC species using monolith column, solvent system-A, flow rate of 50 µl/minute using different gradient program. XIC was generated of three representative species for each group: chain shortened, long chain oxidation product and Native PCs and the median elution time with inter-quartile range for each group was plotted for evaluation.

The maximum efficiency of the monolith column, which is longer than the conventional reverse phase columns used in several published research for analysis of OxPL is achieved by using a shallow gradient (26 minute gradient), compared to the steep gradient or the step gradient (figure 3.28).

3.4.6 Method Validation

3.4.6.1 Assessment of reproducibility and repeatability

Oxidised PC mixture samples were analysed at different times of a day and at different days to assess the repeatability and reproducibility of the method. The experiment was repeated 3 times and the relative standard deviation was calculated from the average peak area and standard deviation of sampled species across all groups of oxidised species. The figure 3.30 shows the intra-day repeatability and inter- day reproducibility of the method. The RSD of most of the peaks were below 20 % although, some species showed greater deviation, which could be due to integration error that becomes more prominent for very low abundant species as well as isobaric nature of the species.

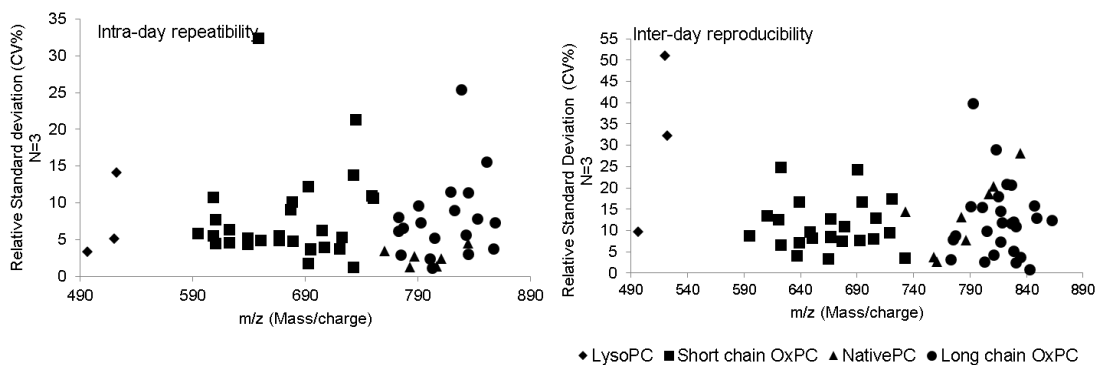


Figure 3.30: Investigation of repeatability and reproducibility of the method by analysing quality control samples at different time points of the day and at different days (N=3). The evaluation was performed by calculating RSD for sampled species in all the replicates. The RSD for most of the species was less than 20 % that conformed to USFDA guidelines for LCMS methods.

As per the US FDA guidelines, the variation should not be more than 20 % for LCMS based methods and the method conforms to the guidelines.

3.4.6.2 Assessment of normalisation approaches

Different approaches were assessed and investigated to minimise technical variation and increase the robustness of the method. Normalisation approaches such as the internal standard method, Total ion intensity and global normalisation approach were compared. The table 3.9 shows the snapshot of the effect and comparison of these 3 normalisation approaches on the relative standard deviation parameter that is calculated from the average normalised peak area and standard deviation of sampled species from 3 independent experiments.

Table 3.9: Evaluation and comparison of the effect of different normalisation approaches on the calculated relative standard deviation for technical replicates (N=3). Five representative species for each group of short chain oxidation product, long chain oxidation product and native PCs were selected and the RSD was calculated post applying the transformation.

m/z	No normalisation	TIC normalisation approach	Global normalisation approach	internal standard normalisation	internal standard normalisation and log transformation
	RSD %				
594.3768	9.58	5.86	9.4	9.4	1.23
610.3724	8.02	4.49	7.94	7.81	1.10
650.4394	8.45	4.98	8.41	8.18	0.75
666.4344	8.02	4.9	8.12	7.61	0.74
678.4706	8.47	4.86	8.35	8.29	0.84
760.5831	1.10	3.45	0.28	2.38	0.17
782.5672	2.76	1.31	2.19	3.41	0.30
786.5990	1.78	2.7	0.79	2.88	0.22
806.5676	3.52	1.36	2.63	4.35	0.42
834.5985	6.25	4.55	4.94	7.43	0.79
790.5566	14.37	10.64	13.72	14.69	1.38
774.5633	6.78	2.99	6.51	6.81	0.58
828.5370	21.43	25.38	22.67	20.57	2.11
842.5881	8.37	7.82	9.2	7.30	0.93
906.5694	7.17	3.42	6.41	7.71	1.02

While all the investigated approaches minimised the variance, the effect of post normalisation processing using log transformation was substantial in smoothening and homogenising the variance.

The global normalisation approach and internal standard normalisation were softer and had milder effect compared to the total ion intensity approach as well as post processing approach using log transformation. This approaches will be investigated in more detail in other chapters involving profiling phospholipids in biological samples (Chapter 4 & 7).

3.4.6.3 Assessment of extraction variability

The extraction variability was investigated by preparing a cocktail of phospholipid species of different classes along with commercially available oxidised species. One set was processed through the extraction procedure and another set was directly analysed by LCMS. This experiment was repeated three times and complemented by performing total phospholipid content assay of extracted and not-extracted samples. The figure 3.31 shows comparative analysis of extracted and not-extracted samples using normalised peak area of all the species that was added in equal amount in both the sets.

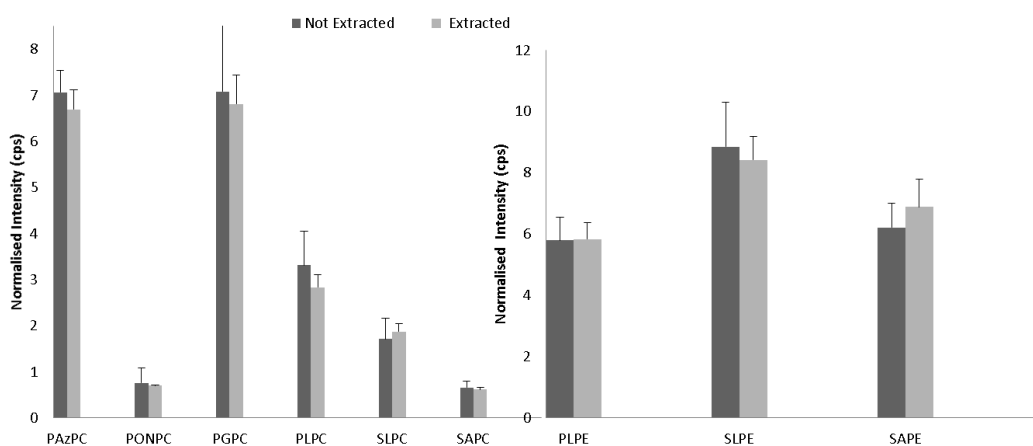


Figure 3.31: Evaluation of extraction variability by LCMS analysis of extracted and not extracted set of cocktail of equimolar amount of phospholipid species from different classes.

The data suggests that the extraction efficiency and recovery is nearly 100 % and there was no biasedness observed in preferential extraction of one species over another. This was further confirmed by measuring the total phospholipid content. The table 3.10 shows the phospholipid content in extracted and not extracted samples that was determined using malachite green assay. The data shows that the phospholipid content was similar in both the set of samples and this reinforces our observation about nearly 100 % extraction efficiency of the method used in this study.

Table 3.10: Malachite green assay to determine the total phospholipid content of extracted and not-extracted samples.

Sample	Average Absorbance at 660 nm	Std. Deviation	Amount of phospholipid (in $\mu\text{g} \pm \text{std.dev}$)
Cocktail (not extracted)	0.5223	0.004	12.81 \pm 0.004
Cocktail (extracted)	0.5225	0.036	12.82 \pm 0.036
PC mixture control	0.411	0.011	8.30 \pm 0.011
PE mixture control	0.3534	0.003	5.97 \pm 0.003
PC mixture oxidised	0.3935	0.005	7.60 \pm 0.005
PE mixture oxidised	0.3435	0.002	5.57 \pm 0.002

3.4.6.4 Assessment of linear dynamic range

The linear dynamic range of the method was investigated by analysing commercially available oxidised PC species like PAzPC, PONPC, POVPC and PGPC at concentration range spread over 6 orders of magnitude. Internal standard (13:0 PC) was added to each concentration, standard curve was prepared and weighted linear regression was used to relate the response and concentration.

The figure 3.32 shows the standard curve of PAzPC that was analysed on Qtrap 5500 and QTOF 5600 instrument. It illustrates that the limit of quantification and linear range for method developed on Qtrap 5500 using targeted approaches and high resolution fast scanning method developed on QTOF 5600 is similar at concentration spread over three orders of magnitude.

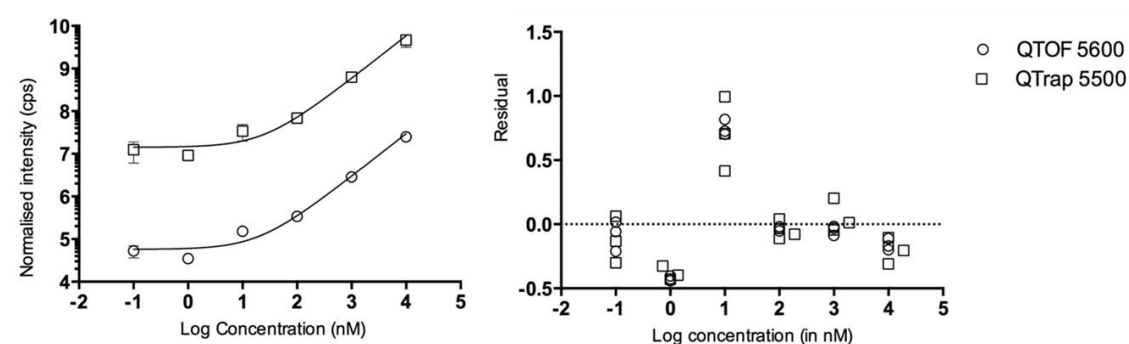


Figure 3.32: Assessment of limit of quantification and linear dynamic range of the method developed using monolith column for chromatographic separation and detection using targeted approaches and validation on QTOF 5600. PAzPC (m/z 666.5) was analysed at different concentrations over 6 orders of magnitude on Qtrap 5500 instrument and QTOF 5600. The limit of quantification was found to be at 10 nM concentration.

The table 3.11 summarises the equation and linearity range for PAzPC, PONPC, POVPC and PGPC that can be used for absolute concentration. The regression analysis for all but POVPC showed linear trend in response and concentration, and this could be due to discrepancy in the integration process of the peak or experimental handling of the standard.

Table 3.11: Analytical parameters for quantification of OxPLs. Internal standard (13:0PC, 153.97pmoles) was applied on the column together with increasing concentration of calibrants. Equation for calculation was obtained using 1/xweightedlinear regression.

Phospholipid	Equation for calculation	Linear range, concentration on column	R ² value (QTOF 5600)	R ² value (Qtrap 5500)
POVPC	$y = 5.53x + 0.11(\text{QTrap}); 0.07x + 0.001(\text{QTOF})$	100 pM – 10 μM	0.69	0.72
PGPC	$y = 4.20x + 0.0006(\text{QTrap}); 0.075x + 0.00003(\text{QTOF})$	100 pM – 10 μM	0.97	0.98
PONPC	$y = 2.05x + 0.02(\text{QTrap}); 0.046x + 0.0001(\text{QTOF}) + 0.001(\text{QTOF})$	100 pM – 10 μM	0.99	0.98
PAzPC	$y = 9.06x + 0.32(\text{QTrap}); 0.049x + 0.001(\text{QTOF})$	100 pM – 10 μM	0.98	0.97

3.4.7 Evaluation of 2D-LCMS analysis for separation of OxPL

Serial coupling of the monolith column to HILIC column and running the gradient simultaneously was set up to investigate the improvement in separation of OXPL species. While reverse phase columns separates the polar oxidised species from their native species, it does not separate the oxidised species belonging to different phospholipid class. Moreover, HILIC column provides effective separation of different phospholipid classes but does not effectively separate oxidised species. Moreover, owing to differential ionisation variability, the analysis of different phospholipid classes in a single run is impractical; therefore, with the objective of further improving the separation that can improve the detection range and reduce the analysis time, the evaluation of 2D LC analysis was investigated. The figure 3.33 shows the separation profile of different groups of oxidised species of PC and PE class when monolith and HILIC column are used for separation alone or in combination by serially coupling the columns and

simultaneous gradient analysis. Median elution time of 5 representative species from each group was used to evaluate the separation.

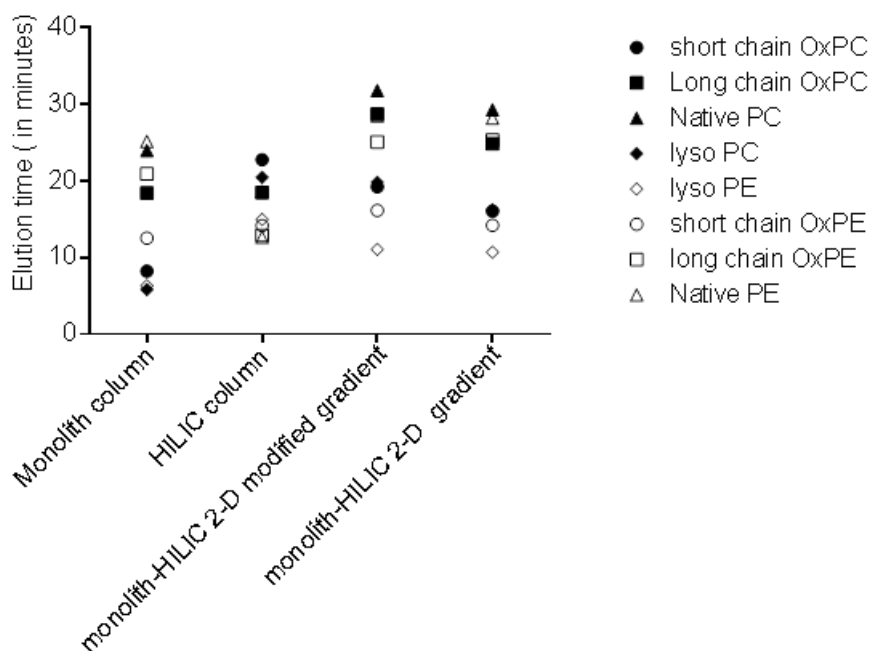


Figure 3.33: Evaluation of chromatographic separation of OxPC species using monolith and HILIC column alone and in combination by serial coupling and simultaneous gradient analysis. Extracted ion chromatogram (XIC) was generated of five representative species for each group from **PC class**: short chain OxPC (POVPC, m/z 594.5; PONPC, m/z 650.5; SONPC, m/z 678.5; SAzPC, m/z 694.5 and KODA-PC, m/z 704.5), long chain OxPC (PLPC-OH, m/z 774.5; PLPC-OOH, m/z 790.5; SEIPC, m/z 856.5; SLPC (2OOH), m/z 850.5 and SLPC-OOH, m/z 818.5) and Native PCs (DPPC, m/z 734.5; PLPC, m/z 758.5; SLPC, m/z 786.5; PAPC, m/z 782.5 and SDHPC, m/z 834.5); **PE class**: short chain OxPE (POVPE, m/z 552.5; PONPE, m/z 608.5; SONPE, m/z 636.5; SAzPE, m/z 652.5 and KODA-PE, m/z 662.5), long chain OxPE (PLPE-OH, m/z 732.5; PLPE-OOH, m/z 748.5; SEIPE, m/z 814.5; SLPE (2OOH), m/z 808.5 and SLPE-OOH, m/z 776.5) and Native PEs (DPPE, m/z 692.5; PLPE, m/z 716.5; SLPE, m/z 744.5; PAPE, m/z 740.5 and SDHPE, m/z 792.5) and the median elution time for each group was used to plot the data

The serial coupling of monolith and HILIC column with modified program showed better separation of the OxPC and OxPE species. However, the native PCs and PE species co-eluted in this setting. Altogether, this was a first step towards evaluation of two dimensional chromatography to improve the oxidised lipidome coverage and enhance high throughput analysis; and it requires further optimisation and experimentation to evaluate its efficiency. The details about the gradient is provided in the appendix I section.

3.4.8 Discussion

Oxidised phospholipids (OxPL's), including chlorinated products, have been implicated in various inflammatory disorders; therefore, a need arises for sensitive methods for detection and quantification of these relatively scarce products in biological samples, in order to correlate

their concentration to the severity or stages of the disease. Earlier methods developed were for specific oxidation products and were limited to the instruments used and scanning methods used to support the identification. For instance, the LC-MS method developed by Gruber et.al (2012) for oxidised phosphatidylcholine compounds was by selective reaction monitoring scanning routine, monitoring the transition to a specific Phosphatidylcholine product ion (m/z 184) which may not be able to distinguish between isomeric and isobaric products of the PC class like a peak at m/z 790.5 would correspond to the mono-hydroperoxide of PLPC or the isotopic peak of the un-oxidised SOPC, owing to low resolution of the instrument used. Similarly, the LC-MS method developed for analysis of chlorohydrins generated in-vitro by Jerlich et.al (2002) used a survey scan for identification of chlorohydrins, which may lack the sensitivity for identification of chlorohydrins in biological samples.

Recently, hybrid mass spectrometers like Qtrap 5500 and QTOF 5600 were introduced, which were capable of performing $(MS)^n$ experiments with 10-fold increase in sensitivity and accuracy for detection of isobaric compounds. Other methods developed were based on improvements in understanding about analyte chemistry and fragmentation patterns on charging with collision energy using inert gases. For example, secondary oxidation products formed having aldehydes or hydroxyaldehydes as functional groups fragmented via following 1-4 diene charge migration and hydrogen elimination mechanism and therefore, providing structural details pertaining to the position of functional groups using tandem mass spectrometry. Similarly, hydroperoxides and chlorinated lipids on collision induced dissociation loses specific neutral compounds like H_2O_2 (34 Da) and HCl (36 or 38 Da) respectively that supports the identification.

Recently, methods were developed through interfacing the separating power of HPLC systems to the sensitivity and resolution power offered by hybrid mass spectrometers like QTrap MS and QTOF instruments. However semi targeted methods using PIS and NL scans have been not utilised effectively in earlier methods. Moreover, earlier methods were limited to analysis of smaller section of the diverse range of oxidised phospholipids species and were not tested on detection of oxidised products in wide range of biological samples. The measurement of low molecular weight biomarkers of lipid peroxidation present in complex matrices such as brain tissue, plasma, urine or cerebrospinal fluid is a delicate and difficult task and there is a need for improved analytical methodology in this field of research. The major objective of this work was to develop methods using semi-targeted approaches to detect a range of oxidised PC species

within one analytical run and is sensitive enough to be translated to analyse OxPC species in different biological samples.

An important aspect of our methodology was to evaluate the separation of several oxidised species using several reverse phase columns and we found that the better separation and robust method was achieved using monolith column as compared to other conventional reverse phase columns and mix mode HILIC column. Chromatographic separation of OxPLs, specifically short chain oxidation products that covered masses from m/z 450 – 750 was better with the system using monolith column and methanol-water solvent system, although similar results were obtained using C-8 column and hexane-methanol-water solvent system, the reproducibility of the retention time was the issue. While many LC-MS based method have been reported for analysis of OxPCs, limited work was done to evaluate the separation of oxidised phospholipid species and achieve chromatographic resolution (Hui et al., 2010). Most of the method reported have concentrated on faster analysis like the method reported for analysis of OxPCs by (Gruber et al., 2012) used a C-18 core shelled column and all the species reported eluted in the first 10 minutes. However, faster analysis can compromise the chromatographic resolution and sensitivity and therefore, can affect the relative quantification process. Moreover, faster analysis of complex samples can also lead to more false positive identification because overlapping of signals of co-eluting analytes and matrix effects. Therefore, better dispersion of separation is required for analysis of samples, when the objective is to identify and characterise several species including isobaric and isomeric species in a single run.

Furthermore our work aimed to develop a method using targeted scanning approaches, which has been reported earlier but lesser exploited to characterise oxidised species in biological samples (Spickett et al., 2011) (Reis et al., 2013). With the fact, that a single poly-unsaturated phospholipid species can give rise to several oxidation products that can make the identification and quantification process of all species in a single run, a difficult task. Moreover, most of the earlier work done was reported and tested on in vitro oxidised samples and concentrated on analysis of pre-determined species. While the approach of multiple reaction monitoring (MRM) is the most used approach to quantify several pre-defined species, it has the limitations of only able to quantify certain number of species in a single run. Moreover, most of the mass spectrometry based methods developed so far have either used MRM based approaches in positive and negative mode or high resolution mass spectrometry based on accurate masses to characterise oxidised PC species (Hui et al., 2010, Gruber et al., 2012, Nakanishi et al., 2009,

Davis et al., 2008). Furthermore, the primary oxidation products that are hydroperoxide species, which are very unstable and they get oxidatively fragmented to short chain oxidation products or are reduced to hydroxides by several enzymes *in-vivo*. Therefore, their abundance level in biological samples can be very low and can be below the detection level of existing methodologies. In our method, we tested a series of targeted approaches to selectively identify several oxPC species in a single run. In this project, the neutral loss scan for 34 Da in combination with precursor ion scanning for head group ions (selective for phospholipid class specific identification) allowed identification of several oxidised phospholipid species in a single run as demonstrated in our results. The experiments with *in-vitro* generated OxPL mixture and using targeted mass spectrometry approach and monolith column for separation demonstrated the detection efficiency as more than 100 different OxPL species were identified in a single run, which is comparable to the MRM analysis method protocols developed by (Gruber, 2012). Moreover, the identification of mono-hydroperoxides, hydroxyl-hydroperoxides, and poly hydroperoxides was facilitated by using the targeted approach and in absence of specific standards.

Although, mass spectrometry technology provides wealth of information about your samples, it brings along the complexity of data analysis and intrinsic variability of instrumentation that can lead to misinterpretation of findings, unless the raw data is appropriately processed and normalised. Therefore, when the developed method is based on scanning approaches on a low resolution mass spectrometer, it is often required to validate the findings using a different chromatographic set-up or transferring the method to another high resolution mass spectrometry instrument. Therefore, we used an approach by transferring the methodology to a high resolution Q-TOF mass spectrometer to validate our findings. The method was also assessed for its qualitative and quantitative use by investigating the injection precision and inter-day variability. The relative standard deviation (CV %) was found to be less than 10 % for substantial number of species. There were some outliers that can be accounted for due to integration errors, peak distortion because of co-eluting species and extraneous level of oxidised species formed during storage.

The similar qualitative assessment was performed for the transferred method on the Q-TOF instrument to assess the technical variability and in-sequence variability. It showed comparable results to that observed on a low resolution Q-Trap instrument. Moreover, data analysis validation was performed by using Progenesis QI software capable of automated pre-processing

the raw mass spectrometry data, thereby facilitating rapid data analysis and further validate the findings.

Finally, a pilot study to improve the chromatographic separation was performed by serially coupling two columns having orthogonal chemistry. This was a first attempt to-date in the field of oxidative lipidomics although, similar work had been carried out in the field of metabolomics (Haggarty, Oppermann et al. 2015). We found that the methodology using two dimensional chromatography has a potential to improve the oxidised lipidome coverage as demonstrated by our work and further work needs to be done to evaluate several columns of different chemistry and mobile phases to highlight this not so popular technology in the field of Lipidomics.

4 Deciphering the oxidised lipidome of ascites of lean and obese rats model of acute pancreatitis

4.1 Background

Acute pancreatitis is a disease caused by localised inflammation of the pancreatic gland that results in acinar tissue damage and interstitial edema; migration of neutrophils; and haemolysis leading to oxidative stress (Schoenberg, Birk et al. 1995, Perez, Pereda et al. 2015). To understand the pathogenesis and etiological factors most experimental studies use animal models like rats and mice induced with acute pancreatitis by treatment with varieties of stimuli. Examples of treatment are free fatty acid infusion to study alcohol induced hyperlipidemic pancreatitis (Anderson, Jeffrey et al. 1986, Morita, Yoshikawa et al. 1998) or two hour period of ischemia to study ischemic induced pancreatitis (Schanaider, de Carvalho et al. 2015)(Sanfey, 1984 #5516), which is termed as ex-vivo perfused canine pancreas preparation model. The other model termed hemorrhagic necrotising pancreatitis model is induced by infusion of sodium taurocholate (0.25 % to 5 %) into the pancreatic duct to study oxidative stress and hemodynamic effects that contributes to symptomatic processes in acute pancreatitis (Pereda, Perez et al. 2012). Although, the mortality rate from acute pancreatitis has decreased over the last decades owing to improvement in treatment and diagnosis, the prevalence in developed countries including United Kingdom still remains very high (Yadav and Lowenfels 2013).

Previous studies reported a link between oxidative stress and pathologies involved in acute pancreatitis using animal models described above (Kruse, Loft et al. 1997, Morita, Yoshikawa et al. 1998, Winterbourn, Bonham et al. 2003). These studies investigated triglyceride levels, reduced glutathione levels, free fatty acid levels, phospholipid levels, lipase activity, protein carbonyls and malondialdehyde levels. All of these provide an indication of the global measure of oxidative stress without providing information at the species level. A recent study reported a significant increase in level of peroxidised products in ascites fluid of rat with acute pancreatitis compared to control samples (Gutierrez, Folch-Puy et al. 2008, Kiziler, Aydemir et al. 2008, Grigor'eva, Romanova et al. 2011). Obesity is considered as a risk factor for acute pancreatitis and it is one of the factors that induce the pro-inflammatory state (Franco-Pons, Gea-Sorli et al. 2010, Robles 2013). High levels of fat necrosis and isoprostanoids were observed in obese rats compared to lean rats with acute pancreatitis and this excess fat was associated with severity of the disease (Pereda, Perez et al. 2012, Perez, Pereda et al. 2015). These results supported the hypothesis for possible role of obesity to the oxidative stress

conditions in acute pancreatitis and therefore, to confirm the translational relevance of the findings in obese and lean model of acute pancreatitis, a study to perform comparative analysis for levels of a range of oxidised phospholipid (OxPL) species is required.

No study to date have been conducted that measures and relatively quantify oxidised phospholipid (oxPL) levels and give information at the species level using mass spectrometry technology in obese and lean model of acute pancreatitis. In addition, a rational approach combining pre-processing of raw data with validation of a statistics method was developed to improve differential profiling of OxPL in biological samples within inherent large biological variation. Such approach has been applied for metabolomics data but it remains yet to be applied in the OxPL field (Bijlsma, Bobeldijk et al. 2006, Want and Masson 2011). While issues in data analysis such as analytical variation, assumption of normality, homoscedasticity and correction for multiple testing with their influence on statistical analysis are known, they are often ignored while analysing LC-MS based datasets (Vinaixa, Samino et al. 2012). Depending on the biological matrix and origin of samples, different approaches are required to minimize systemic variation. For example, samples from obese and lean rats in which the total lipid composition will be very different with obese rats having higher levels of triglyceride levels and therefore, normalisation using total ion intensity will skew the data. OxPL levels that are largely affected by the pathological conditions does not held a self-averaging property i.e. change in levels of a family or a specific class of analytes is not balanced by the level of another class of analytes (Sysi-Aho, Katajamaa et al. 2007).

4.2 Aim and objectives

The aim of this study was to measure and relatively quantify oxidised phospholipids in total lipid extract of ascites of obese and lean rats induced with acute pancreatitis using sodium taurocholate infusion in the pancreatic duct. The hypothesis for this study was that obese rat samples will have high levels of oxidised phospholipids as marker of oxidative stress relative to lean rat samples. To achieve this aim following objectives were outlined:

1. Analysing of total lipid extract of ascites of obese and lean rats with acute pancreatitis on Qtrap 5500 instrument using targeted approaches and monolith column for chromatographic separation to measure and relatively quantify oxidised phospholipids.

2. Cross validation of manual data analysis of data generated on Qtrap 5500 instrument by reacquisition of total lipid extract of ascites of obese and lean rats with acute pancreatitis on Q-TOF 5600 instrument using high resolution general survey scan with data dependent MS/MS scans and monolith column for chromatographic separation followed by automated data analysis using Progenesis QI software.
3. Development and evaluation of rational data analysis approach involving pre-processing of raw data and different normalisation approaches to establish a data analytical flow that can improve the biological information of the data.

4.3 Results

The ascites of lean and obese rats (7 each) was collected by the group of Prof Juan Sastre at University of Valencia; post induction of acute pancreatitis in animal models using sodium taurocholate and was couriered to us. The total lipid was extracted from ascites of seven obese and lean rats' samples followed by analysis on Qtrap 5500 instrument using targeted approaches and QTOF 5600 instrument for validation of findings. The figure 4.1 shows the total ion chromatogram (TIC) of obese and lean rat sample with marked areas indicating the elution time for short chain oxidation products (a); long chain oxidation products (b) and unmodified phospholipid species (c) which were identified as discuss in chapter 3. As discussed in the method development chapter (chapter 3), the monolith column provided better selectivity and separation compared to other reverse phase columns containing C-8, C-18 or C-30 stationary phase and the same method was utilised to profile the ascites of lean and obese rat with acute pancreatitis.

The monolith column provided better separation compared to other reverse phase columns for short chain oxidation products that eluted early from 5 – 10 minutes compared to long chain oxidation products, eluting at 18 – 22 minutes preceding unmodified species that eluted in 22 – 26 minutes.

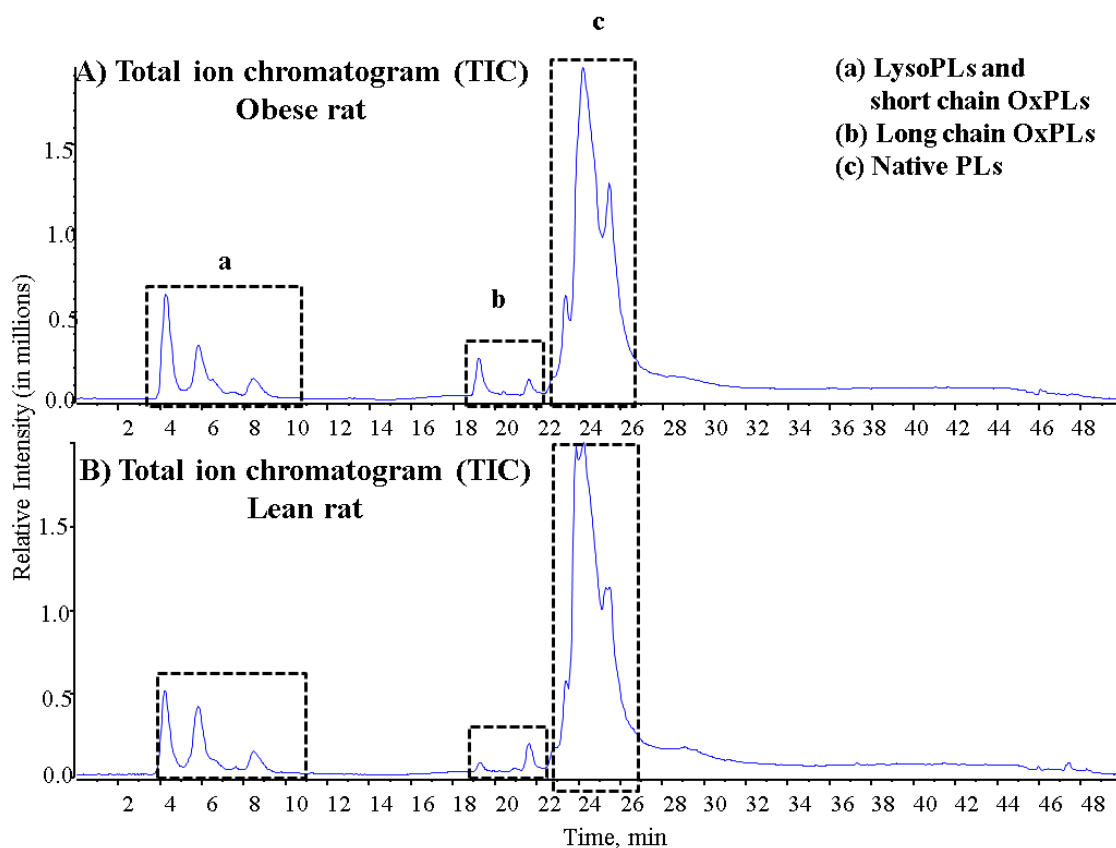


Figure 4.1: Total ion chromatogram (TIC) of total lipid extract of obese and lean rat models of acute pancreatitis. The marked shapes shows the elution time for short chain oxidised species including lyso species, long chain oxidised species and native species.

Subsequently, several oxidised species were identified by studying the fragmentation pattern, looking at signature fragment ions related to the head group as well as fragments related to the fatty acyl chains as illustrated in figure 4.2 with examples of XIC, fragmentation spectra and QTOF-MS spectra for m/z 594.3765 (POVPC) and m/z 774.5643 (PLPC-OH) respectively. The fragmentation spectra of POVPC shows more than two fragments linked to different groups within the structure, thereby providing more confidence in the identification whereas, that of PLPC-OH shows only the fragment of the headgroup at m/z 184.07 Da that corresponds to the phosphocholine group. The experimental masses for samples acquired on high resolution Q-TOF instrument were compared to theoretical masses with tolerance set to 5 ppm and any difference greater than the tolerance level was highlighted and categorised in a putative identification category. All this information together was utilised to develop a holistic approach for categorising the identification process of species with different level of confidence as shown in table 4.1.

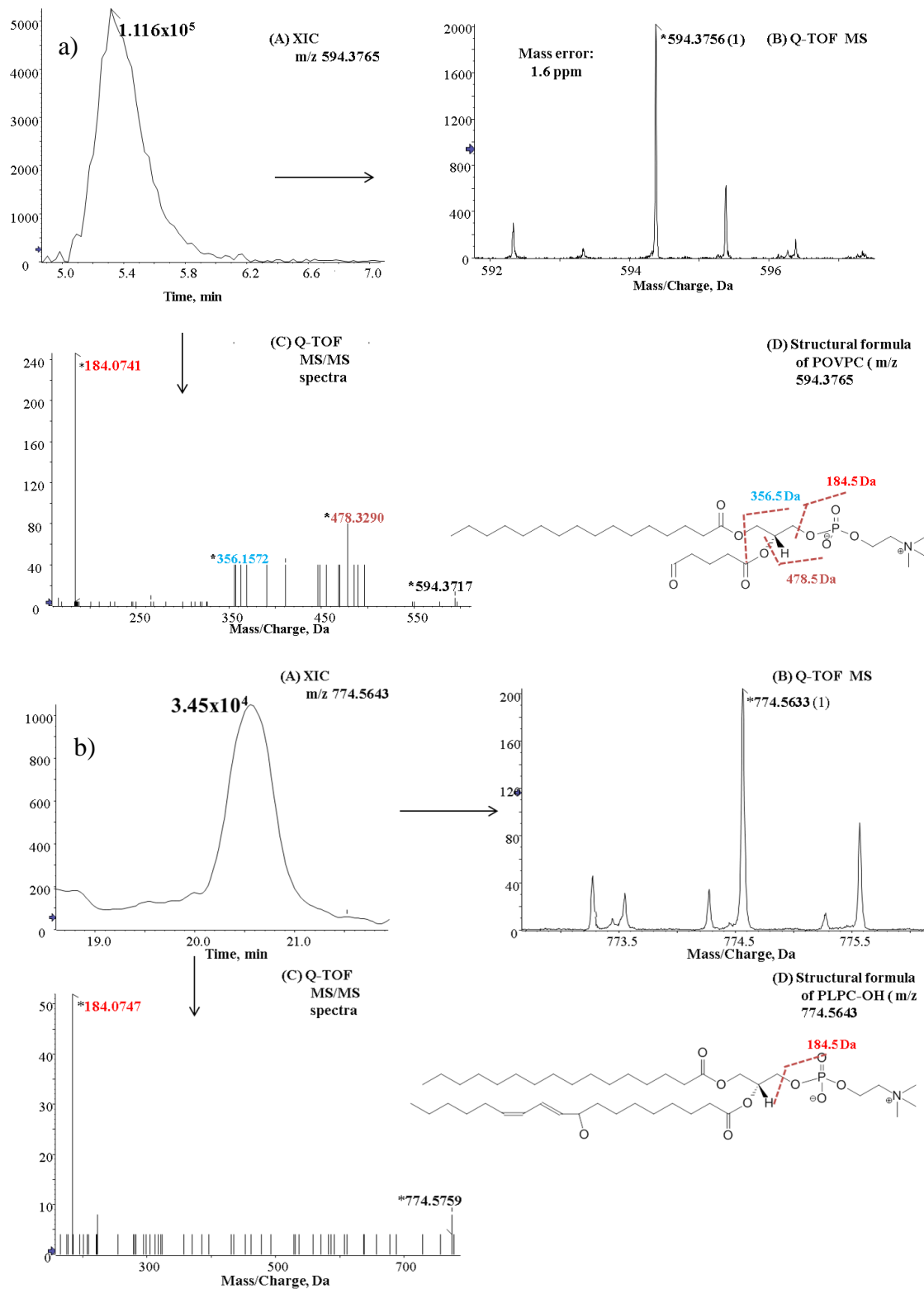


Figure 4.2: Representative strategy used in identification of oxidised species. The top panel a) shows the extracted ion chromatogram (XIC) (A) for m/z 594.3765 with the MS spectra (B) and MS-MS spectra (C) supporting the identification with the fragmentation pattern linked to the structure (D). The bottom panel shows XIC with MS and MS/MS profile for m/z 774.5643.

Table 4.1: Holistic approach for categorising the identification process based on interpretation of MS and MS/MS spectra acquired on low resolution Qtrap 5500 and high resolution QTOF 5600 instrument.

Description	Category
Species identified on low resolution QTrap 5500 as well as high resolution QTOF 5600 instrument	a
Species identified only on Qtrap 5500 or QTOF 5600	b
Fragmentation spectra with three or more peaks on either of the instrument	c
Fragmentation spectra with less than 3 peaks for identification purpose	d
No fragmentation spectra (identification solely based on accurate mass)	e
Missing values for ≥ 20 % of samples in a set	f

The identification process was categorised based on the observation of peaks on both of the instruments that is low resolution Qtrap 5500 using targeted approaches and the high resolution QTOF 5600 (see table 4.1) as well as the number of fragment ions that aided the identification. For example, the peak that corresponded to POVPC at m/z 594.3756 in TOF MS spectra showed 3 fragmented peaks in the MS/MS spectra and was also observed in the precursor ion scan spectra on Qtrap 5500 instrument therefore, the identification was categorised as “a, c”.

The extracted ion chromatograms (XIC) were calculated for m/z 594.3761 (POVPC), 650.4391 (PONPC) and 774.5649 (PLPC-OH) for all samples acquired on Qtrap 5500 and QTOF 5600 and the distribution profile of normalised peak area of each species was compared to check for any systemic errors as shown in figure 4.3. It displays the distribution of abundance of species under investigation on the two different instruments using scatter plot with 95 % confidence interval. The distribution of abundance for m/z 594.3761, 650.4391 and 774.5649 on Qtrap 5500 matched the pattern observed for same masses on QTOF 5600 instrument. Moreover, noticeable variability was observed in the distribution pattern of these species in one or 2 samples that exceeded the 95 % confidence interval, thereby skewing the distribution, and significantly affecting the average abundance.

Conversely, the distribution profile for m/z 842.5 acquired on Qtrap 5500 and QTOF 5600 instrument showed a very different profile as shown in figure 4.4. Further investigation revealed that the profile observed for Qtrap 5500 instrument that used targeted approaches for species identification matched the profile of only one of three co-eluting isobaric species (m/z 842.5905) identified on high resolution QTOF MS owing to narrow mass detection window whereas, the other two species with m/z 842.5112 and 842.5221 that are not observed on Qtrap instrument (low resolving power) did not affected the distribution of the matched profile because of lower abundance.

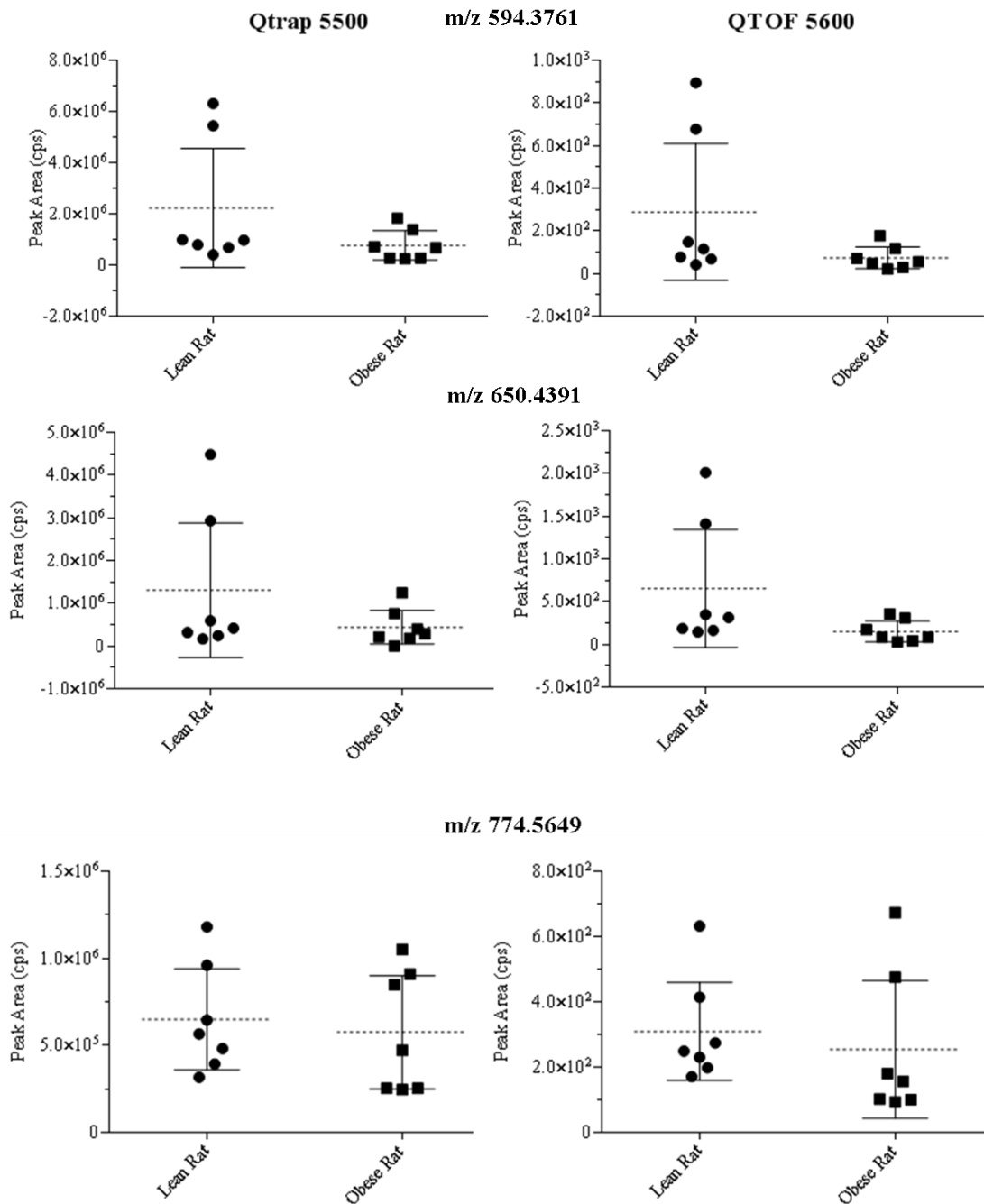


Figure 4.3: Differential profiling of oxidised phosphatidylcholine (OxPC) species in lean and obese rat model of acute pancreatitis. Total lipid extract of ascites of 7 lean and obese rats each were analysed on Qtrap 5500 using targeted approaches (left panel) and high resolution Q-TOF mass spectrometer (right panel) and extracted ion chromatogram (XIC) for m/z 594.5, 650.5 and 774.5 that corresponded to POVPC, PONPC and PLPC-OH respectively was calculated and scatter plot with mean and 95 % confidence interval was plotted to investigate the difference in profiling and response for lean and obese rats on two different instruments.

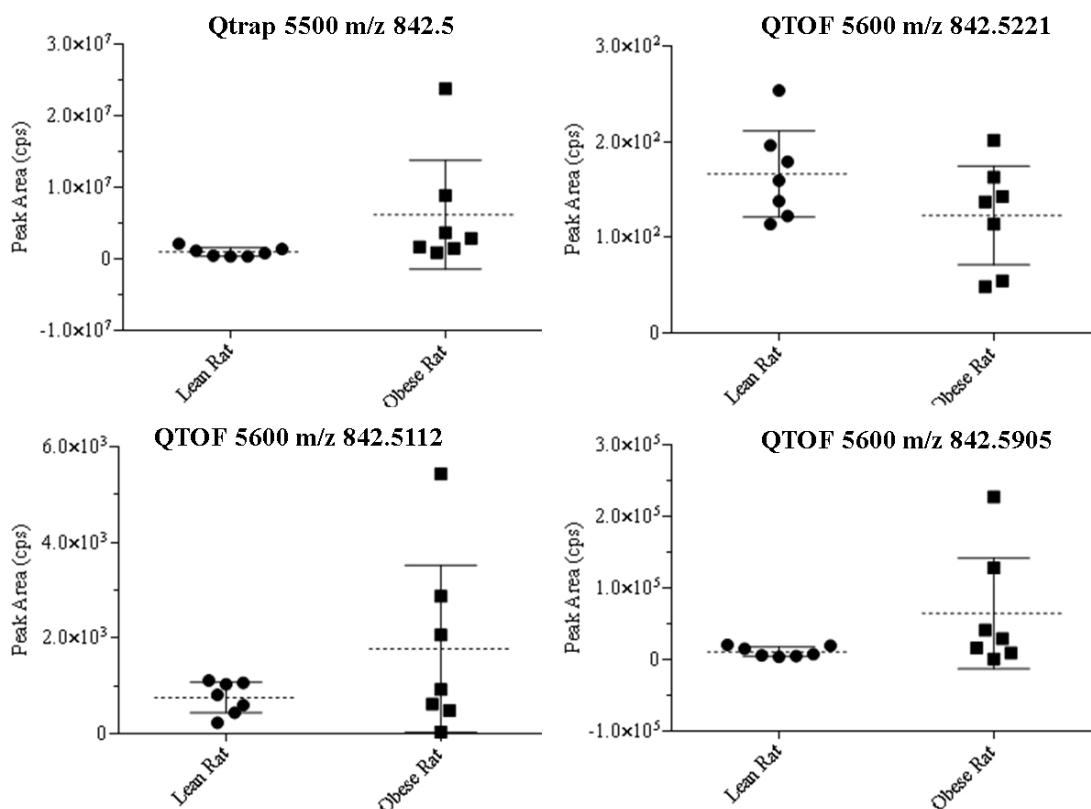


Figure 4.4: Differential profiling of oxidised phosphatidylcholine (OxPC) species in lean and obese rat model of acute pancreatitis. Total lipid extract of ascites of 7 lean and obese rats each were analysed on Qtrap 5500 using targeted approaches (top-left panel) and high resolution Q-TOF mass spectrometer (top-right panel & bottom panels) Only single peak at m/z 842.5 was observed on a low resolution QTrap 5500 instrument whereas, three peaks that corresponded to co-eluting isobaric species were observed on a high resolution QTOF instrument. Graphpad prism was used to plot scatter plot with mean and 95 % confidence interval to investigate the difference in profiling and response for lean and obese rats on two different instruments.

Similarly, the peak areas of all identified species for all samples run on Qtrap 5500 and QTOF 5600 respectively were calculated and the abundance distributions were compared to investigate the difference in instrument response and check overall distribution as shown in figure 4.5. While the abundance distribution for most of the species on two different instruments matched, differences in distribution were observed for low abundant long chain oxidation products, specifically the ones that were formed from species bearing polyunsaturated fatty acids. For example, the peak at m/z 798.5 and 814.5 that corresponds to the hydroxylated product (+ 16 Da) and di-hydroxylated (+ 32 Da) of PAPC (m/z 782.5) can have several co-eluting positional isomers and can lead to chromatographic peak broadening, which affects accurate manual measurement of peak area. Therefore, manual peak area analysis performed on data generated on low resolution Qtrap 5500 for low abundant analytes can be erroneous, in contrast to automated data analysis using progenesis QI for high resolution data generated on the QTOF 5600 instrument. Moreover, the peak at m/z 830.5 was not observed on Qtrap 5500 but was observed on QTOF 5600. However, no MS/MS profile was collected for this species

on QTOF instrument and it not being detected on Qtrap 5500 using targeted approaches (PIS 184 Da) suggested the ion to be extraneous.

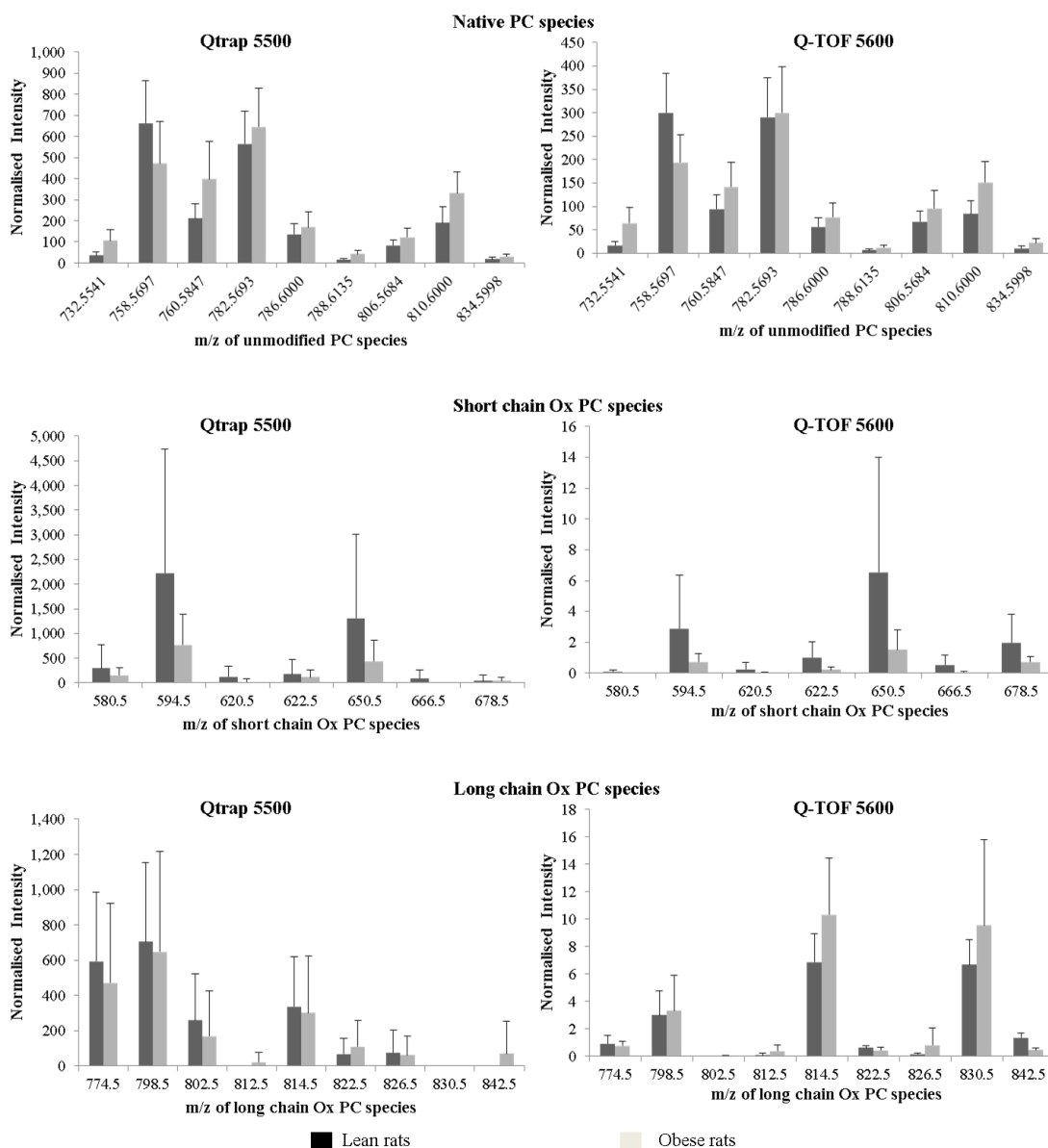


Figure 4.5: Comparative profiling of oxidised phosphatidylcholine (OxPC) species in lean and obese rat model of acute pancreatitis. Total lipid extract of ascites of 7 lean and obese rats each were analysed on Qtrap 5500 using targeted approaches (left panel) and high resolution Q-TOF mass spectrometer (right panel) and extracted ion chromatogram (XIC) for m/z of native PC species, short chain oxidation products and long chain oxidation products was calculated and bar graphs were plotted to investigate the difference in profiling and response for lean and obese rats on two different instruments.

A database was prepared in which all ions were annotated based on their experimental masses, observation of fragmentation spectra and comparison of retention time against standards. The categorisation based on the holistic approach described earlier in table 4.1 was also included. A summary of the database is shown in table 4.2 with information on compound identification and error listing the identification category according to the information generated on two instruments.

Table 4.2: List of all the species identified in total lipid extract of ascites of lean and obese rats with acute pancreatitis.

m/z	Retention Time	Accepted compound Identification	Identification category	Mass error (in ppm)
594.3761	5.29	POVPC	a, c	-0.68
620.3921	5.71	(7-keto,5-heptenoic acid)-PPC	a, e, f	-0.19
622.4116	6.60	(7-hydroxy,5-heptanoic acid)-PPC	a, e	6.08
650.4390	6.27	PONPC	a, d	-0.21
666.4369	6.46	PAzPC	a, e	4.28
678.4734	7.21	SONPC	a, d	4.29
732.5541	21.74	PC(15:1(9Z)/17:0)	a, d	0.41
758.5697	22.36	PC(16:0/18:2(9Z,12Z))	a, d	0.32
760.5847	22.94	PC(16:0/18:1(9Z))	a, c	-0.52
774.5649	20.36	PLPC-OH	a, d	0.74
782.5693	22.66	PC(16:0/20:4(5Z,8Z,11Z,14Z))	a, d	-0.16
786.6000	23.80	PC(18:0/18:2(9Z,12Z))	a, d	-0.93
788.6135	24.27	PC(18:0/18:1(9Z))	a, d	-3.63
798.5604	19.54	PAPC-OH	a, d	-4.95
802.5946	21.91	SLPC-OH	a, e, f	-1.25
806.5684	23.05	PC(16:0/22:6(4Z,7Z,10Z,13Z,16Z,19Z))	a, d	-1.30
810.6000	23.99	SAPC	a, c	-0.60
812.5449	23.46	15-J2IsoP with Palmitoyl	a, e, f	1.27
814.5599	18.64	PAPC-OOH	a, d	1.04
822.5572	21.45	PLPC-2(OOH)	a, e	9.87
826.5935	21.27	SAPC-OH	a, d	-2.58
830.5687	22.94	Not known	a, d	
834.5998	24.38	PC(18:0/22:6(4Z,7Z,10Z,13Z,16Z,19Z))	a, d	-1.18
842.5221	22.42	J2IsoProstane with stearoyl	a, d	4.74
842.5112	21.80	Not known	b, e	
842.5915	21.40	SAPC-OOH	b, d	0.60
(b) Phosphatidylethanolamine class (PE)				
454.2932	5.02	LysoPE(0:0/16:0)	a, d	1.41
482.3254	5.68	LysoPE(0:0/18:0)	a, d	2.73
580.3587	5.29	SOVPE	a, e, f	-3.49
586.3103	5.02	LysoPE(0:0/24:6(6Z,9Z,12Z,15Z,18Z,21Z))	b, d	-6.60
690.5065	19.80	PE(16:1(9Z)/16:0)	a, d	-0.49
716.5240	20.62	PE(18:1(9Z)/16:1(9Z))	a, d	2.18
724.5276	23.24	PE(O-16:0/20:5(5Z,8Z,11Z,14Z,17Z))	b, e, f	0.00
740.5243	22.72	PE(16:0/20:4(5Z,8Z,11Z,14Z))	a, e, f	2.52
764.5225	23.38	PE(16:0/22:6)	a, e, f	0.30
768.5557	24.05	PE(18:0/20:4(5Z,8Z,11Z,14Z))	a, d	2.44

Subsequent step was to develop a rational approach involving post-acquisition data processing and statistical analysis that can minimise the inherent biological variation of biological samples caused by genetic and environmental factors, thereby improving the information generated from the data.

One of the data processing normalisation approaches that was developed and evaluated was the total phospholipid content approach. This was calculated by measuring the total phospholipid content of lean and obese rat samples and the average phospholipid level in each sample was used for normalisation (described later in the chapter), which is shown in figure 4.6 as bar plot with error bars representing the standard deviation calculated for three individual replicates.

Variable amount of total phospholipid was observed in each sample of lean and obese rat with overall total phospholipid higher in obese rats compared to lean rats.

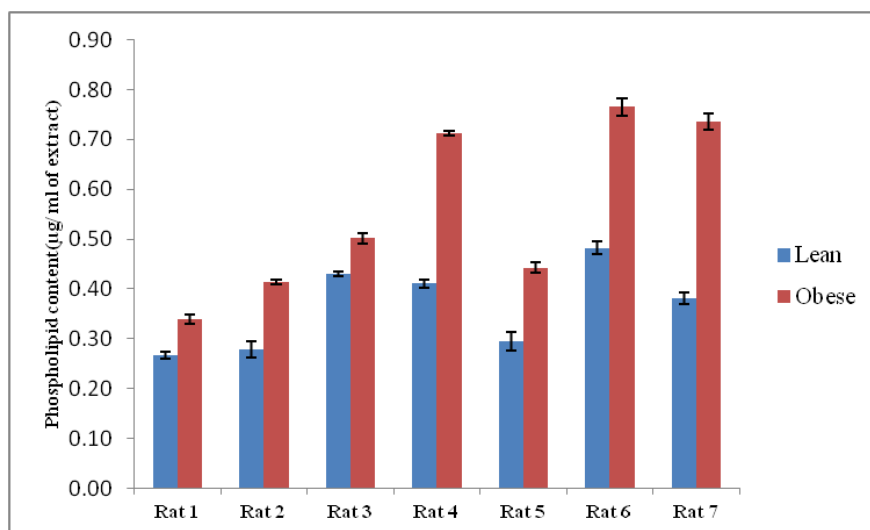


Figure 4.6: Investigation of total phospholipid content of total lipid extract of ascites of lean and obese rats with acute pancreatitis. Ammonium Ferrothiocyanate (AFC) assay with detection using UV spectrophotometry was used to measure the total phospholipid content. The graph represents the average values of three individual replicates with standard deviation that was extrapolated from the calibration curve generated using commercially available phospholipid mixture.

This information about total phospholipid content along with other normalisation approaches like internal standard normalisation, global normalisation, total ion intensity and scaling techniques such as log transformation was utilised to transform the calculated raw peak area with the objective of improving the biological information of the data as well as empowering the statistical analysis, which can be misleading otherwise. Any analyte that was not detected in at least 80 % of the samples within the group was not included in the analysis. For example, a species at m/z 580.3587 (table 4.2) identified as SOVPE , was present only in 2 out of total 7 samples in each group and therefore was not considered for the analysis.

The figure 4.7 illustrates the application of several post data acquisition approaches to calculated raw peak area of unmodified phosphatidylcholine species and comparison of distribution profile pattern. The six different approaches: internal standard normalisation with log transformation, internal standard (IS) normalisation, global normalisation, total ion intensity normalisation, total phospholipid normalisation and total phospholipid normalisation with IS normalisation were applied and statistical analysis was performed with correction for multiple comparison using false discovery rate approach using Graphpad prism software.

While the abundance and distribution pattern of all species matched for all approaches, total ion intensity and total phospholipid content normalisation showed a completely different pattern for some but not all species such as m/z 758.5697, which corresponded to PLPC (16:0/18:2 PC). Moreover, an alternative and unconventional statistical significance rule was proposed and implemented. The proposed rule was defined by the imperative with the prerequisite of calculated p-value to be same in 4 out of 6 total applied approaches in order to be truly significant. Using this rule, relative abundance of no species was found to be statistically significant. However, the relative abundance for peak at m/z 732.5541 that corresponded to 16:0/16:1 PC showed statistically significant difference in abundance in obese rats compared to lean rats in three out of six approaches, it was deemed to be non-significant based on the defined rule.

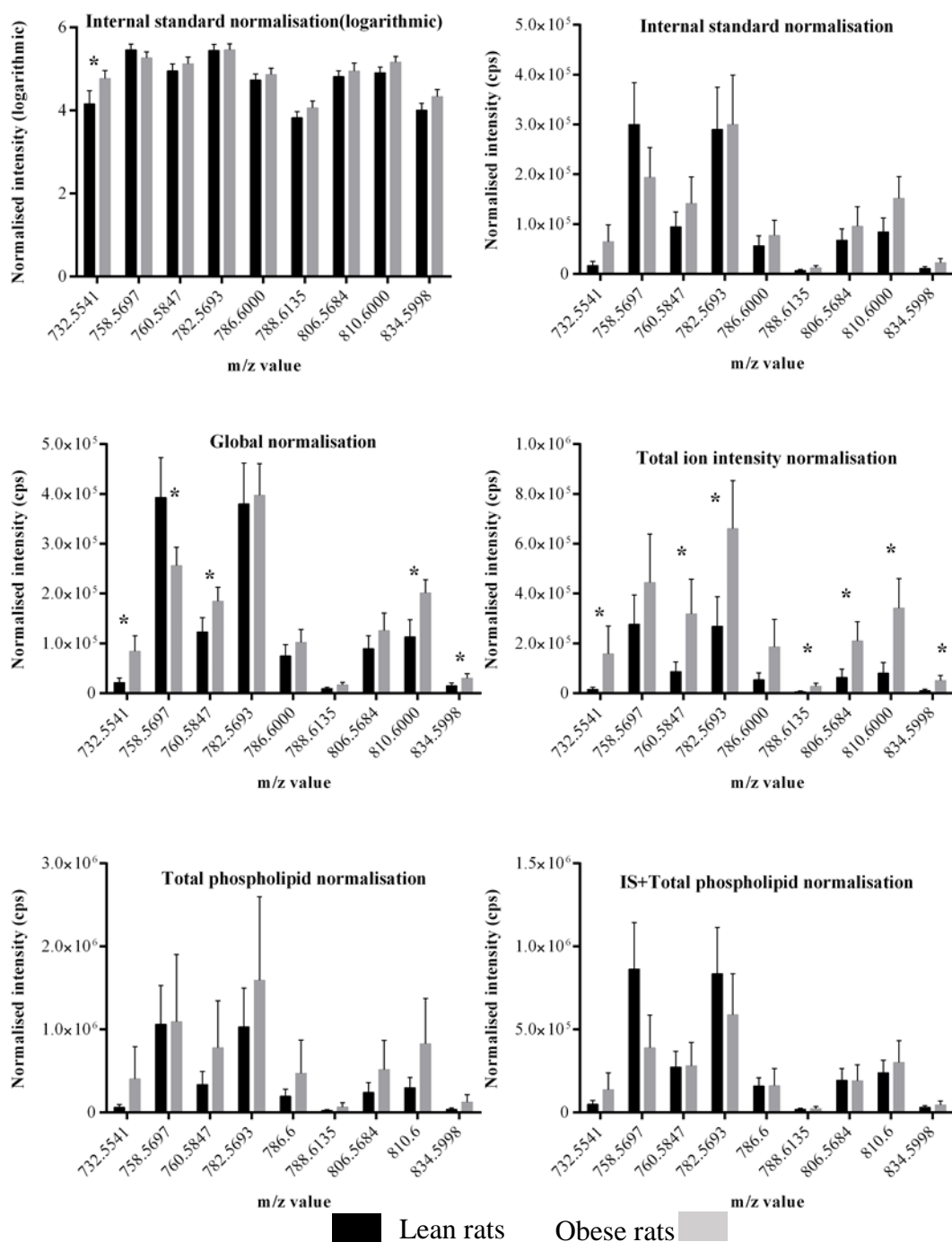


Figure 4.7: Comparison of several post-acquisition data processing approaches on the profile of native PC species in lean and obese rats' samples. Peak area of several species were calculated and processed (transformed) using one of the six approaches as labelled and statistical analysis with correction for multiple comparisons using false discovery rate approach on Graphpad prism was performed. Statistical significance is shown by asterisk (*) mark set at 95 % confidence interval

A similar approach was applied to short chain oxidation products and the same is represented in figure 4.8. The observed pattern suggested minimal difference and influence of post-acquisition approaches on the distribution profile.

No statistical significance was reported in the abundance profile, although, the trend suggested higher abundance in lean rats samples compared to obese rats but the total variance was not possibly accounted by any approaches.

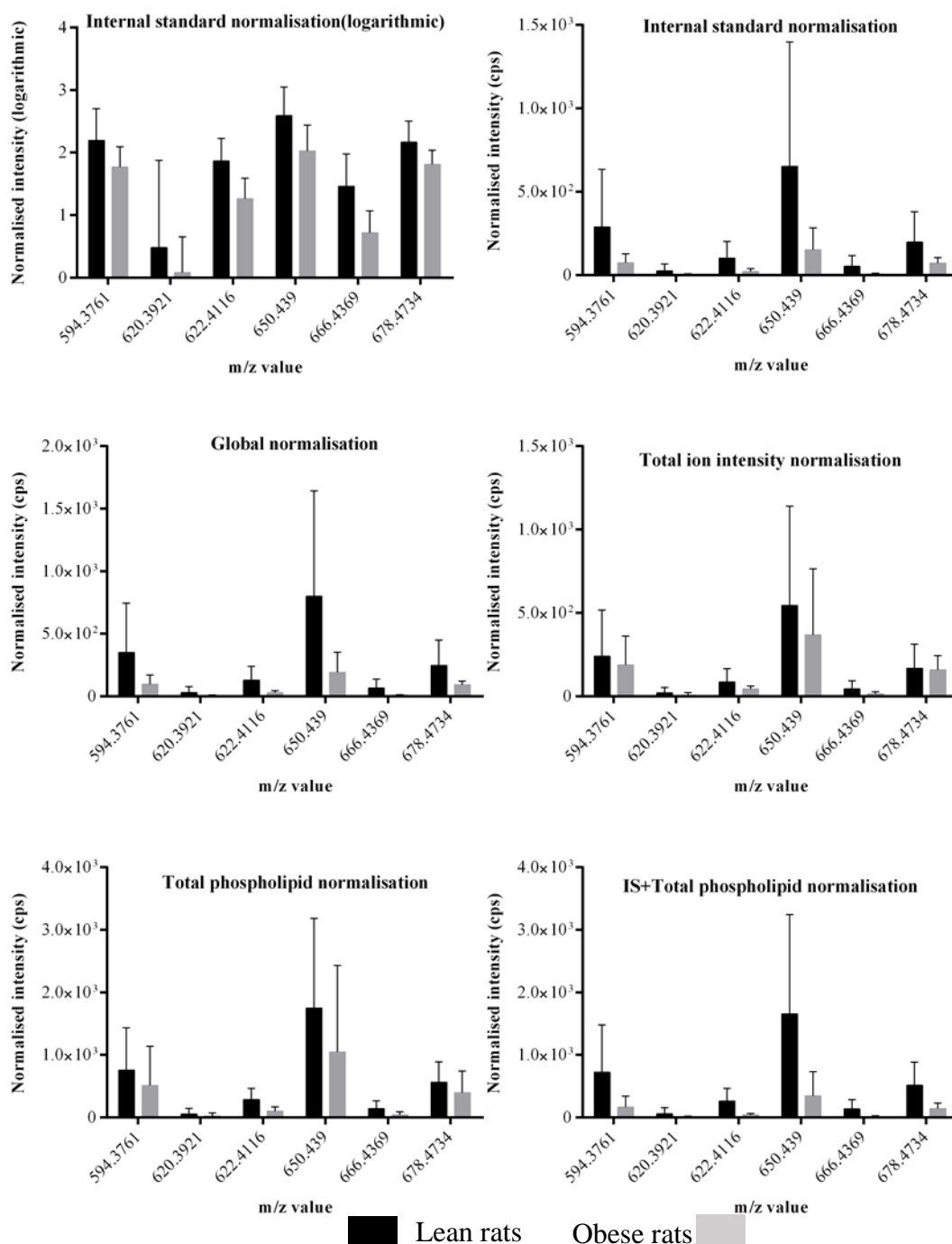


Figure 4.8: Comparison of several post-acquisition data processing approaches on the profile of short chain Ox PC species in lean and obese rats samples. Peak area of several species were calculated and processed (transformed) using one of the six approaches as labelled and statistical analysis with correction for multiple comparisons using false discovery rate approach on Graphpad prism was performed. Statistical significance is shown by asterisk (*) mark with 95 % confidence interval.

The figure 4.9 shows the effect of different post-acquisition approaches on the abundance profile and distribution pattern of long chain oxidation products.

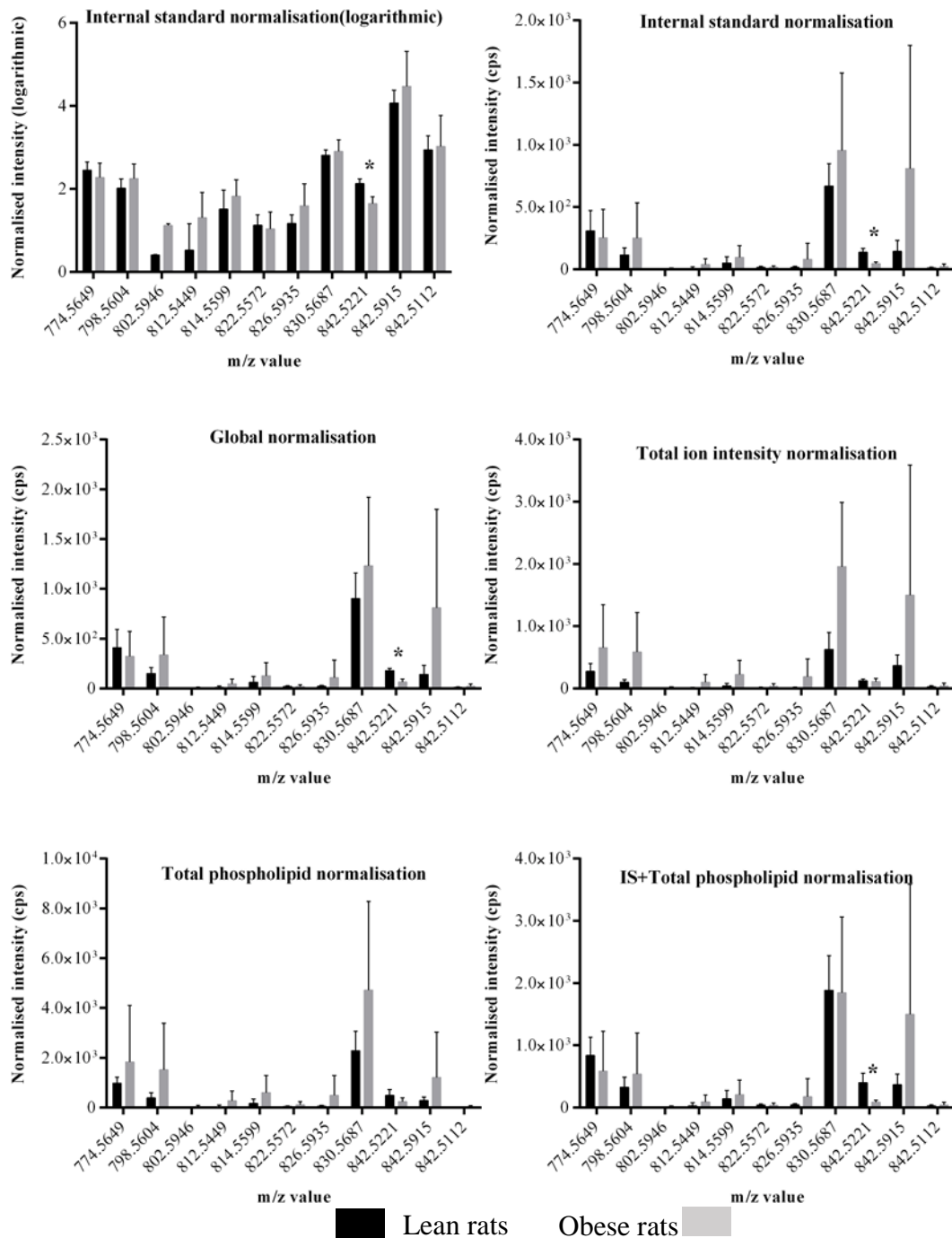


Figure 4.9: Comparison of several post-acquisition data processing approaches on the profile of long chain OxPC species in lean and obese rats' samples. Peak area of several species were calculated and processed (transformed) using one of the six approaches as labelled and statistical analysis with correction for multiple comparisons using false discovery rate approach on Graphpad prism was performed. Statistical significance is shown by asterisk (*) mark.

The peak at m/z 842.5221, which is putatively an oxidised PC species based on the accurate mass and fragmentation pattern showed statistically high levels in lean rats in 4 out of 6 approaches compared to obese rats. However, similar pattern was not observed for this ion for data generated on Qtrap 5500 owing to limitations with the resolution or there might be possibility of extraneous peaks from the matrix or contaminants that can influence the intensity of the analyte peak in high resolution instrument like QTOF MS using general MS survey scan for detection.

All but the total ion intensity normalisation approach and the total phospholipid content approach showed similar distribution profiles, suggesting that these two approaches had greater influence on the distribution pattern, thereby reducing the effectiveness of statistical analysis.

4.4 Discussion

The underlying mechanisms involved in the pathogenesis of acute pancreatitis is ill understood and therefore, several animal models as investigative tools have been developed to understand the pathophysiology of the disease (Hue Su, Cuthbertson et al. 2006). Different non-invasive approaches such as induction with alcohol or hormone as well as invasive approaches such as pancreatic duct perfusion or vascular induced reperfusion have been used to develop animal models to study the disease. Moreover, obesity have shown to be the definitive risk factor of severity and mortality in acute pancreatitis (Martínez, Johnson et al. 2006) (Funnell, Bornman et al. 1993). In this project, bilo-pancreatic duct injection model using sodium taurocholate injection was used for induction of acute pancreatitis in lean and obese rats and the ascites was collected from the peritoneal cavity post 6 hours of induction.

Alteration in lipid metabolism in acute pancreatitis has long been recognised and it has been reported that obesity further exacerbates the pathology (Pereda, Perez et al. 2012, Fujisawa, Kagawa et al. 2016). Higher levels of free fatty acid oxidation products (Gutierrez, Folch-Puy et al. 2008, Grigor'eva, Romanova et al. 2011) and isoprostanoids have been observed in ascites of rats with acute pancreatitis using biological assays and several reports suggested high levels in obese rats with acute pancreatitis (Pereda, Perez et al. 2012). However, comprehensive investigation to decipher the oxidised lipidome using mass spectrometry has never been attempted.

Earlier reports using biochemical assays like TBARS assay showed higher levels of peroxidation products in blood samples of patients with acute pancreatitis suggesting the role of oxidative damage and lipid peroxidation (Verlaan, Roelofs et al. 2006, Milnerowicz, Bukowski et al. 2014). Another clinical study in New Zealand measured oxidative stress markers like protein carbonyls and lipid oxidation using TBARS assay in plasma samples of 90 patients to assess the association and likelihood score of oxidative stress with the disease (Abu-Zidan, 2000).

The mass spectrometry method developed using targeted approaches and chromatographic separation with monolith column enabled identification of several oxidation products in total lipid extract of ascites of lean and obese rat samples with acute pancreatitis (table 4.2) that supported the earlier reports. Moreover, the identification and relative quantification was complemented by the analysis of same samples on high resolution QTOF analysis with automated data analysis using Progenesis QI software that authorised and validated the identification and data analysis. Also, a holistic approach to minimise any inherent biological variability, thereby improving the quantitative information of the data was implemented along with robust statistical analysis to minimise misinterpretation of data. Initial data analysis using mean peak area of all identified species showed that short chain oxidation product species like POVPC (m/z 594.5) and PONPC (m/z 650.5) were abundant in lean rats compared to obese rats but after looking at the distribution in individual samples, it was found that two samples within the set of 7 samples for each set were showing different profile, thereby skewing the results. Therefore, a rational approach was developed that involved normalisation of datasets with five different methods and performing comparative statistical analysis. If 4 out of five data sets treated with different normalisation approach provided similar statistical inference, then only the difference was considered valid.

Although, our investigation did not find any significant difference in the levels of oxidised phospholipid species in lean and obese rats, these findings are only static i.e. they represent the level at a single time point and does not account for the rate of consumption/turnover of these oxidised species. For instance, short chain oxidised phospholipid species bearing terminal aldehydes/ketones with conjugated double bonds are known to be very reactive and they can form Schiff bases and Michael adducts with proteins in the vicinity thereby modulating their functions. Moreover, high lipolytic activity like phospholipase A2 (PLA-2) activity as well as plasminogen activity factor- acetyl hydrolase (PAF-AH) was recently reported in obese model of acute pancreatitis (Patel, Trivedi et al. 2015) (McIntyre, Prescott et al. 2009, Evans,

Papachristou et al. 2010). Therefore, the possibility and the extent of oxidised species that got processed by this higher lipolytic activity cannot not be ruled out. While, mass spectrometry technology is the method of choice for characterization of biological samples owing to the sensitivity and selectivity it offers together with the information rich data it generates, the process of relative quantitation using this technology can be a challenging task considering the fact that several factors and components involved such as ionisation, matrix effects can seriously hamper the quantitative nature (Wasinger, Zeng et al. 2013, Webb-Robertson, Wiberg et al. 2015). While, in this project we attempted to apply and compare several post data acquisition processing approaches along with proposing an all-inclusive unconventional statistical approach to improve the biological content of the data, there is a need of a more robust solution using computational tools to handle the multi factorial, multi dimensionality information that is generated by using this technology.

As stated earlier, there are several approaches to produce animal models that closely mimics the disease condition, although, they differ in pathophysiological nature of the disease that can be studied using this model. For example, alcohol induced acute pancreatitis resembles or is more suitable to study the mild category of the disease with aetiological factors related to alcohol abuse whereas, invasive approach using bile-duodenum injection of sodium taurocholate is associated with more severe form of the disease associated with development of haemorrhagic and necrotic changes in the acinar cells (Hue Su, Cuthbertson et al. 2006). Moreover, recent report attempted to assess the role of ascetic fluid in pathophysiology of the disease and raised the question about the peritoneal cavity fluid to be the location with higher enzymatic activity or the gateway for the toxicological substances to the systemic circulation (Mayer, Airey et al. 1985, Dugernier, Laterre et al. 2000). Nevertheless, protocols need to be standardised to collect the peritoneal fluid along with quenching the proteolytic activity.

Observation of the raw data suggested variability in the levels of species between replicates within treatment group that can add to the variability and obscure the true biological effect. Therefore, care should be taken to minimise any variability that can be caused while handling and induction of disease in the animals. Nevertheless, our study provides useful information about the level of oxidised phospholipid species that reinforces the relationship of oxidative stress with acute pancreatitis and provides a draft of a framework to attempt similar biological characterisation.

5 Oxidised lipidome profiling of isolated components of red blood cell infected with malarial parasite.

5.1 Background

Malaria is a parasitic disease affecting more than 100 countries, causing an estimated of 200 million new infection every year (Percario, Moreira et al. 2012). While active research is being undertaken across the globe to unravel the mechanisms of drug resistance to the current treatment regime for malarial disease caused by *Plasmodium.falciparum* species, factors leading to this resistance are still not well known, owing to a lack of thorough understanding on the pathophysiological mechanism of the disease (Ihekwereme, Esimone et al. 2014).

The malarial parasite resides inside erythrocytes (RBCs) of the infected host during the asexual blood stage of its life cycle. Malaria infection in the host begins with a bite from an infected female anopheline mosquito. As the mosquito feeds, sporozoites are inoculated into the skin. Some drain into the lymph nodes and those that enter the blood stream travel to the liver. In humans, the parasites grow and multiply initially in the liver cells and then in the RBCs. In the RBCs, successive offspring of parasites grow inside and destroy them, releasing daughter parasites (merozoites) that continue the cycle by invading other red cells (Pandey, Babbarwal et al. 2003). The blood stage parasites are those that cause the symptoms of malaria. When certain forms of blood stage parasites (gametocytes) are picked up by a female anopheles mosquito during a blood meal, they start another, different cycle of growth and multiplication in the mosquito. After several days, the parasites are found as sporozoites in the mosquito's salivary glands. When the anopheles mosquito takes a blood meal on another human, the sporozoites are injected with the mosquito's saliva and start another human infection when they parasitize the liver cells. After this initial replication in the liver (exo-erythrocytic schizogony), the parasites undergo asexual multiplication in the RBC's (erythrocytic schizogony). Merozoites infect red blood cells. Alternatively, at this stage (the ring stage trophozoites) mature into schizonts, which rupture releasing merozoites (Sullivan 2002). Thus the mosquito carries the disease from one human to another (acting as a "vector").

The pathophysiology of malaria results from the destruction of RBCs, liberation of the parasite and RBC material or toxins (hemozoin (HZ) or malaria pigment) and cellular debris into the circulation, as well as the host reaction to these events. The parasite digests up to 80% of the host erythrocyte haemoglobin, but the haem is toxic, is dimerized to form the insoluble

crystalline form hemozoin, and is stored in its digestive vacuole (Schwarzer, Kuhn et al. 2003, Sullivan 2005). The hemozoin-containing vacuole is expelled into circulation as a residual body (RB) during schizogony (Coronado, Nadovich et al. 2014).

The liberated hemozoin is bioactive as several reports have been published showing its potential role in modulating biological function such as crucial immune functions, especially targeting phagocytes (Sullivan 2005) (Simoës, Goncalves et al. 2015). Previously, hydroxy fatty acids were identified in saponified hemozoin and found to inhibit monocyte functions, though information about their phospholipid source is scarce (Schwarzer, Kuhn et al. 2003). In another study examining plasma and membrane phospholipids infected RBCs of 60 children with malaria showed a negative correlation between *P.falciparum* infection and phospholipid levels, suggesting modification or increased consumption of phospholipids (Abessolo, Nguete et al. 2009). Similarly, a different lipid profile was observed in RBC infected with the five different sexual stages compared to uninfected RBC and asexual trophozoite infected RBC (Tran, Brown et al. 2016). Total cellular lipidome alteration at different stages of liver infection was observed by shotgun mass spectrometry, which suggested a requirement for host phosphatidylcholine for survival and growth of parasites (Itoe, Sampaio et al. 2014). Moreover, in HZ and parasitized RBCs (pRBCs) monohydroxy derivatives of arachidonic acid (HETEs-hydroxyeicosatetraenoic acid) and linoleic acid (HODEs-hydroxyoctadecanoic acid), and large amounts of the terminal aldehyde: 4-HNE (4-hydroxynonenal) have been determined by the group at University of Turin by demonstrating their role in inhibiting the differentiation of monocytes to macrophages as well as increased cytoadherence and chemotaxis (Schwarzer, Kuhn et al. 2003).

Hemozoin is involved in several aspects of the pathology of the disease as well as in important processes such as the immunogenicity elicited. It is known that the once best antimalarial drug, chloroquine, exerted its effect through interference with the process of hemozoin formation (Martinez, Rajapakse et al. 2008, Coronado, Nadovich et al. 2014).

Moreover, characterisation of isolated components of parasitized red blood cells (RBCs) including Hemozoin (HZ) is yet to be realised that can provide useful insight about the pathology of the disease and may offer novel therapeutic targets. This study was done in collaboration with a research group at University of Turin who provided us with the isolated components of parasitized RBC including the residual bodies (RB), Schizonts (SH), Hemozoin

(HZ) and uninfected RBC (RBC). Our work involved investigation of phospholipid and oxidised phospholipid composition of free HZ and RBs from synchronized cultures of *P. falciparum* parasitized erythrocytes either immediately or 24h after schizogony, with uninfected erythrocytes as controls.

5.2 Aim and Objectives

This study aimed to undertake comparative profiling of oxidised lipidome in isolated components of parasitized RBC like hemozoin (HZ), residual bodies (RB), Schizonts (SH) and uninfected erythrocytes (RBC). To achieve this aim, total lipid extract of the isolated components were analysed on Qtrap 5500 MS instrument using targeted approaches and manual data analysis involving identification of oxidised phospholipid species and peak area integration. This is compared with analysis on high resolution QTOF 5600 instrument and automated data analysis on Progenesis QI software.

5.3 Results

Total lipid extract from isolated components of parasitized red blood cells (RBC's) were analysed on a Qtrap 5500 mass spectrometer using targeted approaches as described in chapter 3. Figures 5.1 and 5.2 illustrate the total ion chromatograms (TIC) for all components under investigation with the corresponding mass spectra in the insets from mass range m/z 450 – 700 in figure 5.1 and m/z 700 – 850 in figure 5.2 respectively. The TICs were obtained using a precursor ion scan of 184 Da, which is selective for the identification of phosphatidylcholine class of phospholipids. Comparison of the ion intensity of the major chromatographic peaks in the 22- 28 minutes region for all samples suggested a difference in the total phospholipid content. Moreover, the averaged spectra for the m/z range 490 – 700 showed high levels of short chain oxidation products in hemozoin samples compared to other samples. The number of oxidised species that were identified in hemozoin samples was higher than in the other isolated components. For example, the mass spectra of the hemozoin sample showed the peaks at m/z 524.5 (18:0 lyso phosphatidylcholine), 594.5 (palmitoyl-oxo-valeroyl phosphatidylcholine (POVPC)), 622.5 (stearoyl – oxo-valeroyl phosphatidylcholine (SOVPC)), 650.5 (palmitoyl- oxononanoyl phosphatidylcholine (PONPC)) and 666.5 (palmitoyl- azealoyl phosphatidylcholine (PAzPC) respectively, whereas the spectra of other isolated components, viz. residual bodies, schizonts and uninfected RBCs did not show all of

these peaks. Additionally, the intensity of these peaks assessed by comparing the peak heights seemed to be higher in hemozoin sample compared to the other isolated components.

The averaged spectra for the m/z range 700 – 850 in figure 5.2 showed high levels of long chain oxidation products in hemozoin samples compared to other samples. The number of oxidised species that were identified in hemozoin samples was higher than in the other isolated components. For example, the mass spectra of the hemozoin sample showed the peaks at m/z 774.5 (hydroxide of palmitoyl, lineoyl phosphatidylcholine -PLPC-OH), 788.5 (keto, hydroxide of palmitoyl, lineoyl phosphatidylcholine -(PLPC-OH, Keto)), 800 (hydroxide of stearoyl, lineoyl phosphatidylcholine -(SLPC-OH)), 818.5 (hydroperoxide of stearoyl, lineoyl phosphatidylcholine -(SLPC-OOH)) and 830.5 (Keto, hydroperoxide of stearoyl, lineoyl phosphatidylcholine -(SLPC-OOH, Keto)) respectively, whereas the spectra of other isolated components, viz. residual bodies, schizonts and uninfected RBCs did not show all of these peaks. Additionally, the intensity of these peaks assessed by comparing the peak heights seemed to be higher in hemozoin sample compared to the other isolated components

To estimate the total phospholipid in samples for loading, a spectrophotometric assay using ammonium ferrothiocyanate was performed and the results suggested that the lipid content varied in different components, as shown in figure 5.3. The residual bodies had lowest amount whereas the schizonts showed the highest amount.

The values of total phospholipid content obtained using these assays were in accordance with the interpretation of the chromatograms in figure 5.1 and figure 5.2. However, owing to limited amount of sample available, this assay was performed without any replicates or technical replicates and therefore, no statistical difference can be inferred using this data. Nevertheless, the information provided by the global analysis of the total phospholipid content suggested the value of an alternative approach for oxidised lipidome profiling, namely analysis of the fold-change in levels of identified species relative to the uninfected RBC's.

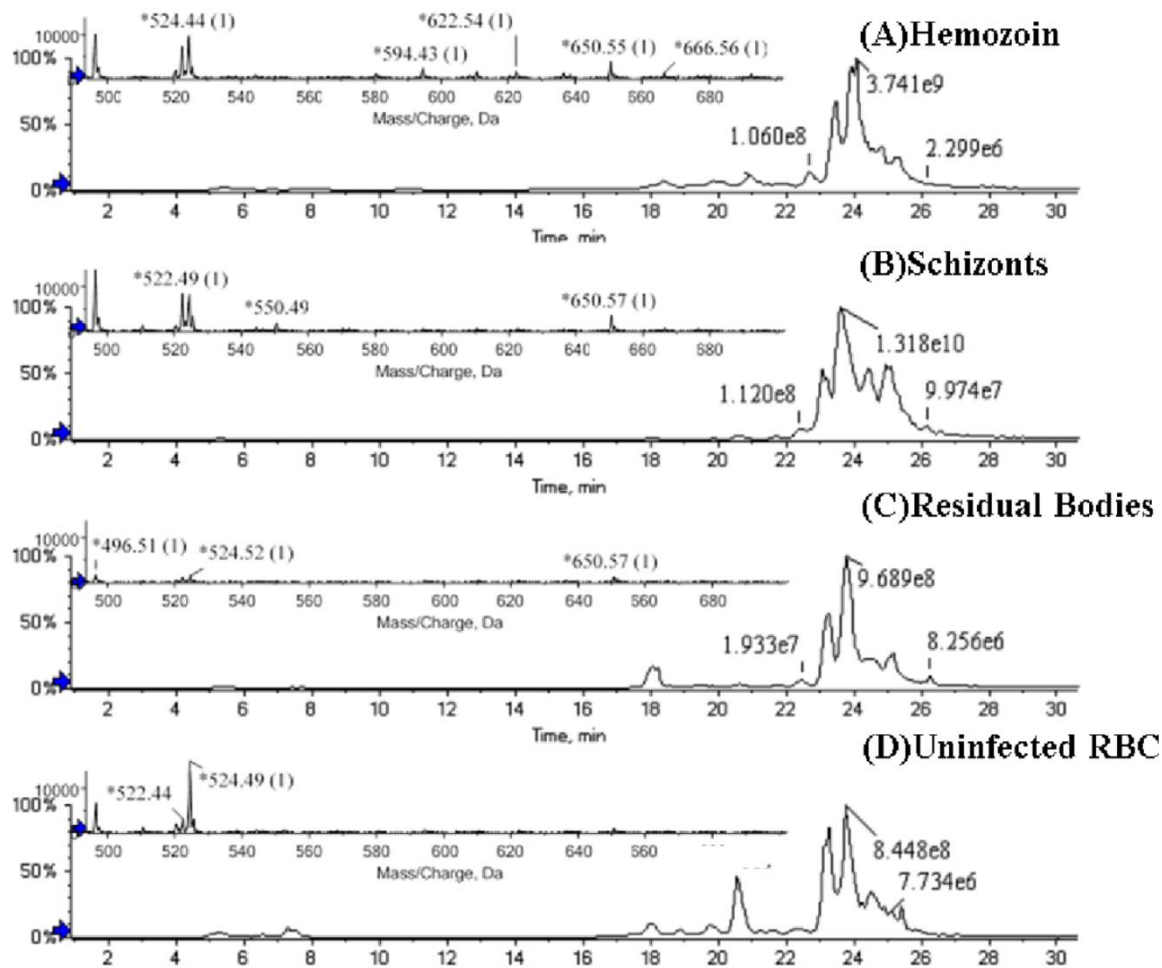


Figure 5.1: Total ion chromatogram with averaged MS spectra from 4-10 minutes in inset for isolated components of parasitized RBCs. (A-C, Hemozoin, Schizonts and Residual bodies) and uninfected RBC's (D) showing different short chain oxidised phosphatidylcholine species profile as well as variable total phospholipid visible by different peak intensities in the region of 20-28 minutes of the chromatogram where the unmodified species elutes. The inset showed the averaged spectra for the 4-10 minutes region of m/z range 450 – 700, which pointed to a different distribution profile for short chain oxidised species. For example, the spectra for hemozoin sample showed peaks at m/z 524.5, 594.5, 622.5, 650.5, 666.5 that corresponded to 18:0 lysoPC, POVPC, SOVPC, PONPC and PAzPC respectively whereas several of these peaks were absent in other samples or were present with low intensity.

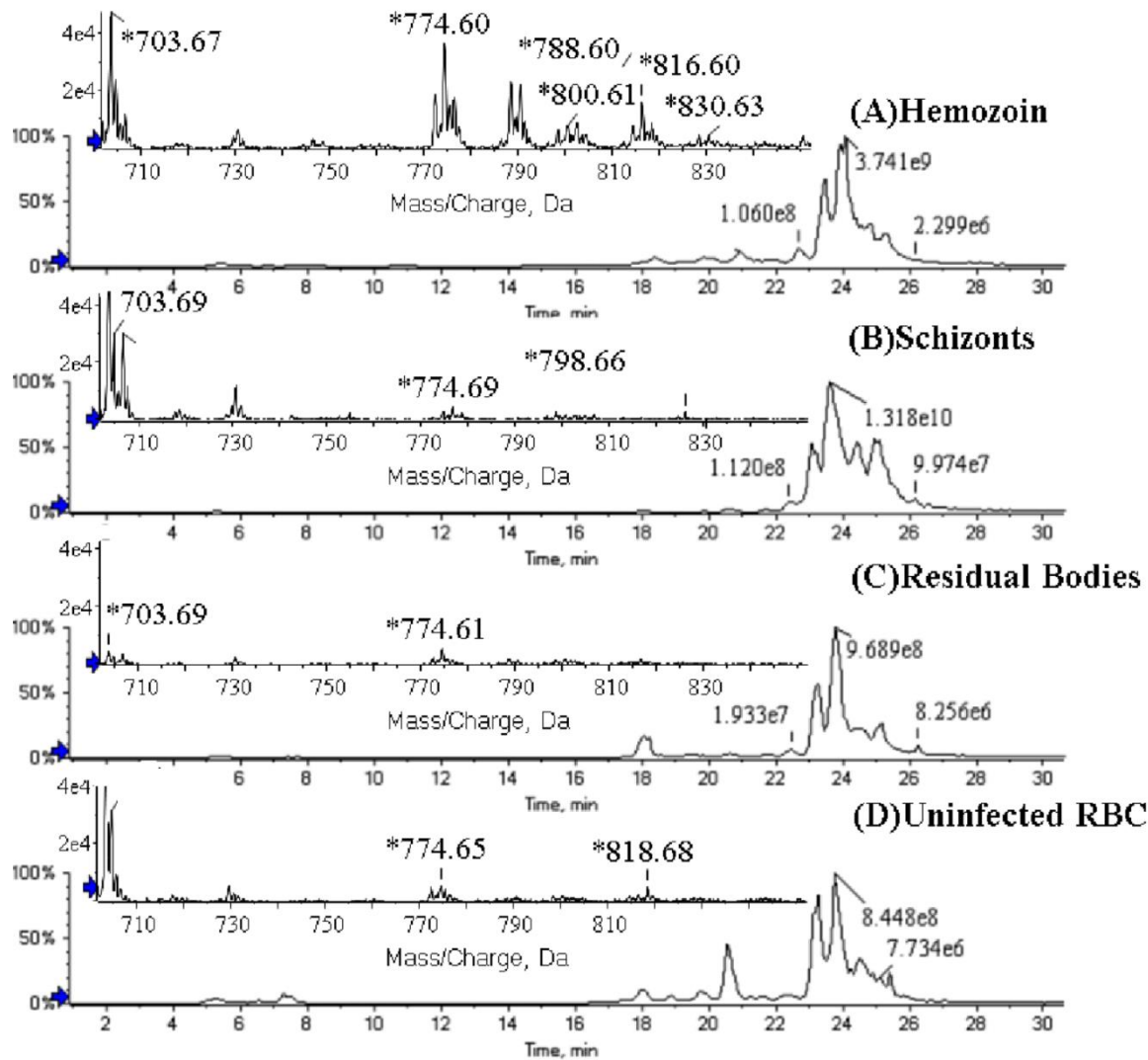


Figure 5.2: Total ion chromatogram with averaged MS spectra from 18-22 minutes in inset for isolated components of parasitized RBCs. (A-C, Hemozoin, Schizonts and Residual bodies) and uninfected RBC's (D) showing different long chain oxidised phosphatidylcholine species spectral profile as well as variable total ion chromatogram by different peak intensities in the region of 18-22 minutes of the chromatogram where the long chain oxidised species elutes. Moreover, the inset is showing the averaged spectral profile for the 18-22 minutes region of m/z range 700 – 850 for all isolated components. For example, the spectra for hemozoin sample showed peaks at m/z 774.5, 788.5, 800.5, 816.5, and 830.5 that corresponded to PLPC-OH, PLPC-OH-keto, SLPC-OH, SLPC-OH-Keto and SLPC-OOH-Keto respectively whereas several of these peaks were absent in other samples or were of lower intensity.

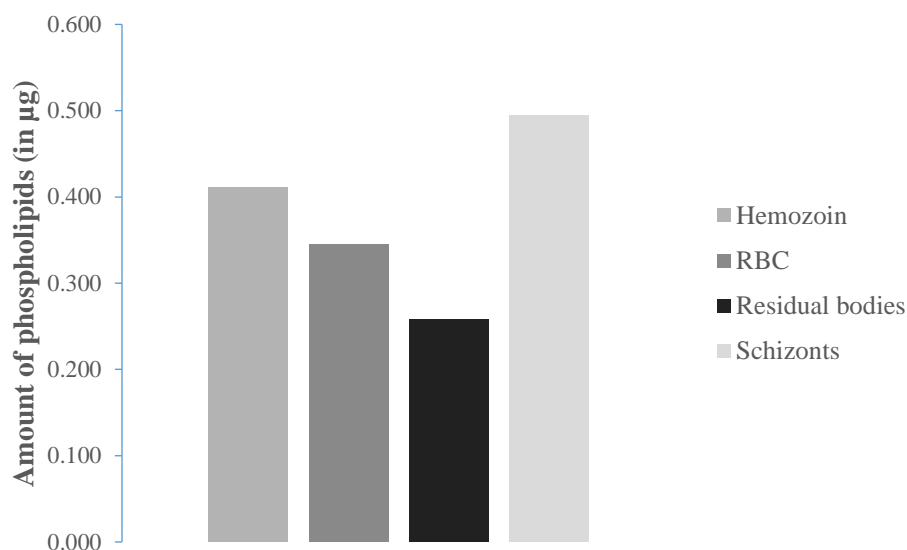


Figure 5.3: Total phospholipid content of isolated components of parasitized RBC's and uninfected RBC determined by Ammonium Ferrothiocyanate assay (AFC). The assay was performed with single sample without any replicates for all components and therefore, no statistics was performed.

The figure 5.4 shows the fold change analysis for all the unmodified phosphatidylcholine species in isolated components of parasitized RBCs relative to the uninfected RBC. The manual peak integration was performed for each species followed by normalisation with the peak area of the internal standard. Subsequently, calculation of the fold change was performed by taking the ratio of normalised peak area of species in each isolated components to corresponding peak area of the species in uninfected RBC that indicated increased or decreased abundance level relative to the uninfected RBC. The error bar represents the standard deviation calculated for the pooled extracted sample. In agreement with the total phospholipids content and interpretation of the chromatogram, schizonts showed high levels of the unmodified species identified using targeted precursor ion scan for 184 Da as well as the MS/MS spectra and the residual bodies showed lowest levels.

Similarly, fold change analysis was performed for short chain oxidation products and long chain oxidation products as represented in figure 5.5 and 5.6 respectively. Here the fold change difference observed was species specific and different to that observed with the unmodified species, where the levels of all the species were higher in schizonts and lower in residual bodies. For example, the relative fold change to uninfected RBC's for (9-OH, 10-dodecenedioic acid)-PPC, m/z 722.5 is negative for schizonts (high phospholipid content) and that of residual bodies (lowest phospholipid content) is equivalent to the uninfected RBC's. Similarly, the relative fold change for (8-oxo-octanoic acid) PPC, at m/z 636.5 is nearly the

same for all isolated components. Overall, the levels of oxidised species were higher in hemozoin compared to other components.

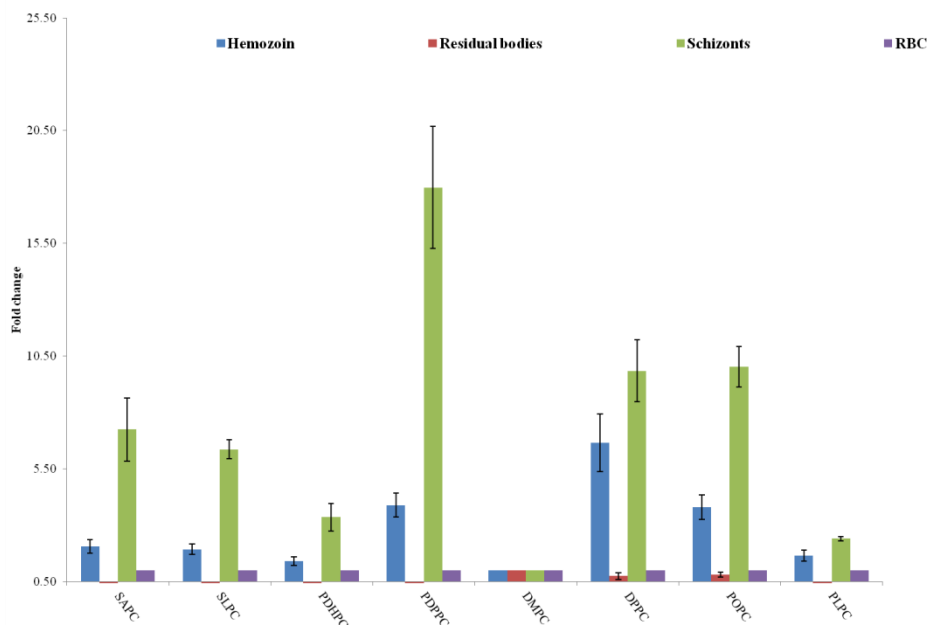


Figure 5.4: Relative fold change analysis of abundance of unmodified PC species in isolated components of infected erythrocytes relative to uninfected RBC. The data were generated on a Qtrap 5500 MS using targeted approaches coupled with a monolith column for chromatographic separation. 10 μ l of total lipid extracts were injected using auto sampler. The data were normalised using 13:0 PC (m/z 650.5) as internal standard and the normalised peak area for each identified species was divided by the peak area of the same species in uninfected RBC sample to calculate relative fold change. The error bars represent the pooled extract sample repeats.

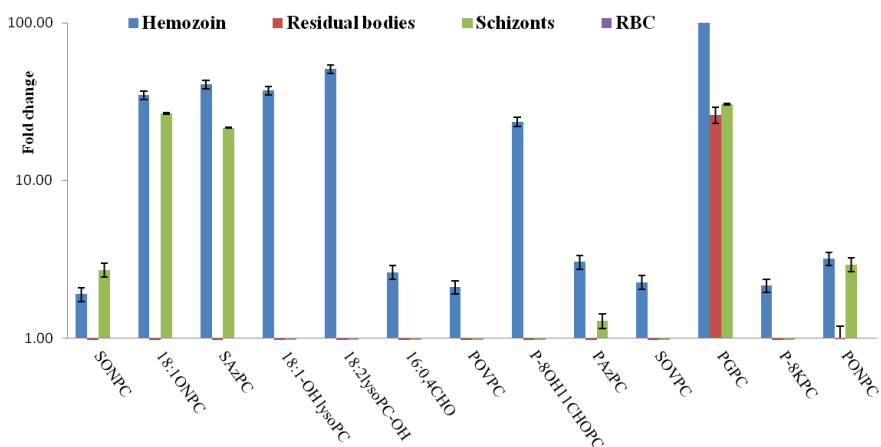


Figure 5.5: Relative fold change analysis of abundance of short chain oxidised PC species in isolated components of infected erythrocytes relative to uninfected RBC. The data were generated on a Qtrap 5500 MS using targeted approaches coupled with a monolith column for chromatographic separation. 10 μ l of total lipid extracts were injected using auto sampler. The data were normalised using 13:0 PC (m/z 650.5) as internal standard and the normalised peak area for each identified species was divided by the peak area of the same species in uninfected RBC sample to calculate relative fold change.

The relative fold change for long chain oxidation products as illustrated in figure 5.6 showed that the levels of entire spectrum of identified species were lower in schizonts compared to other components.

Also, some species such as F2 isoprostanes were found be more than 500 fold higher in hemozoin samples compared to the uninfected RBC samples. Some other species like POPC-OH were equivalent in all components. Moreover, there was substantial number of missing values (species undetectable or below the level of detection) observed in replicates of schizonts samples that could obscure the biological effect or decrease the statistical power of the experiment and therefore, to overcome this, imputed values (mean of the values present) was used and therefore, the error bars in schizonts are skewed.

Nevertheless, some samples were analysed on a high resolution QTOF mass spectrometer and data were analysed using Progenesis QI software, which can handle missing values and unequal variance (assumption of normal distribution) more effectively using their co-detection algorithm and the data analysis is summarised in table 5.1.

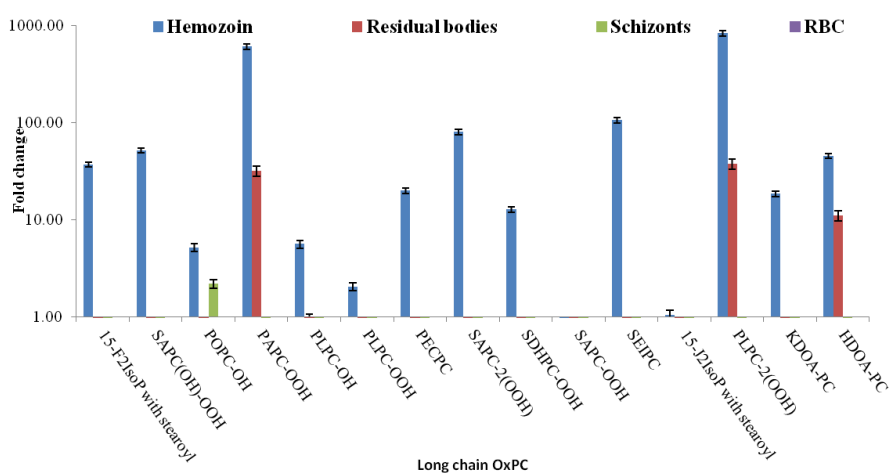


Figure 5.6: Relative fold change analysis of abundance of long chain oxidised PC species in isolated components of infected erythrocytes relative to uninfected RBC. The data were generated on a Qtrap 5500 MS using targeted approaches coupled with monolith column for chromatographic separation. 10 μ l of total lipid extracts was injected using auto sampler. The data were normalised using 13:0 PC, m/z 650.5 as internal standard and the normalised peak area for each identified species was divided with the peak area of the same species in uninfected RBC sample to calculate relative fold change.

The table presents the accurate masses, retention time, p-value of statistical analysis test performed post variance stabilisation and correction for multiple comparison using false discovery rate approach (ANOVA analysis), maximum fold change, information on the samples having highest and lowest levels and accepted identification based on accurate masses and MS/MS spectra with error in ppm for all the identified species in ascending order. It also includes the categorisation of the identification based on the information provided by the MS/MS spectra and mass error i.e. the number of fragments in the MS/MS spectra supporting the identification process and difference between theoretical and experimental masses.

The results obtained with the high resolution mass spectrometry and automated analysis using Progenesis QI software using global normalisation approach were in agreement with the manual data analysis of the data obtained using targeted approaches on low resolution instrument. For instance, the hemozoin samples showed high levels of oxidised species, whereas the unmodified species were high in abundance in schizont samples. Also, mass error of most of the oxidised species was greater than 5 ppm that suggested the possibility of misidentification and they could be alternative isobaric species with similar masses, although, the putative identification cannot be ruled out as the retention time did match the elution profile of oxidised standards as reported in chapter 3. In addition, the MS/MS profile of all these species showed the fragmentation pattern with the most abundant fragment at m/z 184.07 Da suggestive of the phosphatidylcholine class.

Table 5.1: List of oxidised species of phosphatidylcholine class identified in isolated components of parasitized RBC. Samples were acquired on high resolution QTOF instrument and data mining and statistical analysis performed using Progenesis QI software.

m/z	Retention time (min)	Max Fold Change	Accepted Compound ID	Identification category ¹	Formula	Mass Error (ppm)
496.3401	5.21	2.845199	PC(16:0/0:0)	a	C24H50NO7P	0.64
522.3547	5.56	2.794573	PC(18:1(9Z)/0:0)	a	C26H52NO7P	-1.40
524.3702	6.29	17.89929	PC(0:0/18:0)	a	C26H54NO7P	-1.59
544.3377	5.34	7.970868	PC(0:0/20:4)	b		
594.3744	5.65	13.28413	(5-keto-pentanoic acid)-PPC	b	C29H56NO9P	-3.58
622.4058	6.31	20.08312	(5-keto-pentanoic acid)-SPC	c	C31H60NO9P	-3.36
636.4187	6.15	8.633886	2-(8-oxo-octanoic acid)PPC	b, d	C32H62NO9P	-7.60
650.4354	6.56	3.690696	PONPC	a, d	C33H64NO9P	-5.70
666.4365	7.01	2.105689	(nonadioic acid)-PPC	b	C33H64NO10P	3.62
678.4675	15.54	1.669812	Unkown	d		
692.4451	7.56	83.37132	(8-OH,11-keto-9-undecenoic acid)PPC	b, d	C35H66NO10P	-6.62
722.4579	7.03	26.47589	(9-OH,10-dodecenedioic)-PPC	c	C36H68NO11P	-3.25
732.5507	20.20	3.499473	PC(16:1(9Z)/16:0)	a	C40H78NO8P	-4.27
740.5212	20.66	17.49153	PC(18:3(9Z,12Z,15Z)/15:1(9Z))	a	C41H74NO8P	-1.76
756.5476	23.44	7.467103	PC(20:2(11Z,14Z)/14:1(9Z))	a, d	C42H78NO8P	-8.16
758.5656	21.09	4.49116	PC(16:0/18:2(9Z,12Z))	a, d	C42H80NO8P	-5.04
760.5780	24.13	5.876087	PC(16:0/18:1(9Z))	a, d	C42H82NO8P	-9.35
762.5903	24.93	8.791366	PC(18:0/16:0)	a, d	C42H84NO8P	-13.72
770.5256	20.44	5.783693	Unkown	d		
772.5410	21.14	37.71306	PLPC=O	a, d	C42H78NO9P	-10.00
774.5582	19.94	15.1768	PLPC-OH	a, d	C42H80NO9P	-7.90
776.5705	20.35	6.101742	POPC-OH	a, d	C42H82NO9P	-12.28
782.5614	24.02	3.504922	PC(20:4(5Z,8Z,11Z,14Z)/16:0)	a, d	C44H80NO8P	-10.28
786.5922	24.98	5.532142	PC(18:0/18:2(9Z,12Z))	a, d	C44H84NO8P	-10.91
788.5389	16.36	Infinity	PLPC-OH,keto	b, d	C42H78NO10P	-5.93
788.6082	25.31	10.55653	PC(18:0/18:1(9Z))	a, d	C44H86NO8P	-10.41
790.5518	17.86	25.76968	PLPC-2(OH)	a, d	C42H80NO10P	-9.44
798.5528	21.01	1.761227	PAPC-OH	b, d	C44H80NO9P	-14.43
804.5654	18.96	16.1373		d		
806.5607	24.43	3.907098	PC(22:6(4Z,7Z,10Z,13Z,16Z,19Z)/16:0)	a, d	C46H80NO8P	-10.85
810.5920	25.29	6.998587	PC(20:4(5Z,8Z,11Z,14Z)/18:0)	a, d	C46H84NO8P	-10.77
814.5513	21.09	24.8947	PAPC-OOH	b, d	C44H80NO8P	-10.21
816.5663	19.25	27.5427	SLPC-OH,keto	b, d	C44H82NO10P	-10.58
818.5810	20.20	7.123335	SLPC-2(OH)	b, d	C44H84NO10P	-11.72
822.5459	22.96	1.829299	PLPC-2(OOH)	c	C42H80NO12P	-3.94
830.5439	18.15	228.1374	D2isoprostane-Palmitoyl	b, d	C44H80NO11P	-12.43
832.5585	17.35	Infinity	F2isoprostane-Palmitoyl	b, d	C44H82NO11P	-13.67
834.5751	17.92	31.84536	SLPC-OOH,OH	b, d	C44H84NO11P	-12.42
834.5916	25.23	11.99911	PC(18:0/22:6(4Z,7Z,10Z,13Z,16Z,19Z))	b, d	C48H84NO8P	-11.00
842.5091	23.72	1.934857	PAPC-OOH,di-keto	b, d	C44H76NO12P	-10.37
850.6099	13.04	19.95115		d		
852.5358	18.54	Infinity		d		
856.5607	17.92	1369.026	SEIPC	b, d	C46H82NO11P	-10.62
858.5734	19.02	463.8776	D2isoprostane-Stearoyl	b, d	C46H84NO11P	-14.09
874.5689	18.93	187.9257	SAPC-diOOH	b, d	C46H84NO12P	-13.18

¹Identification categories: **a**, MS/MS spectra with more than 3 fragmentation ion peaks; **b**, MS/MS spectrum with only class specific fragmentation ion; **c**, No MS/MS spectrum; **d**, unknown compound or compound identified but with mass error of greater than 5 ppm .

5.4 Discussion

Reactive oxygen species (ROS) have been increasingly implicated in playing a central role in the pathophysiology of malarial infections. The production of ROS is a steady-state event in aerobic respiration. In malaria infections, intra-erythrocytic stages of *P. Falciparum* are mainly responsible for all pathological effects in humans. Uncontrolled production of ROS is problematic for both the host and the parasite. It is generally accepted that oxidative stress is an important mechanism for the destruction of malaria and other intracellular parasites (Vennerstrom and Eaton 1988). ROS are continuously generated by the intra-erythrocytic and hepatic-stage malaria parasites, the RBC or the host immune cells (Golenser et al, 1991). It has been shown that malaria parasites are particularly prone to oxidative stress during the erythrocytic stages (Becker, Tilley et al. 2004).

The malaria parasite haemoglobin digestion produces high concentration of the redox active by-products, free heme and H₂O₂, conferring oxidative stress as a result and formation of hemozoin that have peculiar biological activities (Muller 2004, Wrenger and Muller 2004). The schizont burst releases merozoites and residual bodies containing large amount of parasite products such as hemozoin and parasite membrane fragments, which is able to interact with the innate immune system. The toxic effects of these inflammatory mediators are evident from the characteristic periodicity of malaria paroxysms, including peak fever depending on cyclic schizogony events. During acute malaria infections monocytes and macrophages actively phagocytose HZ released during rupture of schizonts. The presence of HZ-containing monocytes in peripheral blood smears is used as a marker of disease severity. The percentage of HZ-containing monocytes has been reported to be significantly higher in severe malaria cases among Gabonese, Nigerian, Malian and Ugandan children compared to uncomplicated malaria cases (Mujuzi, Magambo et al. 2006) (Metzger, Mordmuller et al. 1995). Apart from inhibiting RBC production, monocyte functions such as the induction of oxidative burst and the ability to perform subsequent rounds of phagocytosis are also impaired upon uptake of HZ (Schwarzer, Turrini et al. 1994, Schwarzer, Kuhn et al. 2003, Skorokhod, Schwarzer et al. 2007, Deroost, Tyberghein et al. 2013, Tyberghein, Deroost et al. 2014, Schwarzer, Arese et al. 2015, Bujila, Schwarzer et al. 2016).

Malaria-infected patients have always reported to show evidence of an increase in lipid peroxidation during infection, particularly in falciparum malaria. This increase is directly proportional to parasitaemia levels. The reduction of antioxidant potency with increased lipid

peroxidation has also been observed to be equally accountable to oxidative stress development in patients. In malaria infection ROS are not only generated as a result of hemoglobin degradation but they are also derived from an immune system activation response leading to the release of ROS as an antimicrobial action (Antoine, Fisher et al. 2014) (Skorokhod, Caione et al. 2010, Uyoga, Skorokhod et al. 2012). These conclusions suggest that oxidative stress is one of the major factors contributing to the development of malarial anemia.

Lipid membrane peroxidation through its final product 4-HNE can be formed by radical-dependent oxidative routes. It has been demonstrated that it generates conjugates with specific aminoacid residues of RBC membranes proteins in Pf -in vitro cultures (Skorokhod, Caione et al. 2010, Tyberghein, Deroost et al. 2014). It has also been reported that the hydroxyl-fatty acids HETE and HODE found present in HZ are final peroxidation products of the arachidonic and linoleic acid. This is due to the continuous generation of lipoperoxidation products in the parasite, during stage maturation in the RBC. (Uchida, 2003).

While the pathological relationship between oxidative stress and malaria parasite have been long established, comprehensive profiling of phospholipid peroxidation products of isolated components of parasitized RBC was not attempted so far. Our study in collaboration with the Schwarzer group at University of Turin, Italy attempted to profile phospholipid oxidation products in isolated components of parasitized RBC using sophisticated mass spectrometry techniques.

The findings showed that the hemozoin samples contained high levels of oxidised species compared to other components like schizonts and residual bodies. This could be one of the reasons for immunogenicity expressed by hemozoin crystals. Several published reports and reviews agreed on unique biological activities of hemozoin. Specifically, isoprostanooids linked phosphatidylcholine species were shown to be higher in hemozoin samples compared to other oxidised species, which were found to be more than 400 fold higher. Also, several short chain oxidation products like POVPC, PONPC and PGPC, whose biological effects have been established in previous studies involving atherogenic models, were shown to be in high abundance in hemozoin samples compared to schizonts or residual bodies. These species have shown to have chemotactic properties as well as pro-inflammatory properties as reported in earlier studies. However, owing to semi quantitative nature of mass spectrometry technique due to several factors that affect the quantitation including missing values, inherent biological

variation and amount of sample loaded; manual data analysis using internal standard normalisation and automated data analysis using Progenesis QI software capable of efficient handling of the missing values and heterodasticity were compared. The results using both the approaches were comparable. Moreover, phospholipids content was estimated using spectrophotometric assay and it showed hemozoin and schizont samples contained phospholipid that is double the amount than found in residual bodies. Nevertheless, the data analysis interpretation does not change even after accounting for this loading variability.

Looking from diagnostic perspectives, blood smear tests are currently the gold standard and the measurement of levels of isoprostanoid like compounds may provide the alternative approach, which can provide information on severity/ occurrence of the disease, although, it may require using sophisticated instruments like mass spectrometry.

Current therapeutic regimens includes artemisinin (an endoperoxide) and quercetin (flavonoids like compounds) that exert their effect by altering the oxidative stress of the parasitized RBC (Ferreira, Luthria et al. 2010). The levels of oxidised phospholipids including the level of isoprostanoids can be used to determine the therapeutic efficacy. Also, the number of different oxidised species identified can offer for alternative therapeutic targets or novel classes of compounds. Moreover, drug resistance being the major factor in malarial treatment, novel therapeutic targets can be developed that can target lipid oxidation products, thereby providing symptomatic relief to patients.

This study was performed using total extract of single replicates and pooled samples and therefore, similar profiling should be conducted on several replicates to validate the findings. Nevertheless, this study provided a comprehensive characterization of oxidised lipidome that can offer further insight about the composition of bioactive components of parasitized RBC and provide novel target to develop newer therapeutic agents.

6 Oxidised lipidome profiling of plasma samples of diabetic patients using mass spectrometry technology: A pilot study

6.1 Background

Type 2 diabetes is a complex polygenic disorder of intermediary metabolism with pathogenesis related to insulin resistance and dyslipidaemia (Krauss 2004). It has also been associated with several metabolic anomalies related to glucose metabolism, lipid metabolism as well as the oxidative stress especially at the mitochondrial site (Schrauwen and Hesselink 2004). It is one of the most prevalent disease of the 21st century and current statistics suggest that about 10 % of the world population aged 60 and above is likely to be suffering from this disease (Chang Wang and Xu 2005). While insulin resistance is the major etiological factor for type 2 and insulin deficiency for type 1 diabetes, several studies have demonstrated that dysregulation of lipid metabolism in the disease (Çakatay, Kayali et al. 2004, Merzouk, Hichami et al. 2004, Niedowicz and Daleke 2005, Kostolanská, Jakuš et al. 2009).

LDL (low density lipoprotein) and HDL (high density lipoprotein) are the lipids carrier present in extracellular fluids including plasma and their levels have long been associated with the development of cardiovascular diseases and metabolic diseases. Insulin resistance and dyslipidaemia have shown negative correlation with the levels of lipoproteins such as LDL and HDL and positive correlation with oxidised form of these lipoproteins (Krauss 2004, Merzouk, Hichami et al. 2004, Silva, Vinagre et al. 2014, Le, El Alaoui et al. 2015, Trpkovic, Resanovic et al. 2015). Moreover, it was reported that the oxLDL reduced preproinsulin mRNA expression and insulin secretion in pancreatic tumor derived islet β cell line (Okajima, Kurihara et al. 2005).

There are very few reports of the use of mass spectrometry to profile the lipidome and oxidised lipidome in biological fluids of patients suffering with type 2 diabetes. Mass spectrometry has been used to measure phospholipids in diabetic plasma using LC coupled to mass spectrometry, and using a range of pre-processing approaches and multivariate analysis the investigators were able to identify biomarkers that could discriminate between control and disease groups (Chang Wang and Xu 2005). A recent study showed altered phosphatidylcholine : phosphatidylethanolamine (PE) ratio related to insulin sensitivity in skeletal muscle cells from type 2 diabetic patients using direct infusion mass spectrometry (Newsom, Brozinick et al. 2016) . Other studies using mass spectrometry and non mass spectrometry based techniques

have focussed on the levels of oxidised fatty acid derived from HDL or LDL in healthy and diabetic conditions (Morgantini, Meriwether et al. 2014) (Silva, Vinagre et al. 2014, Le, El Alaoui et al. 2015, Lokhov, Maslov et al. 2015, Trpkovic, Resanovic et al. 2015). Other types of oxidised lipid compounds such as F2-isoprostanes levels were found to be higher in urine of diabetic patients using gas chromatography mass spectrometry methodology compared to control samples (Devaraj, Hirany et al. 2001).

All the earlier studies demonstrated the extend of lipid peroxidation in the pathogenesis of diabetes by either using colorimetric assays like thiobarbituric acid reactive substances (TBARS assay) or using HPLC-chemiluminescence based assay like FOX assay to measure level of peroxidation or hydroperoxides (Felber, Ferrannini et al. 1987, Nagashima, Oikawa et al. 2002) (Fujiwara, Nishihara et al. 1997). Using these methods, plasma phosphatidylcholine hydroperoxides (PCOOH) concentration was shown to increase in hyperlipidemic and type 2 diabetic patients (Kinoshita, Oikawa et al. 2000, Nagashima, Oikawa et al. 2002). Glycation reaction between amino phospholipid such as PE and reactive aldehydes derived from oxidation of sugar leading to formation of advanced glycation products (AGE) are known to increase in diabetic patients and have shown to increase lipid peroxidation and formation of PCOOH (Miyazawa, Nakagawa et al. 2012) (Bucala, Makita et al. 1993, Kostolanská, Jakuš et al. 2009, Dias and Griffiths 2014).

No attempt so far has been made to identify and quantify specific hydroperoxide bearing oxidised phospholipid species levels as well as other secondary oxidised phospholipid species using LCMS technology. In this chapter we describe a pilot study using plasma samples from diabetic patients (provided by Dr James Brown, Aston University), to develop an optimised method using neutral loss 34 m/z selective scanning approach on a hybrid mass spectrometer Qtrap 5500 that enables detection of all hydroperoxide species. Detection of other oxidised species using head group based scanning approaches was attempted.

6.2 Aim and objectives

The aim of the study was to demonstrate the effectiveness of the selective scanning of neutral loss 34 Da to detect hydroperoxide species in plasma samples of diabetic patients and healthy volunteers, and to use the identified mass to identify the specific oxidised phospholipid species.

To meet the objectives, a total lipid extract of plasma samples of diabetic patients and healthy volunteers were analysed on Qtrap 5500 using targeted approaches and monolithic polyvinylidene column for chromatographic separation. Furthermore, to validate the identification, same samples were analysed on a Sciex tripleTOF 5600 instrument using a high resolution survey scan with data dependent generation of MS/MS scans.

6.3 Results

Chromatographic separation using a monolith column, and detection using targeted approaches such as NL 34 scan for detection of hydroperoxides in conjunction with IDA based MS/MS scans for structural information enabled identification of a number of hydroperoxide species in plasma samples of healthy and diabetic patients. Figure 6.1 (a & b) show representative total ion chromatograms (TIC) for a NL 34 scan of total lipid extract of plasma samples from a diabetic patient and a healthy volunteer. The corresponding summed mass spectra (c & d) illustrates the up regulation of hydroperoxide species in diabetic patient sample relative to healthy plasma sample that eluted between 18-22 minutes. Several peaks corresponding to PLPC-OOH, PAPC-OOH and SAPC-OOH at m/z 790.5, 814.5 and 842.5 were observed in the MS spectra of diabetic sample that were seemingly absent in healthy sample.

Figure 6.2 (a & b) shows the total ion chromatograms (TIC) for PIS 184 Da scan of diabetic plasma and healthy plasma with representative averaged spectra for short chain oxidation products that elute between 4-14 minutes, long chain oxidation products eluting between 18-22 minutes and unmodified phospholipid species eluting between 22 – 26 minutes. Multitude peaks representing oxidised phospholipid species in each category of short chain and long chain oxidation products were observed containing varied functional groups such as: the terminal aldehyde group in POVPC at m/z 594.5, the terminal carboxylic acid in PONPC at m/z 650.5, the epoxy-prostanoid in PEIPC and PECPC at m/z 810.5 and 828.5, as well as hydroxide species like PLPC-OH and PAPC-OH at m/z 774.5 and 798.5. Moreover, unmodified phosphatidylcholine species at m/z 758.5, 786.5 and 810.5 that correspond to PLPC, SLPC and SAPC respectively were observed with similar intensity in the average spectra of healthy and diabetic plasma samples.

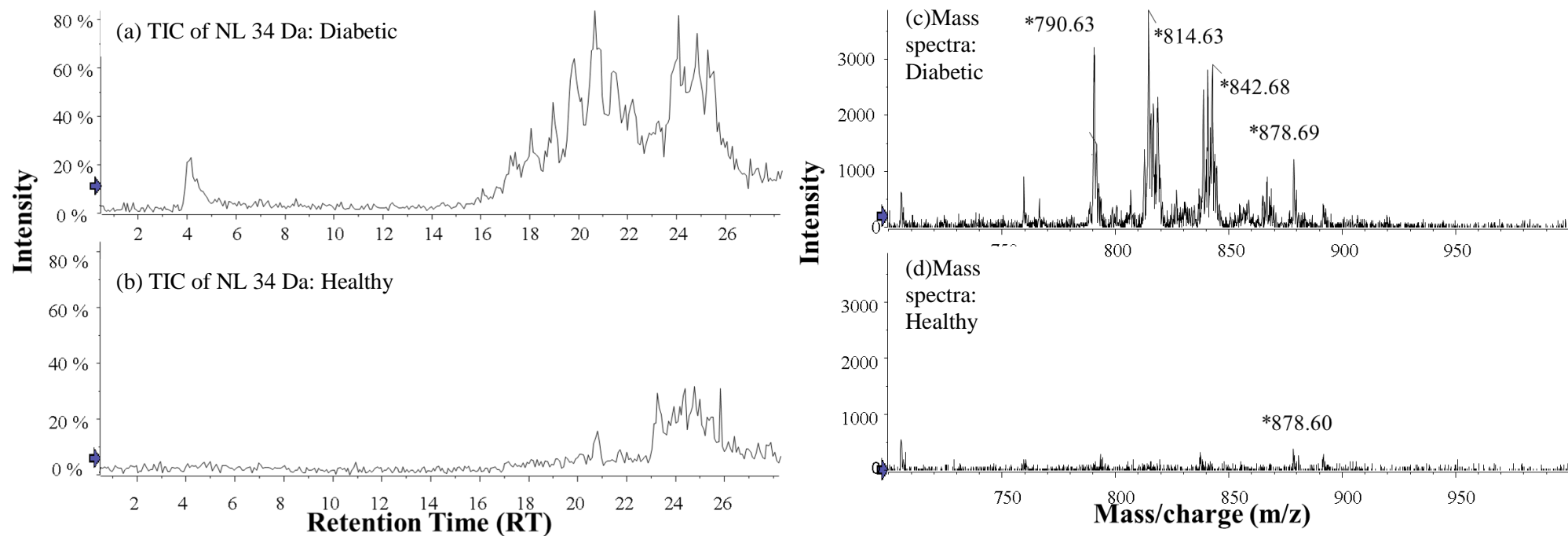


Figure 6.1: Total ion chromatogram (TIC) of neutral loss (NL) scan for 34 Da of total lipid extract of plasma of diabetic and healthy volunteers (a&b) and corresponding spectra (c &d). The TIC along with MS spectra illustrates the unequivocal identification and estimation of abundance of hydroperoxides in diabetic samples relative to healthy plasma. The peaks observed at m/z 790.5, 814.5 and 842.5 corresponded to PLPC-OOH, PAPC-OOH and SAPC-OOH respectively. This experiment was performed using monolith column for separation and Qtrap MS with targeted approaches for detection.

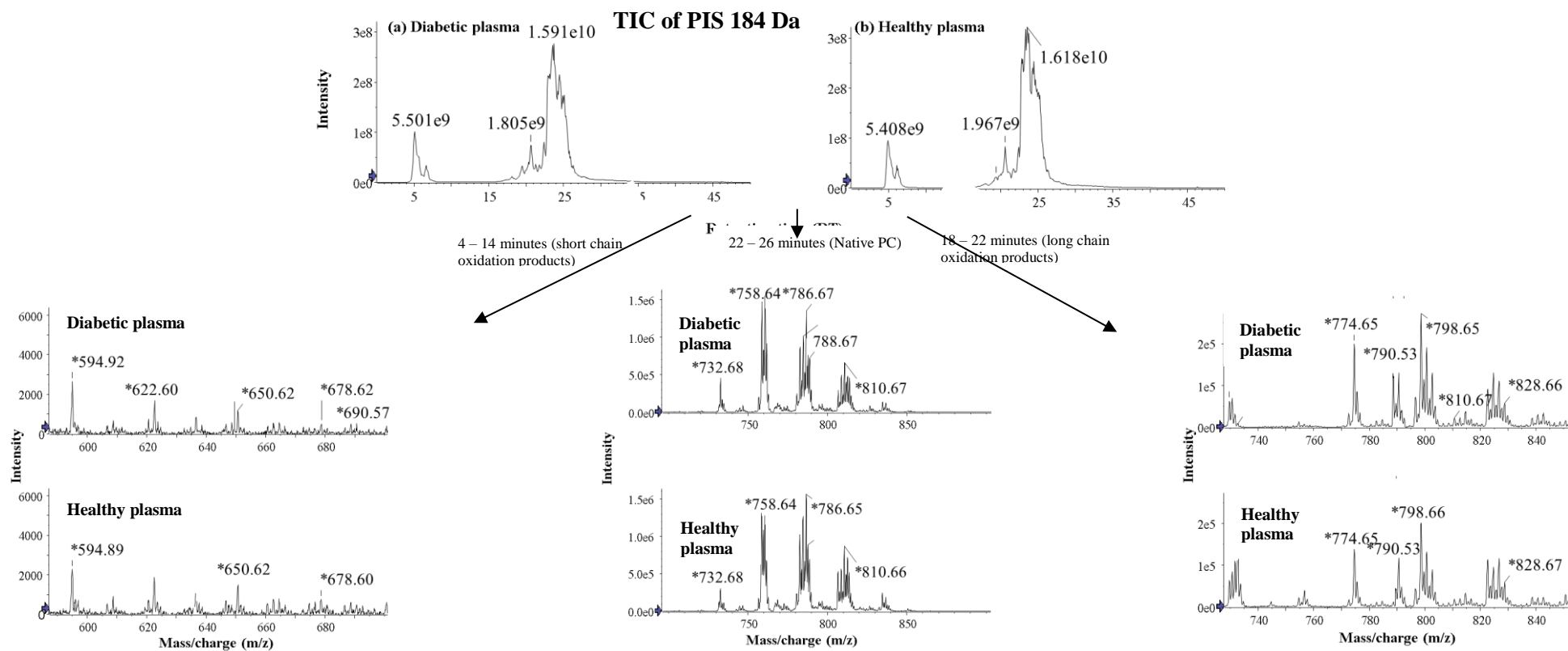


Figure 6.2: Total ion chromatogram (TIC) of precursor ion scan (PIS scan for 184 Da) of total lipid extract of plasma of diabetic and healthy volunteers (a&b) and corresponding spectra representing the elution of short chain oxidation products (4- 14 minutes), long chain oxidation products (18-22 minutes) & native phosphatidylcholine species (22 -26 minutes) respectively .. This experiment was performed using monolith column for separation and Qtrap MS with targeted approaches for detection.

This was followed by identifying of all the oxidised phospholipid species by comparing the elution profile and MS-MS spectra of all of identified m/z with that of the standard mixture generated *in-vitro*, and calculating the peak area of all the observed oxidised species and unmodified species in total 7 biological replicates each of diabetic and healthy plasma samples and normalised using the internal standard approach. Figure 6.3 displays the average abundance of each identified species in diabetic and healthy samples categorised into (a) lyso-PC, (b) hydroperoxide, (c) short chain oxidation products and (d) hydroxide species with the variance being represented by the calculated standard error of the mean. Overall, lysoPCs were more abundant in healthy plasma samples and long chain oxidation products specifically hydroperoxide species in diabetic plasma samples whereas, the level of short chain oxidation products and hydroxide species were similar in diabetic and plasma samples. However, substantial variability was observed in between biological replicates and therefore, no statistical significant difference were found by performing ANOVA analysis. There was a trend for increased level of hydroperoxides in diabetic samples; however, the differences were not statistically significant.

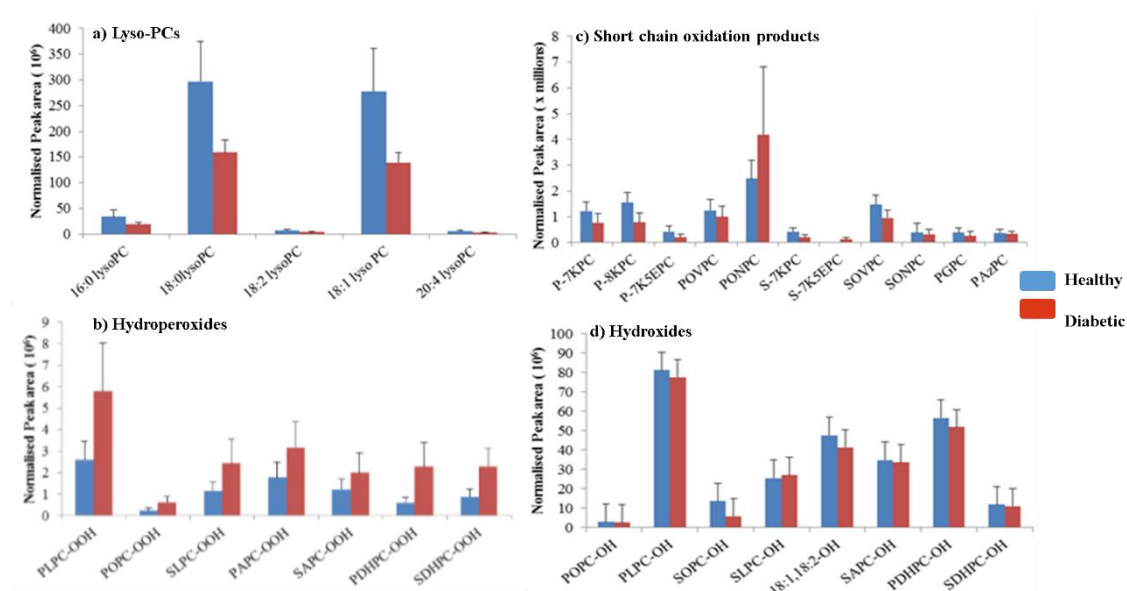


Figure 6.3: Comparative analysis of abundance of several unmodified and OxPC species a) lyso PCs b) Hydroperoxides c) short chain oxidation products d) hydroxides in lipid extracts of diabetic plasma samples (Red) and healthy volunteers (Blue) (N=14). The error bar indicates the standard error of the mean of biological replicates. The data was generated on Q-Trap mass spectrometer using targeted approaches for identification and chromatographic separation was achieved using monolith column.

To further confirm and validate the findings, the same samples were analysed on high resolution QTOF mass spectrometer with IDA based MS/MS scanning. The data was analysed

using the global normalisation approach on Progenesis QI software. Table 6.1 is a list of the experimental masses of the identified species, mass error (ppm) representing the difference in theoretical and experimental mass, verified identification based on accurate mass and MS/MS spectra, and the p-value representing the statistical significance of the difference between control and diabetic samples calculated by performing ANOVA analysis. The results confirmed the manual data analysis performed on data generated using targeted scanning approaches such as NL 34 scan on the Qtrap 5500 instrument. For example, the average abundance difference for POVPC (m/z 594.3776) between healthy and diabetic plasma samples was 1.01 fold found on high resolution QTOF instrument that was in agreement with the levels found by Qtrap instrument. Moreover, statistical analysis using ANOVA analysis showed non-significant difference in levels of all the species identified in diabetic and healthy samples.

Table 6.1: List of oxidised species identified in plasma samples of healthy and diabetic patients using high resolution Q-TOF mass spectrometer. The table also summarises the comparative statistics performed using 2-way ANOVA represented by p-value as well as categorisation of verified identification represented by ranking with letter 'a' and 'b' that is related to confidence in identification > 90 % and < 90% respectively based on MS/MS fragmentation score. The mass error in ppm representing the accuracy in identification based on elemental composition is also listed.

m/z	Retention time (min)	Anova (p)	Max Fold Change	Verified identification category	Verified Compound ID	Formula	Mass Error (ppm)
496.3408	5.29	0.62	1.12	b	PC(16:0/0:0)	C24H50NO7P	2.03
520.3403	5.15	0.80	1.04	b	PC(18:2(9Z,12Z)/0:0)	C26H50NO7P	1.02
524.3721	7.08	0.27	1.25	b	PC(18:0/0:0)	C26H54NO7P	1.92
544.3401	5.34	0.39	1.17	b	PC(0:0/20:4(5Z,8Z,11Z,14Z))	C28H50NO7P	0.58
594.3776	5.86	0.96	1.01	a	(5-keto-pentanoic acid)-PPC	C29H56NO9P	1.76
650.4418	7.54	0.42	1.29	b	PONPC	C33H64NO9P	4.08
732.5521	22.50	0.49	2.38	b	PC(16:1(9Z)/16:0)	C40H78NO8P	-2.32
758.5700	22.32	0.90	1.01	b	PC(16:0/18:2(9Z,12Z))	C42H80NO8P	0.76
774.5655	18.72	0.74	1.10	b	PLPC-OH	C42H80NO9P	1.48
782.5696	22.64	0.91	1.03	b	PC(16:0/20:4(5Z,8Z,11Z,14Z))	C44H80NO8P	0.18
786.5996	23.76	0.98	1.01	b	PC(18:0/18:2(9Z,12Z))	C44H84NO8P	-1.40
790.5600	18.11	0.51	1.78	a	PLPC-2(OH)	C42H80NO10P	0.93
790.5608	19.04	0.51	6.71	a	PLPC-OOH	C42H80NO10P	1.97
798.5645	19.60	0.44	1.11	b	PAPC-OH	C44H80NO9P	0.25
802.5970	20.55	0.91	1.04	b	SLPC-OH	C44H84NO9P	1.64
806.5567	17.35	0.92	2.84	b	PLPC-OH	C42H80NO9P	3.21
806.5691	23.13	0.70	1.10	b	PC(16:0/22:6(4Z,7Z,10Z,13Z,16Z,19Z))	C46H80NO8P	-0.39
810.5989	24.16	0.64	1.16	a	PC(18:0/20:4(8Z,11Z,14Z,17Z))	C46H84NO8P	-2.25
814.5598	16.62	0.49	1.26	a	PAPC-OOH	C44H80NO8P	0.74
818.5903	20.89	0.86	1.99	a	SLPC-2(OH)	C44H84NO10P	-0.32
826.5953	21.27	0.41	1.12	b	SAPC-OH	C46H84NO9P	-0.37
830.5552	16.74	0.59	1.05	b	D2isoprostane-Palmitoyl	C44H80NO11P	1.22
834.5860	19.53	0.90	2.99	b	SLPC-(OOH)OH	C44H84NO9P	0.64
834.5999	24.56	0.51	1.20	b	PC(18:0/22:6(9Z,11Z,13Z,15Z,17Z,19))	C48H84NO8P	-0.99
838.5603	19.39	0.93	4.05	b	SECPC	C46H80NO10P	1.23
842.5912	18.92	0.20	1.45	b	SAPC-OOH	C46H84NO10P	0.78

6.4 Discussion

While the association of oxidative stress with the pathology of type 2 diabetes has long been established, the relationship between phospholipid oxidation and type 2 diabetes is poorly defined as limited studies have been published measuring oxidised phospholipids at the molecular level. We hypothesized that the levels of oxidised species will be abundant in

diabetic patients compared to healthy volunteers and this oxidised lipidome analysis of plasma lipids might improve the understanding of this relationship. Moreover, carbohydrates and lipid metabolism share intimate relationship that suggested a need for further exploration of the association between type 2 diabetes and wide range of oxidised phospholipid species that may provide useful insight into the pathophysiology of the disease. While the recent studies reported the change in plasma lipidome associated with type 2 diabetes (Han, Xia et al. 2011, Zhu, Liang et al. 2011, Meikle, Wong et al. 2013), no study to date has profiled the oxidised lipidome at molecular level in diabetes.

Initially, total lipid extract of seven plasma samples of each healthy and diabetic patients was analysed on Qtrap 5500 using targeted approaches. While, the initial analysis suggested high levels of hydroperoxide species in diabetic patients compared to healthy plasma samples, which was in agreement with other studies conducted using non-mass spectrometry based techniques (Kinoshita, 2000;Fujiwara, 1997; Kostolanská, 2009 ; Nagashima, 2002), the high variance between biological replicates resulted in the differences not being statistically significant. This variance could be due to several biological factors that are associated with the disease such as the difference in glycated haemoglobin (a measure of hyperglycemia), therapeutic drugs that are currently administered and level of HDL, LDL levels etc. A study reported a statistically significant relationship between glycated haemoglobin and the levels of malondialdehyde (MDA) in a case control study involving 30 diabetic patients and healthy volunteers (Goodarzi, Varmaziar et al. 2008). Moreover, a direct cause and effect relationship between oxidative stress and hyperglycemia has been established. Also, a correlation between the levels of HDL, LDL and the levels of F2-isoprostane, which is a kind of oxidised phospholipid species, was examined in a clinical study investigating the role of oxidative stress in rheumatoid arthritis (Rho, Chung et al. 2010). The extent of variability for these biological factors in plasma samples may account for the variance observed in our data analysis. Moreover, hydroperoxide species are relatively unstable species and generally get decomposed to hydroxide species by increased lipolytic enzymatic action, or follows oxidative fragmentation to more stable short chain oxidised species, which can add to the biological variation. Furthermore, the abundance levels observed with the current method provides static abundance levels and does not give any information on the flux magnitude of these identified species.

Similarly, there was no statistically significant difference in short chain oxidation products observed in healthy and diabetic patients although, one of the possible reason could be the marked reactivity of short chain oxidation products. Short chain oxidation products specifically having terminal aldehyde groups are very reactive and they can form Michael adducts and Schiff bases with other biomolecules in the vicinity thereby generating newer species that are not detectable with the current method.

The findings were further validated by re- running the samples on a high resolution mass spectrometer with data dependent MSMS. Similar results were observed with the data generated on high resolution instrument that reinforces the confidence on the detection capability of targeted scanning approaches like neutral loss and precursor ion scan and points us to the direction of designing better experiments that involves further stratification of the subjects in the study.

Further studies need to be carried out integrating several analytical approaches encompassing varied groups of analytes such as proteomics to study lipid protein interaction, glycosylated metabolomics studies and oxidative lipidomics studies to get a clearer picture about the pathology of the disease. Moreover, sample preparation can be modified by isolating HDL, LDL and chylomicrons from plasma of healthy and diabetic patients and extracting lipids from each component followed by mass spectrometric analysis to get a more comprehensive view of the disease. Multivariate analysis (MVA) such as principal component analysis (PCA) and partial least square discriminant analysis (PLS-DA) can facilitate isolating and sharpening the difference between control and diseased samples by accounting for overlapping in signals because of covariance of multiple analytes, thereby aiding in biomarker identification.

Although, our study was not able to reveal the biological difference and association of phospholipid oxidation with type 2 diabetes, it laid a step ahead in the direction that can help design experiments to better understand the pathophysiology of the type 2 diabetes and oxidative stress.

7 Biological effects of antifoaming agents in recombinant protein production

7.1 Background

A life of research scientist working with recombinant protein production can be quite challenging as their work requires handling multi-dimensional data that is produced as well as optimisation of several cultivation strategies that includes but are not limited to design of expression vectors, optimisation of gene copy number or engineering of post-translational processing (Routledge and Clare 2012, Bill and von der Haar 2015, Looser, Bruhlmann et al. 2015). The production of recombinant production on large scale is essential for development and manufacturing of biopharmaceuticals, enzymes and antibodies; to study functional proteomics and to understand cellular mechanisms (Routledge 2012). While transferring or upscaling the process of recombinant production that require aerobic respiration, different mechanical steps are followed like sparging of air from the bottom of reactor flasks and/or use of mechanical stirrers to homogenise and maintain the levels of dissolved oxygen in bioreactors (Garrett 2001, Garrett 2015, Routledge, Mikaliunaite et al. 2015). However, this can lead to the foaming process that affects the quality of recombinant protein produced, sterility environment and may block the exit filters of the bioreactors thereby damaging the equipment (Karakashev and Grozdanova 2012, Routledge 2014). Therefore, one such process and variable optimisation required during protein production is the addition of anti-foaming agents, which are defined as surface active chemical substances, usually derivatives of fatty acids or oils, that, when dispersed in the foaming media, will destroy the foam by bubble coalescence (Schulte 2003, Denkov 2004, Kougiyas, Boe et al. 2015).

Various studies have been performed to investigate the physico-chemical effects of addition of antifoaming agents such as foam height with time and volumetric oxygen mass transfer coefficient (k_{La}) (Routledge, Hewitt et al. 2011); process of foam destruction explained by bridge stretching mechanisms (Etoc, Delvigne et al. 2006, Gao, Yan et al. 2014); hydrophobicity (Ruzickova, Remesova et al. 2005); and growth, metabolic rates and release of lactate dehydrogenase (Hesse, Ebel et al. 2003). Little attention has been given to the biological effects of antifoaming agents on the host cells and recombinant proteins (Routledge 2012).

Previous studies to study the biological effects of the antifoaming agents has been limited to other host organisms like E-Coli K-12 culture producing β galactosidase (Koch, Ruffer et al. 1995), *Geobacillus thermoleovorans* secreting α amylase (Uma Maheswar Rao and Satyanarayana 2003), *Schizosaccharomyces pombe* producing transferrin (Mukaiyama, Giga-Hama et al. 2009), and *Saccharomyces cerevisiae* expressing FC fusion protein (Holmes, Smith et al. 2006, Routledge, Hewitt et al. 2011) and mainly investigated the effect on cell viability, specific growth rate and recombinant protein yield. Moreover, a study using *P. Pastoris* as host strain was published investigating the effect of five different antifoaming agents on several physical properties, growth and viability of the host strain as well as the effect on quality and functionality of recombinant secreted GFP (Routledge, Hewitt et al. 2011). All of these studies highlighted the range of effects different antifoaming agents a various concentrations can have on the host cell as well as the functionality of the protein produced. Single study till date has looked at the effect of antifoaming agents on the functionality and yield of membrane proteins. For instance, the study involving expression of A2aR membrane protein using *P.Pastoris* as host strain investigated the effect of J673A, an alkoxyated fatty acid ester and P2000, a polypropylene glycol on protein yield and cell density (Routledge 2012, Bawa, Routledge et al. 2014).

While a study using *Bacillus* species producing α amylase and investigating the effect of different composition of polyethylene glycol (PEG polymers) pointed out the change in membrane composition, no definitive conclusion was drawn (Andersson, Ramgren et al. 1987). Similar work pointed out the change in lipid composition when PEG8000 was added to the culture of *Schizosaccharomyces Pombe* producing human transferrin (Mukaiyama, Giga-Hama et al. 2009). Moreover, the membrane phospholipid composition and the functionality of the recombinant protein produced, in this case, Vitamin K epoxide reductase, an integral membrane protein was established in a study involving *E.Coli* strain as host with targeted production in the form of inclusion bodies (Jaenecke, Friedrich-Epler et al. 2015). Furthermore, functionality of the membrane protein and the importance of phospholipid environment was extensively reviewed (Phillips, Ursell et al. 2009). However, no study so far investigated the effect of antifoaming agent on total phospholipid composition of the host cell. In this study, the assessment of comparative lipidomic profiling was performed for total lipid extract of *P.pastoris* yeast strain expressing GFP or A2aR protein that were treated with different concentrations of J673-A or P-2000 antifoaming agent.

7.2 Study goals

This study in collaboration with Prof Roslyn Bill and Dr. Sarah Routledge at Aston University was designed to answer the following question:

1. Does the phospholipid profile of total lipid extract of P.Pastoris secreting GFP protein differs from that of expressing A2aR membrane protein?
2. Does the phospholipid profile of total lipid extract of P.Pastoris expressing GFP and A2aR membrane protein changes in response to treatment with different concentrations of J673-A antifoaming agent?
3. Does the phospholipid profile of total lipid extract of P.Pastoris expressing GFP and A2aR membrane protein changes in response to treatment with different concentrations of P-2000 antifoaming agent?

7.3 Results

7.3.1 Comparative Lipidomic profiling for P.Pastoris strain expressing GFP or A2aR protein

7.3.1.1 *Evaluation and comparison of several exploratory data analysis strategies for lipidomic analysis*

This work was done in collaboration with Prof Rosalyn Bill and Dr Sarah Routledge based at Aston University. Handling of P.pastoris yeast strain and setting up of experiments for production of GFP or A2aR protein with treatment of 0.5 % and 1 % J673-A or P-2000 was done by Prof Rosalyn Bill lab and LC-MS analysis to study and compare lipidome for samples expressing different protein and treated with different antifoaming agents was performed by me.

The samples were analysed on high resolution Q-TOF Absciex 5600 instrument with chromatographic separation achieved using HILIC column (Ace silica, 150x 2.1 mm, Hichrom, UK) fitted on Dionex 3000 HPLC system that was interfaced with the mass spectrometer.

7.3.1.1.1 Comparison of lipid profile calculated using automated and manual data analysis approach

To check whether the automated data analysis performed on Progenesis QI complements the manual data analysis that includes generating extracted ion chromatogram (XIC) for individual species. The figure 7.1 summarises the comparison of peak area calculated for representative species manually or co-detection peak peaking algorithm on Progenesis QI. The XIC for m/z 756.5538, 760.5851, 770.564 and 786.6007 that corresponded to 34:3 PC, 34:1 PC, 35:3 PC and 36:2 PC respectively was calculated manually for the lipid extract of P.Pastoris strain expressing GFP and A2aR protein respectively and compared with the peak area calculated for the same species using Progenesis QI software co-detection algorithm. Both approaches showed similar profile for the representative species identified in P.pastoris strain expressing different proteins.

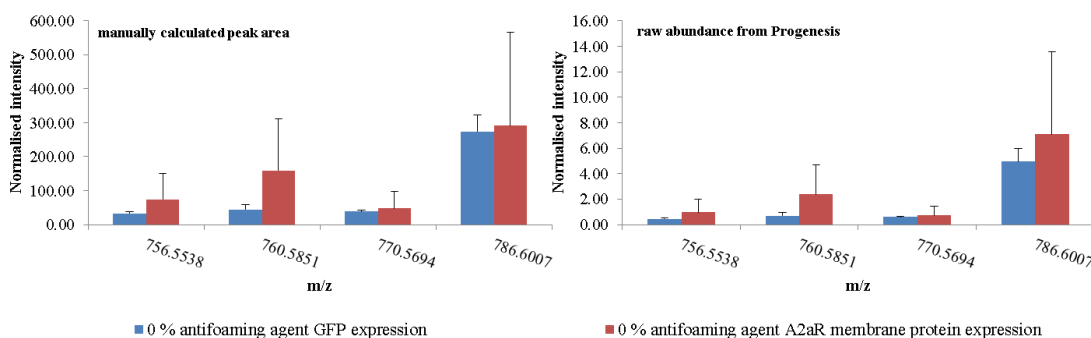


Figure 7.1: Comparison of lipid profile of total lipid extract of P.Pastoris strain expressing GFP and A2aR membrane protein calculated using automated approach on Progenesis QI and manual XIC approach. Peak area for four representative phospholipid species was calculated using both approaches for comparison of profiles.

Subsequently, all the species belonging to the phosphatidylcholine (Melo, Santos et al.), phosphatidylethanolamine (PE) and phosphatidylserine (PS) class were detected on Progenesis QI software by studying the MS and MS/MS spectra and matching the accurate masses and MS-MS fragmentation pattern using Lipidblast database with mass tolerance set to 5 ppm. The table 7.1 lists all the species with retention time, chemical composition and mass error.

Table 7.1: List of all species belonging to PC, PE and PS class identified in total lipid extract of *P.Pastoris* Strain expressing GFP or A2aR membrane protein. The identification was based on accurate mass and Fragmentation matching against Lipidblast database embedded in Progenesis QI software.

Phosphatidylcholine species				
Experimental Mass	Retention Time	Accepted Compound ID	Chemical Formula	Mass error In ppm
482.3246	21.14	PC(15:0/0:0)	C23H48NO7P	1.00
494.3242	21.10	PC(16:1/0:0)	C24H48NO7P	0.10
508.3395	20.99	PC(17:1/0:0)	C25H50NO7P	-0.51
520.3397	20.96	PC(18:2/0:0)	C26H50NO7P	-0.06
522.3554	20.95	PC(18:1/0:0)	C26H52NO7P	-0.12
538.3862	20.80	PC(19:0/0:0)	C27H56NO7P	-1.02
550.3864	20.76	PC(20:1/0:0)	C28H56NO7P	-0.49
636.4955	20.27	PC(26:0/0:0)	C34H70NO7P	-1.16
704.5221	19.26	GPCho(15:1/15:0)	C38H74NO8P	-0.52
718.5382	19.23	GPCho(16:1/15:0)	C39H76NO8P	0.07
726.5040	19.26	GPCho(14:0/18:4)	C40H72NO8P	-3.92
728.5220	19.12	GPCho(17:2/15:1)	C40H74NO8P	-0.64
732.5529	19.18	GPCho(16:1/16:0)	C40H78NO8P	-1.22
744.5534	19.12	GPCho(16:1/17:1)	C41H78NO8P	-0.54
746.5682	19.15	GPCho(15:0/18:1)	C41H80NO8P	-1.61
754.5375	19.07	GPCho(18:3/16:1)	C42H76NO8P	-0.87
756.5532	19.07	GPCho(18:2/16:1)	C42H78NO8P	-0.75
758.5704	18.17	GPCho(16:0/18:2)	C42H80NO8P	1.28
760.5834	19.10	GPCho(18:1/16:0)	C42H82NO8P	-2.20
768.5530	19.04	GPCho(18:3/17:1)	C43H78NO8P	-0.98
770.5689	19.01	GPCho(18:2/17:1)	C43H80NO8P	-0.72
772.5846	19.01	GPCho(17:1/18:1)	C43H82NO8P	-0.59
782.5692	18.99	GPCho(16:0/20:4)	C44H80NO8P	2.93
784.5807	17.41	GPCho(16:0/20:3)	C44H82NO8P	10.6
786.5998	18.99	GPCho(18:0/18:2)	C44H84NO8P	-1.14
796.5251	19.15	GPCho(17:2/18:4)	C43H74NO8P	-1.98
798.5950	18.98	GPCho(18:3/19:0)	C45H84NO8P	-7.15
804.5513	18.99	GPCho(20:5/18:2)	C46H78NO8P	-3.09
812.6132	18.95	GPCho(20:1/18:2)	C46H86NO8P	-3.87
814.6311	18.95	GPCho(20:2/18:0)	C46H88NO8P	-1.17
844.6783	18.84	GPCho(20:0/20:1)	C48H94NO8P	-0.79
872.7094	18.84	GPCho(18:1/24:0)	C50H98NO8P	-1.06
884.7082	19.26	GPCho(22:2/21:0)	C51H98NO8P	-2.31
884.7095	18.75	GPCho(18:2/25:0)	C51H98NO8P	-0.84
896.7091	18.72	GPCho(18:3/26:0)	C52H98NO8P	-1.35
898.7253	18.72	GPCho(18:2/26:0)	C52H100NO8P	-0.69
Phosphatidylethanolamine (PE) species				
452.2771	14.82	PE(16:1/0:0)	C21H42NO7P	-0.05
468.3085	14.68	PE(17:0/0:0)	C22H46NO7P	-0.09
476.2757	14.77	PE(18:3/0:0)	C23H42NO7P	-3.06
480.3086	14.64	PE(18:1/0:0)	C23H46NO7P	0.25
496.3390	14.57	PE(19:0/0:0)	C24H50NO7P	-1.53
502.2903	14.63	PE(20:4/0:0)	C25H44NO7P	-5.02
702.5072	12.71	GPEtn(16:1/17:1)	C38H72NO8P	0.48
704.5221	12.77	GPEtn(18:1/15:0)	C38H74NO8P	-0.49
714.5066	12.66	GPEtn(16:1/18:2)	C39H72NO8P	-0.26
716.5224	12.66	GPEtn(16:0/18:2)	C39H74NO8P	-0.13
718.5374	12.66	GPEtn(16:0/18:1)	C39H76NO8P	-0.95
726.5065	12.61	GPEtn(18:2/17:2)	C40H72NO8P	-0.42
728.5222	12.61	GPEtn(18:3/17:0)	C40H74NO8P	0.16
738.5062	12.59	GPEtn(18:2/18:3)	C41H72NO8P	-0.84
742.5375	12.58	GPEtn(18:2/18:1)	C41H76NO8P	-0.81
744.5533	12.58	GPEtn(18:0/18:2)	C41H78NO8P	-0.68
752.5200	12.59	GPEtn(20:4/17:1)	C42H74NO8P	-3.36
764.5201	12.59	GPEtn(18:2/20:4)	C43H74NO8P	-3.15
766.5349	12.58	GPEtn(18:1/20:4)	C43H76NO8P	-4.22
772.5818	12.58	GPEtn(20:0/18:2)	C43H82NO8P	-4.19
Phosphatidylserine (PS) species				
734.4966	14.28	GPSer(16:1/16:0)	C38H72NO10P	-0.07
760.5121	14.28	GPSer(17:1/17:1)	C40H74NO10P	-0.31
762.5275	14.28	GPSer(17:0/17:1)	C40H76NO10P	-0.57
790.5571	14.28	GPSer(18:1/18:0)	C42H80NO10P	-2.76
798.5247	14.31	GPSer(19:0/18:4)	C43H76NO10P	-4.12
810.5245	14.14	GPSer(20:5/18:0)	C44H76NO10P	-4.33

³GPcho, GPEtn and GPSer correspond to PC, PE and PS class phospholipid. The numerical annotation of species corresponds to carbon chain length and level of unsaturation of fatty acyl chain linked at sn-1 and sn-2 position.

Furthermore, the variability between biological replicates was investigated and several approaches were applied to minimise this uninduced variation (technical and inherent biological variation) that obscured the subtle variation due to the treatment.

7.3.1.1.2 Exploratory analysis to investigate the effect of pre-treatment methods post-acquisition on distribution profile

The figure 7.2 shows the total ion chromatogram (TIC) of three biological replicates of total lipid extract samples of *P.pastoris* strain expressing GFP protein and A2ar membrane protein. The TIC shows the elution time range of PE class species (12-13 minute) and PC class species (18-20 minutes) as well as the contribution of these species of specific class to the total ion intensity (broken boxes). The peak area corresponding to PC class and PE class shows RSD of 52 % and 48 % respectively between replicates. This was further confirmed by comparing the spectra of samples expressing different protein for specific time window that showed the pattern and peak height variability between individual species as shown in figure 7.3.

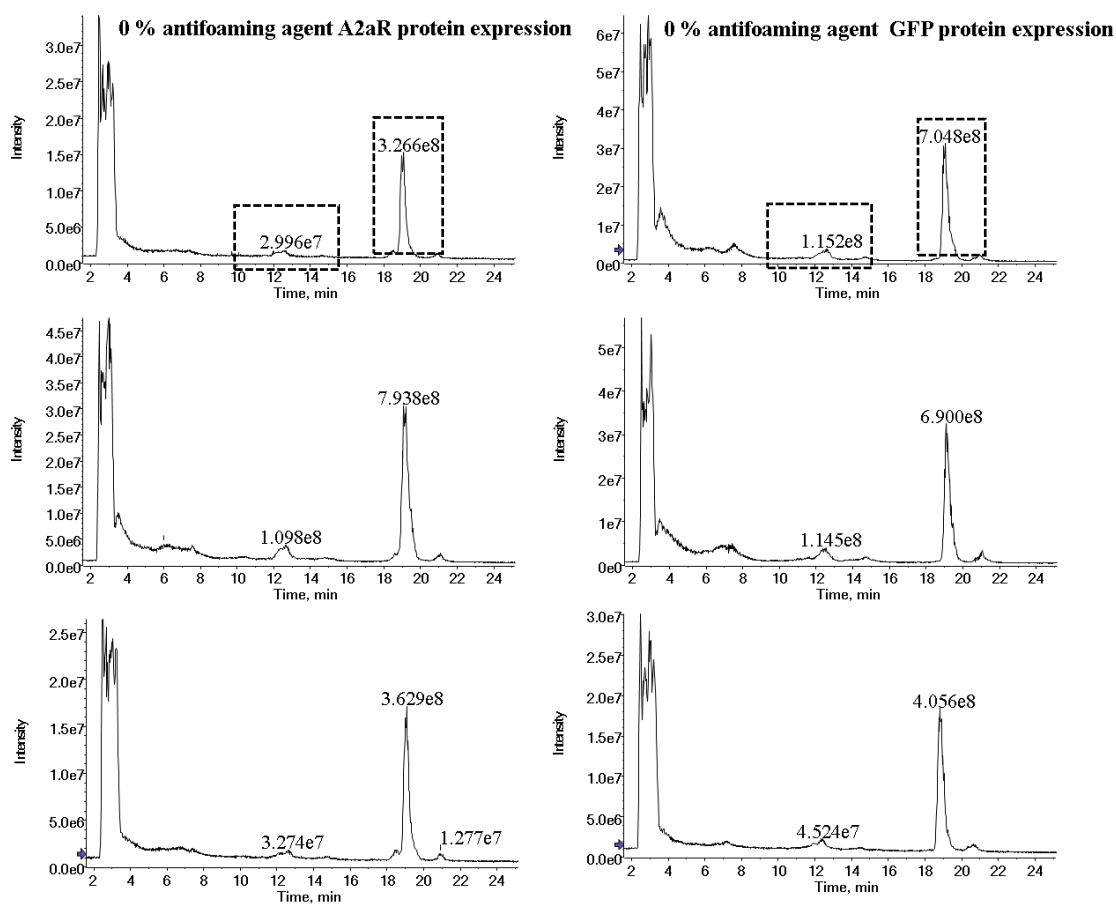


Figure 7.2: Total ion chromatogram (TIC) of biological replicates of total lipid extract of *P.pastoris* strain expressing GFP protein (left panel) and A2aR membrane protein (right panel). The rectangular shape with broken

line represents the elution window of PE and PC class species. The peak area for total PC and PE class shows CV % of 52 % and 48 % respectively between biological replicates.

The figure 7.3 showed the spectral profile of PC and PE class for samples expressing GFP protein (left panel) and A2aR membrane protein. The difference in the pattern of individual species abundance relative to each other within different clusters corresponding to total fatty acyl chain is observed. For example, the sample expressing GFP protein showed high abundance of di-unsaturated species relative to the mono-unsaturated species compared to the A2aR expressing samples. The relative abundance of peak at m/z 758.5 (di-unsaturated species with 34:2 carbon chain and number of double bonds) to m/z 760.5 (mono-unsaturated species with 34:1 carbon chain and number of double bond) is different between samples expressing different protein.

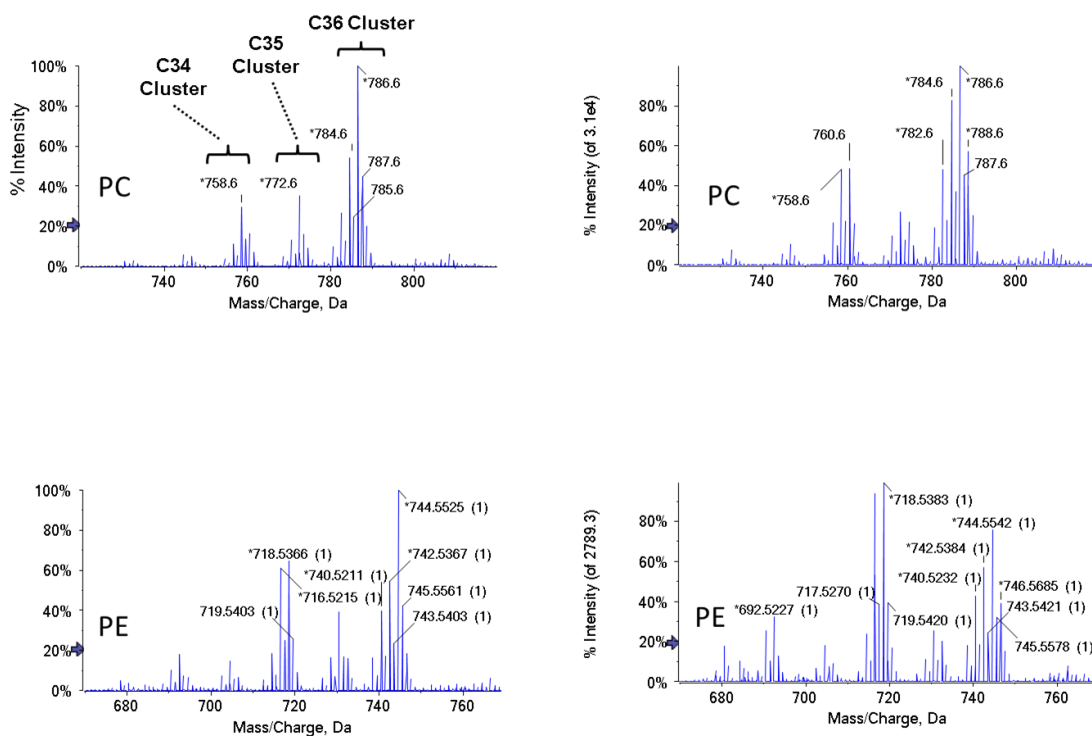


Figure 7.3: LC-MS mass spectra in the positive ion mode of PC class and PE class from *Pichia Pastoris* lipid extracts with GFP secreted membrane (left panel) and A2aR secreted membrane (right panel). The mass spectra of PC class in GFP secreted membrane show the predominance of di-unsaturated and polyunsaturated species, while the mass spectra of PC class in A2aR secreted membrane show the predominance of mono-unsaturated species. The mass spectra of PE class in GFP secreted membrane show the predominance of stearoyl based species (C36 cluster) while the A2aR expressing membrane showed predominance of palmitoyl (C34 cluster) based species.

Furthermore, this uninduced variability can be exemplified by overlaid XICs of individual species for GFP expressing samples and A2aR membrane protein respectively (figure 7.4). The different colour peaks corresponds to biological replicates to demonstrate variability between replicates. The overlaid XIC for m/z 760.5851 of three biological replicates each for the A2aR expressing membrane extract and GFP expressing extract displays one sample differing significant from the rest two replicates suggesting error in sampling or sample preparation. Similar profile is observed in overlaid XIC for m/z 786.6007. These outliers can have profound effect on the average abundance calculation.

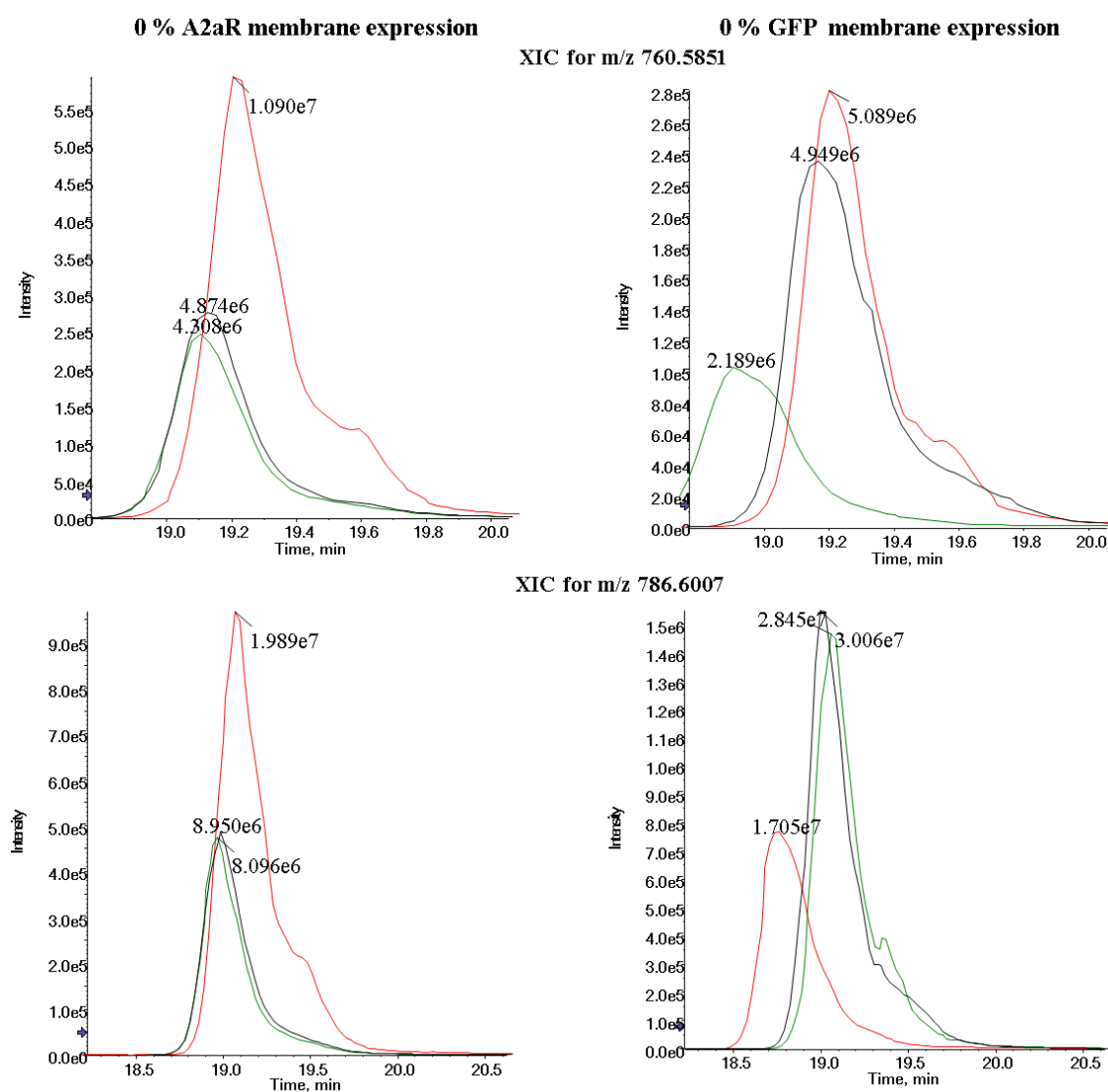


Figure 7.4: The extracted ion current (XIC) obtained for ion at m/z 760.5851 (PC 34:1) of choline class (top panel) and m/z 786.6007 (PC 36:2) (bottom panel) shows variability between biological replicates thereby obscuring the subtle change in abundance due to treatment.

Therefore, to minimise the effect of these outliers we tested several post-acquisition treatments that can account for the skewed variability. Different normalisation approaches like total protein content, pellet weight and global normalisation was used to account for this uninduced variability, thereby minimising its effect on induced variation.

The specific protein concentration was determined by Prof. Roslyn Bill lab and the values were shared with us. Similarly, the weight of the pellet before total lipid extraction was performed using modified Folch method was calculated by Prof. Bill group and the values were shared with us. The raw peak area calculated for all peaks were normalised to the values of specific protein content or pellet weight and its effect on distribution was observed.

The figure 7.5 shows the application of these approaches to calculated peak area of seven species to minimise the variance. However, none of these approaches were able to extract out the subtle biological response or difference. While the distribution and differential analysis for these peaks treated with pellet weight content or global normalisation approach showed similar profile, the treatment with specific protein content completely reversed the distribution profile. Moreover, statistical analysis on graphpad prism with multiple t-test and false discovery rate set to 1% showed no statistical significance in the distribution profile.

Subsequently, the total phospholipid content assay was performed to investigate if the total phospholipid varies between samples as these can affect the distribution profile and alter the abundance level more significantly, if not accounted for in comparative analysis. The figure 7.6 shows the average total phospholipid content in all samples that corresponded to total lipid extract of *P.pastoris* strain expressing different GFP or A2aR membrane protein and treated with either 0.5 % or 1% P-2000 or J673-A antifoaming agent respectively. The distribution shows substantial variability in total phospholipid profile between samples. For instance, the total phospholipid content in extract expressing A2aR protein treated with 0.5 % J673-A is 6 times higher compared to the control extract expressing A2aR protein. Similar profile was observed in extract expressing A2aR membrane protein treated with P-2000 antifoaming agent, although to the lesser extent. However, the total phospholipid content profile for samples expressing GFP with or without treatment did not changed significantly.

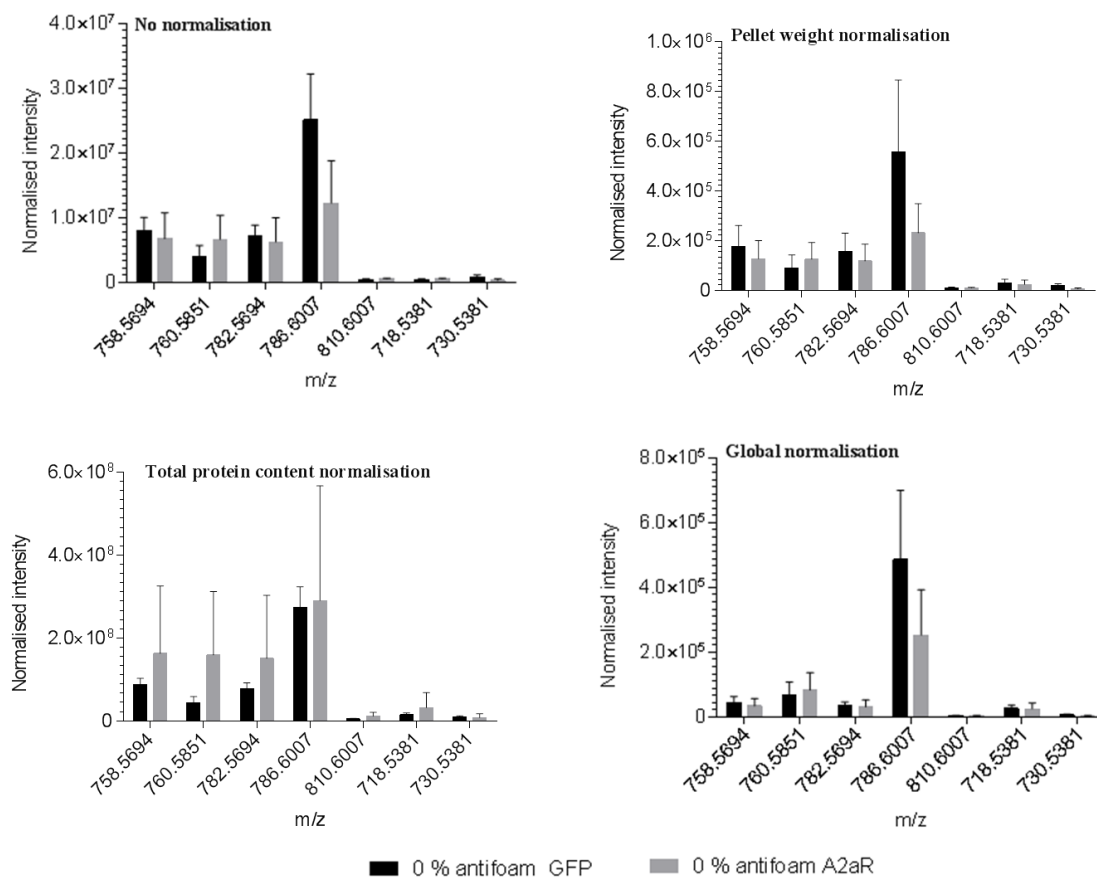


Figure 7.5: Comparison of different normalisation approaches and its effect on the profile of the representative PC and PE species and relative abundance between GFP and A2aR expressing membrane extract. The data plotted is the average of three biological replicates with error bars representing the standard deviation. Statistical analysis was performed on graphpad prism using multiple t-test with false discovery rate correction set to 1 %. No statistical difference was observed.

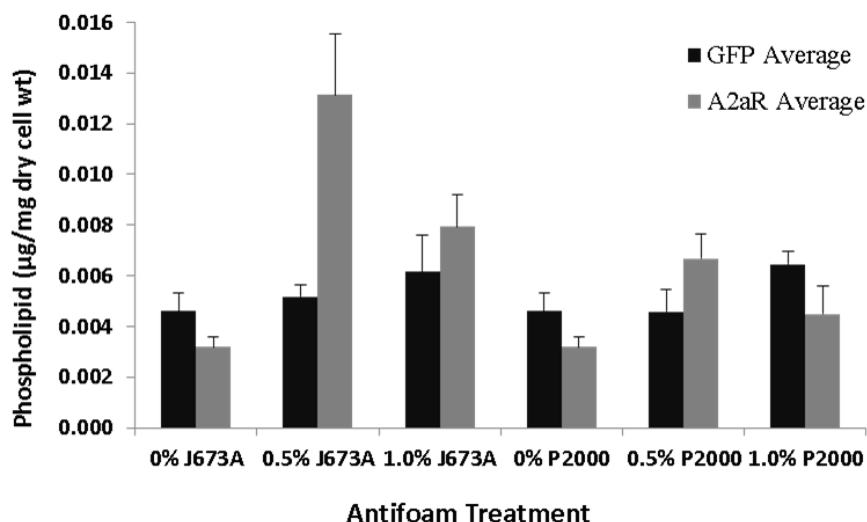


Figure 7.6: The effect of antifoams on total phospholipid content of *P. pastoris*. Cells were grown in shake flasks in the presence of 0%, 0.5% or 1% J673A or P2000 antifoams, and phospholipids were extracted from dry cell pellets by a modified Folch method. Total phospholipid concentration was determined using the ammonium ferrothiocyanate assay. Error bars correspond to 1 S.E.M. (n=3).

Therefore, we applied these values of total phospholipid content to normalise the raw peak area and investigated its effect on the distribution profile. The figure 7.7 shows the effect of normalisation using total phospholipid content on the distribution profile of phospholipid species for extract samples expressing GFP or A2aR membrane protein without any antifoaming treatment. The distribution profile was similar to that observed with normalisation using pellet weight and global weight and this pre-treatment approach also did not significantly minimise the variance to improve the relevant biological information of the data.

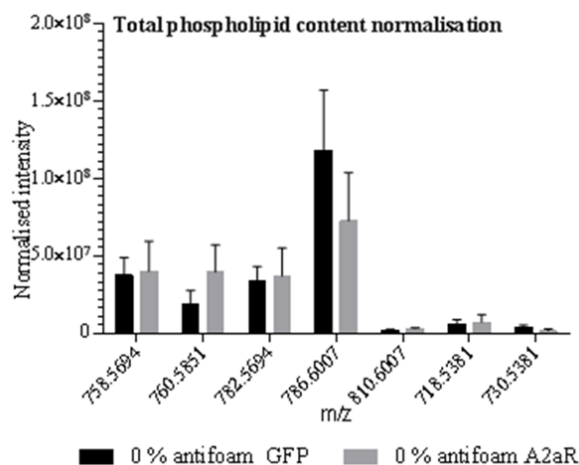


Figure 7.7: Effect of total phospholipid content normalisation on the distribution profile of the representative PC and PE species and relative abundance between GFP and A2aR expressing membrane extract. The data plotted is the average of three biological replicates with error bars representing the standard deviation. Statistical analysis was performed on graphpad prism using multiple t-tests with false discovery rate correction set to 1 %. No statistical difference was observed.

7.3.1.1.3 Ratiometric analysis approach to study the distribution pattern for comparative analysis

However, closer observing the spectra for all the three replicates, we found that the GFP secreting extract showed higher abundance of di-unsaturated and poly unsaturated fatty acyl linked phospholipid species in GFP expressing membrane extract compared to the A2aR expressing membrane extract. However, this biological information was obscured due to variability between replicates and therefore, the ratiometric analysis approach was performed by calculating ratio of peak area of monounsaturated linked phospholipid species to di-unsaturated linked species as well as ratio of monounsaturated to polyunsaturated linked species for all the replicates and the average proportion was calculated, plotted on the graph and statistical analysis performed using multiple t-test comparison with false discovery rate set to 1% using graph pad prism as shown in figure 7.8. For example, ratio of di-unsaturated PC

species (m/z 758.5, 16:0/18:2 PC) to monounsaturated PC species (m/z 760.5, 16:0/18:1 PC) and ratio of polyunsaturated PC species (m/z 782.5, 16:0/20:4 PC) to monounsaturated PC species showed significant higher proportion in GFP expressing species than A2aR expressing species, which was confirmed by the statistical test on graph pad prism using multiple t-test comparison and correction with false discovery rate (FDR) set to 1 %. Interestingly, species with odd carbon chain i.e. 17:0/18:2 PC and 17:0/18:2 PE at m/z 772.5 and 730.5 showed higher abundance in A2aR membrane expressing samples compared to GFP secreting membrane extract. This is illustrated in figure 1-8 by calculating ratio of m/z 758.5 to 772.5 for PC species and m/z 718.5 (16:0/18:1 PE) to 730.5 for PE species and comparing the ratios for both the groups showing statistically significant proportion in A2aR membrane extract.

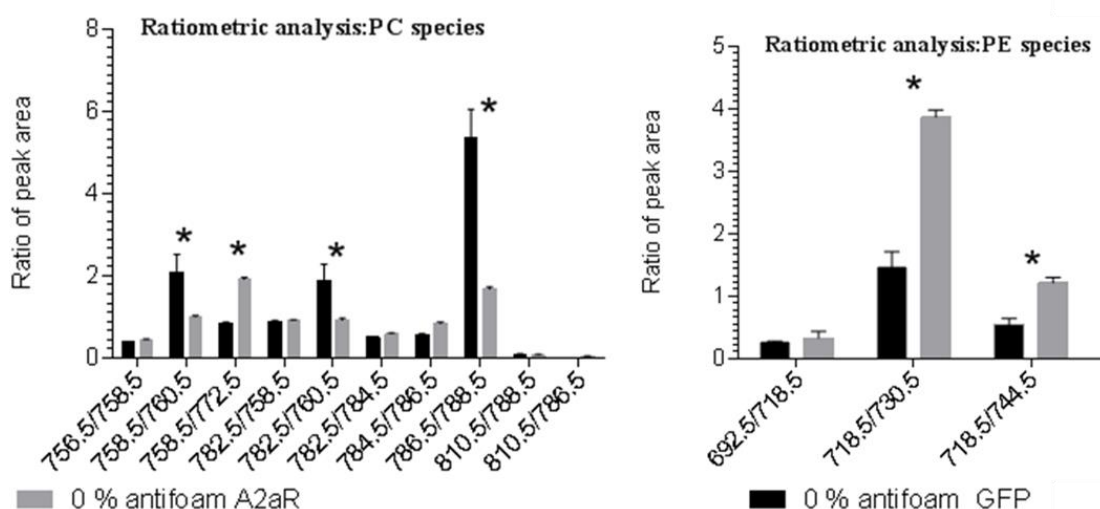


Figure 7.8: Ratiometric analysis approach to study the distribution of lipids in P.Pastoris membrane extract expressing different proteins: GFP and A2aR. Different combination of ratios were calculated where species belonging to same cluster having same number of carbon chain were proportionated as well as species with increasing level of unsaturation from same cluster series. Statistical analysis was performed on graphpad prism using multiple test with FDR set to 1 %. * represents significance set to 95 % confidence interval.

7.3.1.2 Ratiometric analysis approach to study the effect of J673-A antifoaming agent on distribution pattern

7.3.1.2.1 Effect of J673-A antifoaming agent on phospholipid profile of total extract of P.Pastoris expressing GFP protein

The ratiometric analysis approach was applied to study the effect of J673-A antifoaming agent on phospholipid distribution. It was performed by calculating ratio of peak area of monounsaturated linked phospholipid species to di-unsaturated linked species as well as ratio of monounsaturated to polyunsaturated linked species for all the replicates and the average proportion was calculated, plotted on the graph and statistical analysis performed using 2-way ANOVA with multiple comparison and correction using Tukey method and significant level set to 95 % interval as shown in figure 7.9. The investigation suggests concentration dependent increase in abundance level of poly unsaturated fatty acyl chain linked phosphatidylcholine species like 16:0/20:4 PC and diunsaturated fatty acyl chain linked species like 18:/20:4 PC and both species belongs to the C36 cluster whereas there was minimal influence observed on C34 cluster species like peak at m/z 756.5, 758.5 and 760.5.

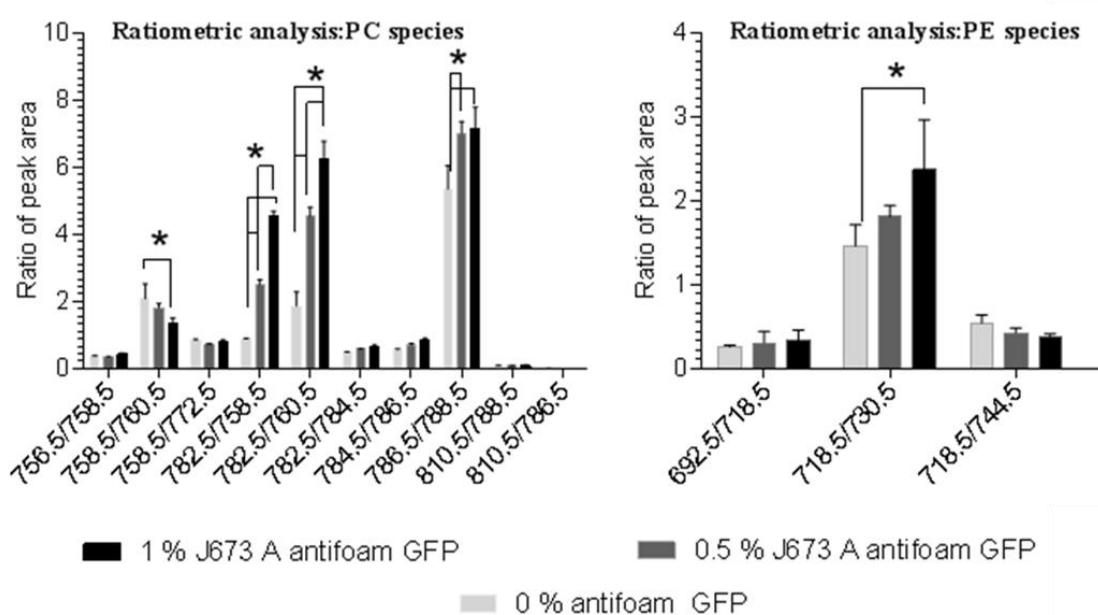


Figure 7.9: Ratiometric analysis approach to study the effect of J673-A on distribution of lipids in *P.Pastoris* membrane extract expressing GFP proteins. Different combination of ratios were calculated where species belonging to same cluster having same number of carbon chain were proportionated as well as species with increasing level of unsaturation from same cluster series. Statistical analysis was performed on graphpad prism using 2-way ANOVA with tukey method for correction for multiple corrections. * represents significance set to 95 % confidence interval.

7.3.1.2.2 Effect of J673-A antifoaming agent on phospholipid profile of total extract of *P.Pastoris* expressing A2aR membrane protein

The effect of J673-A on phospholipid profile of total extract of *P.Pastoris* expressing A2aR membrane protein showed the similar effect as GFP expressing strain, which is illustrated in figure 7.10.

The abundance level of species with higher levels of unsaturation increased relative to saturated or monounsaturated containing species. On the other hand, the ratio of abundance levels of higher masses PE species (m/z 730.5, 17:0/18:2 PE) decreased relative to mono unsaturated lower mass species (m/z 718.5, 16:0/18:1 PE).

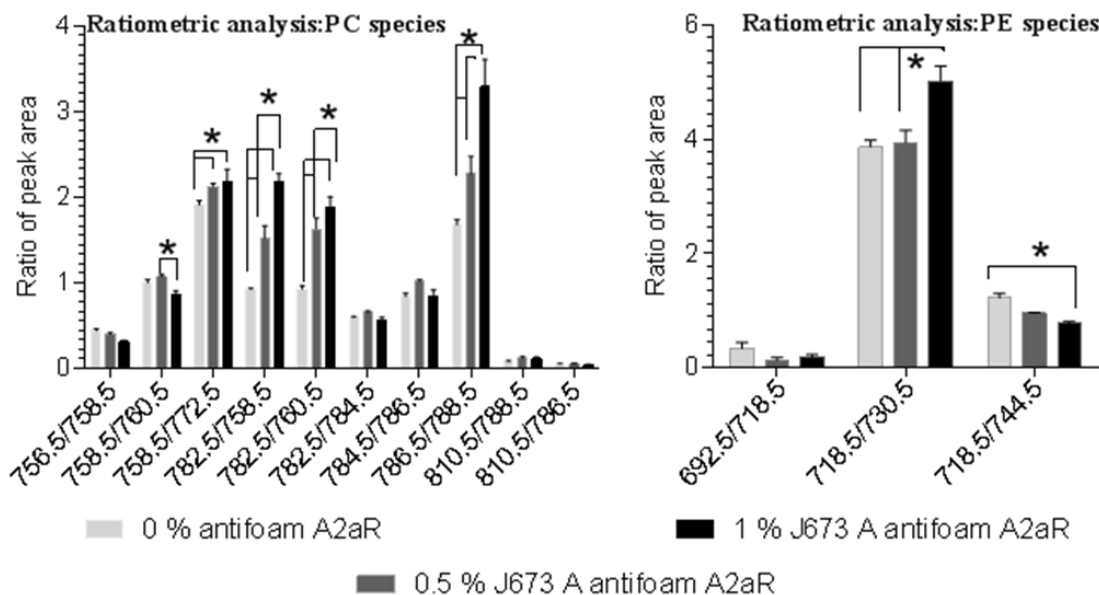


Figure 7.10: Ratiometric analysis approach to study the effect of J673-A on distribution of lipids in P.Pastoris membrane extract expressing A2aR protein. Different combination of ratios were calculated where species belonging to same cluster having same number of carbon chain were proportionated as well as species with increasing level of unsaturation from same cluster series. Statistical analysis was performed on graphpad prism using 2-way ANOVA with tukey method for correction for multiple corrections. * represents significance set to 95 % confidence interval.

7.3.1.3 Ratiometric analysis approach to study the effect of P-2000 antifoaming agent on distribution pattern

7.3.1.3.1 Effect of P-2000 antifoaming agent on phospholipid profile of total extract of P.Pastoris expressing GFP protein

The ratiometric approach was further used to investigate the effect of P-2000 antifoaming agent on the phospholipid profile of total extract of P.Pastoris strain expressing GFP protein. The figure 7.11 with graphs plotted using the average calculated ratios for each group suggested that there was no significant effect on the distribution profile of species belonging to PC class.

Although, the abundance level of a single species of PE class with higher carbon number (m/z 718.5, 16:0/18:1 PE) increased with treatment of 0.5 % P-2000 antifoaming agent.

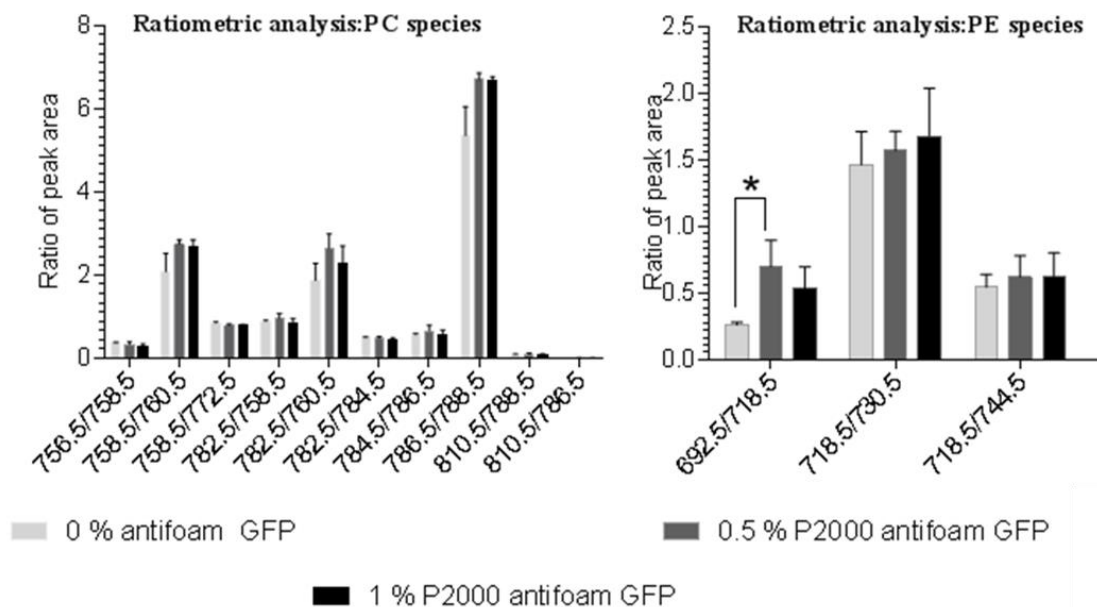


Figure 7.11: Ratiometric analysis approach to study the effect of P-2000 on distribution of lipids in *P.Pastoris* membrane extract expressing GFP proteins. Different combination of ratios were calculated where species belonging to same cluster having same number of carbon chain were proportionated as well as species with increasing level of unsaturation from same cluster series. Statistical analysis was performed on graphpad prism using 2-way ANOVA with tukey method for correction for multiple corrections. * represents significance set to 95 % confidence interval

7.3.1.3.2 Effect of P-2000 antifoaming agent on phospholipid profile of total extract of *P.Pastoris* expressing A2aR membrane protein

The average ratios were calculated to study the relative distribution level of diunsaturated containing species and polyunsaturated containing species to saturated or monounsaturated species. The distribution profile for A2aR membrane expression extract did not changed on addition of P-2000 antifoaming agent as shown in figure 7.12. This effect was similar to that we observed with GFP expressing strain.

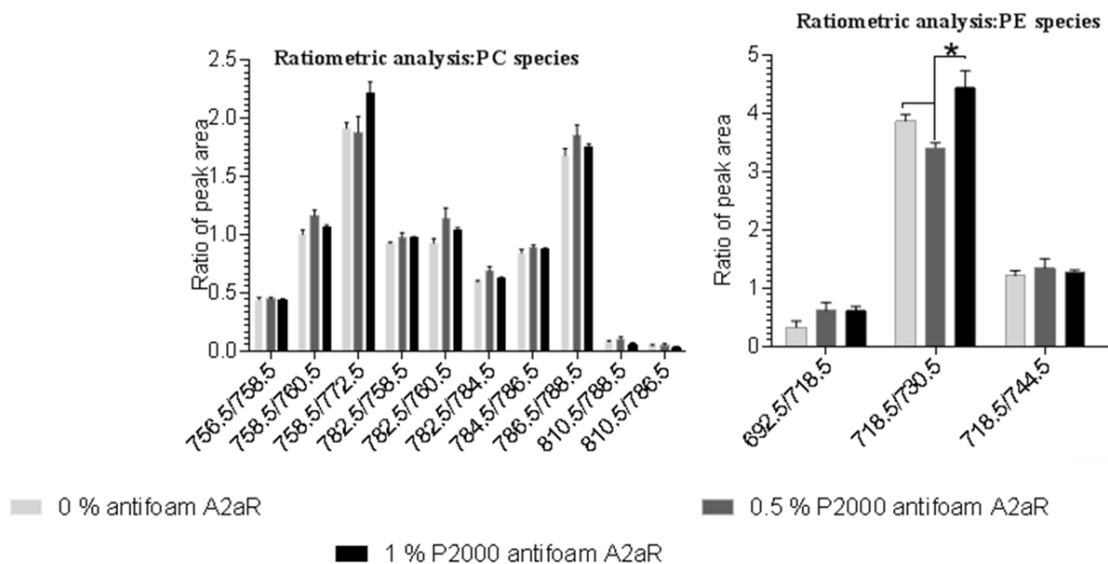


Figure 7.12: Ratiometric analysis approach to study the effect of P-2000 on distribution of lipids in *P.Pastoris* membrane extract expressing A2aR membrane proteins. Different combination of ratios were calculated where species belonging to same cluster having same number of carbon chain were proportionated with species with increasing level of unsaturation from same cluster series. Statistical analysis was performed on graphpad prism using 2-way ANOVA with tukey method for correction for multiple corrections. * represents significance set to 95 % confidence interval

Subsequently, we used the percentage composition analysis approach to investigate the effect on the distribution profile of PC class species and validate the ratiometric analysis. The figure 7.13 shows the % total composition in the total lipis extract of *P.Pastoris* expressing GFP and A2aR membrane protein. The observed distribution profile is similar to that observed with the ratiometric analysis approach in figure 7.8 indicating the GFP expressing strain having higher proportion of di-unsaturated linked phospholipid species compared to A2aR expressing strain such as the (18:0/18:2) PC (m/z 786.6007) and (18:0/18:2) PE (m/z 744.5538).

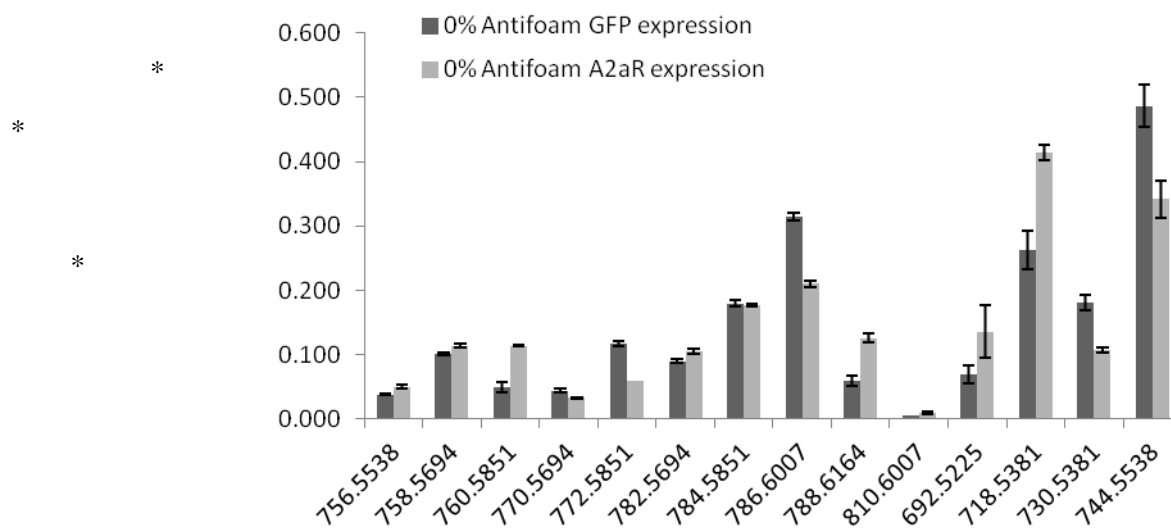


Figure 7.13: Percentage composition analysis approach to study the distribution profile of lipids in *P.Pastoris* membrane extract expressing A2aR membrane proteins and GFP protein. Statistical analysis was performed on graphpad prism using 2-way ANOVA with tukey method for correction for multiple corrections. * represents significance set to 95 % confidence interval.

Similarly, to investigate the effect of antifoaming agents, the percentage composition analysis was applied. The figure 7.14 shows the effect of antifoaming agents: J673-A (A&B) and P2000(C&D) on the distribution profile of phospholipid species in GFP and A2aR expressing strain of *P.Pastoris*. The result suggests J673A having concentration dependent effect on distribution profile of unsaturated linked species which is in agreement with the findings using the ratiometric analysis. Also, there was no significant effect observed for the P2000 antifoaming agent on the distribution profile as shown before with the ratiometric analysis.

The % composition of polyunsaturated containing species such as the (16:0/20:4) PC (m/z 782.5694) and diunsaturated containing species such as at m/z 758.5694, 744.5538 and 786.6007 that corresponds to 16:0/18:2 PC, 18:0/18:2 PE and 18:0/18:2 PC respectively are different in non-treated and J-673A treated strains expressing GFP and A2aR membrane protein.

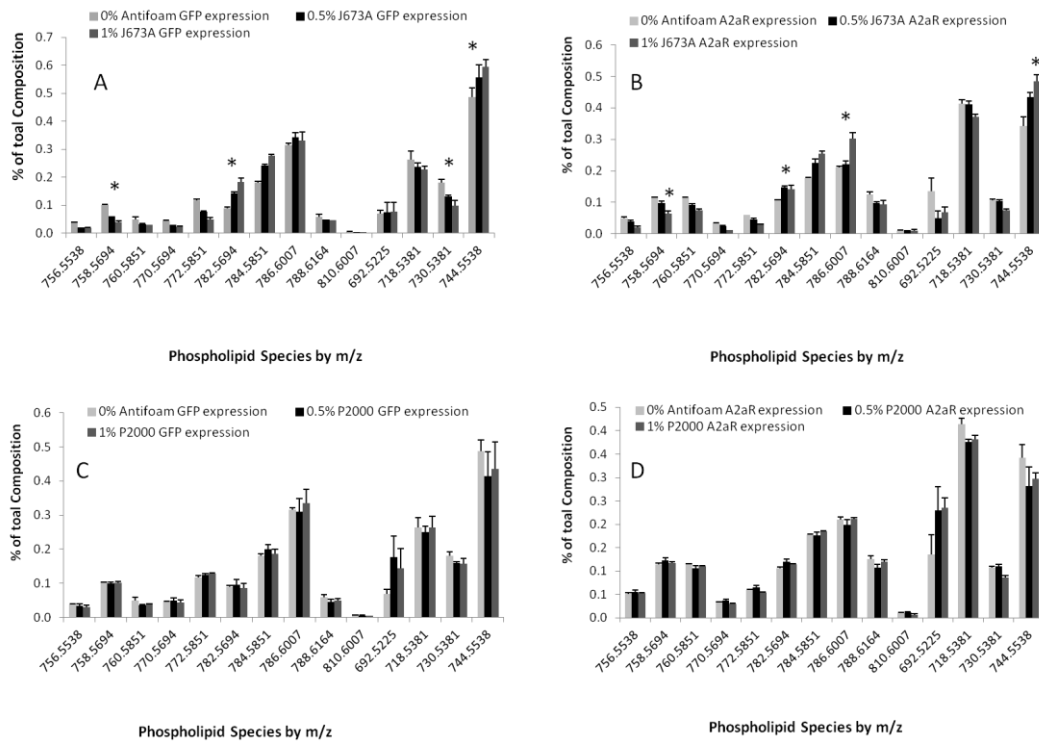


Figure 7.14: Percentage composition analysis approach to study the effect of J673-A (A&B) and P-2000 (C&D) on distribution of lipids in *P. Pastoris* membrane extract expressing GFP and A2aR membrane proteins. Statistical analysis was performed on graphpad prism using 2-way ANOVA with tukey method for correction for multiple corrections. * represents significance set to 95 % confidence interval

7.4 Discussion

The bioreactors for large scale protein production facilitates tighter control of pH, temperature and dissolved oxygen (DO) coupled with more effective feeding strategies which may promote higher product yields (Routledge, Mikaliunaite et al. 2015). However, foaming is an integral problem that can affect the quality and quantity of the protein produced. Foam may accumulate as a result of the gases sparged into the vessel or stirring to sustain the DO conditions required for growth of the organism (Routledge 2014). Moreover, the culture medium and the proteins produced may contribute to foam formation (Doran 2012). In many bioprocesses, foam formation is unwanted; unchecked accumulation leads to blocking of the filter exit and this may damage the bioreactors and also affects the sterility. This problem is commonly managed by the addition of chemical antifoaming agents (Vardar-Sukan 1998, Garrett 2001, Etoc, Delvigne et al. 2006, Junker 2007, Karakashev and Grozdanova 2012). Although, they are commonly used as additives, their effects upon the biological aspects of bioprocesses are not well studied. As demonstrated by the GFP bioreactor experiments, low concentrations of antifoam produced a better yield, whereas the opposite was true in shake flasks where high concentrations produced

more GFP (Bawa, Routledge et al. 2014). Although antifoams are not usually required to alleviate foams formation in these formats, it was observed that the yield of GFP was doubled in the presence of antifoams at higher concentrations than would normally be used. As changes to protein expression could not be explained by the effects of antifoams upon oxygen availability, their effects upon the lipid composition of *P. pastoris* membranes was next investigated in shake flasks to allow a range of conditions to be evaluated. The lipids were extracted from cultures expressing the soluble GFP and membrane protein A2aR grown in the absence of antifoam or treated with 0.5% v/v and 1% v/v of antifoams J673A and P2000.

Yeast plasma membranes is rich in glycerophospholipids and sphingolipids. Ergosterol constitutes the major component of yeast plasma membranes providing structural integrity (Klug and Daum 2014). Membrane fluidity is important for nutrient uptake and exchange of substrates, and glycerophospholipid affects the movement and activity of membrane proteins and insertion sites. The major phospholipids present in *P. pastoris* membranes are phosphatidylcholine (Melo, Santos et al.) accounting for approximately 45% of total phospholipids, phosphatidylethanolamine (PE), (approximately 25%), and the rest proportion constituting phosphatidylserine (PS) and phosphatidylinositol (PI) (Koch, Schmidt et al. 2014).

The method developed on a high resolution QTOF MS instrument along with chromatographic separation achieved using HILIC column enabled detection of 100's of species belonging to the PC, PE and PS class (table 7.1). Molecular level information based on the number of carbon present and the level of unsaturation as well as the head group information was made available by this method. However, owing to inherent limitation in chromatographic separation using HILIC column due to co-elution of all species belonging to same phospholipid class, information on fatty acyl linked at different positions to the glycerol body was not possible. Therefore, it was not possible to tell whether a species belonging to PC class having total 34 carbon and 2 double bond is a 16:0/18:2 PC, 17:1/17:1 PC or 15:1/19:1 PC.

As exemplified in figure 7.1 – 7.3, peak area calculation for different species in replicates showed unaccounted variability. This could be because of several factors including instrument related factors relating to the ion detector and limitations in the dynamic range of QTOF analysers (Chernushevich, Loboda et al. 2001, Thakur 2008, Periat, Kohler et al. 2015, Khoury, El Banna et al. 2016). Although, the possibility of the error in experimental handling cannot be rule out and therefore, we tried different approaches to correct for this variability using several

approaches like protein content including the total phospholipid content (figure 7.5 -7.7) but the distribution profile variability between replicates was not totally accounted.

Subsequently, a novel approach using ratiometric analysis of abundance levels of monounsaturated and unsaturated fatty acyl bearing species to polyunsaturated fatty acyl bearing species within the same cluster was performed and the mean ratio was used for comparative statistical analysis. Our data show that overexpression of different types of protein, either soluble or membrane, can affect the abundance of certain species of phospholipids in addition to affecting the chain length. Recombinant protein production dependent and anti-foaming agent specific response was observed. J673-A treated samples showed higher levels of species bearing polyunsaturated fatty acyl chains compared to the species with monounsaturated fatty acyl chains whereas, P-2000 treated samples did not showed any effect on the abundance level. Recombinant protein production is associated with endoplasmic reticulum stress due to focussing of metabolic machinery for production of target protein and saturated fatty acid has been previously shown to degrade ER (Leamy, Egnatchik et al. 2014). Therefore, this increase production of polyunsaturated fatty acyl containing phospholipid species may be linked to alleviation of the ER stress and thereby improving the production and quality of target protein as it has been reported previously about the beneficial effect of docosahexaenoic acid (a poly unsaturated fatty acid) in resolving oxidative stress in diabetes (Vericel, Colas et al. 2015).

Moreover, several reports suggested the requirement and composition of specific phospholipids for the functionality of recombinant protein production (Seddon, Curnow et al. 2004, Bill and von der Haar 2015, Grison, Brocard et al. 2015, Jaenecke, Friedrich-Epler et al. 2015). This study provides evidence based agreement to the theory. Nevertheless, this study provided useful insight into change in lipid composition in response to different types of antifoaming agents and similar studies with different membrane proteins need to be designed and conducted to reinforce our findings. Moreover, multi-dimensional studies involving multivariate analysis with lipidomics are required to correlate the change in lipid composition with other physical parameters and protein production.

8 Discussion

The major focus of this thesis and the underlying work was the development of an improved mass spectrometry based protocol for measurement of lipid peroxidation and oxidation products and factors that need to be considered when measuring them such as the variability in ionisation efficiency of different classes of phospholipids, consideration of isobaric species during data analysis as well as difference in linear dynamic range of the response for each oxidised species on a mass spectrometer. It is evident from several published articles in the literature that a plethora of oxidised phospholipid species are formed via non enzymatic oxidation and that these may have non- identical biological activities (van Meer 2005, Blanksby and Mitchell 2010, Spickett and Fauzi 2011, Gruber, Bicker et al. 2012). Several other published reports have indicated that oxPL may contribute to development of disease pathologies (Niki 2009, Griffiths, Ogundare et al. 2011, Spickett and Fauzi 2011, Greig, Kennedy et al. 2012, Reis and Spickett 2012). Unsurprisingly, this has led to development of various improved methodologies for measurement of these markers of oxidative damage. However, most of the methodologies developed so far remained driven by technological advancement in the instrumentation aspects of mass spectrometry and separation science or they were focussed on measurement of a predefined list of species (Stutts, Menger et al. 2013) (Gruber, Bicker et al. 2012, Milic, Fedorova et al. 2012, Milic, Hoffmann et al. 2013). Therefore, several oxidised species whose levels may be close to the detection limit remained undetected leading to only partial information from the measurements. Also, semi targeted approaches like precursor ion scanning and neutral loss scanning that can add selectivity and sensitivity to the detection together with broader coverage of the oxidised species have been underutilised in previous studies, although, their potential and advantages have been known and reported extensively (Spickett, Wiswedel et al. 2010, Sandra and Sandra 2013). This suggests the need for development of more focussed & sensitive methodologies that can provide a better coverage of the oxidised lipidome in disease models.

While methods using LCMS technology have been developed over decades for measurement of oxidised lipids, relatively speaking the power of chromatographic separation to improve the sensitivity and dynamic range of detection has been overlooked and limited attempt so far to the best of authors' knowledge has been made for optimisation and evaluation of chromatographic separation. This thesis begins to offer solution to aforementioned issues by initiating the optimisation and evaluation of chromatographic separation of oxidised phospholipid species by testing several reverse phase and mix mode columns and a range of

solvent systems together with application of semi targeted approaches for analysis of in-vitro generated oxidised phospholipid mixture belonging to PC and PE class. We evaluated the selectivity parameter achieved on several reverse phased columns with common stationary phases like C8, C18 and C30, a monolithic column with divinylstyrene benzene chemistry, as well as a mix mode silica based HILIC column together with testing several solvent system and gradient system. Our work suggested that monolithic column with methanol –water solvent system provided a robust method with better selectivity for short chain oxidation products, which eluted in the early part of the chromatographic run compared to other columns. Furthermore, emphasis was also placed on method validation by testing of repeatability and reproducibility along with recovery post extraction of samples. The intra-day and inter-day variability was calculated as less than 20 % for most of the oxidised species. In Parallel, for comparison purpose the method was translated to a high resolution QTOF mass spectrometer and data analysis using Progenesis QI software to reinforce the identification and manual data analysis. A further attempt to evaluate the efficiency of separation using two-dimensional chromatography was also done and presented. This all led to presentation of an improved LCMS method that can be a starting point for research labs interested in oxidative lipidomics work.

As a result of this work, a first attempt was made to perform comparative profiling of oxidised phospholipids in ascites of lean and obese rats induced with acute pancreatitis with the objective of investigation of association of obesity with oxidative stress. In addition, a post data acquisition approach by comparing several normalisation approaches was set up and investigated to improve the biological content of the data by minimising any inherent variation due to sample composition and variation occurred during handling. This analysis proved to be highly sensitive and capable of detecting a range of oxidised species in the total lipid extract of ascites of lean and obese rats. Despite the sensitive analysis and setting up of a post-acquisition data handling approach, it was not possible to ascertain any discriminating levels of oxidised phospholipid species between lean and obese rats model of acute pancreatitis although, the trend suggested high levels of short chain oxidation products in ascites of lean rats compared to obese rats. The difference in the level of several oxidised species like POVPC, PONPC between replicates of the same group were more than 2 standard deviation that obscured any significant difference in the level. However, a likely cause of this is that a single time point to collect the ascite fluid post induction of acute pancreatitis was investigated, thereby only providing a static snapshot of the levels of oxidised species at a single time point and it does not provide any information on the dynamics of oxidative stress. This may contribute to the confounding factors

that may obscure subtle differences in the levels and extent of oxidative stress and further studies are required to investigate it further.

A second study used the methodology to profile the oxidised lipidome in isolated components of RBC infected with the malarial parasite *P. falciparum* was conducted. Statistically significant difference of oxidised species such as POVPC (m/z 594.5), PONPC (m/z 650.5), PLPC-OH (m/z 774.5), SLPC-OH (m/z 800.5), PAPC-OH (m/z 798.5) and isoprostanoids (m/z 832.5) were observed in hemozoin samples compared to other components such as the residual bodies, schizonts and uninfected RBCs. This was in agreement to the high levels of hydroxylated fatty acids detected in hemozoin samples in previous studies. It was also shown the association of these oxidation products and modulation of immune cell functions in monocytes and dendritic cells. While this study was conducted on a single set of pooled samples that was sent to use by our collaborators, it opens up further avenues for investigation of therapeutic efficacy of novel antimalarials that have been developed recently as well as improve our understanding about the pathological process involved in malaria and may contribute in development of novel intervention strategy targeting lipid oxidation.

In the third study, an attempt was made to reproduce the result that was obtained using non-mass spectrometry based methods in plasma samples of diabetic patients in earlier studies. While the trend suggested higher levels of oxidised species like PLPC-OOH (m/z 790.5), SLPC-OOH (m/z 818.5) in diabetic plasma compared to healthy plasma samples, the variability within group obscured the differences. This could be due to the multi-faceted nature of the disease often; it becomes difficult to account and control for all inherent biological variation. Moreover, no information was available on the drugs administered to the diabetic patients that can add to the variability and further stratification of samples based on BMI, drugs taken as well as other biochemical tests may improve the data analysis. Also, the effect of oxidative stress on lipidome may be too subtle to be detected in the plasma owing to its multi component nature and that an analysis of different components of plasma such as low density lipoprotein (LDL), chylomicrons and high density lipoprotein (HDL) may be better suited for studies involving such multi-faceted disease such as diabetes.

During our method development and evaluation of chromatographic separation, it was observed that HILIC column separated different phospholipid classes that enabled profiling all lipid classes in a single chromatographic run. While all the previous chapters measured the oxidised

lipidome, this individual project was conducted to look at the levels of unmodified phospholipids to demonstrate the wider value of lipidomics, and to understand the biological effect of antifoaming agents used in recombinant protein production in bioreactors was carried out using yeast expression system. Same method was tested to assess any statistical difference in the levels of unmodified species of PC, PE and PS class. Concentration and antifoaming specific effect on lipid composition was observed but biological implication of this altered lipid composition is yet to be investigated.

Despite, the advances presented in this thesis, significant challenges in oxidised lipidome studies still exist and the potential solutions are explained below:

a) Sample preparation: While new processes in sample preparation such as high throughput solid phase micro extraction (SPME) with dual reverse phase and cation/anion exchange cartridges have been introduced, their use in routine laboratory preparations is rather limited owing to preference for simple liquid-liquid extraction methodologies that have long been established in the field (Griffiths, Ogundare et al. 2011, Gross and Han 2011, Sandra and Sandra 2013, Emwas 2015). Furthermore, online SPME/ column trapping processes are evolving that may further improve the high throughput and minimise user intervention as well as reducing solvent use and sample preparation time.

b) Chromatographic separation: While this study attempted to optimise and evaluate chromatographic separation, the potential to further improve separation still exist using recently developed convergence chromatography, which uses super critical fluids such as liquid carbon dioxide as the mobile phases. Furthermore, ultra high performance liquid chromatography (UHPLC) using narrowbore columns may improve chromatographic resolution in analysis of oxidised lipids and therefore, minimise co-elution as well as ion suppression (Yamada, Uchikata et al. 2013, Cajka and Fiehn 2014, Gika, Theodoridis et al. 2014). Furthermore, more robust investigation of two-dimensional liquid chromatography (2D-LCMS) is still required, although; we had attempted to evaluate the orthogonal 2D-LCMS for separation of oxidised PC and PE.

c) Mass spectrometry: New developments in the mass spectrometry field happen at the pace with which the field of oxidative lipidomics is not able to cope. Therefore, most studies in the past have used similar platforms and potential new applications and evaluation of newer

developed technologies is rather limited or confined to more sophisticated laboratories that have the revenue to incorporate these advancements in their day to day analysis platform. One such technology that has the potential to improve the detection is the ion mobility mass spectrometry, which can offer a third dimension in LCMS separation by incorporation of drift cell between ionisation step and the entry to the mass analyser (Baker, Armando et al. 2014). Ions are separated based upon their collisional cross sectional area (CSS) where ions are passed into the drift chamber filled with collision gas usually helium or nitrogen and weak uniform electric field is applied to drag the ions through the drift chamber and the time taken for an ion to pass through the drift chamber is directly proportional to the number of collisions with the inert gas, which in turn is the direct result of the surface area of the molecule.

d) Data analysis: One of the most rate-limiting yet overlooked processes in the study of oxidative lipidomics is the development of pragmatic approaches to handle and process mass spectrometric data. While commercial software and freeware exist to extract information from the mass spectrometric raw data, there is fundamental difference in how each software processes the data based on the mathematical model and algorithms it utilises from the step of chromatographic alignment to peak picking (Bro and Smilde 2003, van den Berg, Hoefsloot et al. 2006, Hartler, Tharakan et al. 2013, Chawade, Alexandersson et al. 2014, Mizuno, Ueda et al. 2016). Moreover, manual intervention is usually required and recommended as the information can be distorted by the process of data handling by this software. One of the most important process is the normalisation method that these softwares allow and usually limited number of approaches are incorporated by these softwares with the view of one size fits all approach, often overlooking the type of biological samples. This can add to the discrepancy of reporting and publication of the data that can hamper scientific development. Therefore, a more rational approach needs to be established. Also, no universal database exists for oxidative lipidomics platform and there is utmost need for development of database with harmonising the name of the species that can help speed up the development in this field. In this project, database that covered a wide range of oxidation products for PC, PE and PS class was developed in an excel file that included the chemical formula, exact mass, retention time, list of fragment ions and structures of all species in sdf format, which was uploaded onto the progenesis software to aid in the identification process.

e) Future oxidative lipidomics studies: There are still several areas where oxidative lipidomics is underutilised and could provide valuable insight. One such area includes mitochondrial diseases as mitochondrial membrane consists of specific type of lipid: cardiolipin and the

alteration in the composition of cardiolipin lipids may be associated with the pathology involving mitochondrial function (Bird, Marur et al. 2011). Furthermore, other disease pathologies involving oxidative stress may have association with altered lipid composition and this field of oxidative lipidomics needs to be integrated to further understand disease biochemistry.

Concluding remarks: The work presented in this thesis offers a potential solution through development of several mass spectrometry protocols with semi-targeted approaches and chromatographic separation using monolith column; to increase sensitivity and detection of low abundant oxidised species in several disease models. It also provides a starting point to conduct oxidative lipidomics studies that has the potential to uncover more subtle changes in the lipidome thereby further increasing our understanding of biochemistry underlying disease and exposure and provide discovery based solutions.

9 List of References

- Abessolo, F. O., J. C. Nguele, E. Legault and E. Ngou-Milama (2009). "[Plasma and erythrocyte membrane phospholipids in children with Plasmodium falciparum malaria: relation to blood parasite counts and lactate levels]." *Sante* **19**(1): 39-42.
- Adachi, J., M. Asano, N. Yoshioka, H. Nushida and Y. Ueno (2006). "Analysis of phosphatidylcholine oxidation products in human plasma using quadrupole time-of-flight mass spectrometry." *Kobe J Med Sci* **52**(5): 127-140.
- Adachi, J., N. Yoshioka, M. Sato, K. Nakagawa, Y. Yamamoto and Y. Ueno (2005). "Detection of phosphatidylcholine oxidation products in rat heart using quadrupole time-of-flight mass spectrometry." *Journal of chromatography. B, Analytical technologies in the biomedical and life sciences* **823**(1): 37-43.
- Akbarzadeh, A., R. Rezaei-Sadabady, S. Davaran, S. W. Joo, N. Zarghami, Y. Hanifehpour, M. Samiei, M. Kouhi and K. Nejadi-Koshki (2013). "Liposome: classification, preparation, and applications." *Nanoscale Research Letters* **8**(1): 102-102.
- Aldrovandi, M. and V. B. O'Donnell (2013). "Oxidized PLs and vascular inflammation." *Current atherosclerosis reports* **15**(5): 323-323.
- Anderson, R. J. L., I. J. M. Jeffrey, P. M. Kay and J. M. Braganza (1986). "PEROXIDIZED LINOLEIC-ACID AND EXPERIMENTAL PANCREATITIS." *International Journal of Pancreatology* **1**(3-4): 237-248.
- Andersson, E., M. Ramgren and B. Hahnagerdal (1987). "THE INFLUENCE OF PEG ON ALPHA-AMYLASE PRODUCTION WITH BACILLUS SPECIES." *Annals of the New York Academy of Sciences* **506**: 613-616.
- Antoine, T., N. Fisher, R. Amewu, P. M. O'Neill, S. A. Ward and G. A. Biagini (2014). "Rapid kill of malaria parasites by artemisinin and semi-synthetic endoperoxides involves ROS-dependent depolarization of the membrane potential." *Journal of Antimicrobial Chemotherapy* **69**(4): 1005-1016.
- Arnhold, J., A. N. Osipov, H. Spalteholz, O. M. Panasenko, J. Schiller, E. Of, H. Acid and O. N. Unsaturated (2001). "Effects of hypochlorous acid on unsaturated phosphatidylcholines." *Free Radical Biology and Medicine* **31**(9): 1111-1119.
- Baker, P. R. S., A. M. Armando, J. L. Campbell, O. Quehenberger and E. A. Dennis (2014). "Three-dimensional enhanced lipidomics analysis combining UPLC, differential ion mobility spectrometry, and mass spectrometric separation strategies." *Journal of Lipid Research* **55**(11): 2432-2442.
- Bawa, Z., S. J. Routledge, M. Jamshad, M. Clare, D. Sarkar, I. Dickerson, M. Ganzlin, D. R. Poyner and R. M. Bill (2014). "Functional recombinant protein is present in the pre-induction phases of Pichia pastoris cultures when grown in bioreactors, but not shake-flasks." *Microbial Cell Factories* **13**.
- Becker, K., L. Tilley, J. L. Vennerstrom, D. Roberts, S. Rogerson and H. Ginsburg (2004). "Oxidative stress in malaria parasite-infected erythrocytes: host-parasite interactions." *Int J Parasitol* **34**(2): 163-189.
- Bijlsma, S., I. Bobeldijk, E. R. Verheij, R. Ramaker, S. Kochhar, I. A. Macdonald, B. van Ommen and A. K. Smilde (2006). "Large-scale human metabolomics studies: a strategy for data (pre-) processing and validation." *Anal Chem* **78**(2): 567-574.
- Bill, R. M. and T. von der Haar (2015). "Hijacked then lost in translation: the plight of the recombinant host cell in membrane protein structural biology projects." *Current Opinion in Structural Biology* **32**: 147-155.
- Bird, S. S., V. R. Marur, M. J. Sniatynski, H. K. Greenberg and B. S. Kristal (2011). "Lipidomics Profiling by High-Resolution LC-MS and High-Energy Collisional Dissociation Fragmentation: Focus on Characterization of Mitochondrial Cardiolipins and Monolysocardiolipins." *Analytical Chemistry* **83**(3): 940-949.
- Birukova, A. a., V. Starosta, X. Tian, K. Higginbotham, L. Koroniak, J. a. Berliner and K. G. Birukov (2013). "Fragmented oxidation products define barrier disruptive endothelial cell response to OxPAPC." *Translational research : the journal of laboratory and clinical medicine* **161**(6): 495-504.
- Blanksby, S. J. and T. W. Mitchell (2010). "Advances in mass spectrometry for lipidomics." *Annual review of analytical chemistry (Palo Alto, Calif.)* **3**: 433-465.
- Boccard, J., J. L. Veuthey and S. Rudaz (2010). "Knowledge discovery in metabolomics: an overview of MS data handling." *J Sep Sci* **33**(3): 290-304.

- Bochkov, V. N. (2007). "Inflammatory profile of oxidized phospholipids." Thrombosis and Haemostasis: 348-354.
- Bochkov, V. N., O. V. Oskolkova, K. G. Birukov, A.-L. Levonen, C. J. Binder and J. Stöckl (2010). "Generation and biological activities of oxidized phospholipids." Antioxidants & redox signaling **12**(8): 1009-1059.
- Bonomini, F., S. Tengattini, A. Fabiano, R. Bianchi and R. Rezzani (2008). "Atherosclerosis and oxidative stress." Histology and histopathology **23**(3): 381-390.
- Breusing, N., T. Grune, L. Andrisic, M. Atalay, G. Bartosz, F. Biasi, S. Borovic, L. Bravo, I. Casals, R. Casillas, A. Dinischiotu, J. Drzewinska, H. Faber, N. M. Fauzi, A. Gajewska, J. Gambini, D. Gradinaru, T. Kokkola, A. Lojek, W. Luczaj, D. Margina, C. Mascia, R. Mateos, A. Meinitzer, M. T. Mitjavila, L. Mrakovcic, M. C. Munteanu, M. Podborska, G. Poli, P. Sicinska, E. Skrzydlewska, J. Vina, I. Wiswedel, N. Zarkovic, S. Zelzer and C. M. Spickett (2010). "An inter-laboratory validation of methods of lipid peroxidation measurement in UVA-treated human plasma samples." Free Radic Res **44**(10): 1203-1215.
- Bro, R. and A. K. Smilde (2003). "Centering and scaling in component analysis." J Chemom **17**.
- Brügger, B., G. Erben, R. Sandhoff, F. T. Wieland and W. D. Lehmann (1997). "Quantitative analysis of biological membrane lipids at the low picomole level by nano-electrospray ionization tandem mass spectrometry." Proceedings of the National Academy of Sciences of the United States of America **94**(6): 2339-2344.
- Bucala, R., Z. Makita, T. Koschinsky, A. Cerami and H. Vlassara (1993). "Lipid advanced glycosylation: pathway for lipid oxidation in vivo." Proceedings of the National Academy of Sciences **90**(14): 6434-6438.
- Buetler, T. M., A. Krauskopf and U. T. Ruegg (2004). "Role of superoxide as a signaling molecule." News in physiological sciences : an international journal of physiology produced jointly by the International Union of Physiological Sciences and the American Physiological Society **19**: 120-123.
- Bujila, I., E. Schwarzer, O. Skorokhod, J. M. Weidner, M. Troye-Blomberg and A. K. Ostlund Farrants (2016). "Malaria-derived hemozoin exerts early modulatory effects on the phenotype and maturation of human dendritic cells." Cell Microbiol **18**(3): 413-423.
- Cajka, T. and O. Fiehn (2014). "Comprehensive analysis of lipids in biological systems by liquid chromatography-mass spectrometry." TrAC Trends in Analytical Chemistry **61**: 192-206.
- Çakatay, U., R. Kayali, S. Salman, A. Sivas and I. Satman (2004). "Relationship between lipid profile and lipid hydroperoxide levels in early stage type 1 diabetic patients." Biomedical Research **25**(4): 189-193.
- Cao, M., A. Koulman, L. J. Johnson, G. A. Lane and S. Rasmussen (2008). "Advanced data-mining strategies for the analysis of direct-infusion ion trap mass spectrometry data from the association of perennial ryegrass with its endophytic fungus, *Neotyphodium lolii*." Plant Physiol **146**(4): 1501-1514.
- Carrasco-Pancorbo, A., N. Navas-Iglesias and L. Cuadros-Rodríguez (2009). "From lipid analysis towards lipidomics, a new challenge for the analytical chemistry of the 21st century. Part I: Modern lipid analysis." TrAC Trends in Analytical Chemistry **28**(3): 263-278.
- Chang Wang, H. K., Yufeng Guan, Jun Yang, Jianren Gu, Shengli Yang and G. Xu (2005). "Plasma Phospholipid Metabolic Profiling and Biomarkers of Type 2 Diabetes Mellitus Based on High-Performance Liquid Chromatography/ Electrospray Mass Spectrometry and Multivariate Statistical Analysis." Analytical Chemistry, **77**(13).
- Chawade, A., E. Alexandersson and F. Levander (2014). "Normalizer: A Tool for Rapid Evaluation of Normalization Methods for Omics Data Sets." Journal of Proteome Research **13**(6): 3114-3120.
- Chernushevich, I. V., A. V. Loboda and B. A. Thomson (2001). "An introduction to quadrupole-time-of-flight mass spectrometry." J Mass Spectrom **36**(8): 849-865.
- Christer S. Ejsing, K. E. (2006). "Automated Identification and Quantification of Glycerophospholipid Molecular Species by Multiple Precursor Ion Scanning." Anal Chem.
- Clendinen, C. S., G. S. Stupp, R. Ajredini, B. Lee-McMullen, C. Beecher and A. S. Edison (2015). "An overview of methods using ¹³C for improved compound identification in metabolomics and natural products." Frontiers in Plant Science **6**(611).
- Coronado, L. M., C. T. Nadovich and C. Spadafora (2014). "Malarial Hemozoin: From target to tool." Biochimica et biophysica acta **1840**(6): 2032-2041.
- Davies, M. J. (2011). "Myeloperoxidase-derived oxidation: mechanisms of biological damage and its prevention." Journal of clinical biochemistry and nutrition **48**(1): 8-19.

Denkov, N. D. (2004). "Mechanisms of foam destruction by oil-based antifoams." Langmuir **20**(22): 9463-9505.

Deroost, K., A. Tyberghein, N. Lays, S. Noppen, E. Schwarzer, E. Vanstreels, M. Komuta, M. Prato, J. W. Lin, A. Pamplona, C. J. Janse, P. Arese, T. Roskams, D. Daelemans, G. Opdenakker and P. E. Van den Steen (2013). "Hemozoin induces lung inflammation and correlates with malaria-associated acute respiratory distress syndrome." Am J Respir Cell Mol Biol **48**(5): 589-600.

Devaraj, S., S. V. Hirany, R. F. Burk and I. Jialal (2001). "Divergence between LDL Oxidative Susceptibility and Urinary F2-Isoprostanes as Measures of Oxidative Stress in Type 2 Diabetes." Clinical Chemistry **47**(11): 1974-1979.

Dever, G., L.-J. Stewart, A. R. Pitt and C. M. Spickett (2003). "Phospholipid chlorohydrins cause ATP depletion and toxicity in human myeloid cells." FEBS Letters **540**(1): 245-250.

Dever, G., C. L. Wainwright, S. Kennedy and C. M. Spickett (2006). "Fatty acid and phospholipid chlorohydrins cause cell stress and endothelial adhesion." Acta Biochimica Polonica **53**(4): 761-768.

Dever, G. J., R. Benson, C. L. Wainwright, S. Kennedy and C. M. Spickett (2008). "Phospholipid chlorohydrin induces leukocyte adhesion to ApoE(-/-) mouse arteries via upregulation of P-selectin." Free Radical Biology and Medicine **44**(3): 452-463.

Dias, I. H. and H. R. Griffiths (2014). "Oxidative stress in diabetes - circulating advanced glycation end products, lipid oxidation and vascular disease." Ann Clin Biochem **51**(Pt 2): 125-127.

Domingues, M. R., A. Reis and P. Domingues (2008). "Mass spectrometry analysis of oxidized phospholipids." Chem Phys Lipids **156**(1-2): 1-12.

Doran, P. M. (2012). Bioprocess engineering principles: Second edition, Academic Press.

Dugernier, T., P. F. Laterre and M. S. Reynaert (2000). "Ascites fluid in severe acute pancreatitis: from pathophysiology to therapy." Acta Gastroenterol Belg **63**(3): 264-268.

Edzes, H. T., T. Teerlink, M. S. V. D. Knaap and J. Valk (1992). "Analysis of phospholipids in brain tissue by 31P NMR at different compositions of the solvent system chloroform-methanol- water." Magnetic Resonance in Medicine **26**(1): 46-59.

Ejsing, C. S., E. Duchoslav, J. Sampaio, K. Simons, R. Bonner, C. Thiele, K. Ekroos and A. Shevchenko (2006). "Automated identification and quantification of glycerophospholipid molecular species by multiple precursor ion scanning." Analytical chemistry **78**(17): 6202-6214.

Ejsing, C. S., J. L. Sampaio, V. Surendranath, E. Duchoslav, K. Ekroos, R. W. Klemm, K. Simons and A. Shevchenko (2009). "Global analysis of the yeast lipidome by quantitative shotgun mass spectrometry." Proc Natl Acad Sci U S A **106**(7): 2136-2141.

Ekroos, K. (2002). "Quantitative Profiling of Phospholipids by Multiple Precursor Ion Scanning on a Hybrid Quadrupole Time-of-Flight Mass Spectrometer." Anal. Chem. **74**.

Emwas, A.-H. M. (2015). The Strengths and Weaknesses of NMR Spectroscopy and Mass Spectrometry with Particular Focus on Metabolomics Research. Metabonomics: Methods and Protocols. J. T. Bjerrum. New York, NY, Springer New York: 161-193.

Etoc, A., F. Delvigne, J. P. Lecomte and P. Thonart (2006). "Foam control in fermentation bioprocess - From simple aeration tests to bioreactor." Applied Biochemistry and Biotechnology **130**(1-3): 392-404.

Evans, A. C., G. I. Papachristou and D. C. Whitcomb (2010). "Obesity and the risk of severe acute pancreatitis." Minerva Gastroenterol Dietol **56**(2): 169-179.

Felber, J.-P., E. Ferrannini, A. Golay, H. U. Meyer, D. Theibaud, B. Curchod, E. Maeder, E. Jequier and R. A. DeFronzo (1987). "Role of Lipid Oxidation in Pathogenesis of Insulin Resistance of Obesity and Type II Diabetes." Diabetes **36**(11): 1341-1350.

Ferreira, J. F. S., D. L. Luthria, T. Sasaki and A. Heyerick (2010). "Flavonoids from Artemisia annua L. as Antioxidants and Their Potential Synergism with Artemisinin against Malaria and Cancer." Molecules **15**(5).

Finnigan, R. E. (1994). "Quadrupole mass spectrometers." Analytical Chemistry **66**(19): 969A-975A.

Franco-Pons, N., S. Gea-Sorli and D. Closa (2010). "Release of inflammatory mediators by adipose tissue during acute pancreatitis." J Pathol **221**(2): 175-182.

Fruhwith, G. O., A. Loidl and A. Hermetter (2007). "Oxidized phospholipids: from molecular properties to disease." Biochimica et biophysica acta **1772**(7): 718-736.

Fu, M., W. Xu, Q. Lu, G. Pan and C. Varga (2014). "Evaluation and optimization of high-performance liquid chromatography coupled with high-resolution mass spectrometry for phospholipid quantitation." Rapid Communications in Mass Spectrometry **28**(7): 811-821.

Fujisawa, T., K. Kagawa, K. Hisatomi, K. Kubota, H. Sato, A. Nakajima and N. Matsuhashi (2016). "Obesity with abundant subcutaneous adipose tissue increases the risk of post-ERCP pancreatitis." Journal of Gastroenterology: 1-8.

Fujiwara, Y., H. Nishihara, T. Nakakoshi, T. Hasegawa, S. Tagami and Y. Kawakami (1997). "Elevation of plasma lipid peroxides in non-insulin dependent diabetics with multiple lacunar infarcts." J Atheroscler Thromb **4**(2): 90-95.

Funnell, I. C., P. C. Bornman, S. P. Weakley, J. Terblanche and I. N. Marks (1993). "Obesity: An important prognostic factor in acute pancreatitis." British Journal of Surgery **80**(4): 484-486.

Gao, F., H. Yan, Q. Wang and S. Yuan (2014). "Mechanism of foam destruction by antifoams: a molecular dynamics study." Physical Chemistry Chemical Physics **16**(32): 17231-17237.

Garrett, P. R. (2001). Foams and antifoams. Food Colloids: Fundamentals of Formulation. E. Dickinson and R. Miller: 55-72.

Garrett, P. R. (2015). "Defoaming: Antifoams and mechanical methods." Current Opinion in Colloid & Interface Science **20**(2): 81-91.

German, J. B., L. A. Gillies, J. T. Smilowitz, A. M. Zivkovic and S. M. Watkins (2007). "Lipidomics and lipid profiling in metabolomics." Curr Opin Lipidol **18**(1): 66-71.

Gika, H. G., G. A. Theodoridis, R. S. Plumb and I. D. Wilson (2014). "Current practice of liquid chromatography–mass spectrometry in metabolomics and metabonomics." Journal of Pharmaceutical and Biomedical Analysis **87**: 12-25.

Glish, G. L. and R. W. Vachet (2003). "The basics of mass spectrometry in the twenty-first century." Nature reviews. Drug discovery **2**(2): 140-150.

Gonnella, N. C. (2012). "Chromatographic Separation and NMR An Integrated Approach in Pharmaceutical Development." Adv Chromatogr **50**: 93-138.

Goodarzi, M. T., L. Varmaziar, A. A. Navidi and K. Parivar (2008). "Study of oxidative stress in type 2 diabetic patients and its relationship with glycated hemoglobin." Saudi Med J **29**(4): 503-506.

Greig, F. H., S. Kennedy and C. M. Spickett (2012). "Physiological effects of oxidized phospholipids and their cellular signaling mechanisms in inflammation." Free Radic Biol Med **52**(2): 266-280.

Griffiths, W. J., M. Ogundare, C. M. Williams and Y. Wang (2011). "On the future of "omics": lipidomics." Journal of Inherited Metabolic Disease **34**(3): 583-592.

Grigor'eva, I. N., T. I. Romanova and I. I. Ragino (2011). "Lipid peroxidation in patients with acute and chronic pancreatitis." Ekspierimental'naia i klinicheskaia gastroenterologija = Experimental & clinical gastroenterology(7): 24-27.

Grintzalis, K., D. Zisimopoulos, T. Grune, D. Weber and C. D. Georgiou (2013). "Method for the simultaneous determination of free/protein malondialdehyde and lipid/protein hydroperoxides." Free Radic Biol Med **59**: 27-35.

Grison, M. S., L. Brocard, L. Fouillen, W. Nicolas, V. Wewer, P. Dormann, H. Nacir, Y. Benitez-Alfonso, S. Claverol, V. Germain, Y. Boutte, S. Mongrand and E. M. Bayer (2015). "Specific membrane lipid composition is important for plasmodesmata function in Arabidopsis." Plant Cell **27**(4): 1228-1250.

Groessler, M., S. Graf and R. Knochenmuss (2015). "High resolution ion mobility-mass spectrometry for separation and identification of isomeric lipids." Analyst.

Gross, Richard W. and X. Han (2011). "Lipidomics at the Interface of Structure and Function in Systems Biology." Chemistry & Biology **18**(3): 284-291.

Gruber, F., W. Bicker, O. V. Oskolkova, E. Tschachler and V. N. Bochkov (2012). "A simplified procedure for semi-targeted lipidomic analysis of oxidized phosphatidylcholines induced by UVA irradiation." Journal of lipid research **53**(6): 1232-1242.

Guilhaus, M., D. Selby and V. Mlynski (2000). "Orthogonal acceleration time-of-flight mass spectrometry." Mass Spectrometry Reviews **19**(2): 65-107.

Gutierrez, P. T., E. Folch-Puy, O. Bulbena and D. Closa (2008). "Oxidised lipids present in ascitic fluid interfere with the regulation of the macrophages during acute pancreatitis, promoting an exacerbation of the inflammatory response." Gut **57**(5): 642-648.

Haeggstrom, J. Z. and C. D. Funk (2011). "Lipoxygenase and leukotriene pathways: biochemistry, biology, and roles in disease." Chem Rev **111**(10): 5866-5898.

Haggarty, J., M. Oppermann, M. Dalby, R. Burchmore, K. Cook, S. Weidt and K. V. Burgess (2015). "Serially coupling hydrophobic interaction and reversed-phase chromatography with simultaneous gradients provides greater coverage of the metabolome." Metabolomics **11**(5): 1465-1470.

Hajjar, D. and A. Gotto (2013). "Biological Relevance of Inflammation and Oxidative Stress in the Pathogenesis of Arterial Diseases." American Journal of Pathology **182**(5): 1474-1481.

Han, L. D., J. F. Xia, Q. L. Liang, Y. Wang, Y. M. Wang, P. Hu, P. Li and G. A. Luo (2011). "Plasma esterified and non-esterified fatty acids metabolic profiling using gas chromatography-mass spectrometry and its application in the study of diabetic mellitus and diabetic nephropathy." Anal Chim Acta **689**(1): 85-91.

Han, X. (2016). "Lipidomics for studying metabolism." Nat Rev Endocrinol **advance online publication**.

Han, X. and R. W. Gross (1994). "Electrospray ionization mass spectroscopic analysis of human erythrocyte plasma membrane phospholipids." Proceedings of the National Academy of Sciences of the United States of America **91**(22): 10635-10639.

Han, X. and R. W. Gross (2003). "Global analyses of cellular lipidomes directly from crude extracts of biological samples by ESI mass spectrometry: a bridge to lipidomics." Journal of lipid research **44**(6): 1071-1079.

Han, X. and R. W. Gross (2005). "Shotgun lipidomics: electrospray ionization mass spectrometric analysis and quantitation of cellular lipidomes directly from crude extracts of biological samples." Mass Spectrom Rev **24**(3): 367-412.

Han, X., K. Yang, J. Yang, K. N. Fikes, H. Cheng and R. W. Gross (2006). "Factors influencing the electrospray intrasource separation and selective ionization of glycerophospholipids." Journal of the American Society for Mass Spectrometry **17**(2): 264-274.

Harrison, D., K. K. Griendling, U. Landmesser, B. Hornig and H. Drexler (2003). "Role of oxidative stress in atherosclerosis." The American journal of cardiology **91**(3A): 7A-11A.

Hartler, J., R. Tharakan, H. C. Kofeler, D. R. Graham and G. G. Thallinger (2013). "Bioinformatics tools and challenges in structural analysis of lipidomics MS/MS data." Brief Bioinform **14**(3): 375-390.

Hesse, F., M. Ebel, N. Konisch, R. Sterlinski, W. Kessler and R. Wagner (2003). "Comparison of a production process in a membrane-aerated stirred tank and up to 1000-L airlift bioreactors using BHK-21 cells and chemically defined protein-free medium." Biotechnology Progress **19**(3): 833-843.

Holmes, W., R. Smith and R. Bill (2006). "Evaluation of antifoams in the expression of a recombinant FC fusion protein in shake flask cultures of *Saccharomyces cerevisiae* & *Pichia pastoris*." Microbial Cell Factories **5**(1): 1-3.

Hue Su, K., C. Cuthbertson and C. Christophi (2006). "Review of experimental animal models of acute pancreatitis." HPB : The Official Journal of the International Hepato Pancreato Biliary Association **8**(4): 264-286.

Hui, S.-P., H. Chiba, S. Jin, H. Nagasaka and T. Kurosawa (2010). "Analyses for phosphatidylcholine hydroperoxides by LC/MS." Journal of chromatography. B, Analytical technologies in the biomedical and life sciences **878**(20): 1677-1682.

Hulsmans, M. and P. Holvoet (2010). "The vicious circle between oxidative stress and inflammation in atherosclerosis." Journal of cellular and molecular medicine **14**(1-2): 70-78.

Ihekwereme, C. P., C. O. Esimone and E. C. Nwanegbo (2014). "Hemozoin inhibition and control of clinical malaria." Adv Pharmacol Sci **2014**: 984150.

Isaac, G., R. Jeannotte, S. W. Esch and R. Welti (2007). "New mass-spectrometry-based strategies for lipids." Genetic engineering **28**: 129-157.

Itoe, Maurice A., Júlio L. Sampaio, Ghislain G. Cabal, E. Real, V. Zuzarte-Luis, S. March, Sangeeta N. Bhatia, F. Frischknecht, C. Thiele, A. Shevchenko and Maria M. Mota (2014). "Host Cell Phosphatidylcholine Is a Key Mediator of Malaria Parasite Survival during Liver Stage Infection." Cell Host & Microbe **16**(6): 778-786.

Jaenecke, F., B. Friedrich-Epler, C. Parthier and M. T. Stubbs (2015). "Membrane Composition Influences the Activity of in Vitro Refolded Human Vitamin K Epoxide Reductase." Biochemistry **54**(42): 6454-6461.

Jerlich, A., A. R. Pitt, R. J. Schaur and C. M. Spickett (2000). "Pathways of phospholipid oxidation by HOCl in human LDL detected by LC-MS." Free Radical Biology and Medicine **28**(5): 673-682.

Johnson, A. R. and E. E. Carlson (2015). "Collision-Induced Dissociation Mass Spectrometry: A Powerful Tool for Natural Product Structure Elucidation." Analytical Chemistry **87**(21): 10668-10678.

Junker, B. (2007). "Foam and its mitigation in fermentation systems." Biotechnology Progress **23**(4): 767-784.

- Karakashev, S. I. and M. V. Grozdanova (2012). "Foams and antifoams." Advances in Colloid and Interface Science **176**: 1-17.
- Karpievitch, Y. V., T. Taverner, J. N. Adkins, S. J. Callister, G. A. Anderson, R. D. Smith and A. R. Dabney (2009). "Normalization of peak intensities in bottom-up MS-based proteomics using singular value decomposition." Bioinformatics **25**(19): 2573-2580.
- Khalil, M. B., W. Hou and H. Zhou (2010). "Lipidomics era: Accomplishments and challenges." Mass Spectrometry ...: 877-929.
- Khandelwal, P., S. Stryker, H. Chao, N. Aranibar, R. M. Lawrence, M. Madireddi, W. Zhao, L. Chen and M. D. Reily (2014). "¹H NMR-based lipidomics of rodent fur: species-specific lipid profiles and SCD1 inhibitor-related dermal toxicity." J Lipid Res **55**(7): 1366-1374.
- Khoury, S., N. El Banna, S. Tfaili and P. Chaminade (2016). "A study of inter-species ion suppression in electrospray ionization-mass spectrometry of some phospholipid classes." Anal Bioanal Chem **408**(5): 1453-1465.
- Kinoshita, M., S. Oikawa, K. Hayasaka, A. Sekikawa, T. Nagashima, T. Toyota and T. Miyazawa (2000). "Age-related increases in plasma phosphatidylcholine hydroperoxide concentrations in control subjects and patients with hyperlipidemia." Clin Chem **46**(6 Pt 1): 822-828.
- Kiziler, A. R., B. Aydemir, T. Gulyasar, E. Unal and P. Gunes (2008). "Relationships among iron, protein oxidation and lipid peroxidation levels in rats with alcohol-induced acute pancreatitis." Biological Trace Element Research **124**(2): 135-143.
- Klug, L. and G. Daum (2014). "Yeast lipid metabolism at a glance." FEMS Yeast Res **14**(3): 369-388.
- Koch, B., C. Schmidt and G. Daum (2014). "Storage lipids of yeasts: a survey of nonpolar lipid metabolism in *Saccharomyces cerevisiae*, *Pichia pastoris*, and *Yarrowia lipolytica*." FEMS Microbiol Rev **38**(5): 892-915.
- Koch, V., H. M. Ruffer, K. Schugerl, E. Innertsberger, H. Menzel and J. Weis (1995). "EFFECT OF ANTIFOAM AGENTS ON THE MEDIUM AND MICROBIAL CELL PROPERTIES AND PROCESS PERFORMANCE IN SMALL AND LARGE REACTORS." Process Biochemistry **30**(5): 435-446.
- Koch, W., S. Forcisi, R. Lehmann and P. Schmitt-Kopplin (2014). "Sensitivity improvement in hydrophilic interaction chromatography negative mode electrospray ionization mass spectrometry using 2-(2-methoxyethoxy)ethanol as a post-column modifier for non-targeted metabolomics." J Chromatogr A **1361**: 209-216.
- Kofeler, H. C., A. Fauland, G. N. Rechberger and M. Trotsmuller (2012). "Mass spectrometry based lipidomics: an overview of technological platforms." Metabolites **2**(1): 19-38.
- Koivusalo, M., P. Haimi, L. Heikinheimo, R. Kostianen and P. Somerharju (2001). "Quantitative determination of phospholipid compositions by ESI-MS: effects of acyl chain length, unsaturation, and lipid concentration on instrument response." Journal of lipid research **42**(4): 663-672.
- Konishi, M., M. Iwasa, J. Araki, Y. Kobayashi, A. Katsuki, Y. Sumida, N. Nakagawa, Y. Kojima, S. Watanabe, Y. Adachi and M. Kaito (2006). "Increased lipid peroxidation in patients with non-alcoholic fatty liver disease and chronic hepatitis C as measured by the plasma level of 8-isoprostane." J Gastroenterol Hepatol **21**(12): 1821-1825.
- Korotaeva, A., E. Samoilova, T. Pavlunina and O. M. Panasenko (2013). "Halogenated phospholipids regulate secretory phospholipase A2 group IIA activity." Chemistry and Physics of Lipids **167**: 51-56.
- Kostolanská, J., V. Jakuš and L. Barák (2009). "Glycation and lipid peroxidation in children and adolescents with type 1 diabetes mellitus with and without diabetic complications." Journal of Pediatric Endocrinology and Metabolism **22**(7): 635-643.
- Kougias, P. G., K. Boe, E. S. Einarsdottir and I. Angelidaki (2015). "Counteracting foaming caused by lipids or proteins in biogas reactors using rapeseed oil or oleic acid as antifoaming agents." Water Research **79**: 119-127.
- Krauss, R. M. (2004). "Lipids and Lipoproteins in Patients With Type 2 Diabetes." Diabetes Care **27**(6): 1496-1504.
- Kruse, P., S. Loft, M. E. Anderson and H. E. Poulsen (1997). "The involvement of reactive oxygen species in early Cerulein induced acute pancreatitis in rats." Digestion **58**(SUPPL. 2): 28-28.
- Kuhn, H. and V. B. O'Donnell (2006). "Inflammation and immune regulation by 12/15-lipoxygenases." Prog Lipid Res **45**(4): 334-356.
- Le, Q. H., M. El Alaoui, E. Vericel, B. Segrestin, L. Soulere, M. Guichardant, M. Lagarde, P. Moulin and C. Calzada (2015). "Glycoxidized HDL, HDL Enriched With Oxidized Phospholipids and HDL From

Diabetic Patients Inhibit Platelet Function." Journal of Clinical Endocrinology & Metabolism **100**(5): 2006-2014.

Leamy, A. K., R. A. Egnatchik, M. Shiota, P. T. Ivanova, D. S. Myers, H. A. Brown and J. D. Young (2014). "Enhanced synthesis of saturated phospholipids is associated with ER stress and lipotoxicity in palmitate treated hepatic cells." J Lipid Res **55**(7): 1478-1488.

Lee, J. Y., S. Lim, S. Park and M. H. Moon (2013). "Characterization of oxidized phospholipids in oxidatively modified low density lipoproteins by nanoflow liquid chromatography-tandem mass spectrometry." Journal of Chromatography A **1288**: 54-62.

Li, M., L. Yang, Y. Bai and H. Liu (2014). "Analytical Methods in Lipidomics and Their Applications." Analytical Chemistry **86**(1): 161-175.

Lokhov, P. G., D. L. Maslov, E. E. Balashova, O. P. Trifonova, N. V. Medvedeva, T. I. Torkhovskaya, O. M. Ipatova, A. I. Archakov, P. P. Malyshev, V. V. Kukharchuk, E. A. Shestakova, M. V. Shestakova and Dedov, II (2015). "Mass Spectrometry Analysis of Blood Plasma Lipidome as the Method of Disease Diagnostics, Evaluation of Effectiveness and Optimization of Drug Therapy." Biochemistry Moscow-Supplement Series B-Biomedical Chemistry **9**(2): 95-105.

Looser, V., B. Bruhlmann, F. Bumbak, C. Stenger, M. Costa, A. Camattari, D. Fotiadis and K. Kovar (2015). "Cultivation strategies to enhance productivity of *Pichia pastoris*: A review." Biotechnology Advances **33**(6, Part 2): 1177-1193.

Louw, S., A. S. Pereira, F. Lynen, M. Hanna-Brown and P. Sandra (2008). "Serial coupling of reversed-phase and hydrophilic interaction liquid chromatography to broaden the elution window for the analysis of pharmaceutical compounds." J Chromatogr A **1208**(1-2): 90-94.

Mahrous, E. A., R. B. Lee and R. E. Lee (2008). "A rapid approach to lipid profiling of mycobacteria using 2D HSQC NMR maps." Journal of Lipid Research **49**(2): 455-463.

Martinez, A., C. S. K. Rajapakse, B. Naoulou and R. A. Sanchez-Delgado (2008). "INOR 165-Mechanism of antimalarial action of the ruthenium(II)-chloroquine complex [RuCl₂(CQ)]₂." Abstracts of Papers of the American Chemical Society **236**.

Martínez, J., C. D. Johnson, J. Sánchez-Payá, E. de Madaria, G. Robles-Díaz and M. Pérez-Mateo (2006). "Obesity Is a Definitive Risk Factor of Severity and Mortality in Acute Pancreatitis: An Updated Meta-Analysis." Pancreatology **6**(3): 206-209.

Mayer, A. D., M. Airey, J. Hodgson and M. J. McMahon (1985). "Enzyme transfer from pancreas to plasma during acute pancreatitis. The contribution of ascitic fluid and lymphatic drainage of the pancreas." Gut **26**(9): 876-881.

McIntyre, T. M., S. M. Prescott and D. M. Stafforini (2009). "The emerging roles of PAF acetylhydrolase." Journal of Lipid Research **50**(Supplement): S255-S259.

Meikle, P. J., G. Wong, C. K. Barlow, J. M. Weir, M. A. Greeve, G. L. MacIntosh, L. Almasy, A. G. Comuzzie, M. C. Mahaney, A. Kowalczyk, I. Haviv, N. Grantham, D. J. Magliano, J. B. M. Jowett, P. Zimmet, J. E. Curran, J. Blangero and J. Shaw (2013). "Plasma Lipid Profiling Shows Similar Associations with Prediabetes and Type 2 Diabetes." PLoS ONE **8**(9): e74341.

Melo, T., N. Santos, D. Lopes, E. Alves, E. Maciel, M. Faustino, J. Tome, M. Neves, A. Almeida, P. Domingues, M. Segundo and M. Domingues (2013). "Photosensitized oxidation of phosphatidylethanolamines monitored by electrospray tandem mass spectrometry." Journal of Mass Spectrometry **48**(12): 1357-1365.

Merzouk, S., A. Hichami, A. Sari, S. Madani, H. Merzouk, A. Yahia Berrouguet, J. J. Lenoir-Rousseaux, N. Chabane-Sari and N. A. Khan (2004). "Impaired oxidant/antioxidant status and LDL-fatty acid composition are associated with increased susceptibility to peroxidation of LDL in diabetic patients." General Physiology and Biophysics **23**(4): 387-399.

Messner, M. C., C. J. Albert, J. McHowat and D. A. Ford (2008). "Identification of lysophosphatidylcholine-chlorohydrin in human atherosclerotic lesions." Lipids **43**(3): 243-249.

Metzger, W. G., B. G. Mordmuller and P. G. Kremsner (1995). "Malaria pigment in leucocytes." Trans R Soc Trop Med Hyg **89**(6): 637-638.

Milic, I., M. Fedorova, K. Teuber, J. Schiller and R. Hoffmann (2012). "Characterization of oxidation products from 1-palmitoyl-2-linoleoyl-sn-glycerophosphatidylcholine in aqueous solutions and their reactions with cysteine, histidine and lysine residues." Chem Phys Lipids **165**(2): 186-196.

Milic, I., R. Hoffmann and M. Fedorova (2013). "Simultaneous detection of low and high molecular weight carbonylated compounds derived from lipid peroxidation by electrospray ionization-tandem mass spectrometry." Anal Chem **85**(1): 156-162.

Milnerowicz, H., R. Bukowski, M. Jabłonowska, M. Ściskalska and S. Milnerowicz (2014). "The Antioxidant Profiles, Lysosomal and Membrane Enzymes Activity in Patients with Acute Pancreatitis." Mediators of Inflammation **2014**: 376518.

Miyazawa, T., K. Nakagawa, S. Shimasaki and R. Nagai (2012). "Lipid glycation and protein glycation in diabetes and atherosclerosis." Amino Acids **42**(4): 1163-1170.

Mizuno, H., K. Ueda, Y. Kobayashi, N. Tsuyama, K. Todoroki, J. Z. Min and T. Toyo'oka (2016). "The great importance of normalization of LC-MS data for highly-accurate non-targeted metabolomics." Biomedical Chromatography: n/a-n/a.

Morgan, A. H., V. J. Hammond and L. Morgan (2010). "Quantitative assays for esterified oxylipins generated by immune cells." Nature protocols **5**(12): 1919-1931.

Morgan, A. H., V. J. Hammond, L. Morgan, C. P. Thomas, K. A. Tallman, Y. R. Garcia-Diaz, C. McGuigan, M. Serpi, N. A. Porter, R. C. Murphy and V. B. O'Donnell (2010). "Quantitative assays for esterified oxylipins generated by immune cells." Nat Protoc **5**(12): 1919-1931.

Morgantini, C., D. Meriwether, S. Baldi, E. Venturi, S. Pinnola, A. C. Wagner, A. M. Fogelman, E. Ferrannini, A. Natali and S. T. Reddy (2014). "HDL lipid composition is profoundly altered in patients with type 2 diabetes and atherosclerotic vascular disease." Nutrition Metabolism and Cardiovascular Diseases **24**(6): 594-599.

Morita, Y., T. Yoshikawa, S. Takeda, K. Matsuyama, S. Takahashi, N. Yoshida, M. G. Clemens and M. Kondo (1998). "Involvement of lipid peroxidation in free fatty acid-induced isolated rat pancreatic acinar cell injury." Pancreas **17**(4): 383-389.

Mouritsen, O. G. (2011). "Lipidology and lipidomics--quo vadis? A new era for the physical chemistry of lipids." Phys Chem Chem Phys **13**(43): 19195-19205.

Mousavi, F., B. Bojko and J. Pawliszyn (2015). "Development of high throughput 96-blade solid phase microextraction-liquid chromatography-mass spectrometry protocol for metabolomics." Anal Chim Acta **892**: 95-104.

Mujuzi, G., B. Magambo, B. Okech and T. G. Egwang (2006). "Pigmented monocytes are negative correlates of protection against severe and complicated malaria in Ugandan children." Am J Trop Med Hyg **74**(5): 724-729.

Mukaiyama, H., Y. Giga-Hama, H. Tohda and K. Takegawa (2009). "Dextran sodium sulfate enhances secretion of recombinant human transferrin in *Schizosaccharomyces pombe*." Applied Microbiology and Biotechnology **85**(1): 155-164.

Muller, S. (2004). "Redox and antioxidant systems of the malaria parasite *Plasmodium falciparum*." Mol Microbiol **53**(5): 1291-1305.

Murphy, R. C. and P. H. Axelsen (2011). "MASS SPECTROMETRIC ANALYSIS OF LONG-CHAIN LIPIDS." 579-599.

Murphy, R. C. and S. J. Gaskell (2011). "New applications of mass spectrometry in lipid analysis." J Biol Chem **286**(29): 25427-25433.

Nagashima, T., S. Oikawa, Y. Hirayama, Y. Tokita, A. Sekikawa, Y. Ishigaki, R. Yamada and T. Miyazawa (2002). "Increase of serum phosphatidylcholine hydroperoxide dependent on glycemic control in type 2 diabetic patients." Diabetes Research and Clinical Practice **56**(1): 19-25.

Nakanishi, H., Y. Iida, T. Shimizu and R. Taguchi (2009). "Analysis of oxidized phosphatidylcholines as markers for oxidative stress, using multiple reaction monitoring with theoretically expanded data sets with reversed-phase liquid chromatography/tandem mass spectrometry." Journal of chromatography. B, Analytical technologies in the biomedical and life sciences **877**(13): 1366-1374.

Navas-Iglesias, N., A. Carrasco-Pancorbo and L. Cuadros-Rodríguez (2009). "From lipids analysis towards lipidomics, a new challenge for the analytical chemistry of the 21st century. Part II: Analytical lipidomics." TrAC Trends in Analytical Chemistry **28**(4): 393-403.

Negre-Salvayre, A., N. Auge, V. Ayala, H. Basaga, J. Boada, R. Brenke, S. Chapple, G. Cohen, J. Feher, T. Grune, G. Lengyel, G. E. Mann, R. Pamplona, G. Poli, M. Portero-Otin, Y. Riahi, R. Salvayre, S. Sasson, J. Serrano, O. Shamni, W. Siems, R. C. Siow, I. Wiswedel, K. Zarkovic and N. Zarkovic (2010). "Pathological aspects of lipid peroxidation." Free Radic Res **44**(10): 1125-1171.

Newsom, S. A., J. T. Brozinick, K. Kiseljak-Vassiliades, A. N. Strauss, S. D. Bacon, A. A. Kerege, H. H. Bui, P. Sanders, P. Siddall, T. Wei, M. Thomas, M. S. Kuo, T. Nemkov, A. D'Alessandro, K. C. Hansen, L. Perreault and B. C. Bergman (2016). "Skeletal muscle phosphatidylcholine and phosphatidylethanolamine are related to insulin sensitivity and respond to acute exercise in humans." Journal of Applied Physiology **120**(11): 1355-1363.

Niedowicz, D. M. and D. L. Daleke (2005). "The role of oxidative stress in diabetic complications." Cell Biochemistry and Biophysics **43**(2): 289-330.

Niki, E. (2009). "Lipid peroxidation: physiological levels and dual biological effects." Free radical biology & medicine **47**(5): 469-484.

Nusshold, C., M. Kollrosier, H. Köfeler, G. Rechberger, H. Reicher, A. Ullen, E. Bernhart, S. Waltl, I. Kratzer, A. Hermetter, H. Hackl, Z. Trajanoski, A. Hrzencak, E. Malle and W. Sattler (2010). "Hypochlorite modification of sphingomyelin generates chlorinated lipid species that induce apoptosis and proteome alterations in dopaminergic PC12 neurons in vitro." Free radical biology & medicine **48**(12): 1588-1600.

Nuszkowski, A., R. Gräbner, G. Marsche, A. Unbehaun, E. Malle and R. Heller (2001). "Hypochlorite-modified low density lipoprotein inhibits nitric oxide synthesis in endothelial cells via an intracellular dislocalization of endothelial nitric-oxide synthase." The Journal of biological chemistry **276**(17): 14212-14221.

O'Donnell, V. B. (2011). "Mass spectrometry analysis of oxidized phosphatidylcholine and phosphatidylethanolamine." Biochimica et biophysica acta **1811**(11): 818-826.

Okajima, F., M. Kurihara, C. Ono, Y. Nakajima, K. Tanimura, H. Sugihara, A. Tatsuguchi, K. Nakagawa, T. Miyazawa and S. Oikawa (2005). "Oxidized but not acetylated low-density lipoprotein reduces preproinsulin mRNA expression and secretion of insulin from HIT-T15 cells." Biochimica et Biophysica Acta (BBA) - Molecular and Cell Biology of Lipids **1687**(1-3): 173-180.

Ozbalci, C., T. Sachsenheimer and B. Brügger (2013). "Quantitative analysis of cellular lipids by nano-electrospray ionization mass spectrometry." Methods in molecular biology (Clifton, N.J.) **1033**: 3-20.

Panasenko, O. M., H. Spalteholz, J. Schiller and J. Arnhold (2003). "Myeloperoxidase-induced formation of chlorohydrins and lysophospholipids from unsaturated phosphatidylcholines." Free Radical Biology and Medicine **34**(5): 553-562.

Pandey, A. V., V. K. Babbarwal, J. N. Okoyeh, R. M. Joshi, S. K. Puri, R. L. Singh and V. S. Chauhan (2003). "Hemozoin formation in malaria: a two-step process involving histidine-rich proteins and lipids." Biochemical and Biophysical Research Communications **308**(4): 736-743.

Parsons, B. J. and C. M. Spickett (2015). "Special issue on "Analytical methods for the detection of oxidized biomolecules and antioxidants"." Free Radical Research **49**(5): 473-476.

Patel, K., R. N. Trivedi, C. Durgampudi, P. Noel, R. A. Cline, J. P. DeLany, S. Navina and V. P. Singh (2015). "Lipolysis of Visceral Adipocyte Triglyceride by Pancreatic Lipases Converts Mild Acute Pancreatitis to Severe Pancreatitis Independent of Necrosis and Inflammation." The American Journal of Pathology **185**(3): 808-819.

Patti, G. J., O. Yanes and G. Siuzdak (2012). "Innovation: Metabolomics: the apogee of the omics trilogy." Nat Rev Mol Cell Biol **13**(4): 263-269.

Pegorier, S., D. Stengel, H. Durand, M. Croset and E. Ninio (2006). "Oxidized phospholipid: POVPC binds to platelet-activating-factor receptor on human macrophages. Implications in atherosclerosis." Atherosclerosis **188**(2): 433-443.

Percario, S., D. R. Moreira, B. A. Gomes, M. E. Ferreira, A. C. Goncalves, P. S. Laurindo, T. C. Vilhena, M. F. Dolabela and M. D. Green (2012). "Oxidative stress in malaria." Int J Mol Sci **13**(12): 16346-16372.

Pereda, J., S. Perez, J. Escobar, A. Arduini, M. Asensi, G. Serviddio, L. Sabater, L. Aparisi and J. Sastre (2012). "Obese rats exhibit high levels of fat necrosis and isoprostanes in taurocholate-induced acute pancreatitis." PLoS One **7**(9): e44383.

Perez, S., J. Pereda, L. Sabater and J. Sastre (2015). "Pancreatic ascites hemoglobin contributes to the systemic response in acute pancreatitis." Free Radical Biology and Medicine **81**: 145-155.

Periat, A., I. Kohler, A. Thomas, R. Nicoli, J. Boccard, J. L. Veuthey, J. Schappler and D. Guillaume (2015). "Systematic evaluation of matrix effects in hydrophilic interaction chromatography versus reversed phase liquid chromatography coupled to mass spectrometry." J Chromatogr A.

Peterson, B. L. and B. S. Cummings (2006). "A review of chromatographic methods for the assessment of phospholipids in biological samples." Biomed Chromatogr **20**(3): 227-243.

Philippova, M., T. Resink, P. Erne and V. Bochkov (2014). "Oxidised phospholipids as biomarkers in human disease." Swiss Med Wkly **144**: w14037.

Phillips, R., T. Ursell, P. Wiggins and P. Sens (2009). "Emerging roles for lipids in shaping membrane-protein function." Nature **459**(7245): 379-385.

Podrez, E. A., E. Poliakov, Z. Z. Shen, R. L. Zhang, Y. J. Deng, M. J. Sun, P. J. Finton, L. Shan, B. Gugiu, P. L. Fox, H. F. Hoff, R. G. Salomon and S. L. Hazen (2002). "Identification of a novel family of oxidized phospholipids that serve as ligands for the macrophage scavenger receptor CD36." Journal of Biological Chemistry **277**(41): 38503-38516.

Ravandi, A., S. Babaei, R. Leung, J. C. Monge, G. Hoppe, H. Hoff, H. Kamido and A. Kuksis (2004). "Phospholipids and oxophospholipids in atherosclerotic plaques at different stages of plaque development." Lipids **39**(2): 97-109.

Reis, A., M. R. Domingues, F. M. Amado, A. J. Ferrer-Correia and P. Domingues (2007). "Radical peroxidation of palmitoyl-linoleoyl-glycerophosphocholine liposomes: Identification of long-chain oxidised products by liquid chromatography-tandem mass spectrometry." J Chromatogr B Analyt Technol Biomed Life Sci **855**(2): 186-199.

Reis, A., P. Domingues and M. R. Domingues (2013). "Structural motifs in primary oxidation products of palmitoyl-arachidonoyl-phosphatidylcholines by LC-MS/MS." J Mass Spectrom **48**(11): 1207-1216.

Reis, a., P. Domingues, a. J. V. Ferrer-Correia and M. R. M. Domingues (2004). "Fragmentation study of short-chain products derived from oxidation of diacylphosphatidylcholines by electrospray tandem mass spectrometry: identification of novel short-chain products." Rapid communications in mass spectrometry : RCM **18**(23): 2849-2858.

Reis, A., A. Rudnitskaya, G. J. Blackburn, N. M. Fauzi, A. R. Pitt and C. M. Spickett (2013). "A comparison of five lipid extraction solvent systems for lipidomic studies of human LDL." Journal of Lipid Research **54**(7): 1812-1824.

Reis, A. and C. M. Spickett (2012). "Chemistry of phospholipid oxidation." Biochimica et biophysica acta **1818**(10): 2374-2387.

Rho, Y. H., C. P. Chung, A. Oeser, J. F. Solus, T. Gebretsadik, A. Shintani, P. Raggi, G. L. Milne and C. M. Stein (2010). "Interaction between Oxidative Stress and HDL Cholesterol Is Associated with Severity of Coronary Artery Calcification in Rheumatoid Arthritis." Arthritis care & research **62**(10): 1473-1480.

Robaszekiewicz, A., G. Bartosz, A. R. Pitt, A. Thakker, R. A. Armstrong, C. M. Spickett and M. Soszyński (2014). "HOCl-modified phosphatidylcholines induce apoptosis and redox imbalance in HUVEC-ST cells." Archives of Biochemistry and Biophysics **548**: 1-10.

Roberts, L. D., G. McCombie, C. M. Titman and J. L. Griffin (2008). "A matter of fat: An introduction to lipidomic profiling methods." Journal of Chromatography B **871**(2): 174-181.

Robles, L. (2013). "Role of Oxidative Stress in the Pathogenesis of Pancreatitis: Effect of Antioxidant Therapy." Pancreatic Disorders & Therapy **03**(01).

Routledge, S. J. (2012). "Beyond de-foaming: the effects of antifoams on bioprocess productivity." Computational and structural biotechnology journal **3**: e201210014-e201210014.

Routledge, S. J. and M. Clare (2012). Setting Up a bioreactor for recombinant protein production in yeast. Methods in Molecular Biology. **866**: 99-113.

Routledge, S. J., C. J. Hewitt, N. Bora and R. M. Bill (2011). "Antifoam addition to shake flask cultures of recombinant *Pichia pastoris* increases yield." Microbial Cell Factories **10**.

Routledge, S. J., L. Mikaliunaite, A. Patel, M. Clare, S. P. Cartwright, Z. Bawa, M. D. B. Wilks, F. Low, D. Hardy, A. J. Rothnie and R. M. Bill (2015). "The synthesis of recombinant membrane proteins in yeast for structural studies." Methods.

Routledge, S. J. B., R.M., Poyner, D. R. (2014). "Antifoams: the overlooked additive?" Pharmaceutical Bioprocessing **2**(2): 103-106.

Ruzickova, I., Z. Remesova and K. Vanzurova (2005). "Biological foam control by chemical additives dosing - Part II: Biological and physicochemical aspects." Acta Hydrochimica Et Hydrobiologica **33**(3): 262-265.

Samhan-Arias, A. K., J. Ji, O. M. Demidova, L. J. Sparvero, W. Feng, V. Tyurin, Y. Y. Tyurina, M. W. Epperly, A. A. Shvedova, J. S. Greenberger, H. Bayir, V. E. Kagan and A. A. Amoscato (2012). "Oxidized phospholipids as biomarkers of tissue and cell damage with a focus on cardiolipin." Biochim Biophys Acta **1818**(10): 2413-2423.

Sandra, K., S. Pereira Ados, G. Vanhoenacker, F. David and P. Sandra (2010). "Comprehensive blood plasma lipidomics by liquid chromatography/quadrupole time-of-flight mass spectrometry." J Chromatogr A **1217**(25): 4087-4099.

Sandra, K. and P. Sandra (2013). "Lipidomics from an analytical perspective." Curr Opin Chem Biol **17**(5): 847-853.

Sauer, S. and M. Kliem (2010). "Mass spectrometry tools for the classification and identification of bacteria." Nat Rev Micro **8**(1): 74-82.

Schanaider, A., T. P. de Carvalho, S. d. O. Coelho, J. M. Renteria, E. C. Araujo Eleutherio, M. T. Lima Castelo-Branco, K. Madi, W. Baetas-da-Cruz and H. S. Pereira de Souza (2015). "Ischemia-reperfusion rat model of acute pancreatitis: protein carbonyl as a putative early biomarker of pancreatic injury." Clinical and Experimental Medicine **15**(3): 311-320.

Schiller, J., O. Zschornig, M. Petkovic, M. Muller, J. Arnhold and K. Arnold (2001). "Lipid analysis of human HDL and LDL by MALDI-TOF mass spectrometry and ³¹P-NMR." J. Lipid Res. **42**(9): 1501-1508.

Schoenberg, M. H., D. Birk and H. G. Beger (1995). "Oxidative stress in acute and chronic pancreatitis." The American Journal of Clinical Nutrition **62**(6): 1306S-1314S.

Schrauwen, P. and M. K. C. Hesselink (2004). "Oxidative Capacity, Lipotoxicity, and Mitochondrial Damage in Type 2 Diabetes." Diabetes **53**(6): 1412-1417.

Schulte, H. G. (2003). Antifoams.

Schwartz, J. C., M. W. Senko and J. E. P. Syka (2002). "A two-dimensional quadrupole ion trap mass spectrometer." Journal of the American Society for Mass Spectrometry **13**(6): 659-669.

Schwarzer, E., P. Arese and O. A. Skorokhod (2015). "Role of the lipoperoxidation product 4-hydroxynonenal in the pathogenesis of severe malaria anemia and malaria immunodepression." Oxid Med Cell Longev **2015**: 638416.

Schwarzer, E., H. Kuhn, E. Valente and P. Arese (2003). "Malaria-parasitized erythrocytes and hemozoin nonenzymatically generate large amounts of hydroxy fatty acids that inhibit monocyte functions." Blood **101**(2): 722-728.

Schwarzer, E., F. Turrini and P. Arese (1994). "A luminescence method for the quantitative determination of phagocytosis of erythrocytes, of malaria-parasitized erythrocytes and of malarial pigment." Br J Haematol **88**(4): 740-745.

Schwudke, D., J. Oegema, L. Burton, E. Entchev, J. T. Hannich, C. S. Ejsing, T. Kurzchalia and A. Shevchenko (2006). "Lipid profiling by multiple precursor and neutral loss scanning driven by the data-dependent acquisition." Anal Chem **78**(2): 585-595.

Seddon, A. M., P. Curnow and P. J. Booth (2004). "Membrane proteins, lipids and detergents: not just a soap opera." Biochimica et Biophysica Acta (BBA) - Biomembranes **1666**(1-2): 105-117.

Sherwood, C. A., A. Eastham, L. W. Lee, J. Risler, H. Mirzaei, J. A. Falkner and D. B. Martin (2009). "Rapid Optimization of MRM-MS Instrument Parameters by Subtle Alteration of Precursor and Product m/z Targets." Journal of proteome research **8**(7): 3746-3751.

Shrivastava, A. and V. Gupta (2011). "Methods for the determination of limit of detection and limit of quantitation of the analytical methods." Chronicles of Young Scientists **2**(1): 21.

Shurubor, Y. I., U. Paolucci, B. F. Krasnikov, W. R. Matson and B. S. Kristal (2005). "Analytical precision, biological variation, and mathematical normalization in high data density metabolomics." Metabolomics **1**.

Silva, V. M., C. G. C. Vinagre, L. A. O. Dallan, A. P. M. Chacra and R. C. Maranhão (2014). "Plasma Lipids, Lipoprotein Metabolism and HDL Lipid Transfers are Equally Altered in Metabolic Syndrome and in Type 2 Diabetes." Lipids **49**(7): 677-684.

Simoës, M. L., L. Goncalves and H. Silveira (2015). "Hemozoin activates the innate immune system and reduces Plasmodium berghei infection in Anopheles gambiae." Parasit Vectors **8**(1): 12.

Skorokhod, A., E. Schwarzer, G. Gremo and P. Arese (2007). "HNE produced by the malaria parasite Plasmodium falciparum generates HNE-protein adducts and decreases erythrocyte deformability." Redox Rep **12**(1): 73-75.

Skorokhod, O. A., L. Caione, T. Marrocco, G. Migliardi, V. Barrera, P. Arese, W. Piacibello and E. Schwarzer (2010). "Inhibition of erythropoiesis in malaria anemia: role of hemozoin and hemozoin-generated 4-hydroxynonenal." Blood **116**(20): 4328-4337.

Sparvero, L. J., A. A. Amoscato, P. M. Kochanek, B. R. Pitt, V. E. Kagan and H. Bayir (2010). "Mass-spectrometry based oxidative lipidomics and lipid imaging: applications in traumatic brain injury." J Neurochem **115**(6): 1322-1336.

Sparvero, L. J., A. A. Amoscato, P. M. Kochanek, B. R. Pitt, V. E. Kagan and H. Bayir (2010). "Mass-Spectrometry Based Oxidative Lipidomics and Lipid Imaging: Applications in Traumatic Brain Injury." Journal of Neurochemistry **115**(6): 1322-1336.

Spickett, C. (2001). "Detection of phospholipid oxidation in oxidatively stressed cells by reversed-phase HPLC coupled with positive-ionization electroscopy MS." Biochem. J.

Spickett, C. M. (2005). "Studies of phospholipid oxidation by electrospray mass spectrometry: from analysis in cells to biological effects." BioFactors **24**.

Spickett, C. M. (2007). "Chlorinated lipids and fatty acids: an emerging role in pathology." Pharmacology & therapeutics **115**(3): 400-409.

Spickett, C. M. and N. M. Fauzi (2011). "Analysis of oxidized and chlorinated lipids by mass spectrometry and relevance to signalling." Biochemical Society transactions **39**(5): 1233-1239.

Spickett, C. M. and A. R. Pitt (2015). "Oxidative Lipidomics Coming of Age: Advances in Analysis of Oxidized Phospholipids in Physiology and Pathology." Antioxid Redox Signal.

Spickett, C. M. and A. R. Pitt (2015). "Oxidative Lipidomics Coming of Age: Advances in Analysis of Oxidized Phospholipids in Physiology and Pathology." Antioxidants & Redox Signaling **22**(18): 1646-1666.

Spickett, C. M., A. R. Pitt and A. J. Brown (1998). "Direct observation of lipid hydroperoxides in phospholipid vesicles by electrospray mass spectrometry." Free Radical Biology and Medicine **25**(4-5): 613-620.

Spickett, C. M., A. Reis and A. R. Pitt (2011). "Identification of oxidized phospholipids by electrospray ionization mass spectrometry and LC-MS using a QQLIT instrument." Free radical biology & medicine **51**(12): 2133-2149.

Spickett, C. M., N. Rennie, H. Winter, L. Zambonin, L. Landi, A. Jerlich, R. J. Schaur and A. R. Pitt (2001). "Detection of phospholipid oxidation in oxidatively stressed cells by reversed-phase HPLC coupled with positive-ionization electrospray [correction of electroscopy] MS." Biochemical Journal **355**(Pt 2): 449-457.

Spickett, C. M., N. Rennie, H. Winter, L. Zambonin, L. Landi, a. Jerlich, R. J. Schaur and a. R. Pitt (2001). "Detection of phospholipid oxidation in oxidatively stressed cells by reversed-phase HPLC coupled with positive-ionization electrospray [correction of electroscopy] MS." The Biochemical journal **355**(Pt 2): 449-457.

Spickett, C. M., I. Wiswedel, W. Siems, K. Zarkovic and N. Zarkovic (2010). "Advances in methods for the determination of biologically relevant lipid peroxidation products." Free radical research **44**(10): 1172-1202.

Spickett, C. M., I. Wiswedel, W. Siems, K. Zarkovic and N. Zarkovic (2010). "Advances in methods for the determination of biologically relevant lipid peroxidation products." Free Radical Research **44**(10): 1172-1202.

Steinberg, D. (2009). "The LDL modification hypothesis of atherogenesis: an update." Journal of lipid research **50** Suppl: S376-381.

Stewart, J. C. M. (1980). "Colorimetric determination of phospholipids with ammonium ferrothiocyanate." Analytical Biochemistry **104**(1): 10-14.

Strassburg, K., A. M. Huijbrechts, K. A. Kortekaas, J. H. Lindeman, T. L. Pedersen, A. Dane, R. Berger, A. Brenkman, T. Hankemeier, J. van Duynhoven, E. Kalkhoven, J. W. Newman and R. J. Vreeken (2012). "Quantitative profiling of oxylipins through comprehensive LC-MS/MS analysis: application in cardiac surgery." Anal Bioanal Chem **404**(5): 1413-1426.

Stutts, W., R. Menger, A. Kiss, R. Heeren and R. Yost (2013). "Characterization of Phosphatidylcholine Oxidation Products by MALDI MSn." Analytical Chemistry **85**(23): 11410-11419.

Stutts, W. L., R. F. Menger, A. Kiss, R. M. A. Heeren and R. A. Yost (2013). "Characterization of Phosphatidylcholine Oxidation Products by MALDI MSn." Analytical Chemistry **85**(23): 11410-11419.

Subramaniam, S., E. Fahy, S. Gupta, M. Sud, R. W. Byrnes, D. Cotter, A. R. Dinasarapu and M. R. Maurya (2011). "Bioinformatics and systems biology of the lipidome." Chem Rev **111**(10): 6452-6490.

Sullivan, D. J. (2002). "Theories on malarial pigment formation and quinoline action." Int J Parasitol **32**(13): 1645-1653.

Sullivan, D. J. (2005). Hemozoin: a Biocrystal Synthesized during the Degradation of Hemoglobin. Biopolymers Online, Wiley-VCH Verlag GmbH & Co. KGaA.

Sysi-Aho, M., M. Katajamaa, L. Yetukuri and M. Oresic (2007). "Normalization method for metabolomics data using optimal selection of multiple internal standards." BMC Bioinformatics **8**: 93.

Thakur, R. K., Reiko; McNally, Jonathan; Cook, Kevin; Zabrouskov, Vlad (2008). The Importance of Linear-Dynamic Range for Small-Molecule and targeted Peptide LC-MS-MS-Quantitation. S. J. Thermo Fisher Scientific, CA, USA. San Jose, CA, USA., Thermo Fisher Scientific, San Jose, CA, USA.

Thomas, C. P., L. T. Morgan, B. H. Maskrey, R. C. Murphy, H. Kuhn, S. L. Hazen, A. H. Goodall, H. A. Hamali, P. W. Collins and V. B. O'Donnell (2010). "Phospholipid-esterified eicosanoids are generated in agonist-activated human platelets and enhance tissue factor-dependent thrombin generation." J Biol Chem **285**(10): 6891-6903.

Tran, P. N., S. H. J. Brown, M. Rug, M. C. Ridgway, T. W. Mitchell and A. G. Maier (2016). "Changes in lipid composition during sexual development of the malaria parasite Plasmodium falciparum." Malaria Journal **15**(1): 1-13.

Trpkovic, A., I. Resanovic, J. Stanimirovic, D. Radak, S. A. Mousa, D. Cenic-Milosevic, D. Jevremovic and E. R. Isenovic (2015). "Oxidized low-density lipoprotein as a biomarker of cardiovascular diseases." Critical Reviews in Clinical Laboratory Sciences **52**(2): 70-85.

Tyberghein, A., K. Deroost, E. Schwarzer, P. Arese and P. E. Van den Steen (2014). "Immunopathological effects of malaria pigment or hemozoin and other crystals." Biofactors **40**(1): 59-78.

Tyurina, Y. Y., V. A. Tyurin, V. I. Kapralova, A. A. Amoscato, M. W. Epperly, J. S. Greenberger and V. E. Kagan (2009). "Mass-spectrometric characterization of phospholipids and their hydroperoxide derivatives in vivo: effects of total body irradiation." Methods in molecular biology (Clifton, N.J.) **580**: 153-183.

Uchikata, T., A. Matsubara, E. Fukusaki and T. Bamba (2012). "High-throughput phospholipid profiling system based on supercritical fluid extraction-supercritical fluid chromatography/mass spectrometry for dried plasma spot analysis." Journal of Chromatography A **1250**: 69-75.

Uchikata, T., A. Matsubara, S. Nishiumi, M. Yoshida, E. Fukusaki and T. Bamba (2012). "Development of oxidized phosphatidylcholine isomer profiling method using supercritical fluid chromatography/tandem mass spectrometry." Journal of Chromatography A **1250**: 205-211.

Uchikata, T., A. Matsubara, S. Nishiumi, M. Yoshida, E. Fukusaki and T. Bamba (2012). "Development of oxidized phosphatidylcholine isomer profiling method using supercritical fluid chromatography/tandem mass spectrometry." J Chromatogr A **1250**: 205-211.

Ulmer, C. Z. (2015). "Liquid Chromatography-Mass Spectrometry Metabolic and Lipidomic Sample Preparation Workflow for Suspension-Cultured Mammalian Cells using Jurkat T lymphocyte Cells." Journal of Proteomics & Bioinformatics **08**(06).

Uma Maheswar Rao, J. L. and T. Satyanarayana (2003). "Enhanced secretion and low temperature stabilization of a hyperthermostable and Ca²⁺-independent alpha-amylase of *Geobacillus thermoleovorans* by surfactants." Letters in applied microbiology **36**(4): 191-196.

Uppu, R. M., S. N. Murthy, W. A. Pryor and N. L. Parinandi (2010). "Simultaneous analysis of multiple lipid oxidation products in-vivo by liquid chromatography-mass spectrometry." Free radicals and antioxidant protocols-methods in molecular biology **610**.

Uyoga, S., O. A. Skorokhod, M. Opiyo, E. N. Orori, T. N. Williams, P. Arese and E. Schwarzer (2012). "Transfer of 4-hydroxynonenal from parasitized to non-parasitized erythrocytes in rosettes. Proposed role in severe malaria anemia." Br J Haematol **157**(1): 116-124.

van den Berg, R. A., H. C. Hoefsloot, J. A. Westerhuis, A. K. Smilde and M. J. van der Werf (2006). "Centering, scaling, and transformations: improving the biological information content of metabolomics data." BMC Genomics **7**(1): 142.

van Meer, G. (2005). "Cellular lipidomics." The EMBO journal **24**(18): 3159-3165.

Vardar-Sukan, F. (1998). "Foaming: Consequences, prevention and destruction." Biotechnology Advances **16**(5-6): 913-948.

Vennerstrom, J. L. and J. W. Eaton (1988). "Oxidants, oxidant drugs, and malaria." J Med Chem **31**(7): 1269-1277.

Vericel, E., R. Colas, C. Calzada, Q. H. Le, N. Feugier, C. Cugnet, H. Vidal, M. Laville, P. Moulin and M. Lagarde (2015). "Moderate oral supplementation with docosahexaenoic acid improves platelet function and oxidative stress in type 2 diabetic patients." *Thrombosis and Haemostasis* **114**(2): 289-296.

Verlaan, M., H. M. J. Roelofs, A. van Schaik, G. J. A. Wanten, J. B. M. J. Jansen, W. H. M. Peters and J. P. H. Drenth (2006). "Assessment of oxidative stress in chronic pancreatitis patients." *World Journal of Gastroenterology : WJG* **12**(35): 5705-5710.

Veselkov, K. A., L. K. Vingara, P. Masson, S. L. Robinette, E. Want, J. V. Li, R. H. Barton, C. Boursier-Neyret, B. Walther, T. M. Ebbels, I. Pelczer, E. Holmes, J. C. Lindon and J. K. Nicholson (2011). "Optimized Preprocessing of Ultra-Performance Liquid Chromatography/Mass Spectrometry Urinary Metabolic Profiles for Improved Information Recovery." *Analytical Chemistry* **83**(15): 5864-5872.

Vinaixa, M., S. Samino, I. Saez, J. Duran, J. J. Guinovart and O. Yanes (2012). "A Guideline to Univariate Statistical Analysis for LC/MS-Based Untargeted Metabolomics-Derived Data." *Metabolites* **2**(4): 775-795.

Vogesser, M. and C. Seger (2010). "Pitfalls associated with the use of liquid chromatography-tandem mass spectrometry in the clinical laboratory." *Clin Chem* **56**(8): 1234-1244.

Volinsky, R. and P. K. J. Kinnunen (2013). "Oxidized phosphatidylcholines in membrane-level cellular signaling: from biophysics to physiology and molecular pathology." *Febs Journal* **280**(12): 2806-2816.

Wacker, B. K., C. J. Albert, B. a. Ford and D. a. Ford (2013). "Strategies for the analysis of chlorinated lipids in biological systems." *Free radical biology & medicine* **59**: 92-99.

Wang, C., S. Xie, J. Yang, Q. Yang and G. Xu (2004). "Structural identification of human blood phospholipids using liquid chromatography/quadrupole-linear ion trap mass spectrometry." *Analytica Chimica Acta* **525**(1): 1-10.

Want, E. and P. Masson (2011). "Processing and analysis of GC/LC-MS-based metabolomics data." *Methods Mol Biol* **708**: 277-298.

Wasinger, V. C., M. Zeng and Y. Yau (2013). "Current Status and Advances in Quantitative Proteomic Mass Spectrometry." *International Journal of Proteomics* **2013**: 12.

Webb-Robertson, B.-J. M., H. K. Wiberg, M. M. Matzke, J. N. Brown, J. Wang, J. E. McDermott, R. D. Smith, K. D. Rodland, T. O. Metz, J. G. Pounds and K. M. Waters (2015). "Review, Evaluation, and Discussion of the Challenges of Missing Value Imputation for Mass Spectrometry-Based Label-Free Global Proteomics." *Journal of Proteome Research* **14**(5): 1993-2001.

Weng, N. D. (2014). "Mini-Review: Important Roles of Chromatography in the Quantization of Biomarkers Using Liquid Chromatography and Mass Spectrometry (LC-MS)." *Austin Chromatogr.* **1**(4).

Wenk, M. R. (2005). "The emerging field of lipidomics." *Nature reviews. Drug discovery* **4**(7): 594-610.

Willmann, J., D. Leibfritz and H. Thiele (2008). "Hyphenated Tools for Phospholipidomics." *Journal of Biomolecular Techniques : JBT* **19**(3): 211-216.

Winterbourn, C. C., M. J. D. Bonham, H. Buss, F. M. Abu-Zidan and J. A. Windsor (2003). "Elevated protein carbonyls as plasma markers of oxidative stress in acute pancreatitis." *Pancreatology* **3**(5): 375-382.

Winterbourn, C. C., J. J. M. van den Berg, E. Roitman and F. A. Kuypers (1992). "Chlorohydrin formation from unsaturated fatty acids reacted with hypochlorous acid." *Archives of Biochemistry and Biophysics* **296**(2): 547-555.

Wörmer, L., J. S. Lipp, J. M. Schröder and K.-U. Hinrichs (2013). "Application of two new LC-ESI-MS methods for improved detection of intact polar lipids (IPLs) in environmental samples." *Organic Geochemistry* **59**: 10-21.

Wrenger, C. and S. Muller (2004). "The human malaria parasite *Plasmodium falciparum* has distinct organelle-specific lipoylation pathways." *Mol Microbiol* **53**(1): 103-113.

Wu, R., E. Svenungsson, I. Gunnarsson, B. Andersson, I. Lundberg, L. S. Elinder and J. Frostegard (1999). "Antibodies against lysophosphatidylcholine and oxidized LDL in patients with SLE." *Lupus* **8**(2): 142-150.

Wu, Z., J. C. Shon and K.-H. Liu (2014). "Mass Spectrometry-based Lipidomics and Its Application to Biomedical Research." *Journal of Lifestyle Medicine* **4**(1): 17-33.

Yadav, D. and A. B. Lowenfels (2013). "The Epidemiology of Pancreatitis and Pancreatic Cancer." *Gastroenterology* **144**(6): 1252-1261.

- Yamada, T., T. Uchikata, S. Sakamoto, Y. Yokoi, S. Nishiumi, M. Yoshida, E. Fukusaki and T. Bamba (2013). "Supercritical fluid chromatography/Orbitrap mass spectrometry based lipidomics platform coupled with automated lipid identification software for accurate lipid profiling." Journal of Chromatography A **1301**: 237-242.
- Yang, K., H. Cheng, R. W. Gross and X. Han (2009). "Automated lipid identification and quantification by multidimensional mass spectrometry-based shotgun lipidomics." Anal Chem **81**(11): 4356-4368.
- Yang, K. and X. Han (2011). "Accurate quantification of lipid species by electrospray ionization mass spectrometry - Meet a key challenge in lipidomics." Metabolites **1**(1): 21-40.
- Yetukuri, L., K. Ekroos, A. Vidal-Puig and M. Oresic (2008). "Informatics and computational strategies for the study of lipids." Mol Biosyst **4**(2): 121-127.
- Yin, H., B. E. Cox, W. Liu, N. A. Porter, J. D. Morrow and G. L. Milne (2009). "Identification of intact oxidation products of glycerophospholipids in vitro and in vivo using negative ion electrospray iontrap mass spectrometry." J Mass Spectrom **44**(5): 672-680.
- Zehethofer, N. and D. M. Pinto (2008). "Recent developments in tandem mass spectrometry for lipidomic analysis." Analytica chimica acta **627**(1): 62-70.
- Zhang, J. R., A. R. Cazars, B. S. Lutzke and E. D. Hall (1995). "Hplc Chemiluminescence and Thermospray Lc/Ms Study of Hydroperoxides Generated from Phosphatidylcholine." Free Radical Biology and Medicine **18**(1): 1-10.
- Zhang, W. J. and R. G. Salomon (2005). "Oxidized phospholipids, isolevuglandins, and atherosclerosis." Molecular Nutrition & Food Research **49**(11): 1050-1062.
- Zhang, X. and G. E. Reid (2006). "Multistage tandem mass spectrometry of anionic phosphatidylcholine lipid adducts reveals novel dissociation pathways." International Journal of Mass Spectrometry **252**(3): 242-255.
- Zhou, S. L., Q. Song, Y. Tang and N. D. Weng (2005). "Critical review of development, validation, and transfer for high throughput bioanalytical LC-MS/MS methods." Current Pharmaceutical Analysis **1**(1): 3-14.
- Zhou, X. and G. Arthur (1992). "Improved procedures for the determination of lipid phosphorus by malachite green." Journal of Lipid Research **33**(8): 1233-1236.
- Zhu, C., Q. L. Liang, P. Hu, Y. M. Wang and G. A. Luo (2011). "Phospholipidomic identification of potential plasma biomarkers associated with type 2 diabetes mellitus and diabetic nephropathy." Talanta **85**(4): 1711-1720.

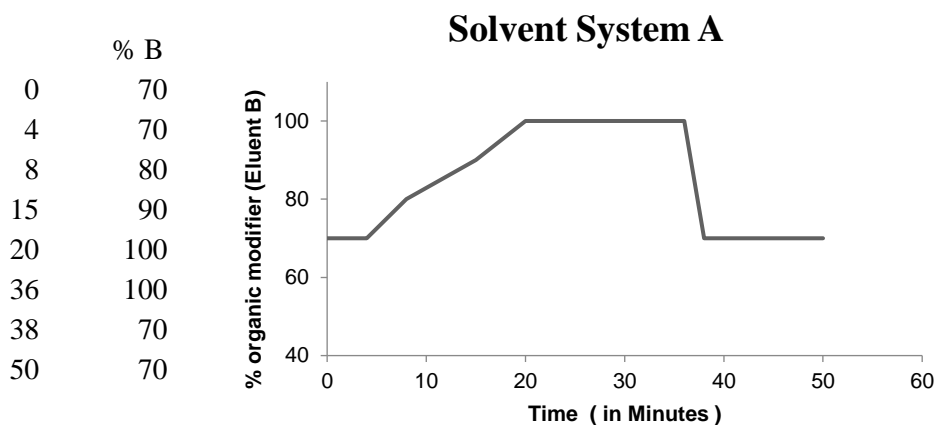
1 Appendix 1

1.1 Graphical representation of chromatographic program and solvent system used for optimisation of chromatographic separation as detailed in chapter 2: section 2.3.1.9.

Solvent System A

Eluent A: Water with 0.1 % formic acid and 5 mM Ammonium Formate

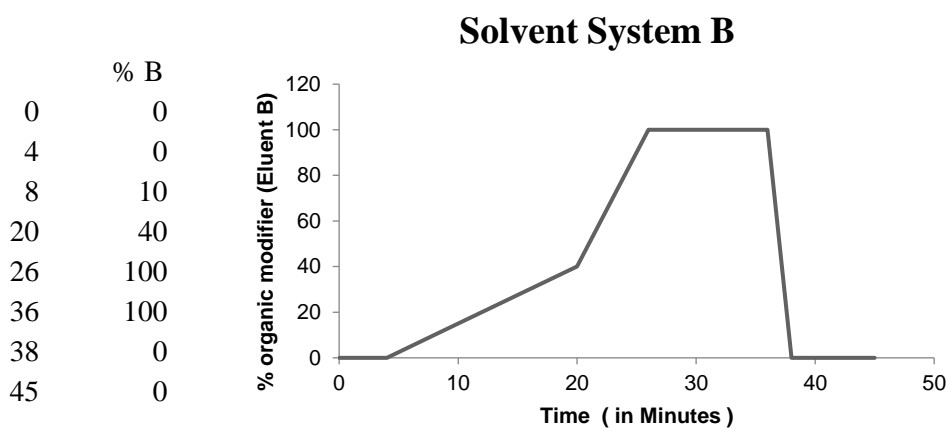
Eluent B: Methanol with 0.1 % formic acid and 5 mM Ammonium Formate



Solvent System B

Eluent A: Methanol: Hexane: 0.1M Ammonium Acetate (71:5:7)

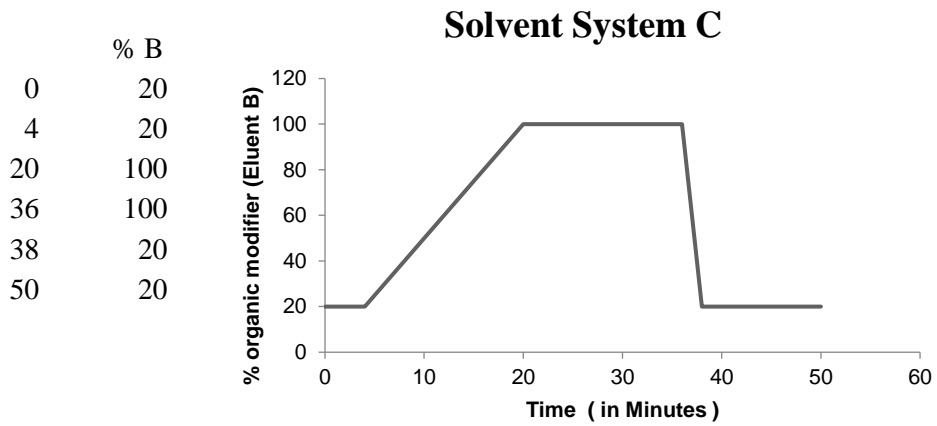
Eluent B: (95:5:0) Methanol: Hexane



Solvent System C

Eluent A: THF:MeOH:Water (30:20:50) with 10mM Ammonium Acetate

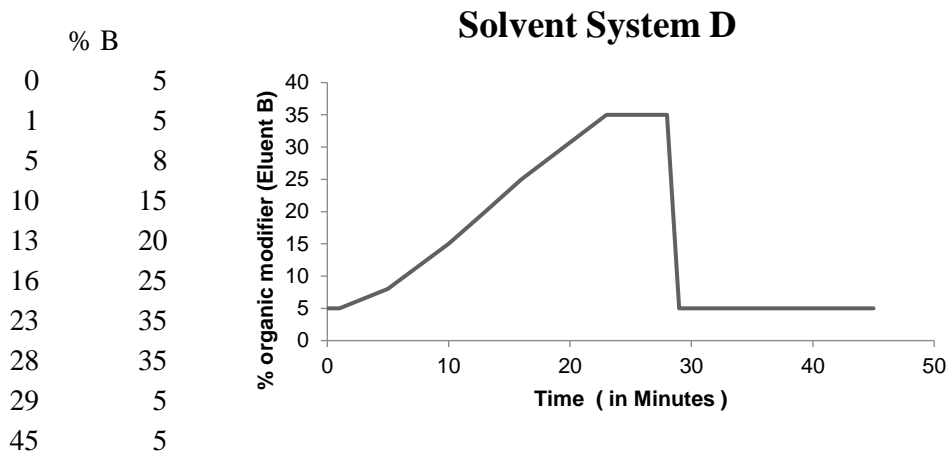
Eluent B: THF:MeOH:Water (70:20:10) with 10mM Ammonium Acetate



Solvent System D

Eluent A: 20 % Isopropyl alcohol (IPA) in Acetonitrile (ACN)

Eluent B: 20 % Isopropyl alcohol (IPA) in 20 mM Ammonium Formate

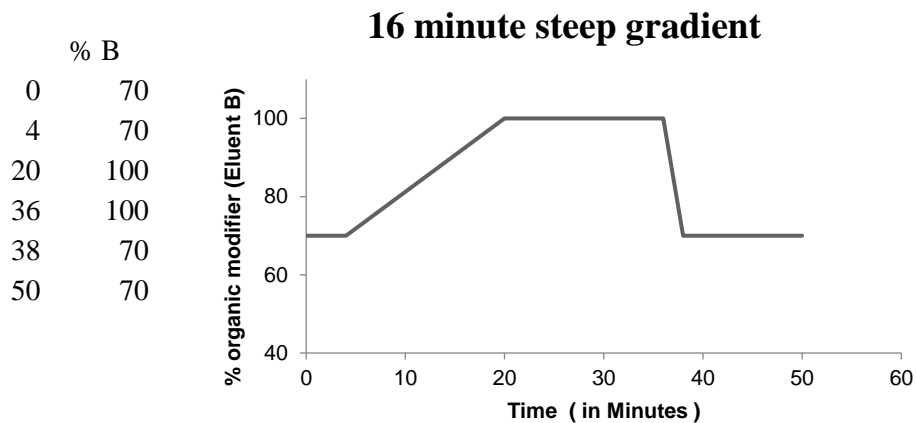


1.2 Graphical representation of chromatographic program for evaluation of chromatographic separation using monolith column with different gradients (Chapter 2 section 2.3.1.9)

16 minute steep gradient

Eluent A: Water with 0.1 % formic acid and 5 mM Ammonium Formate

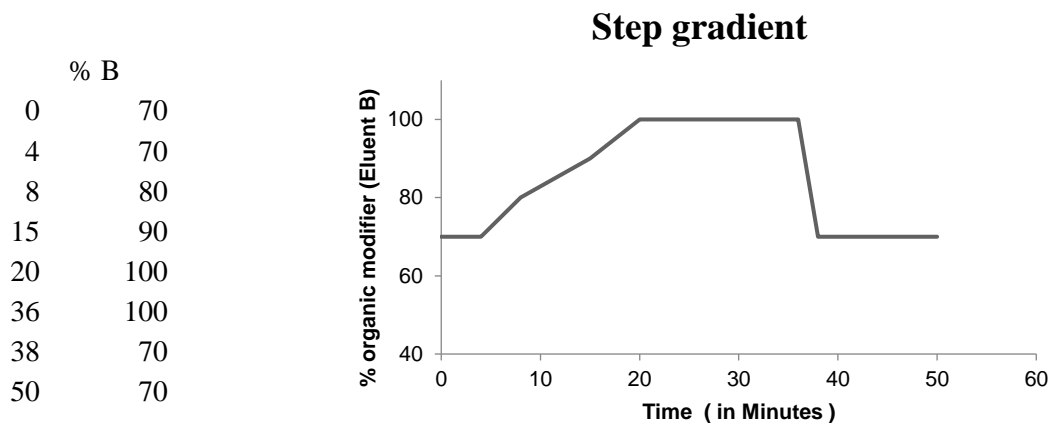
Eluent B: Methanol with 0.1 % formic acid and 5 mM Ammonium Formate



Step gradient

Eluent A: Water with 0.1 % formic acid and 5 mM Ammonium Formate

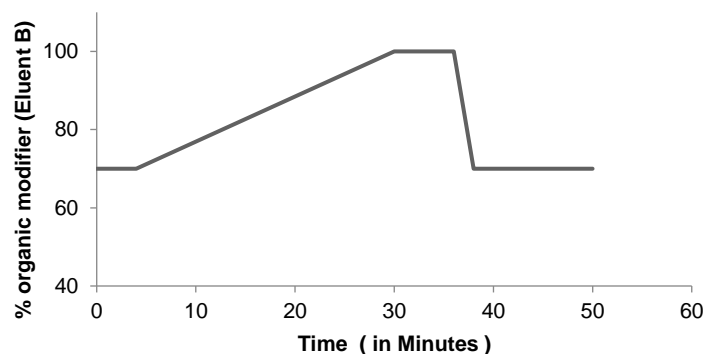
Eluent B: Methanol with 0.1 % formic acid and 5 mM Ammonium Formate



Eluent A: Water with 0.1 % formic acid and 5 mM Ammonium Formate
 Eluent B: Methanol with 0.1 % formic acid and 5 mM Ammonium Formate

26 minute shallow gradient

% B	
0	70
4	70
30	100
36	100
38	70
50	70



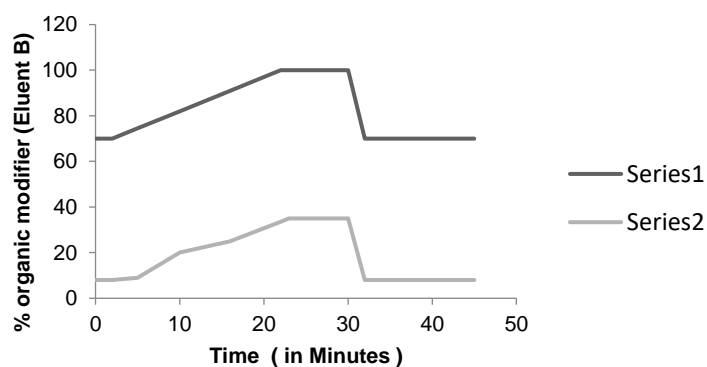
1.3 Graphical representation of chromatographic program for evaluation of chromatographic separation using 2D-LCMS technology using monolith column and HILIC column with solvent system A and D (Chapter 2 section 2.3.1.9)

Solvent System

Eluent A: Water with 0.1 % formic acid and 5 mM Ammonium Formate
 Eluent B: Methanol with 0.1 % formic acid and 5 mM Ammonium Formate
 Eluent A': 20 % Isopropyl alcohol (IPA) in Acetonitrile (ACN)
 Eluent B': 20 % Isopropyl alcohol (IPA) in 20 mM Ammonium Formate

	% B	% B'
0	70	8
2	70	8
5	74.5	9
10	82	20
16	91	25
22	100	33.5
23	100	35
30	100	35
32	70	8
45	70	8

Program 1



Solvent System

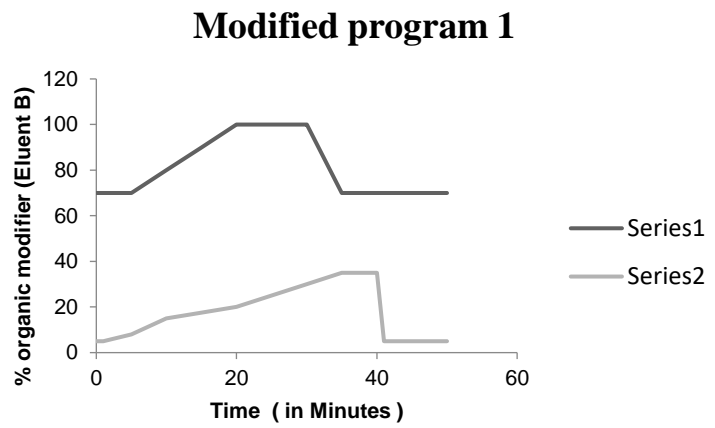
Eluent A: Water with 0.1 % formic acid and 5 mM Ammonium Formate

Eluent B: Methanol with 0.1 % formic acid and 5 mM Ammonium Formate

Eluent A: 20 % Isopropyl alcohol (IPA) in Acetonitrile (ACN)

Eluent B': 20 % Isopropyl alcohol (IPA) in 20 mM Ammonium Formate

	% B	% B'
0	70	5
1	70	5
5	70	8
10	80	15
15	90	17.5
20	100	20
30	100	30
35	70	35
40	70	35
41	70	5
50	70	5



2 Appendix II

2.1 Full spectra of precursor ion scan for 184 Da of control, UV treated as well as AAPH oxidised phosphatidylcholine mixture (PC mix)

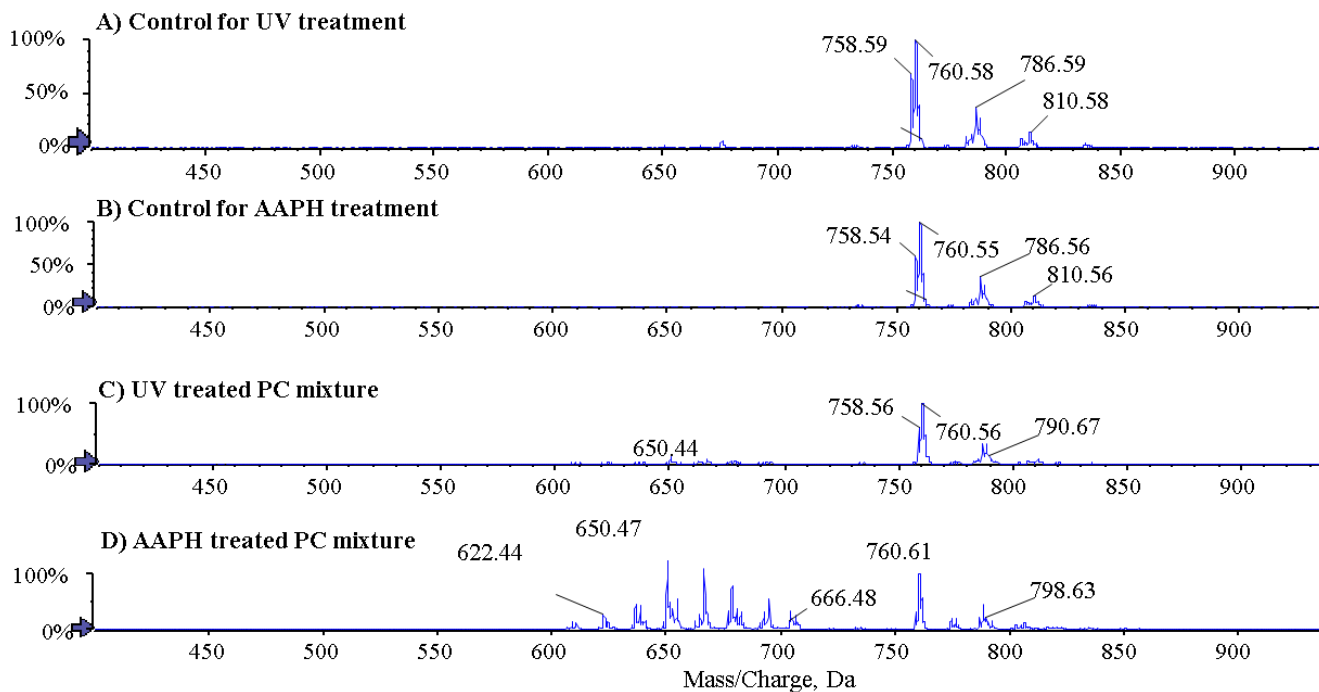


Figure 2.1: Direct infusion mass spectrometry of UV treated and AAPH treated PC mixture. The panel shows the different profile of oxidised phosphatidylcholine (OxPC) that are formed through UV exposure and AAPH treatment.

2.2 Tuning parameters optimisation

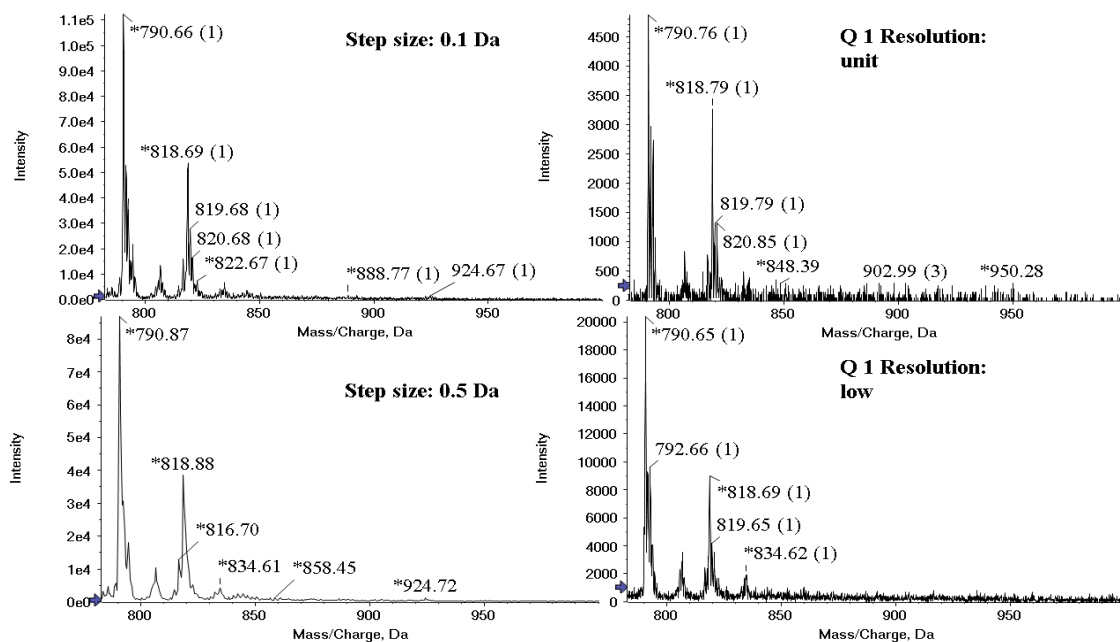


Figure 2.2: Direct infusion mass spectrometry (DIMS) analysis of 10 mM AAPH treated phosphatidylcholine mixture using NL 34 scan for optimisation of compound parameters. Hydroperoxides peaks at increment of 32 Da are observed at m/z 790.5 ($758.5 + 32$ Da) and 818.5 ($786.5 + 32$ Da) in 10 mM AAPH treated samples. The panel shows that the scan with step size of 0.1 and low Q1 resolution maximised ion intensity.

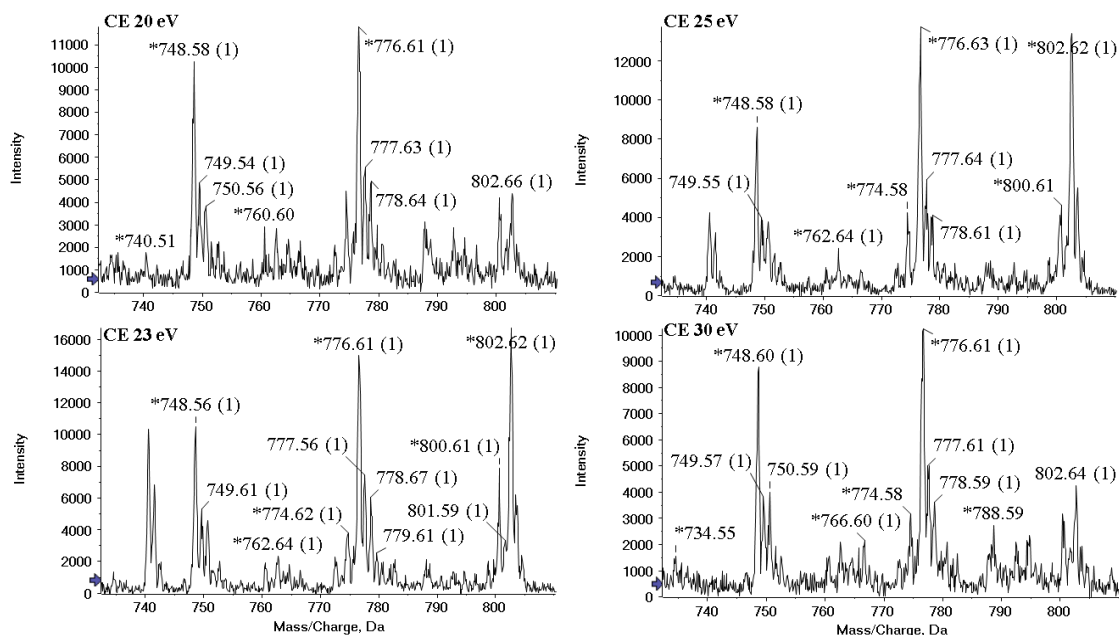


Figure 2.3: Direct infusion mass spectrometry (DIMS) analysis of 10 mM AAPH treated phosphatidylethanolamine (PE) mixture using NL 34 scan for optimisation of compound parameters. Hydroperoxides peaks at increment of 32 Da are observed at m/z 748.5 ($716.5 + 32$ Da) and 776.5 ($744.5 + 32$ Da) in 10 mM AAPH treated samples. The 4 panel shows that the scan with CE set between 23 -25 eV provided better sensitivity

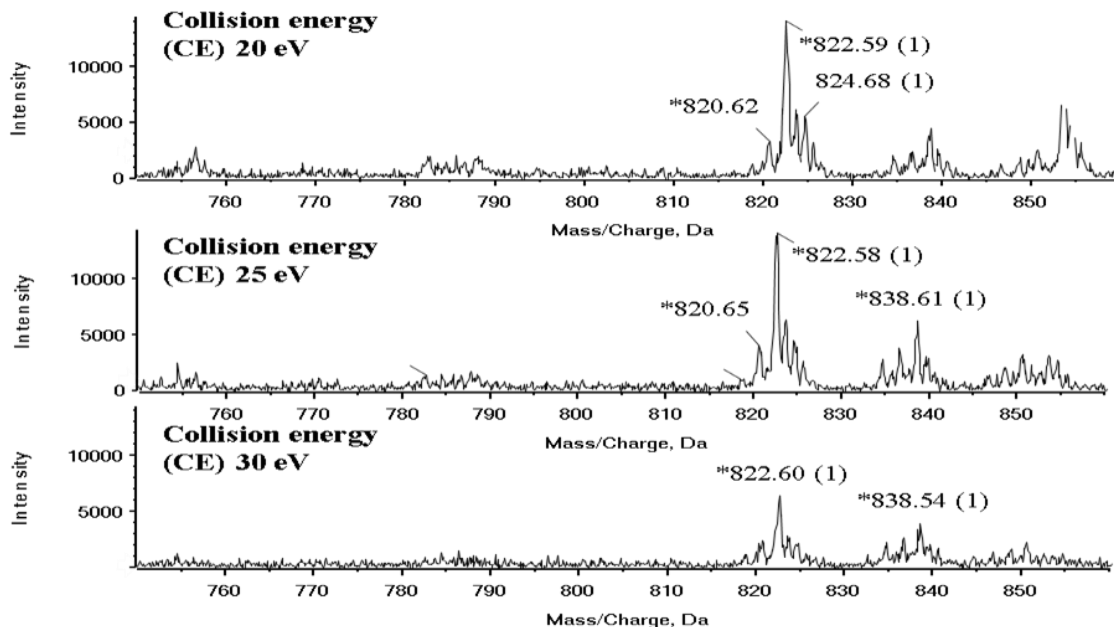


Figure 2.4: Direct infusion mass spectrometry (DIMS) analysis of 10 mM AAPH treated phosphatidylserine (PS) mixture using NL 34 scan for optimisation of compound parameters. Hydroperoxides peaks at increment of 32 Da are observed at m/z 822.5 ($790.5 + 32$ Da) in 10 mM AAPH treated samples. The 3 panel shows that the scan with CE set between 20 -25 eV provided better sensitivity.

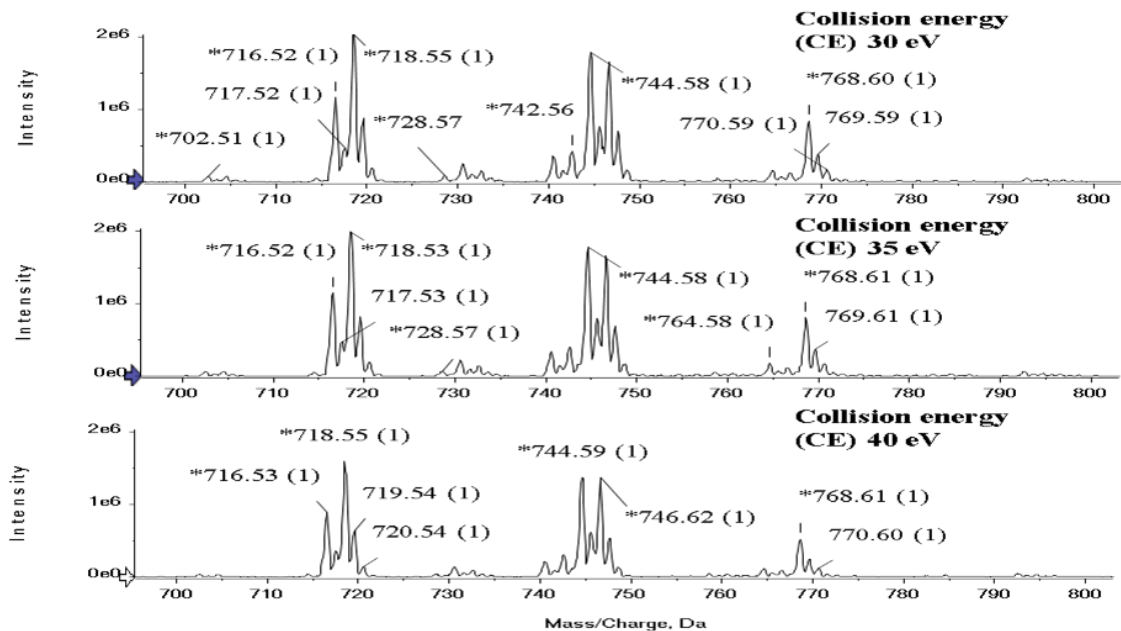


Figure 2.5: Direct infusion mass spectrometry (DIMS) analysis of 10 mM AAPH treated phosphatidylethanolamine (PE) mixture using NL 141 scan for optimisation of compound parameters. The 3 panel shows that the scan with CE set between 30 -35 eV provided better sensitivity.

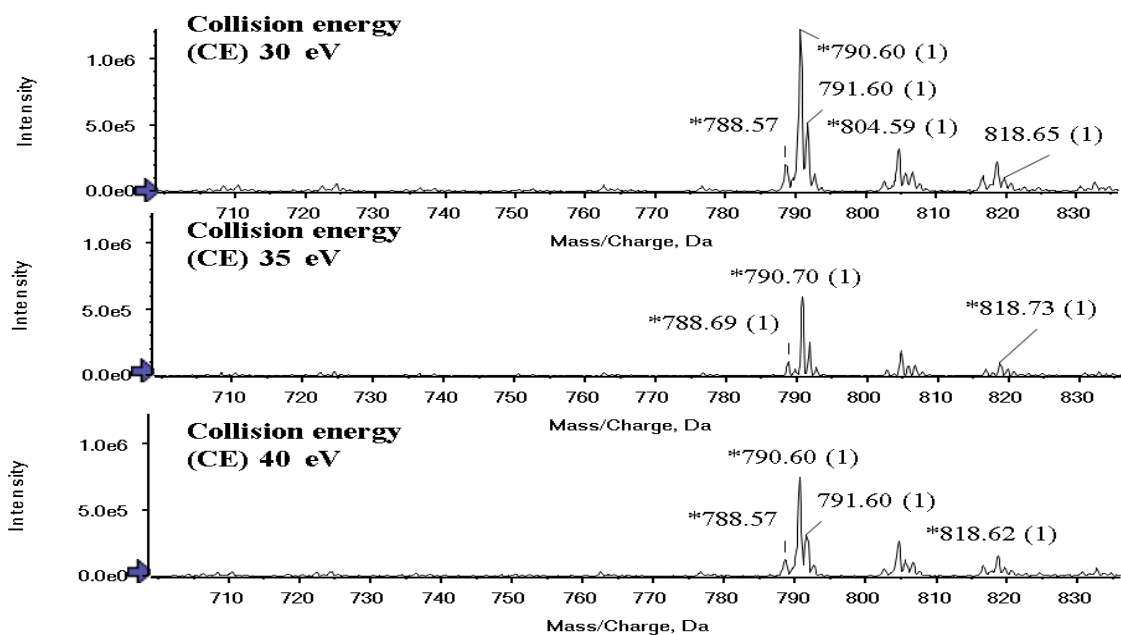


Figure 2.6: Direct infusion mass spectrometry (DIMS) analysis of 10 mM AAPH treated phosphatidylserine (PS) mixture using NL 185 Da scan for optimisation of compound parameters. The 3 panel shows that the scan with CE set between 30 -35 eV provided better sensitivity

2.3 Permission for re-printing the figure showing proton NMR analysis of SOPC, SLPC and SAPC chlorohydrin species

RightsLink



Thank You For Your Order!

Dear Mr. Alpesh Thakker,

Thank you for placing your order through Copyright Clearance Center's RightsLink service. Elsevier has partnered with RightsLink to license its content. This notice is a confirmation that your order was successful.

Your order details and publisher terms and conditions are available by clicking the link below:

<http://s100.copyright.com/CustomerAdmin/PLF.jsp?ref=97c3a958-38ae-4dcc-b031-a49b5f661656>

Order Details

Licensee: Alpesh Thakker

License Date: Sep 5, 2016

License Number: 3942440391751

Publication: Archives of Biochemistry and Biophysics

Title: HOCl-modified phosphatidylcholines induce apoptosis and redox imbalance in HUVEC-ST cells

Type Of Use: reuse in a thesis/dissertation

Total: 0.00 GBP

To access your account, please visit <https://myaccount.copyright.com>.

Please note: Online payments are charged immediately after order confirmation; invoices are issued daily and are payable immediately upon receipt.

To ensure that we are continuously improving our services, please take a moment to complete our [customer satisfaction survey](#).

2.4 Liquid-chromatography mass spectrometry (LC-MS) analysis of chlorohydrin species from PC mixture on Qtrap 5500 mass spectrometer using targeted approaches and cross validation on QTOF MS.

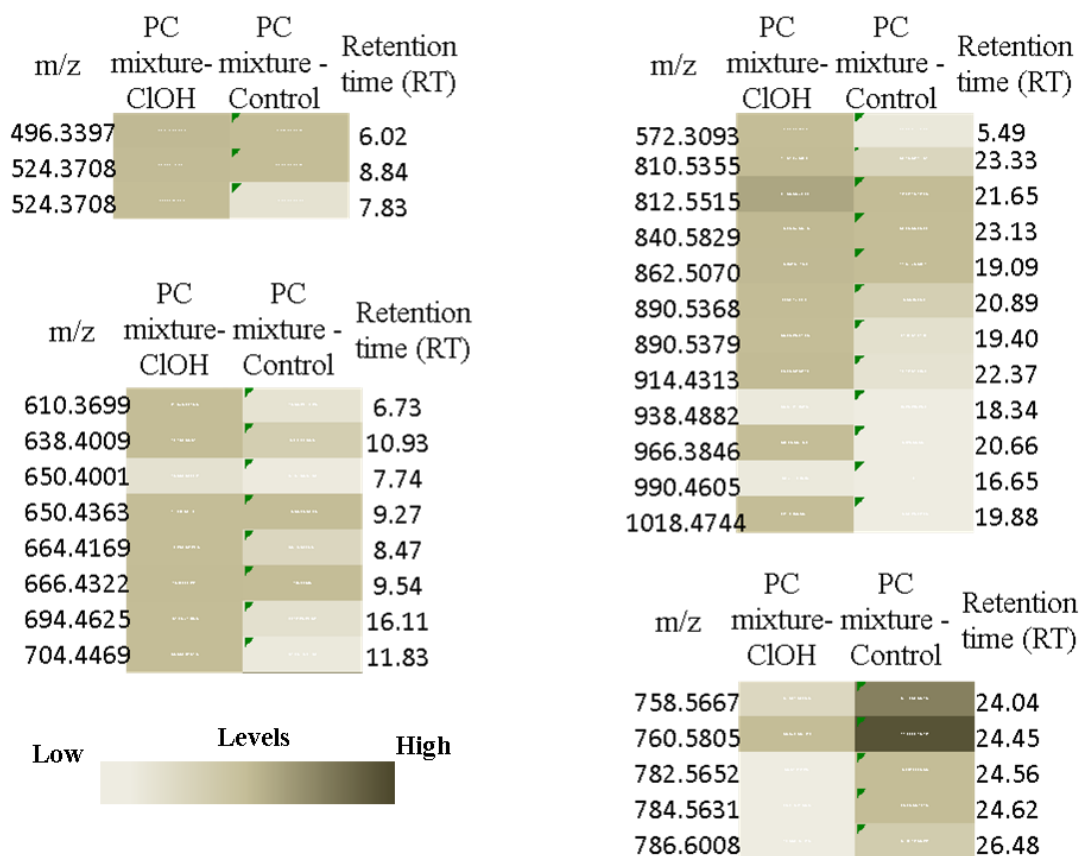


Figure 2.7: LC-MS analysis of HOCl treated PC mixture using monolith column for chromatographic separation and NL 36, NL 38 and IDA based product ion scanning for identification of species on Absciex Qtrap 5500 mass spectrometer (N=3). The individual peak areas were calculated by generating extracted ion chromatogram (XIC) for individual species, normalised using peak area of internal standard (13:0 /PC) added before extraction step and represented as heat map where light colour corresponds to low abundance level and dark colour corresponds to relative high abundance

Table 2.1: Automated data analysis using Progenesis QI of high resolution data of chlorohydrin samples PC mixture generated on Absciex 5600 QTOF instrument. The table shows the retention time, statistical analysis p-value post ANOVA, accepted identification, mass error and the sample where high levels was found.

m/z	Retention time (min)	Anova (p)	Accepted Compound ID	Formula	Mass Error (ppm)
496.3397	6.02	5.82E-05	PC(16:0/0:0)	C24H50NO7P	-0.09
524.3708	8.84	0.000203	PC(18:0/0:0)	C26H54NO7P	-0.60
524.3708	7.83	0.00091	PC(18:0/0:0)	C26H54NO7P	-0.42
572.3093	5.49	0.001028	Lyso-18-1-CIOH PC	C26H51ClNO8P	-3.68
610.3699	6.73	2.90E-06	(pentanedioic)-PPC	C29H56NO10P	-2.61
638.4009	10.93	0.000164	SGPC	C31H60NO10P	-2.91
650.4001	7.74	0.000214	(5-OH,8-keto,6-octenoic acid)-PPC	C32H60NO10P	-4.04
650.4363	9.27	0.002842	PONPC	C33H64NO9P	-4.32
664.4169	8.47	0.000405	(5-heptenedioic)-SPC	C33H62NO10P	-2.22
666.4322	9.54	3.05E-06	PAzPC	C33H64NO10P	-2.85
694.4625	16.11	1.47E-05	SAzPC	C35H68NO10P	-4.15
704.4469	11.83	3.64E-06	KODA-PC	C36H66NO10P	-4.05
758.5667	24.04	5.02E-08	PC(16:0/18:2(9E,11Z))	C42H80NO8P	-3.66
760.5805	24.45	3.70E-08	PC(16:0/18:1(9Z))	C42H82NO8P	-6.01
782.5652	24.56	1.12E-05	PC(16:0/20:4(5Z,8Z,11Z,14Z))	C44H80NO8P	-5.44
784.5631	24.62	0.000419			
786.6008	26.48	0.000206	PC(18:0/18:2(9Z,12Z))	C44H84NO8P	0.09
810.5355	23.33	5.64E-06	PLPC-CIOH	C42H81ClNO9P	-6.77
812.5515	21.65	9.65E-06	POPC-CIOH	C42H83ClNO9P	-6.38
840.5829	23.13	2.89E-06	SOPC-CIOH	C44H87ClNO9P	-6.07
862.5070	19.09	2.96E-07	PLPC-2(CIOH)	C42H82Cl2NO10P	-6.56
890.5368	20.89	3.87E-06	SLPC-2(CIOH)	C44H86Cl2NO10P	-8.03
890.5379	19.40	5.45E-06	SLPC-2(CIOH)	C44H86Cl2NO10P	-6.76
914.4313	22.37	1.09E-07			
938.4882	18.34	0.000163	PAPC-3(CIOH)	C44H83Cl3NO11P	4.26
966.3846	20.66	2.90E-06			
990.4605	16.65	9.81E-05	PAPC-4(CIOH)	C44H84Cl4NO12P	4.77
1018.4744	19.88	0.001422	SAPC-4(CIOH)	C46H88Cl4NO12P	-2.32

2.5 Liquid-chromatography mass spectrometry (LC-MS) analysis of peroxidation species from PC mixture on Qtrap 5500 mass spectrometer using targeted approaches and cross validation on QTOF MS.

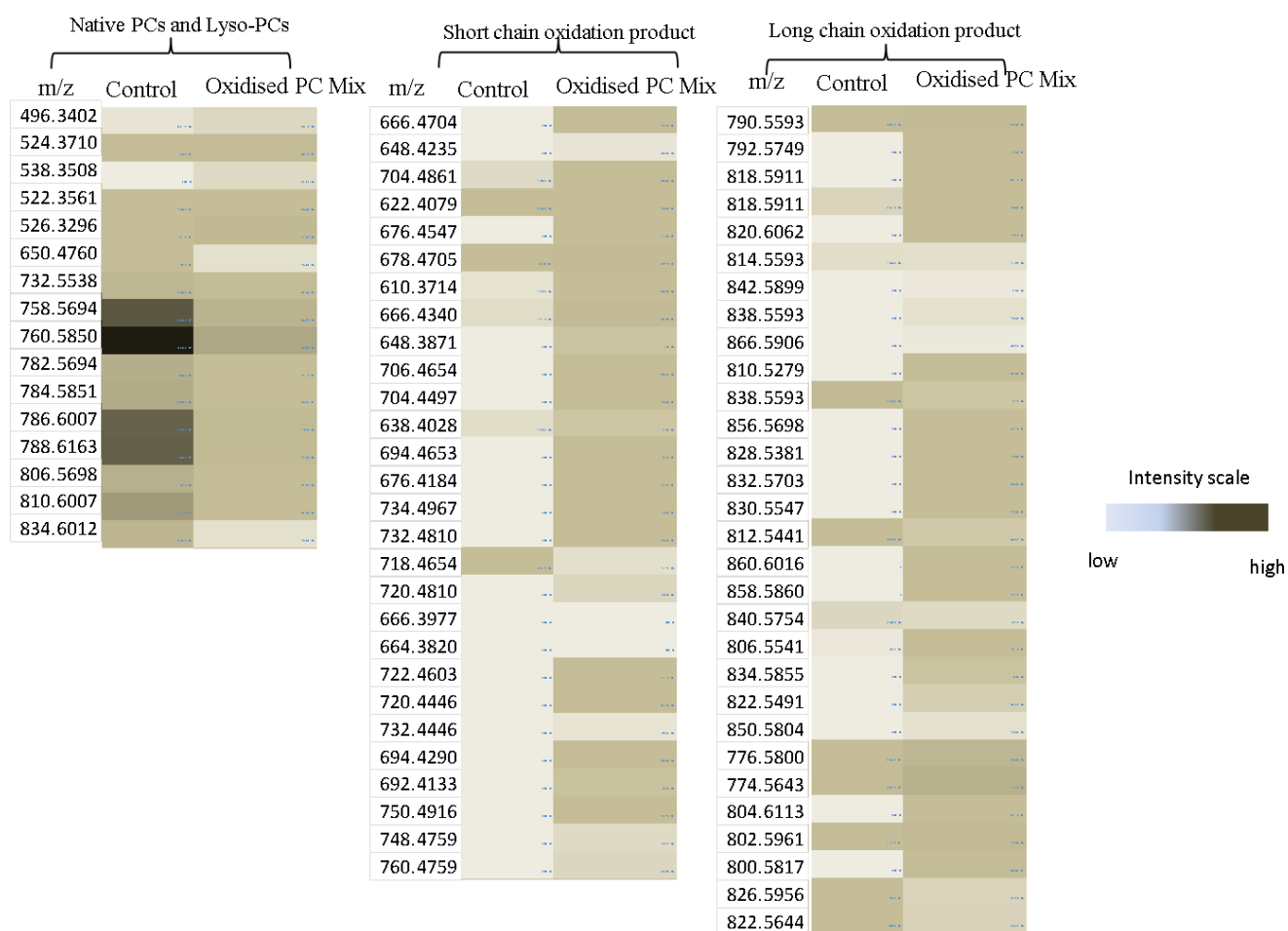


Figure 2.8: Qualitative analysis of all OxPC species identified in control and oxidised PC mixture samples by generating heat map representing colour coded abundance levels of OxPCs. Over 50 different OxPC species were identified and shows upregulation in oxidised sample, compared to control sample.

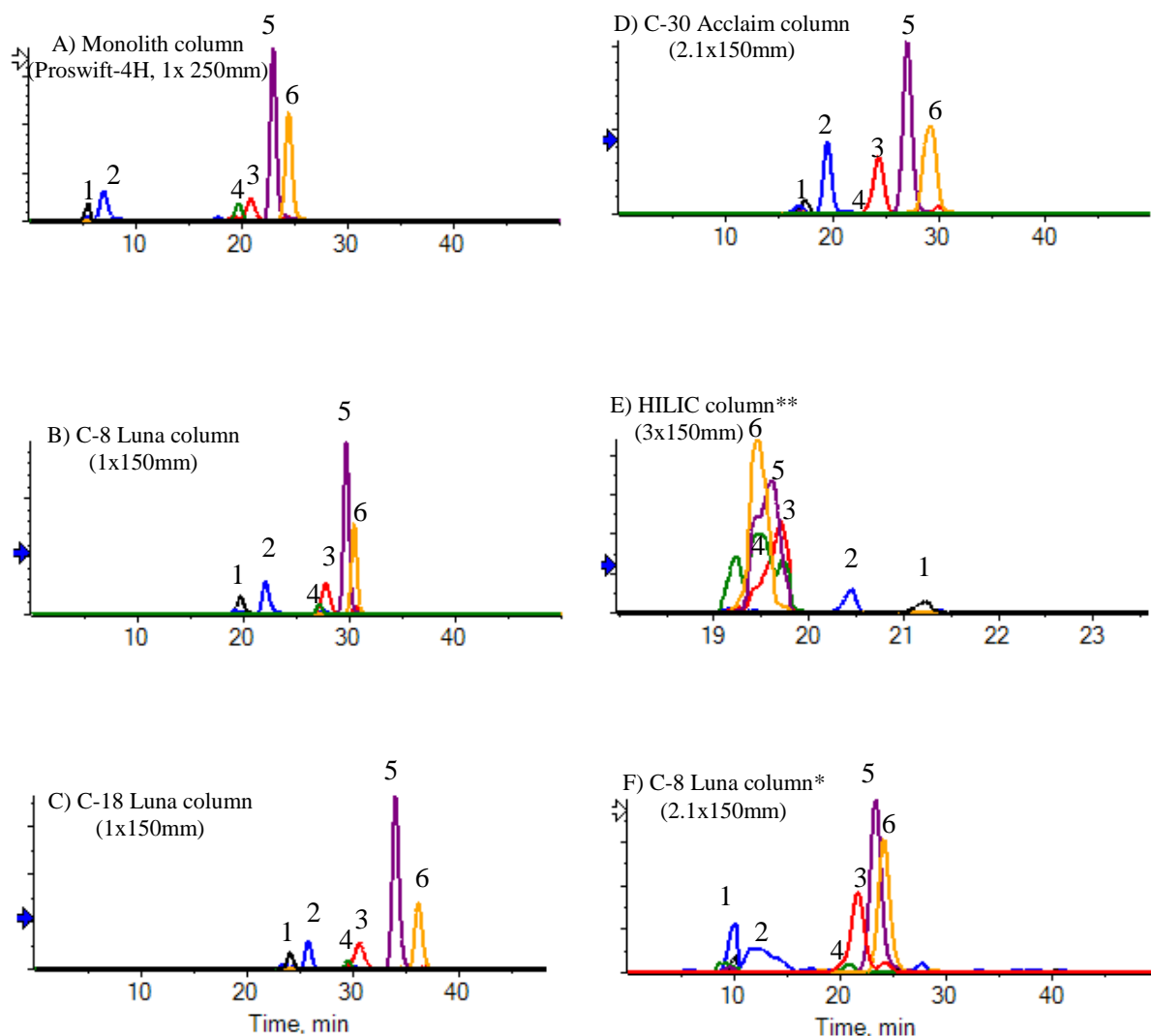
Table 2.2: List of oxidised phosphatidylcholine (OxPC) species with accurate masses, experimental masses, measured retention time and molecular formula.

Compound	Theoretical mass	Experimental mass	Error in ppm	Retention time
16:0 lysoPC	496.3402	496.3406	-0.81	5.6
18:0lysoPC	524.371	524.3718	-1.53	7.93
18:2 lysoPC	520.3407	520.3404	0.58	5.51
18:1 lyso PC	522.3561	522.3563	-0.38	6.21
20:4 lysoPC-OH	560.33468	560.3383	-6.46	4.51
20:4 lysoPC	544.3403	544.34	0.55	5.71
18:2lysoPC-OH	536.3356	536.3347	1.68	4.61
18:2lysoPC-OOH	552.3317	552.33	3.08	4.33
18:2lysoPC=O	534.3203	534.323	-5.05	4.56
13:0PC (internal standard)	650.4755	650.4765	-1.54	18.12
PLPC	758.5694	758.569	0.53	22.87
POPC	760.585	760.5848	0.26	23.38
PAPC	782.5694	782.568	1.79	23.11
OLPC	784.5851	784.5836	1.91	23.47

SLPC	786.6007	786.6001	0.76	24.23
SOPC	788.6163	788.6154	1.14	24.68
PDHPC	806.5698	806.5687	1.36	23.63
SAPC	810.6007	810.5998	1.11	24.53
SDHPC	834.6012	834.5993	2.28	24.87
P-7KPC(1palmitoyl-2-(7-oxoheptanoic acid)	622.40785	622.4082	-0.56	6.93
P-8KPC(1palmitoyl-2-(8-oxo-octanoic acid)	636.4235	636.4237	-0.31	7.55
P-7K5EPC (1palmitoyl-2-(7-oxo-5-heptenoic acid)	620.3922	620.3931	-1.45	7.52
P-11K9EPC(1-palmitoyl-2-(11-oxo-9-undecenoic acid)PC	676.4548	676.4556	-1.18	10.17
POVPC	594.3763	594.3775	-2.02	6.2
PONPC	650.4391	650.4395	-0.61	8.43
S-7KPC	650.43915	650.4388	0.54	11.51
S-8KPC	664.4548	664.456	-1.81	13.28
S-7K5EPC	648.4235	648.4236	-0.15	13.47
S-11K9EPC	704.4861	704.4857	0.57	17.79
SOVPC	622.40785	622.4084	-0.88	9.71
SONPC	678.47045	678.471	-0.81	14.91
PGPC	610.3714	610.3724	-1.64	6.27
PAzPC	666.434	666.4347	-1.05	8.41
HOOA-PC	650.40276	650.4035	-1.14	6.25
KOOA-PC	648.38711	648.3866	0.79	6.21
HDOA-PC	706.46536	706.4649	0.65	8.39
KDOA-PC	704.44971	704.4483	2.00	8.44
1-palmitoyl -2-(5-hydroxy-6,8-undecedienoic acid)PC	690.43406	690.435	-1.36	13.95
1-palmitoyl-2-(8-hydroxy-11-oxo-9-undecenoic acid)PC	692.44971	692.4502	-0.71	10.42
SGPC	638.40276	638.4035	-1.16	9.68
SAzPC	694.4653	694.4659	-0.86	14.85
HOOA-PC with 1 stearoyl	678.43406	678.4342	-0.21	9.72
KOOA-PC with 1 stearoyl	676.41841	676.4197	-1.91	8.33
HDOA-PC with 1 stearoyl	734.49666	734.4953	1.85	14.88
KDOA-PC with 1 stearoyl	732.48101	732.4792	2.47	14.85
1-stearoyl -2-(5-hydroxy-6,8-undecedienoic acid)PC	718.46536	718.4662	-1.17	13.92
1-stearoyl-2-(8-hydroxy-11-oxo-9-undecenoic acid)PC	720.48101	720.4794	2.23	13.67
HOdiA-PC	666.39768	666.3984	-1.08	6.39
HDdiA-PC	722.46028	722.4651	-6.67	7.25
KDdiA-PC	720.44463	720.4425	2.96	8.26
1-palmitoyl-2-(10-hydroxy-5,8,11-tridecatrienedioic acid)PC	732.44463	732.4456	-1.32	8.36
HDdiA-PC with 1 stearoyl	750.49158	750.4921	-0.69	16.07
KDdiA-PC with 1 stearoyl	748.47593	748.4761	-0.23	15.54
1-stearoyl-2-(10-hydroxy-5,8,11-tridecatrienedioic acid)PC	760.47593	760.4765	-0.75	14.75
PLPC-OOH	790.55926	790.5595	-0.30	17.7
POPC-OOH	792.5749	792.5745	0.50	20.04
SLPC-OOH	818.5911	818.5906	0.61	19.77
SOPC-OOH	820.60621	820.6037	3.06	21.55
PAPC-OOH	814.55926	814.5585	0.93	20.36

SAPC-OOH	842.5899	842.5898	0.12	20.95
PDHPC-OOH	838.55926	838.5596	-0.41	20.92
SDHPC-OOH	866.59056	866.5891	1.68	21.27
PECPC	810.5279	810.5257	2.71	19.66
SECPC	838.55926	838.5597	-0.52	19.5
SEIPC	856.56983	856.5707	-1.02	19.55
PEIPC	828.5381	828.5396	-1.81	17.16
PLPC(OH)-OOH	806.5541	806.5554	-1.61	18.29
SLPC(OH)-OOH	834.58548	834.5855	-0.02	17.74
SAPC(OH)-OOH	858.58548	858.5843	1.37	19.46
PAPC(OH)-OOH	830.55418	830.5563	-2.55	18.49
PDHPC(OH)-OOH	854.55418	854.5563	-2.48	19.04
SAPC-2(OOH)	874.58039	874.5805	-0.13	18.4
PLPC-2(OOH)	822.54909	822.5502	-1.35	15
SLPC-2(OOH)	850.58039	850.5992	-22.11	18.13
POPC-OH	776.58	776.5801	-0.13	21.58
PLPC-OH	774.5643	774.5641	0.26	21.02
SOPC-OH	804.6113	804.6089	2.98	22.72
SLPC=O	800.58	800.5796	0.50	22.09
SLPC-OH	802.5959	802.5953	0.75	21.13
SAPC-OH	826.5956	826.5956	0.00	21.78
PDHPC-OH	822.56435	822.5636	0.91	20.58
SDHPC-OH	850.59565	850.595	0.76	22.16

2.6 Evaluation of chromatographic separation of oxidised phosphatidylcholines (OxPC) using different chromatographic system



1 - m/z 594.5, POVPC (short chain oxidation product); **2** - m/z 650.5, PONPC (short chain oxidation product); **3** - m/z 774.5, PLPC-OH (long chain oxidation product); **4** - m/z 790.5, PLPC-OOH (long chain oxidation product); **5** - m/z 758.5, PLPC (native PC); **6** - m/z 786.5, SLPC (native PC)

Figure 2.9: Extracted ion chromatogram (XIC) were generated of two representative species for each group; chain shortened products (POVPC, m/z 594.5; PONPC, m/z 650.5), long chain oxidation product (PLPC-OH, m/z 774.5; PLPC-OOH, m/z 790.5) and Native PCs (PLPC, m/z 758.5; SLPC, m/z 786.5) and overlaid to evaluate the elution profile of OxPCs using different column. Different solvent systems were also used to optimise the separation of different species. ** indicates solvent system for HILIC column: eluent A- 20% Isopropyl alcohol (IPA) in Acetonitrile (ACN) and eluent B- 20 % IPA in ammonium formate (20mM); * indicates another solvent system consisting of eluent A as Tetrahydrofuran (THF):methanol:water (30:20:50) and eluent B as THF: methanol: water (70:20:10) with 10mM ammonium acetate

Flow rate	50 µl/minute			100 µl/minute			200 µl/minute		
compound	Monoisotopic mass (M+H)+	Molecular Formula (neutral compound)							
16:0 lysoPC	496.3402	C24H50O7NP	4.71	3.15E+06	2.25	2.82E+06	1.18	3.36E+05	
18:0lysoPC	524.3710	C26H54O7NP	5.53	2.35E+08	2.66	1.29E+08	1.38	3.62E+07	
18:2 lysoPC	520.3407	C26H50O7NP	4.8	2.45E+05	2.34	3.53E+05	0	0.00E+00	
18:1 lyso PC	522.3561	C26H52O7NP	5.05	3.29E+07	2.44	2.13E+07	1.22	4.71E+06	
20:4 lysoPC	544.3403	C28H50NO7P	5.11	5.33E+05	0	0.00E+00		0.00E+00	
13:0PC (internal standard)	650.4755	C34H68O8NP	17.79	1.69E+07	10.94	1.07E+07	7	2.24E+06	
PLPC	758.5694	C42H80NO8P	22.99	7.10E+08	15.83	6.72E+08	11.85	2.31E+08	
POPC	760.5850	C42H82NO8P	23.52	1.61E+09	16.33	1.81E+09	12.32	6.73E+08	
SLPC	786.6007	C44H84O8NP	24.45	5.49E+08	17.22	6.42E+08	13.21	1.44E+08	
SAPC	810.6007	C46H84NO8P	24.77	5.86E+07	17.56	8.19E+07	13.54	2.18E+07	
P-7KPC(1palmitoyl-2-(7-oxoheptanoic acid)	622.4079	C31H60O9NP	6.02	1.68E+07	2.89	1.12E+07	1.54	2.23E+06	
P-8KPC(1palmitoyl-2-(8-oxo-octanoic acid)	636.4235	C32H62O9NP	6.4	4.01E+07	3.14	3.41E+07	1.6	7.26E+06	
P-7K5EPC (1palmitoyl-2-(7-oxo-5-heptenoic acid)	620.3922	C31H58O9NP	6.28	4.48E+06	3.08	3.30E+06	1.53	6.08E+05	
P-11K9EPC(1-palmitoyl-2-(11-oxo-9-undecenoic acid)PC	676.4548	C35H66O9NP	8.11	1.51E+07	4.08	1.02E+07	2.29	4.29E+06	
POVPC	594.3763	C29H56O9NP	5.55	3.48E+06	2.66	2.55E+06	1.32	3.95E+05	
PONPC	650.4391	C33H64NPO9	6.96	1.48E+08	3.42	1.21E+08	1.79	2.33E+07	
S-7KPC	650.4392	C33H64O9NP	9.69	2.91E+06	0	0.00E+00	0		
SOVPC	622.4079	C31H60O9NP	7.55	2.22E+07	3.76	1.53E+07	2.02	3.10E+06	
SONPC	678.4705	C35H68NPO9	10.77	4.51E+07	5.57	2.99E+07	3.23	7.76E+06	
PAzPC	666.4340	C33H64O10NP	6.86	5.37E+07	3.39	5.23E+07	2.38	5.12E+06	
SGPC	638.4028	C31H60O10NP	7.48	1.47E+07	3.06	3.33E+07	1.56	6.43E+06	
SAzPC	694.4653	C35H68O10NP	10.44	2.24E+07	5.45	1.53E+07	3.18	3.24E+06	
PLPC-OOH	790.5593	C42H80O10NP	19.71	8.53E+07	12.99	7.02E+07	9.42	1.61E+07	
SLPC-OOH	818.5911	C44H84NO10P	21.42	2.96E+07	14.54	3.87E+07	10.79	9.74E+06	
PEIPC	828.5381	C44H78O11NP	18.55	2.88E+06	11.74	1.41E+06	5.17	1.58E+06	
PLPC(OH)-OOH	806.5541	C42H80NPO11	17.93	2.05E+07	11.21	1.31E+07	7.4	2.67E+06	
SLPC(OH)-OOH	834.5855	C44H84NO11P	19.97	5.05E+06	13.24	4.60E+06	9.62	1.40E+06	
POPC-OH	776.5800	C42H82NO9P	21.47	8.79E+07	14.5	8.90E+07	10.72	2.90E+07	
PLPC-OH	774.5643	C42H80O9NP	20.86	1.29E+08	13.96	1.35E+08	10.25	4.19E+07	
SAPC-OH	826.5956	C46H84NO9P	21.76	3.78E+06	12.42	2.53E+06	8.75	8.73E+05	

Table 2.3: Effect of flow rates on retention, sensitivity and resolution of representative oxidised species calculated by generating extracted ion chromatogram (XIC) and measuring peak area. The OxPC mixture was separated using monolith column at different flow rates and detection was performed on Q-trap mass spectrometer

3 Appendix III

3.1 List of publications

- Robaszkiewicz, A., Bartosz, G., Pitt, A.R., **Thakker, A.**, Spickett, M.C., et al. (2014). HOCl – modified phosphatidylcholines induce apoptosis and redox imbalance in HUVEC – ST cells. Arch Biochem Biophys, 1-10.
- Routledge, S., **Thakker, A.**, Reis, A., Spickett, C., Bill, R. (2016). Antifoam addition to *Pichia pastoris* cultures alters recombinant protein yield and membrane phospholipid composition (manuscript submitted)
- Popat, R., **Thakker, A.**, Spickett, C., Robson, M. (2016). Anti-myeloperoxidase antibodies attenuate the monocyte response to LPS and shape macrophage development (manuscript submitted)

Page [redacted] removed for copyright restrictions.